AD-A091 657 ARMY ENGINEER WATERWAYS EXPERIMENT STATION VICKSBURG--ETC F/G 8/3
TYPE 19 FLOOD INSURANCE STUDY: TSUNAMI PREDICTIONS FOR SOUTHERN--ETC(U)
SEP 80 J R HOUSTON FEMA-IAA-H-9-79
UNCLASSIFIED WES/TR/HL-80-18 NL

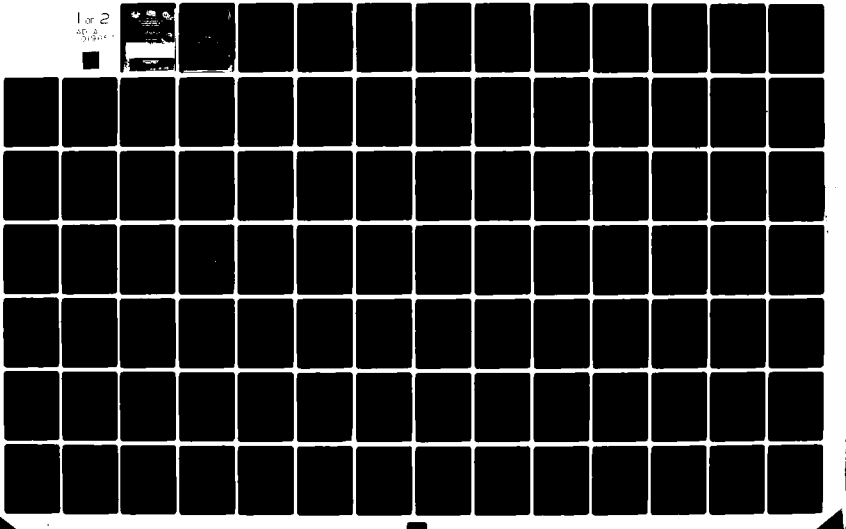

Unclassified

SECURITY CLASSIFICATION OF THIS PAGE (When Data Entered)

REPORT DOCUMENTATION PAGE

READ INSTRUCTIONS BEFORE COMPLETING FORM

1. REPORT NUMBER: Technical Report HL-80-18	2. GOVT ACCESSION NO.: AD-A091 657
3. RECIPIENT'S CATALOG NUMBER	
4. TITLE (and Subtitle): TYPE 19 FLOOD INSURANCE STUDY: TSUNAMI PREDICTIONS FOR SOUTHERN CALIFORNIA	5. TYPE OF REPORT & PERIOD COVERED: Final report; Jul 79 - May 80
	6. PERFORMING ORG. REPORT NUMBER
7. AUTHOR(s): James R. Houston	8. CONTRACT OR GRANT NUMBER(s)
9. PERFORMING ORGANIZATION NAME AND ADDRESS: U. S. Army Engineer Waterways Experiment Station, Hydraulics Laboratory, P. O. Box 631, Vicksburg, Miss. 39180	10. PROGRAM ELEMENT, PROJECT, TASK AREA & WORK UNIT NUMBERS
11. CONTROLLING OFFICE NAME AND ADDRESS: Federal Insurance Administration, Federal Emergency Management Agency, Washington, D. C. 20472	12. REPORT DATE: September 1980
	13. NUMBER OF PAGES: 174
14. MONITORING AGENCY NAME & ADDRESS (if different from Controlling Office): FEMA-IAA-H-9-79	15. SECURITY CLASS. (of this report): Unclassified
	15a. DECLASSIFICATION/DOWNGRADING SCHEDULE

16. DISTRIBUTION STATEMENT (of this Report)

Approved for public release; distribution unlimited.

17. DISTRIBUTION STATEMENT (of the abstract entered in Block 20, if different from Report)

18. SUPPLEMENTARY NOTES

19. KEY WORDS (Continue on reverse side if necessary and identify by block number)

Floodplain insurance	Shorelines
Mathematical models	Southern California
Numerical analysis	Tsunamis

20. ABSTRACT (Continue on reverse side if necessary and identify by block number)

Calculations of shoreline elevations due to tsunamis of distant origin were made for the southern California region. Elevations were determined that were expected to be equaled or exceeded on the average of once per 100 or once per 500 yr. In addition, exceedance frequency distributions for arbitrary frequencies of occurrence were presented. Historical data of tsunami activity in distant generation regions were used in the investigation in conjunction

(Continued)

DD FORM 1 JAN 73 1473 EDITION OF 1 NOV 65 IS OBSOLETE

Unclassified

SECURITY CLASSIFICATION OF THIS PAGE (When Data Entered)

AD A091389

20. ABSTRACT (Continued).

with numerical models that generated tsunamis and propagated them across the deep-ocean and nearshore region. The combined effects of the astronomical tides and tsunamis were incorporated in the analysis. Numerical simulations of the 1964 Alaskan tsunami in southern California were performed and comparisons with historical tide gage recordings were presented. Tsunami elevation predictions based upon the methods presented in the investigation were shown to be in good agreement with predictions based solely upon historical data of tsunami activity (at the limited number of locations in southern California with sufficient historical data to allow reasonable predictions to be made).

PREFACE

The investigation reported herein was authorized by the Office, Chief of Engineers (OCE), U. S. Army, in a letter dated 11 July 1979 and was performed for the Federal Insurance Administration, Federal Emergency Management Agency, under Inter-Agency Agreement (IAA)-H-9-79, Project Order No. 20. Project coordinator was Mr. Jerome Peterson, OCE.

The investigation was conducted from July 1979 to May 1980 by personnel of the Hydraulics Laboratory, U. S. Army Engineer Waterways Experiment Station (WES), under the direction of Mr. H. B. Simmons, Chief of the Hydraulics Laboratory, and Dr. R. W. Whalin, Chief of the Wave Dynamics Division. Dr. J. R. Houston, Research Hydraulic Engineer, conducted the study and prepared this report. Mrs. L. Chou made computer plots and aided in the computer computations.

Directors of WES during the investigation and the preparation and publication of this report were COL John L. Cannon, CE, and COL Nelson P. Conover, CE. Technical Director was Mr. F. R. Brown.

CONTENTS

TYPE 19 FLOOD INSURANCE STUDY: TSUNAMI PREDICTIONS FOR SOUTHERN CALIFORNIA

PART I: INTRODUCTION

Background

1. Of all water waves that occur in nature, one of the most destructive is the tsunami. The term "tsunami," originating from the Japanese words "tsu" (harbor) and "nami" (wave), is used to describe sea waves of seismic origin. Tectonic earthquakes, i.e., earthquakes that cause a deformation of the seabed, appear to be the principal seismic mechanism responsible for the generation of tsunamis. Coastal and submarine landslides and volcanic eruptions also have triggered tsunamis.

2. Tsunamis are principally generated by undersea earthquakes of magnitudes greater than 6.5 on the Richter scale with focal depths less than 30 miles.* They are very long-period waves (5 min to several hours) of low height (a few feet or less) when traversing water of oceanic depth. Consequently, they are not discernible in the deep ocean and go unnoticed by ships. Tsunamis travel at the shallow-water wave celerity equal to the square root of acceleration due to gravity times water depth even in the deepest oceans because of their very long wavelengths. This speed of propagation can be in excess of 500 mph in the deep ocean.

3. When tsunamis approach a coastal region where the water depth decreases rapidly, wave refraction, shoaling, and bay or harbor resonance may result in significantly increased wave heights. The great periods and wavelengths of tsunamis preclude their dissipating energy as a breaking surf; instead, they are apt to appear as rapidly rising water levels and only occasionally as bores.

4. Over 500 tsunamis have been reported within recorded history. Virtually all of these tsunamis have occurred in the Pacific Basin. This

---

* Multiply miles by 1.609344 to convert to kilometres.

is because most tsunamis are associated with earthquakes, and most seismic activity beneath the oceans is concentrated in the narrow fault zones adjacent to the great oceanic trench systems which are predominantly confined to the Pacific Ocean.

5. The loss of life and destruction of property due to tsunamis have been immense. The Great Hoei Tokaido-Nankaido tsunami of Japan killed 30,000 people in 1707. In 1868, the Great Peru tsunami caused 25,000 deaths and carried the frigate U.S.S. Waterlee 1,300 ft inland. The Great Meiji Sanriku tsunami of 1896 killed 27,122 persons in Japan and washed away over 10,000 houses.

6. In recent times, three tsunamis have caused major destruction in areas of the United States. The Great Aleutian tsunami of 1946 killed 173 persons in Hawaii, where heights as great as 55 ft were recorded. The 1960 Chilean tsunami killed 330 people in Chile, 61 in Hawaii, and 199 in distant Japan. The most recent major tsunami to affect the United States, the 1964 Alaskan tsunami, killed 107 people in Alaska, 4 in Oregon, and 11 in Crescent City, California, and caused over 100 million dollars in damage on the west coast of North America.

Purpose of Study

7. The purpose of this study was to establish 100- and 500-yr tsunami elevations in southern California produced by distantly generated tsunamis. This study is an update of a previous study that predicted 100- and 500-yr tsunami elevations in southern California (Houston and Garcia 1974). Whereas the previous study by Houston and Garcia (1974) used simple analytical solutions to propagate tsunamis over the nearshore region and to statistically combine tsunamic and astronomical tides, this study used complex numerical solutions for nearshore propagation and for superposition of tsunamis and tides. Two other reports (Garcia and Houston 1975 and Houston and Garcia 1978) established tsunami elevations for the west coast of the continental United States excluding Southern California. The 100- and 500-yr tsunami elevations are required by the Federal Insurance Administration (FIA) of the Federal Emergency Management Agency (FEMA) for use in flood insurance rate calculations.

PART II: NUMERICAL MODELS

Background

8. Unlike other areas of the Pacific Ocean such as the Hawaiian Islands, southern California lacks sufficient data to allow reasonable tsunami elevation predictions based upon local historical records of tsunami activity. Virtually all of southern California is completely without data of tsunami occurrence, even data for the prominent 1960 and 1964 tsunamis. Only a handful of locations have historical data for tsunamis other than the 1960 and 1964 tsunamis. However, the FIA requires information on tsunami elevations for all of southern California, even for the many locations that have no known historical data of tsunami activity and for coastal areas that are currently not developed (since these areas may be developed in the future).

9. The lack of historical data of tsunami activity in southern California necessitates the use of numerical models to predict tsunami elevations. The Aleutian-Alaskan area and the west coast of South America were found by Houston and Garcia (1974) to be the tsunamigenic regions of concern to southern California. Both regions have sufficient data on the generation of major tsunamis to allow a statistical investigation of tsunami generation. A numerical model employing a fairly coarse grid to cover a large section of the Pacific Ocean was used to generate representative tsunamis and propagate them across the deep ocean. A second numerical model employing a fine grid was used to propagate tsunamis from the deep ocean over the continental slope and shelf to shore. Previous studies by Houston and Garcia (1974) and Garcia and Houston (1975) used analytical methods to solve one-dimensional linear equations that described the transformation of tsunamis as they propagated from deep water to shore. Houston and Garcia (1978) used a two-dimensional numerical model. In this study a two-dimensional model is used for nearshore propagation that is similar to the model used by Houston and Garcia (1978) but allows a numerical grid with a varying spatial grid cell size.

10. There has been disagreement among tsunami researchers concerning the equations that govern tsunami generation, deep-ocean propagation, and nearshore propagation. The significance of frequency dispersion and nonlinear advection on tsunami propagation has been determined only in recent years. Using the nonlinear and dispersive Korteweg-deVries equation, Hammack and Segur (1978) concluded that "if the length of the initial wave is approximately 100 miles, the lead wave is described by a linear nondispersive model from source region until shoaling occurs near the shoreline." This conclusion also applies to leading waves that have reflected off land areas and traveled to a distant location. Thus two or three of the initial waves may be governed by linear nondispersive equations. Similarly, in studying tsunami propagation from the deep ocean to the nearshore region, Goring (1978) concluded that "... because of the small relative height of tsunamis and their large lengths relative to the lengths of the continental slope, the propagation of tsunamis from the deep ocean to the continental shelf-break and for some distance onto the shelf will be predicted as well by the linear nondispersive theory as by the nonlinear theories." Furthermore, Tuck (1979) found that "... linear long-wave equations are adequate to describe most of the tsunami generation, propagation and reception processes." Also, numerical studies by Hwang et al. (1972) have indicated that linear nondispersive equations govern tsunami propagation over the deep ocean. Numerical studies by Houston (1978) have shown that linear nondispersive equations govern tsunami generation, propagation over the deep ocean, and interaction with the Hawaiian Islands.

11. In this study, only large tsunamis (initial wavelengths greater than 100 miles) are considered; therefore, linear nondispersive equations are used for tsunami generation and deep-ocean propagation. The nearshore numerical model includes bottom friction and nonlinear advection terms. However, it was found by numerical experiments that these terms have no significant effect on tsunamis propagated from the deep ocean to the shoreline in the southern California region.

12. In this report, only tsunamis of distant origin (at least two or three tsunami wavelengths away from the west coast) are considered in

the analysis. Hammack (1972) has shown that near the generation area of a tsunami, details of ground motion during the earthquake and details of the permanent deformation of the sea floor influence the form of the resulting tsunami. Very little is known about the actual time-dependent ground motion during earthquakes generating major tsunamis, and small-scale details of the permanent deformation of the sea floor following earthquakes cannot be predicted in advance. Thus, accurate predictions of the properties of locally generated tsunamis are not possible at this time. However, Hammack (1972) has shown that the time-dependent ground motions and small-scale details of the permanent ground deformation produce waves which are not significant far from the source region. Thus, distantly generated tsunamis can be studied only knowing major features of the permanent ground deformation.

13. The probability is not considered great that an extremely destructive, locally generated tsunami will occur in southern California. Tsunamis are generally produced by earthquakes having fault movements that exhibit a pronounced "dip-slip," or vertical component of motion. "Strike-slip," or horizontal displacement, fault movements are inefficient generators of tsunamis. Faults in southern California characteristically exhibit strike-slip motion since the Pacific block of the earth's crust is moving horizontally relative to the North American block.

14. There have been reports of significant locally generated tsunamis in southern California. For example, a recent publication of the California Division of Mines and Geology (Weber and Kiessling 1978) mentions that Wood and Heck (1966) reported that runup heights of a tsunami generated by the 1812 Santa Barbara earthquake reached 50 ft* at Gaviota, 30-35 ft at Santa Barbara, and 15 ft or more at Ventura in southern California. However, an exhaustive study (Marine Advisors, Inc., 1965**) of this event that included an investigation of the unpublished notes of the late Professor G. D. Lauderback, University of California,

---

* Multiply feet by 0.3048 to convert to metres.

** Marine Advisors, Inc. 1965. "An Examination of the Evidence for the Reported Santa Barbara Coast Tsunami of December 1812" (unpublished report submitted to the Southern California Edison Company).

Berkeley (cited by Wood and Heck (1966) as a basis for their reported runup heights) has shown that the runup heights for this possible tsunami were not nearly as large as those reported. Professor Lauderback took an old report that said that the sea flowed 1/2 mile inland and transferred it to the present day topographic chart in the vicinity of Gaviota Canyon. This yielded a 50-ft level. However, the study by Marine Advisors, Inc. (1965), discovered that the old report actually referred to an estuary near Santa Barbara that is approximately at sea level. In addition, they learned that there were no reported drownings even though Indian villages were on the beach at the time and many people were there. (The mission padres kept meticulous records of Indian births, deaths, and other statistics). Other evidence indicates that there may have been a runup as great as 10 to 12 ft at Gaviota and a smaller runup at Santa Barbara (Marine Advisors, Inc., see footnote on page 7). A report of a tsunami at Santa Cruz, California, in 1840 also has been shown to be erroneous.

15. The largest authenticated locally generated tsunami in southern California was generated by the 1927 Point Arguello earthquake and produced runup elevations as great as 6 ft in the immediate vicinity. The only other reports of locally generated tsunamis in southern California were for possible tsunamis of very small heights in Santa Monica Bay (Joy 1968).

16. Thus relatively small locally generated tsunamis have been known to occur in southern California, but there are no reliable reports of major locally generated tsunamis. There could be a few locations in southern California (e.g. Gaviota) for which locally generated tsunamis are more significant than distantly generated tsunamis because the elevations produced by distantly generated tsunamis are small. However, the frequency of occurrence of locally generated tsunamis in southern California is not known and predictions of locally generated tsunami elevations are beyond the scope of this report.

17. The finite-difference numerical model used to simulate the generation of tsunamis in the Alaskan region and their propagation across the deep ocean was originally developed by Hwang et al. (1972), and

described in detail in an earlier report (Houston and Garcia 1974). A numerical model developed at WES (Garcia 1976) that used a more efficient solution scheme (explicit) than the Hwang et al. (1972) model (implicit-explicit scheme) was used to simulate the generation of tsunamis in the Peru-Chile region and their propagation across the deep ocean. This model was needed as a result of the extremely large grids (approximately 100,000 grid cells) used to propagate tsunamis over the great distance from Peru-Chile to southern California. In this study, the model employed 1/5° by 1/3° spherical coordinate grids to solve the linearized long-wave equations. Such coarse grids adequately resolve the very long tsunami wavelengths in the deep ocean. The grids covered very large sections of the Pacific Ocean including either Alaska and the west coast of the United States or South America and the west coast of the United States. The boundary condition on the solid boundaries (land) of the grids was that the component of the velocity normal to the boundary equaled zero. On open boundaries (ocean), a first-order approximation of total transmission was made.

18. The deep-ocean finite-difference model solved an initial value problem starting with an uplift deformation of the water surface identical with the major features of the permanent deformation (permanent in the sense that the time scale associated with it is much longer than the period of the tsunami) of the sea floor following the seismic disturbance. The transient movements within the time-history of the ground motion were neglected because Hammack (1972) has further shown that the initial deformation of the water surface will closely approximate major features of the permanent deformation of the ocean floor, provided these features have characteristic lengths that are at least four times as great as the water depth. The neglect of smaller features is unimportant because such small-scale details produce waves that are negligible in the far field.

Nearshore Numerical Model

19. The nearshore finite-difference numerical model used in this study is described in detail by Butler (1978). The model solves the

classical shallow-water wave equations that govern tsunami propagation in the nearshore region. A highly efficient implicit solution scheme that employs a centered, alternating-direction procedure is used.

20. The nearshore propagation numerical model employed in this study uses a smoothly varying grid that allows cells to be small in shallow water and larger in deeper water. A piecewise reversible transformation (analogous to that used by Wanstrath (1976)) is used independently in the x- and y-directions to map the grid into a uniform grid used in computational space. The coordinate transformation has the form

$$x = p + q\alpha^{r}$$

where p, q, and r are arbitrary constants and the transformation is applied piecewise for each axis. The transformation is such that there is a regular grid in computational space and all derivatives in computational space are centered. Many stability problems commonly occurring in variable grid schemes are eliminated using this transformation since the real space grid is smoothly varying with the variation and its first derivative being continuous. The variable grid allows accurate resolution of the tsunami wave form as it enters shallow water and its wavelength decreases.

21. The nearshore numerical model used as input the time-history calculated by the generation and deep-ocean propagation numerical model. A tsunami was generated in the Aleutian-Alaskan area or the west coast of South America and propagated across the deep ocean to a 500-m depth off the west coast of the United States. Wave forms calculated at this depth by the deep-ocean numerical model were recorded all along the west coast. These wave forms then were used as input to the nearshore numerical model, which propagated the tsunamis from the 500-m depths across the continental slope and shelf to shore.

22. The nearshore numerical grid covered an area approximately 280 miles by 142 miles. It extended from Point Conception, California, to Ensenada, Mexico. The grid was oriented approximately parallel to the 500-m contour, since refraction would have bent the wave fronts to such

an orientation before they reached the 500-m contour. Grid cells in water depths less than 500-m were slightly less than 1 mile on a side.

Verification

23. The numerical models used in this report were verified by numerical simulations of the 1964 Alaskan tsunami. This was the only large tsunami for which reliable information exists concerning source characteristics. The initial condition used in the generation and deep-ocean propagation numerical model was that the uplift of the ocean's surface in the source region was identical with the permanent deformation of the ocean bottom following the earthquake. The permanent deformation of the ocean's bottom as a function of spatial location was taken from Plafker (1964). The generation and deep-ocean propagation numerical model was used to propagate the 1964 Alaskan tsunami to a water depth of approximately 500 m off the coast of southern California. The nearshore numerical model then was used to propagate the tsunami to shore.

24. There were seven tide gages in operation along the coast of southern California from Point Conception to San Diego. Figures 1-7 show comparisons between recordings of the 1964 Alaskan tsunami by these tide gages and wave forms calculated using the generation and deep-ocean propagation and the nearshore numerical models to propagate the 1964 tsunami from Alaska to southern California. The comparisons extend over a period of 1.5 to 2.0 hr. This time period was selected since numerical models that generate tsunamis and propagate them across the deep ocean to distant locations will provide good values only for the first 1.5 to 2.0 hr (Houston 1978).

25. The numerical model calculations agree remarkably well with the tide gage recordings shown in Figures 1-7, considering the fact that the uplift used to generate the 1964 tsunami is only approximately known. In addition, tide gages do not record tsunamis without distortion of amplitude, period, and phase. Even so, the amplitudes, periods, and phases of the calculated and recorded wave forms shown in Figures 1-7 are in good general agreement. The greatest amplitude difference is for the second

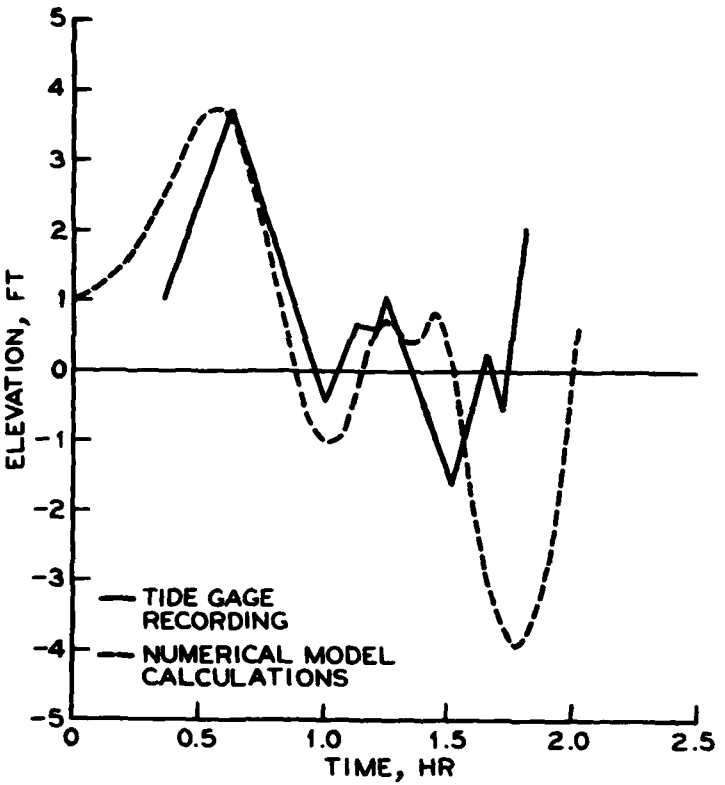

Figure 1. 1964 tsunami at Rincon Island, California

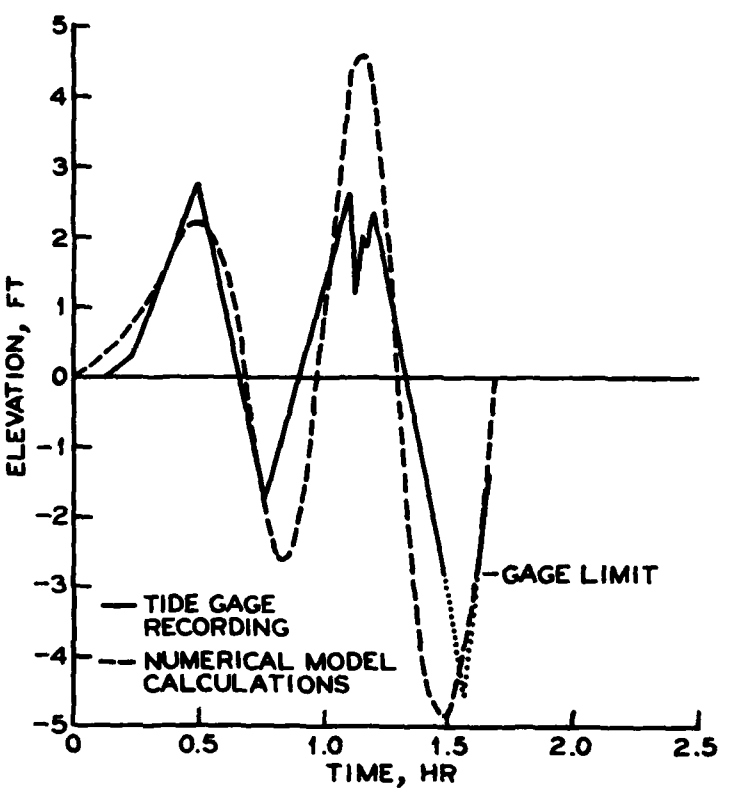

Figure 2. 1964 tsunami at Santa Monica, California

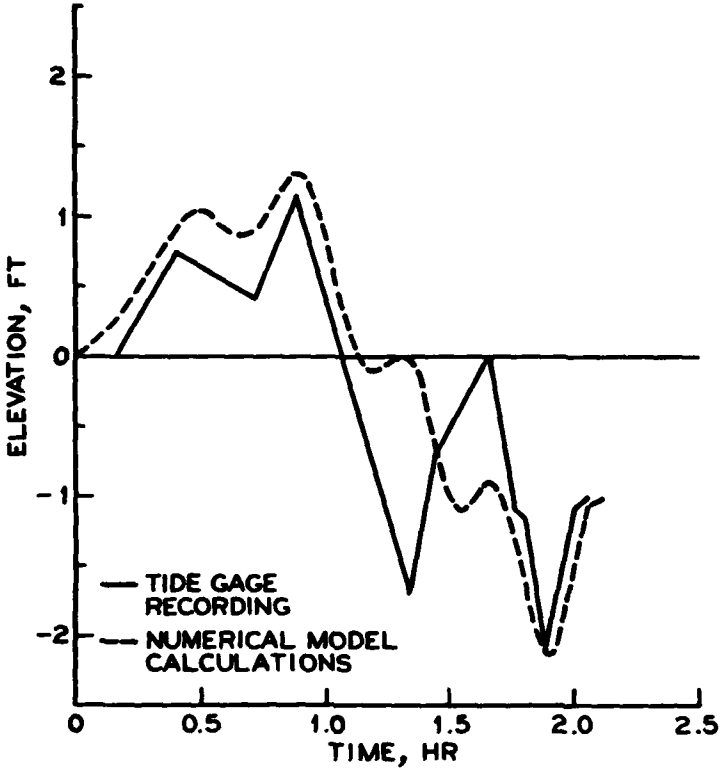

Figure 3. 1964 tsunami at Los Angeles (Berth 60), California

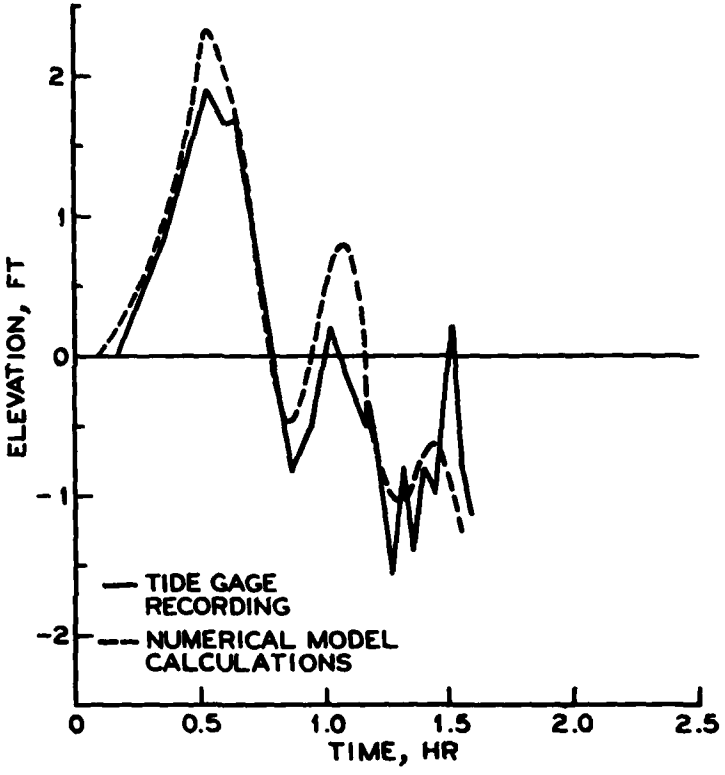

Figure 4. 1964 tsunami at Alamitos Bay, California

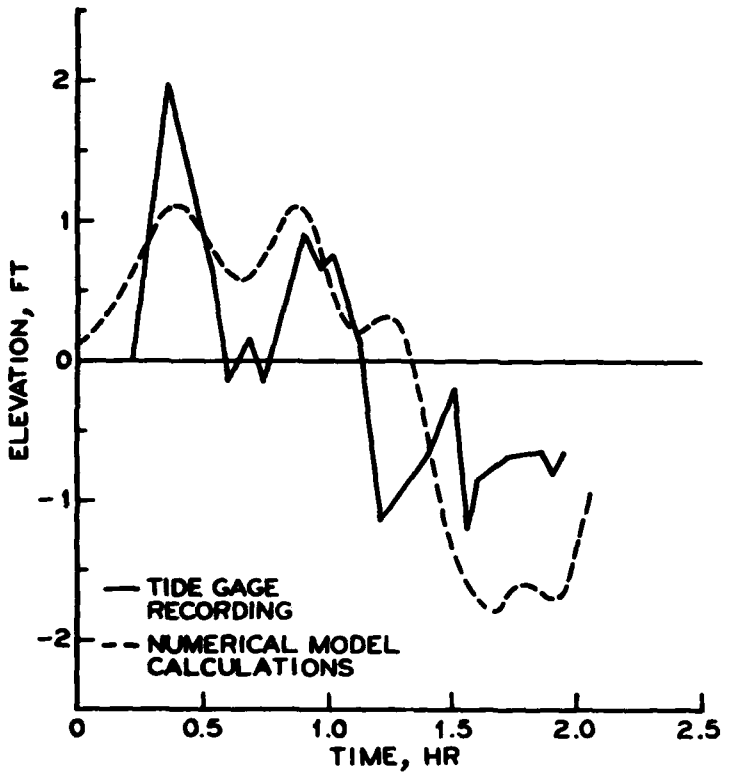

Figure 5. 1964 tsunami at La Jolla, California

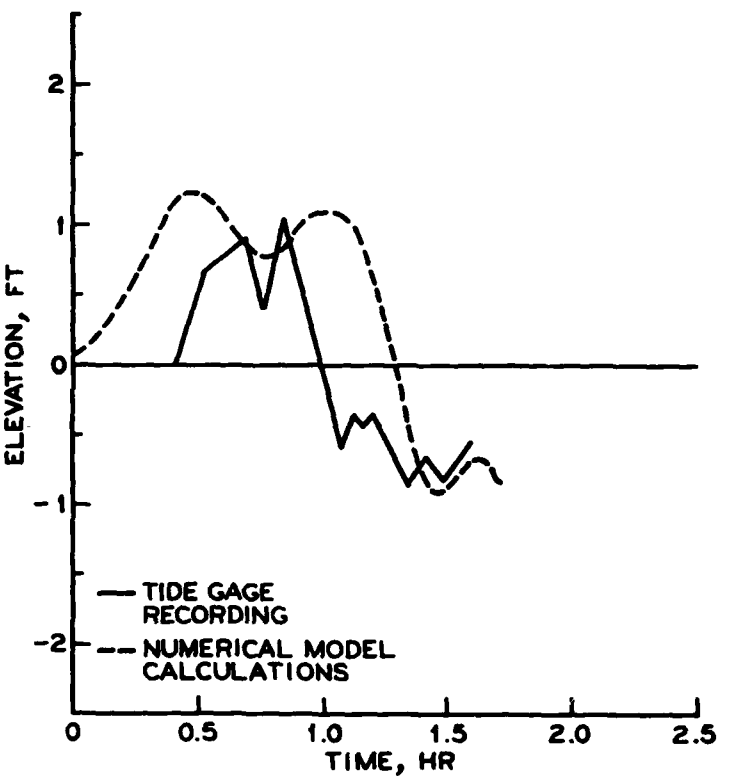

Figure 6. 1964 tsunami at San Diego, California

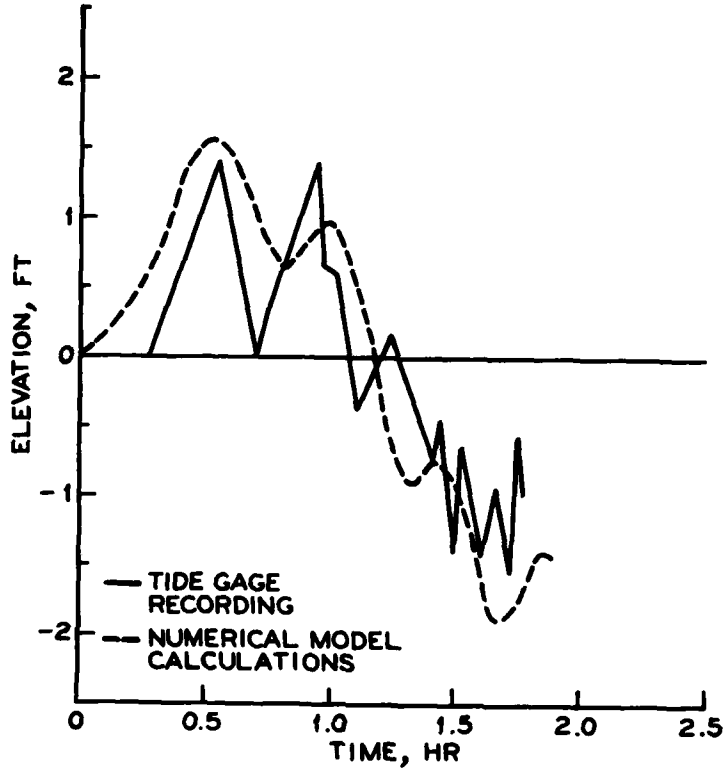

Figure 7. 1964 tsunami at Newport Bay, California

wave crest at Santa Monica, California, shown in Figure 2. However, the tide gage may have had response problems while recording this wave crest since the recording appears to be truncated and there are unusual high frequency oscillations in this truncated region of the wave form.

PART III: METHODOLOGY FOR ELEVATION PREDICTIONS

Tsunami Occurrence Probabilities

26. Historical data on tsunami generation must be the basis for an analysis that considers the probability of tsunami generation in the two tsunamigenic areas in the Pacific Ocean of concern to southern California--the Aleutian and Peru-Chile Trench areas. A satisfactory correlation between earthquake magnitude and tsunami intensity has never been demonstrated. Not all large earthquakes occurring in the ocean even generate noticeable tsunamis. Furthermore, earthquake parameters of importance to tsunami generation, such as focal depth and vertical ground motion, have only been measured for earthquakes occurring in recent years. Therefore, data on earthquake occurrence cannot be used to determine occurrence probabilities of tsunamis. Historical data of tsunami occurrence in generation regions must be used to determine these probabilities.

27. In South America, a wealth of information exists concerning tsunami occurrence. Reliable data (grouped in intensity increments of 0.5) exist for tsunamis with intensity greater than or equal to 0 for a 169-yr period and greater than or equal to 2.5 for a 417-yr period. The intensity scale used was a modification (by S. L. Soloviev of the Soviet Union) of the standard Imamura-Iida tsunami intensity scale. Intensity is defined as

$$i = \log_2 \left(\sqrt{2H_{avg}} \right)$$

This definition in terms of an average runup (in metres) over a coast instead of a maximum runup elevation at a single location (used for the standard Imamura-Iida scale) tends to eliminate a spurious intensity magnitude caused by often observed anomalous responses (due, for example, to local resonances) of single isolated locations.

28. Using the most recent and complete catalog of tsunami occurrence in the Pacific Ocean (Soloviev and Go 1969), a relation between

tsunami intensity and frequency of occurrence was determined for the tsunami-generating trench running the length of the Peru-Chile coast. Tsunamis with intensity greater than or equal to 0 were considered. It was assumed that the logarithm of the tsunami frequency of occurrence was linearly related to the tsunami intensity. Earthquake magnitude and frequency of occurrence have been similarly related by Gutenberg and Richter (1965) and used extensively in earthquake predictions. Soloviev (1970) has shown a similar relation between tsunami intensity and frequency of generation for moderate to large tsunamis throughout the Pacific Ocean. Furthermore, Wiegel (1965) found the same type of relation between tsunami occurrence and runup levels for historical tsunamis at Hilo, Hawaii; San Francisco, California; and Crescent City, California; and Adams (1970) for tsunamis at Kahuku Point, Oahu. A recent study by Rascon and Villarreal (1975) revealed this same relation for historical tsunamis on the west coast of Mexico (data from 1732) and on the Pacific west coast of North America, excluding Mexico.

29. Letting $n(i)$ equal the probability of a tsunami with an intensity i being generated during any given year and using statistics for the entire trench along the Peru-Chile coast, a least-squares analysis resulted in the following expression:

$$n(i) = 0.074e^{-0.63i} \qquad (1)$$

30. In using statistics for the entire trench area along the Peru-Chile coast, it was assumed that the probability of tsunami occurrence was uniform along the trench. This is a standard assumption for earthquake frequency analysis (Gutenberg and Richter 1965). The tectonic justification of this assumption lies in the fact that a single sialic block or plate of the earth's crust or lithosphere is dipping into the Peru-Chile Trench (Wilson 1969). It can be reasonably expected that the movement of this single plate is similar along its entire length.

31. In the Aleutian Trench area, only large tsunamis occurring in relatively recent years (since 1788) have been recorded due to the

isolation of the area. Assuming an exponential coefficient of -0.71 for this trench area (determined by Soloviev 1970) as a mean value for areas of the Pacific with the most data on tsunamis and using only the reliable data for large tsunamis (intensity greater than or equal to 3.5), the following relation was determined by a least-squares analysis:

$$n(i) = 0.113e^{-0.71i} \tag{2}$$

Again, the probability of tsunami occurrence was assumed to be uniform along the trench.

Use of Numerical Models

32. To relate the probability distribution of tsunami intensities to source characteristics, it was assumed that the ratio of the source uplift heights producing two tsunamis of different intensities (as defined in the previous section) is equal to the ratio of the average runup heights produced on the coasts near these tsunami sources. This ratio is equal to $2(i_1 - i_2)$ for two tsunamis with intensities i_1 and i_2.

33. If H_a is the wave height emitted in the direction parallel to the major axis of length a by a tsunami source with an elliptical shape (large tsunamis have historically had elliptically shaped uplifts) and H_b is the wave height emitted in the direction parallel to the minor generation axis of length b, then experimental research of tsunami generation has shown that $H_b/H_a \approx a/b$ (Hatori 1963). For a large tsunami, H_b can be larger than H_a by a factor of as much as 5 or 6. Thus, the orientation of the tsunami source relative to the area where elevations are to be determined is very important; that is, the elevation at a distant site due to the generation of a tsunami at one location along a trench cannot be considered as being representative of all possible placements of the tsunami source in the entire trench region. Hence, the Aleutian and Peru-Chile Trenches had to be segmented and elevations along the coast of southern California determined for

tsunami sources located at the center of each of the segments.

34. The spatial size of a tsunami source was standardized because there is not an apparent correlation between tsunami intensity and spatial size of a tsunami source. For example, the 1946 Aleutian tsunami had an uplift region of very small spatial extent, whereas the 1957 Aleutian tsunami had an uplift region that covered perhaps the greatest spatial extent of any known earthquake (Kelleher et al. 1974); yet the 1946 tsunami had the greater tsunami intensity, producing, in general, greater runup elevations in the near and distant regions.

35. The standard source employed (described in Houston and Garcia 1974), represents a large tsunami with intensity 4 on the modified Imamura-Iida scale. Certainly, tsunamis of low intensity may have smaller spatial extents; however, large tsunamis pose the greatest threat to a distant area such as southern California. These large tsunamis can be expected to have similar spatial extents, with any spatial differences being unimportant in the far field compared with the effects of source orientation and vertical uplift.

36. Figures 8 and 9 show the Aleutian Trench divided into 12 segments and the Peru-Chile Trench into 3 segments. The segments in the Aleutian Trench were approximately one-quarter the length of the major axis of the standard source, whereas the segments in the Peru-Chile Trench were approximately the length of the major axis of the standard source. The standard source was centered in each segment such that the major axis of the source was parallel to the trench axis. Uplift regions historically have had such an orientation relative to trench systems. The Aleutian Trench was segmented much finer than the Peru-Chile Trench because the Aleutian Trench is oriented relative to southern California such that elevations produced in southern California are very sensitive (Houston et al. 1975) to the location of a source along the trench. Uplifts along the Peru-Chile Trench do not radiate energy directly toward southern California regardless of their position along the trench. Therefore elevations in southern California are not very sensitive (Garcia 1976) to source location within these sections.

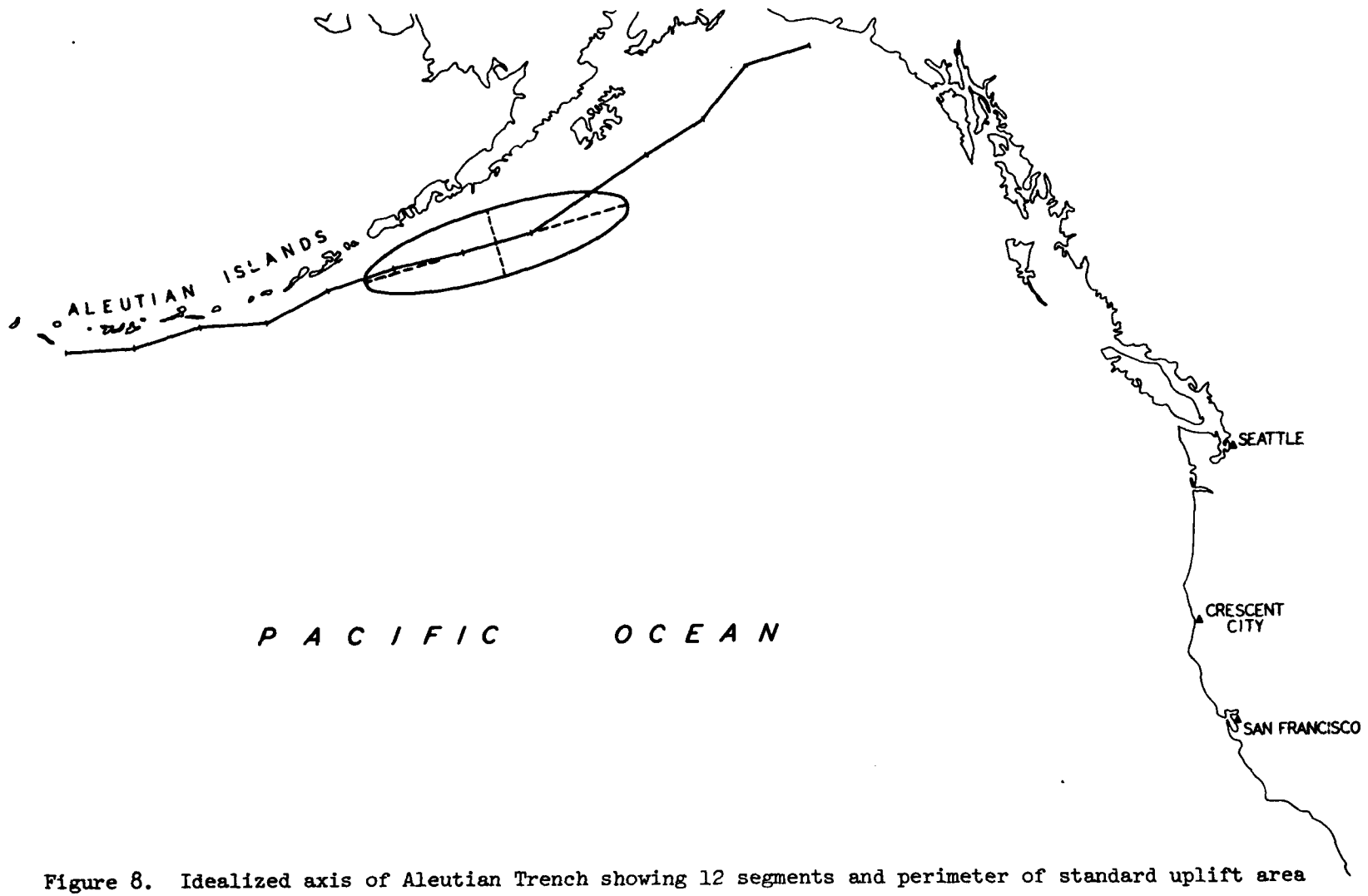

Figure 8. Idealized axis of Aleutian Trench showing 12 segments and perimeter of standard uplift area

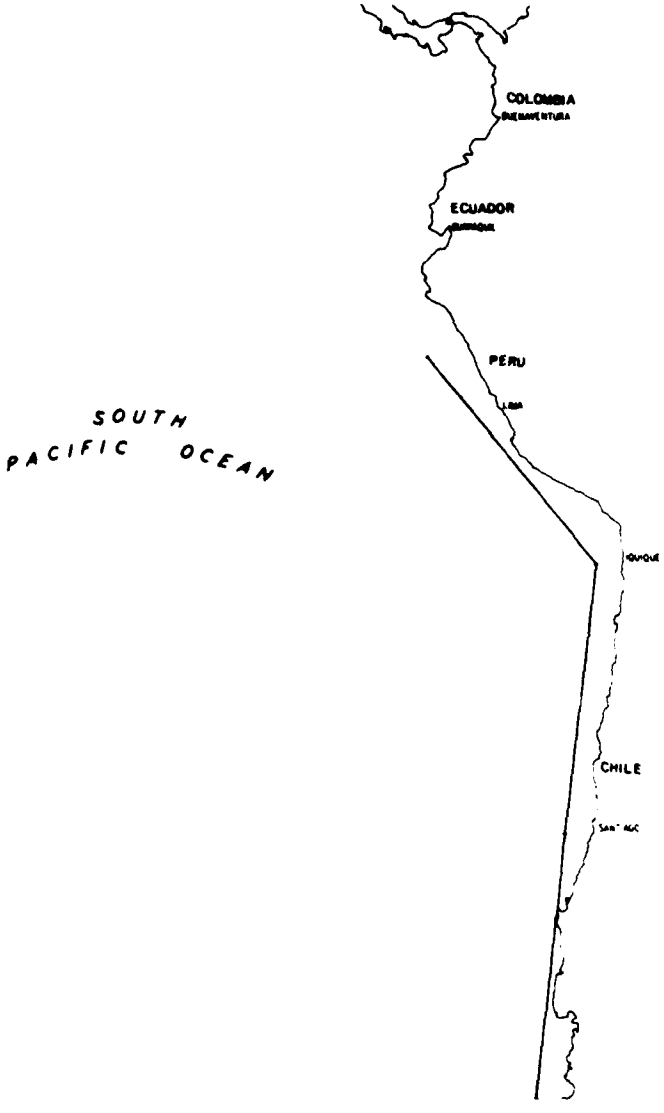

Figure 9. Idealized axis of Peru-Chile Trench showing 3 segments

37. In each of the segments of the Aleutian and Peru-Chile Trenches, tsunamis with intensities from 2.5 to 4.5 in increments of 0.5 were generated and propagated across the deep ocean using the deep-ocean numerical model discussed in an earlier section. Tsunamis with intensities less than 2.5 are too small to produce significant elevations in southern California. An upper limit of 4.5 was chosen because the largest tsunami intensity ever reported was less than 4.5 (Soloviev and Go 1969). Gutenburg and Richter (1965) indicate that there is an upper limit to the strain which can be supported by rock before fracture. Thus, earthquakes only reach certain maximum magnitudes and tsunamis can be expected to have analogous upper limits of intensity. Perkins (1972) and McGarr (1976) have demonstrated that future earthquakes cannot have seismic moments (measure of earthquake magnitude for large earthquakes) much larger than those of earthquakes that occurred in recorded history.

38. The wave forms propagated to southern California by the deep-ocean propagation numerical model were used as input to the nearshore propagation numerical model. Each wave form was propagated from a water depth of 500 m to shore using the nearshore model. Thus, at each grid location on the shoreline of the west coast, there was a group of 75 wave forms--5 wave forms (for intensities from 2.5 to 4.5 in increments of 0.5) for each segment of the Aleutian and Peru-Chile Trenches. Each of these wave forms had an associated probability equal to the probability that a certain intensity tsunami would be generated in a particular segment of a trench region.

Effect of Astronomical Tides

39. The maximum "still water" elevation produced during tsunami activity is the result of a superposition of tsunami and astronomical tide wave forms. Therefore, the statistical effect of astronomical tides on total tsunami runup must be included in the predictive scheme presented in this report. Since the wave forms calculated by the

near-shore model did not have a simple form (e.g., sinusoidal), the statistical effect of the astronomical tide on tsunami runup had to be determined through a numerical approach.

40. The wave forms calculated by the nearshore numerical model extended over a period of time of approximately 2 hr. One to three wave crests (the largest waves in the tsunami) arrived during this time. Smaller waves arriving at later times, however, have often persisted for days during historical tsunamis. An analysis of tide gage records of the 1960 and 1964 tsunamis in southern California indicated that these smaller waves have amplitudes on the average of 50 percent of the maximum wave amplitude of the tsunami; therefore a sinusoidal group of these small waves was added to each of the calculated wave forms so that the total wave form extended over a 12-hr period. These smaller waves are important for locations where tsunami waves are fairly small compared with tidal variations. At such locations, the maximum combined tsunami and astronomical elevation occurs during the maximum tidal elevation.

41. A computer program was developed to predict time-histories of the astronomical tides in southern California. The program was based upon the harmonic analysis methods used in the past by the National Ocean Survey for mechanical tide-predicting machines (Schureman 1948). Tidal constants available from the National Ocean Survey were used as input to the computer program. A year of tidal elevations was then predicted for grid locations in southern California. The year 1964 was selected because all the major tidal components for tides in southern California had a node factor of approximately 1.00 during this year, thus making it an average year. The node factor is associated with the revolution of the moon's node and has an 18.6-yr cycle. Since a tsunami can arrive at any time during this 18.6-yr period (arrival at a low of the node factor is equally likely as an arrival at a high), the statistical effect of the temporally varying node factor on the predicted runup elevations is shown to be very small in Appendix A of this report.

43. The many maximum elevations with associated probabilities were used to determine exceedance frequency distributions of combined

tsunami and astronomical tide elevations. The maximum elevations were ordered and frequencies summed, starting with the largest elevations, until a desired frequency was obtained. The elevation encountered when the summed frequency reached a desired value F was the elevation that is equaled or exceeded with an average frequency of once every 1/F yr. Thus, when the summed frequencies reached the value 0.01, the elevation associated with the last frequency summed was the 100-yr elevation.

PART IV: RESULTS

Explanation

44. Figures 10-23 present predicted 100- and 500-yr elevations (in feet) in southern California produced by distantly generated tsunamis. These elevations include the effects of the astronomical tide; that is, they are maximum elevations due to the superposition of tsunami and tidal wave forms (see PART III). The lower curves in Figures 10-23 represent the 100-yr elevation and the upper curves, the 500-yr elevation. A 100-yr elevation is one that is equaled or exceeded with an average frequency of once every 100 yr (i.e. 100-yr return period); a 500-yr elevation has a corresponding definition. Elevations in this report are referenced to the mean sea level (msl) datum.

45. The elevations presented in Figures 10-23 extend along more than 200 miles of coastline in southern California from Santa Barbara to San Diego. Similar elevations north and west of Santa Barbara are presented in an earlier report (Houston and Garcia 1978). Calculations were made at 240 locations (presented in Figures 24-31) along this coastline. The latitude and longitude of each of these gage locations are presented in Table 1. The elevations calculated at each gage location are connected by straight lines in Figures 10-23.

46. Plates 1-120 present exceedance distributions at all 240 gage locations. The y-axis of the plots presents tsunami frequency in events per year. Tsunami frequency is the inverse of the tsunami return period. Thus the 100-yr tsunami has a frequency of 0.01 events per year and the 500-yr tsunami a frequency of 0.002 events per year. The tsunami frequency is presented in Plates 1-120 on a logarithmic scale. Each tick mark from a frequency of 0.001 to 0.01 represents an increment of 0.001. Each tick mark from a frequency of 0.01 to 0.1 represents an increment of 0.01. Figure 32 illustrates how to determine 100- and 500-yr elevations using an exceedance frequency distribution.

47. The tsunami elevations presented in Figures 10-23 and Plates 1-120 are elevations at the shoreline. As discussed by Houston

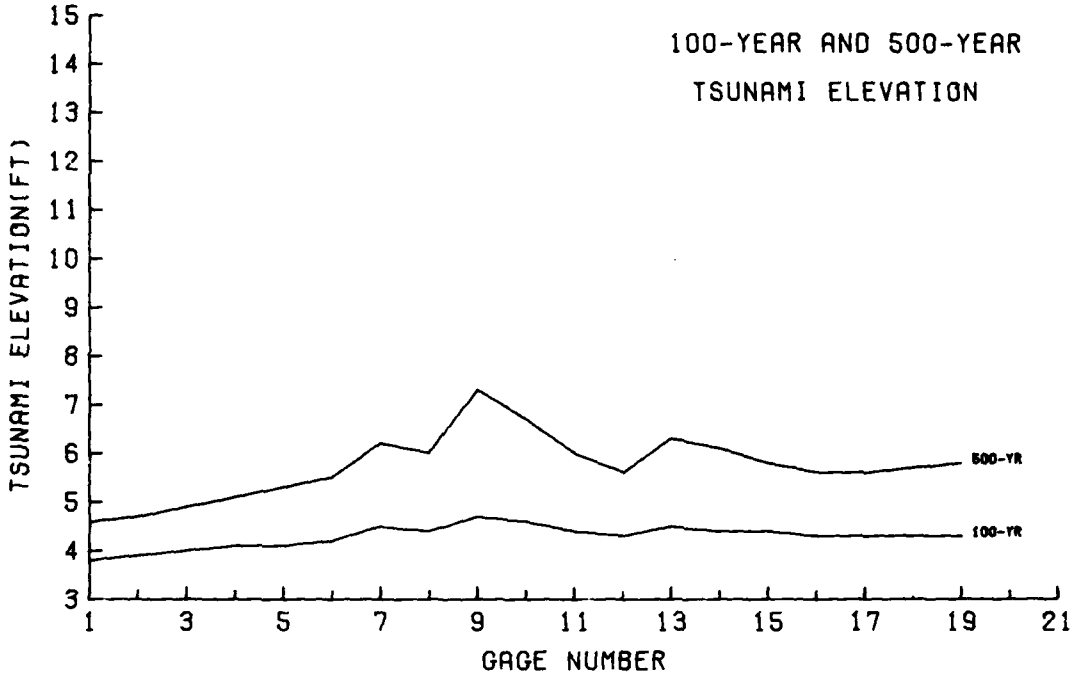

Figure 10. Gage numbers 1-19

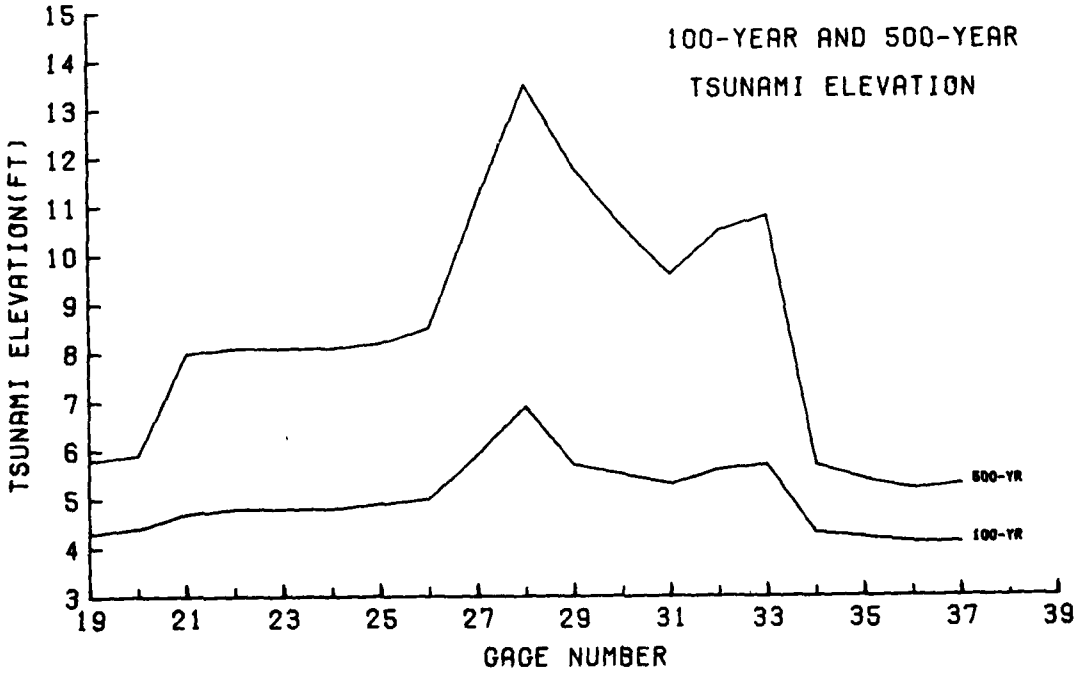

Figure 11. Gage numbers 19-37

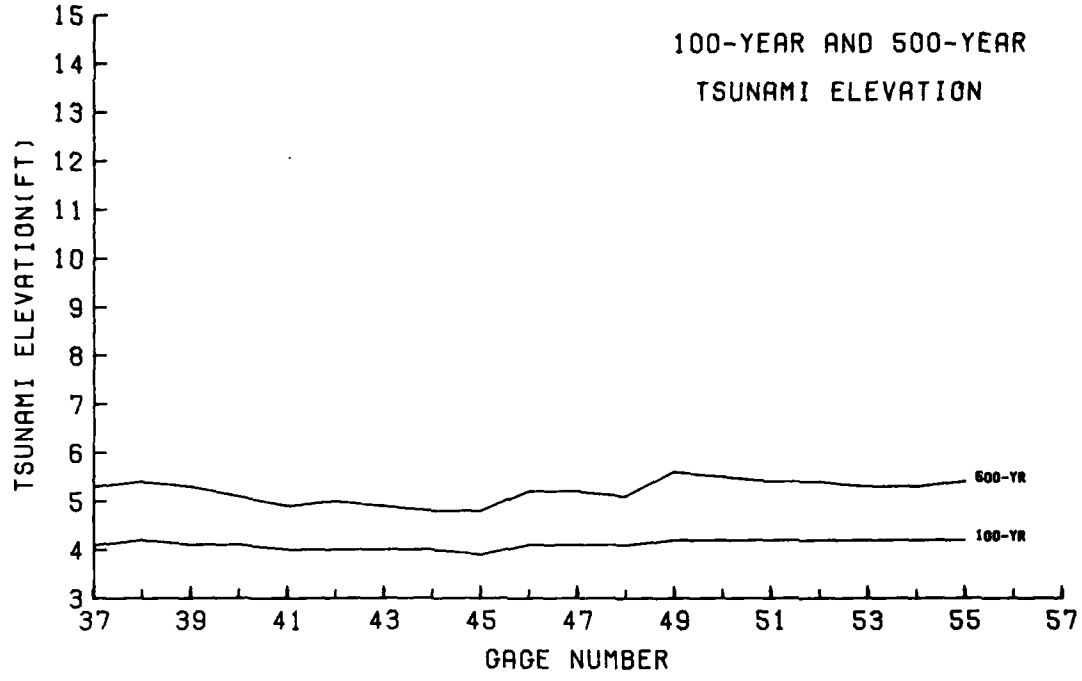

Figure 12. Gage numbers 37-55

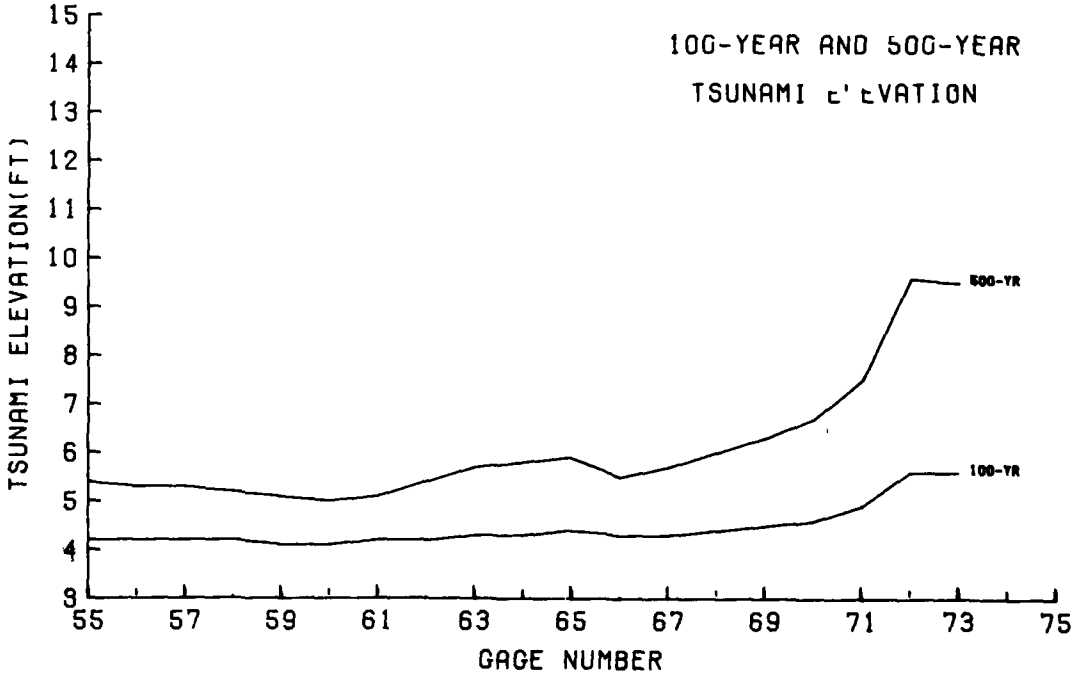

Figure 13. Gage numbers 55-73

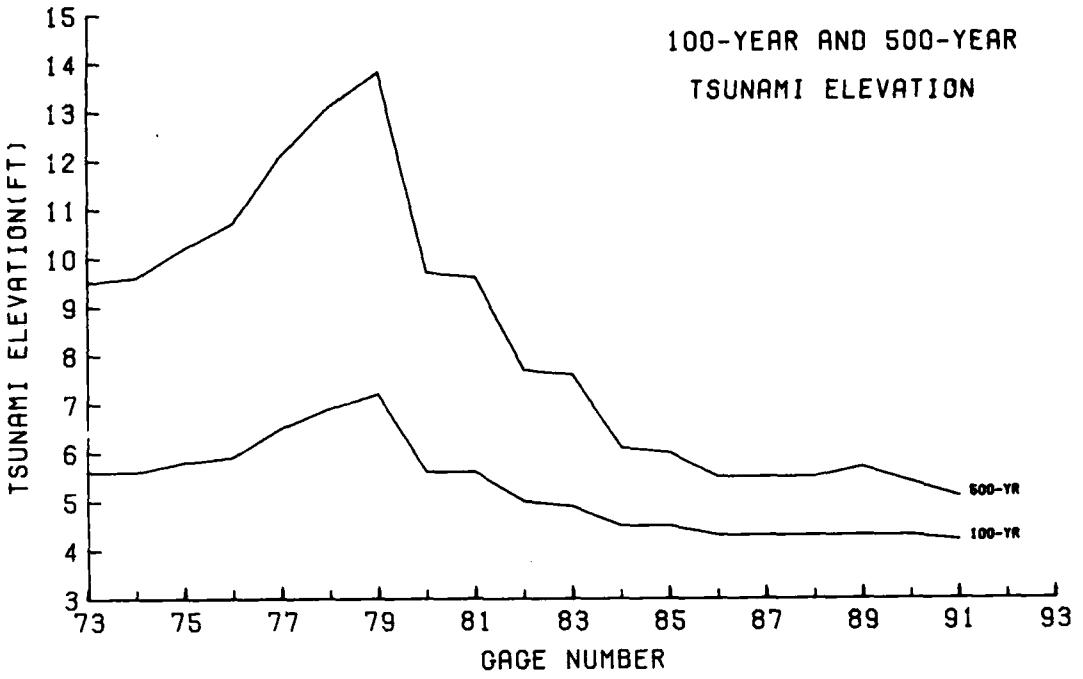

Figure 14. Gage numbers 73-91

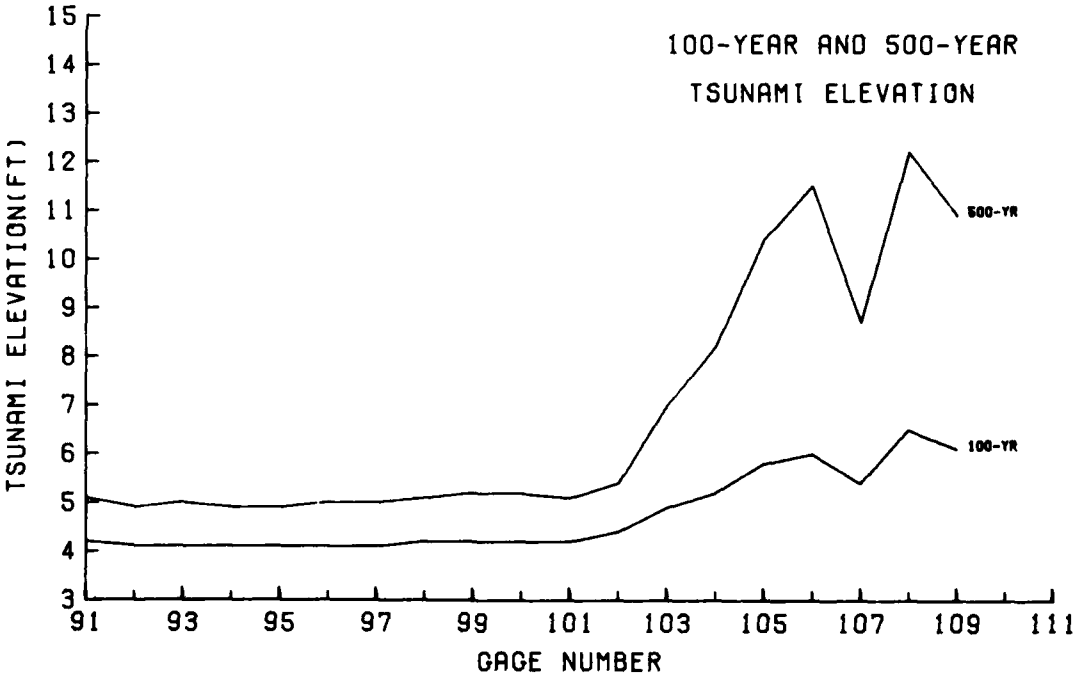

Figure 15. Gage numbers 91-109

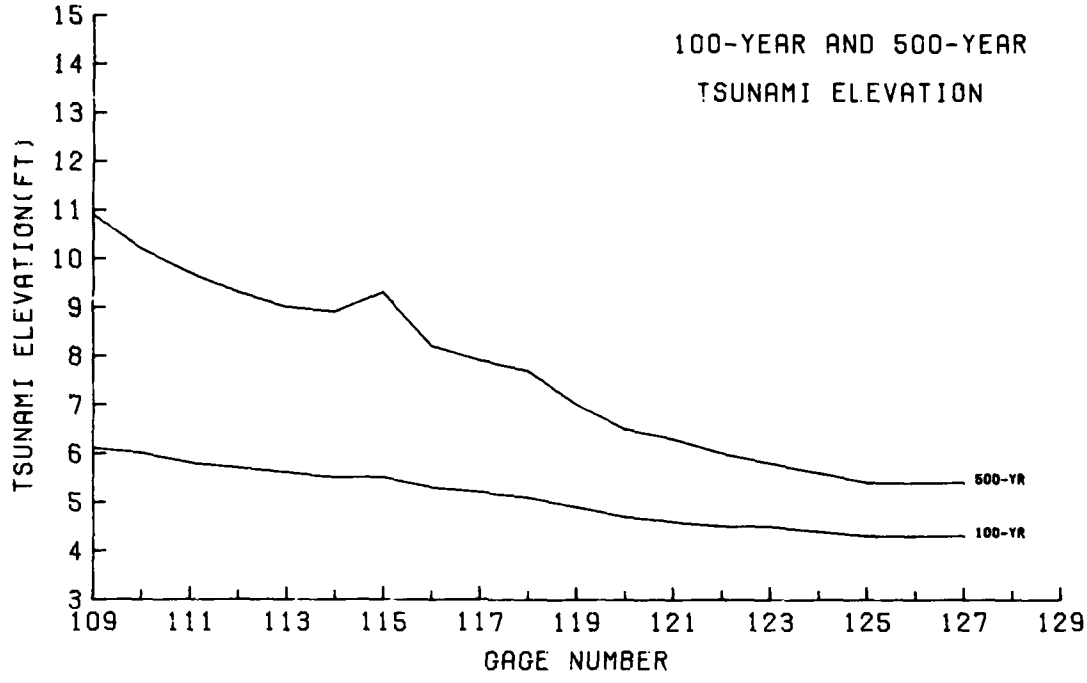

Figure 16. Gage numbers 109-127

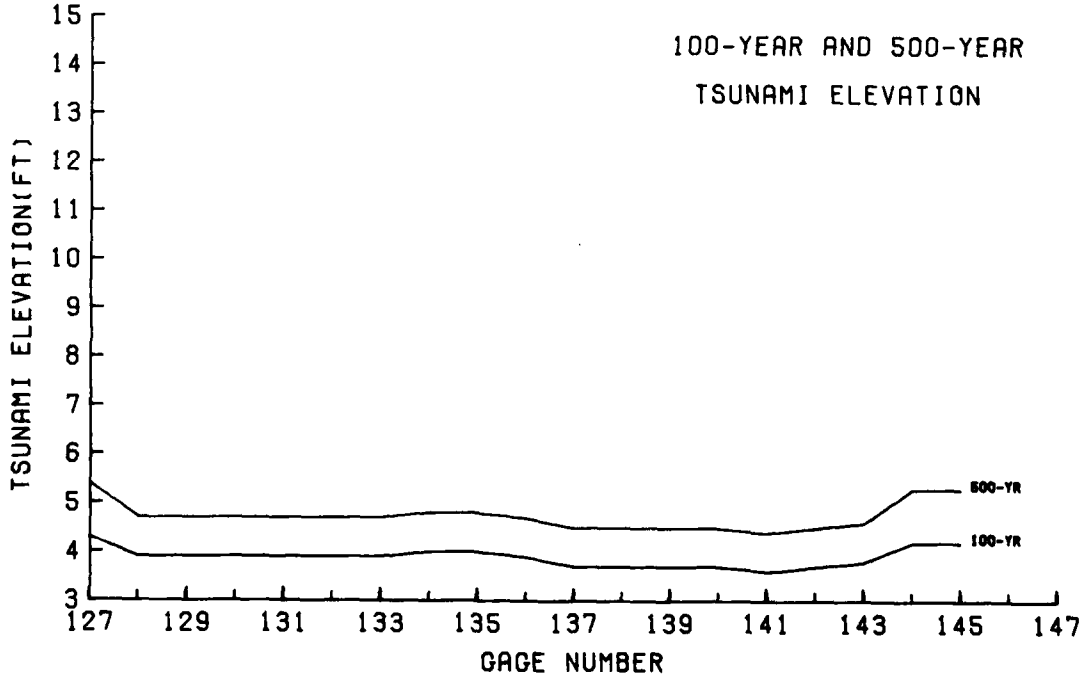

Figure 17. Gage numbers 127-145

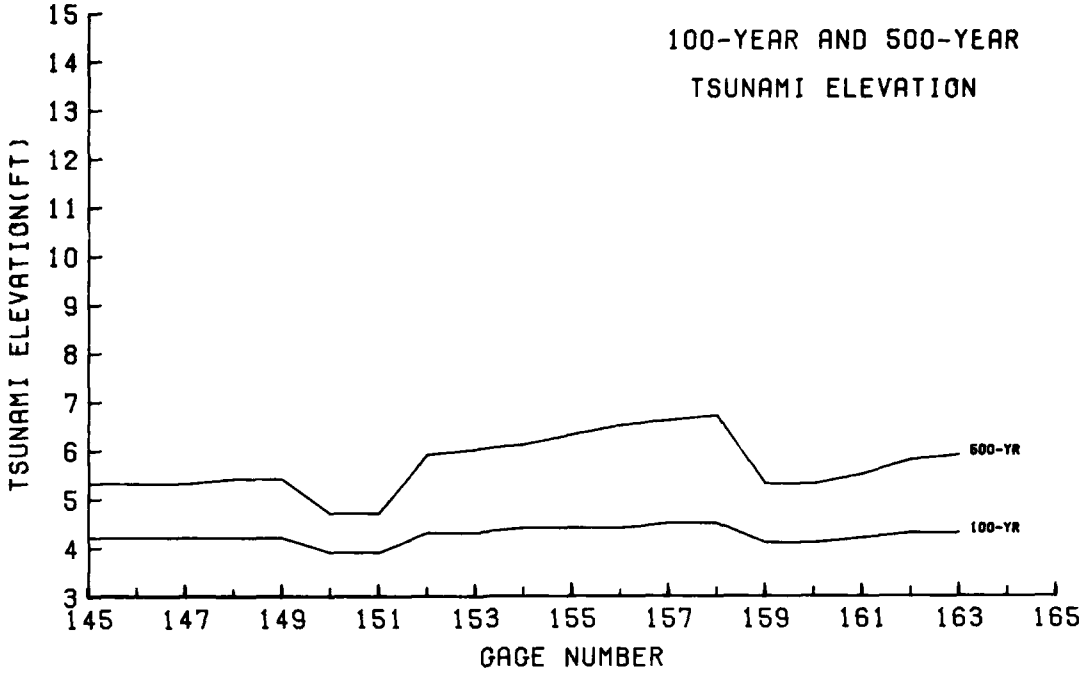

Figure 18. Gage numbers 145-163

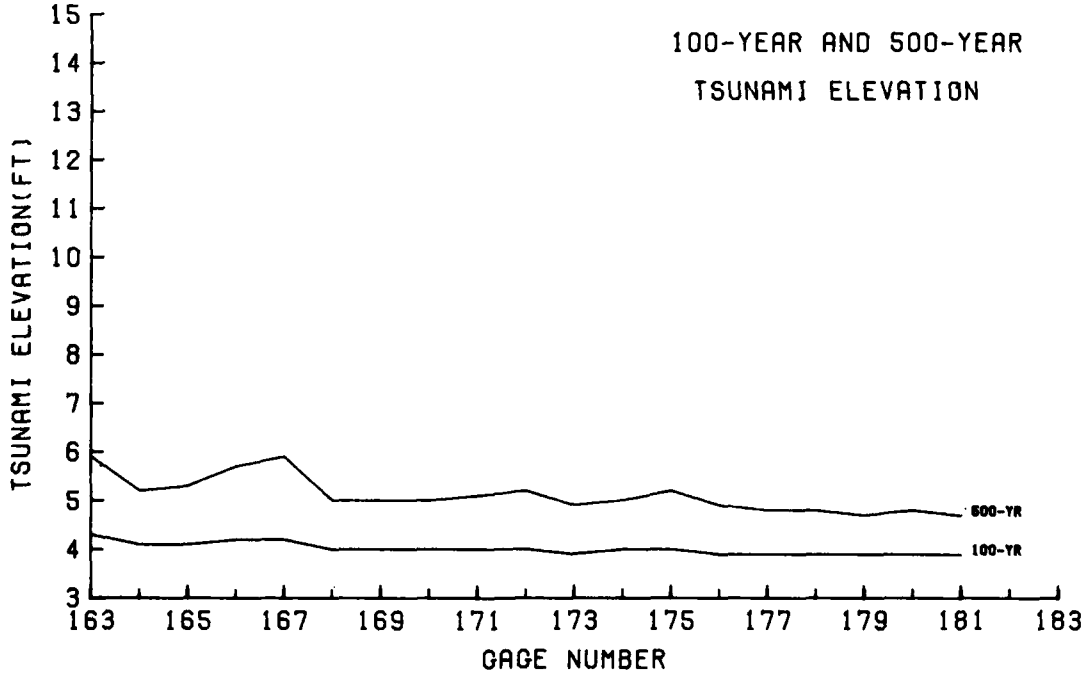

Figure 19. Gage numbers 163-181

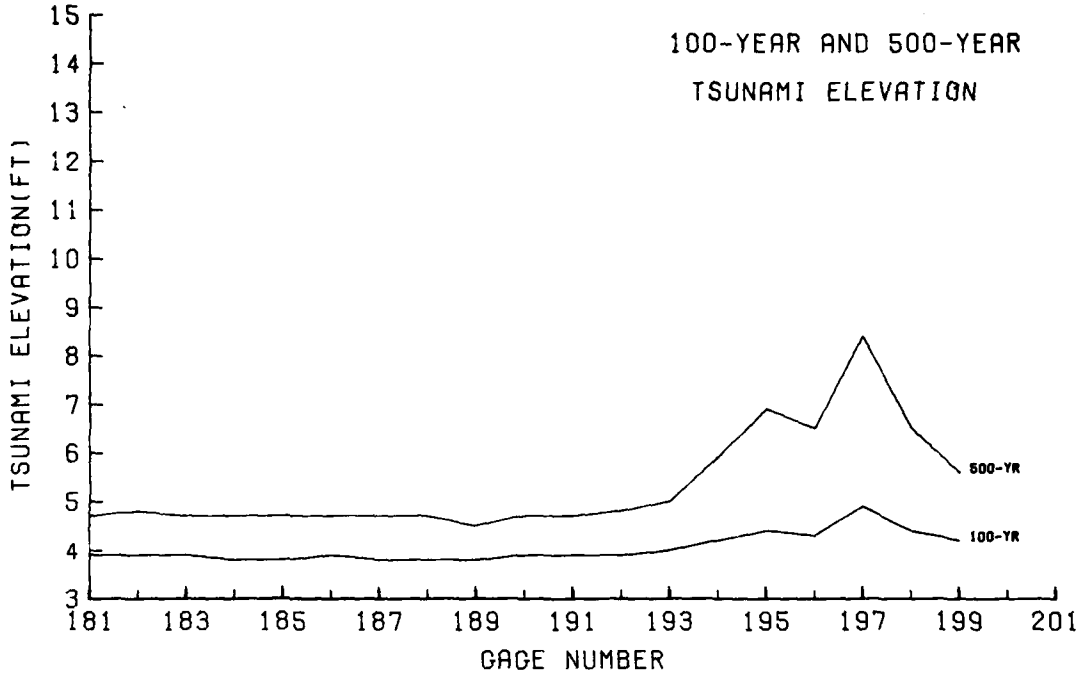

Figure 20. Gage numbers 181-199

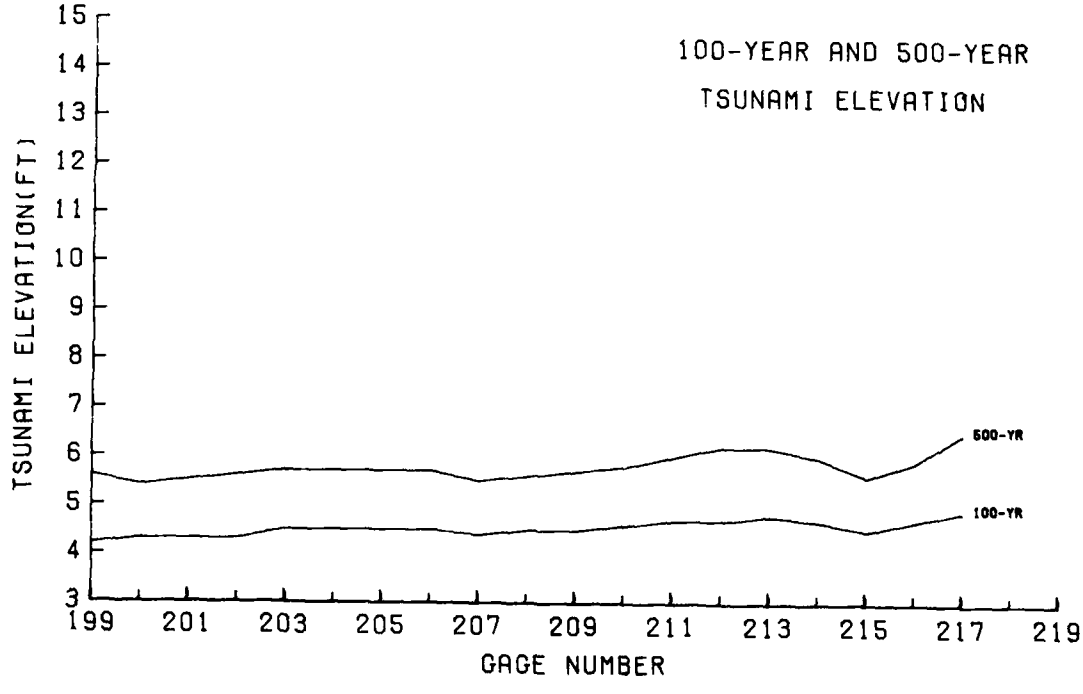

Figure 21. Gage numbers 199-217

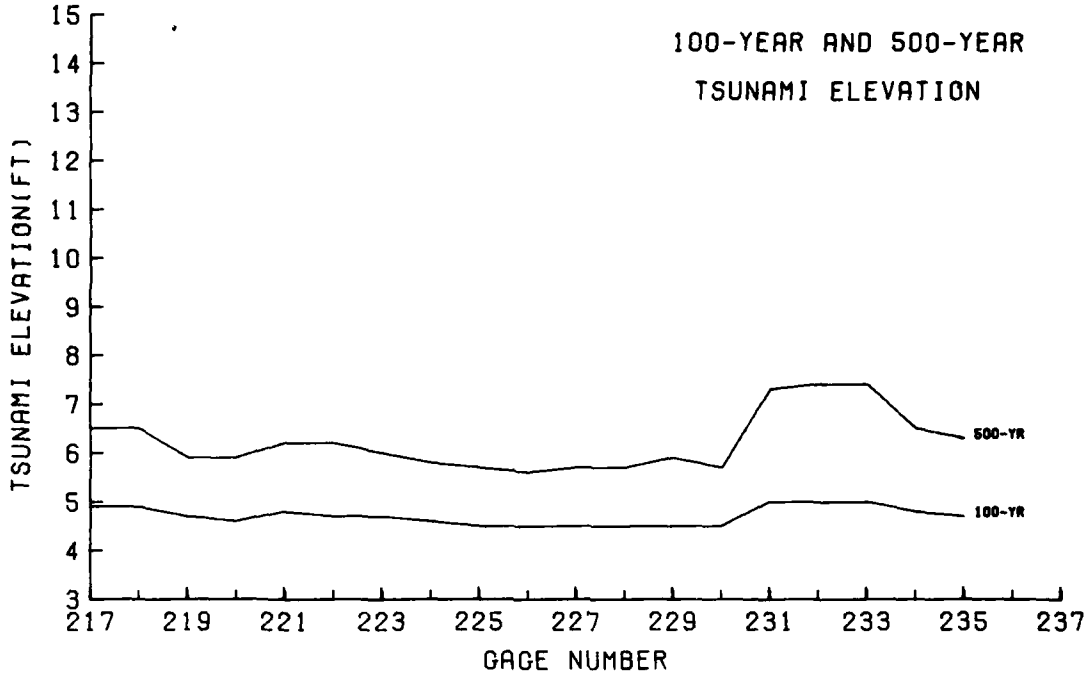

Figure 22. Gage numbers 217-235

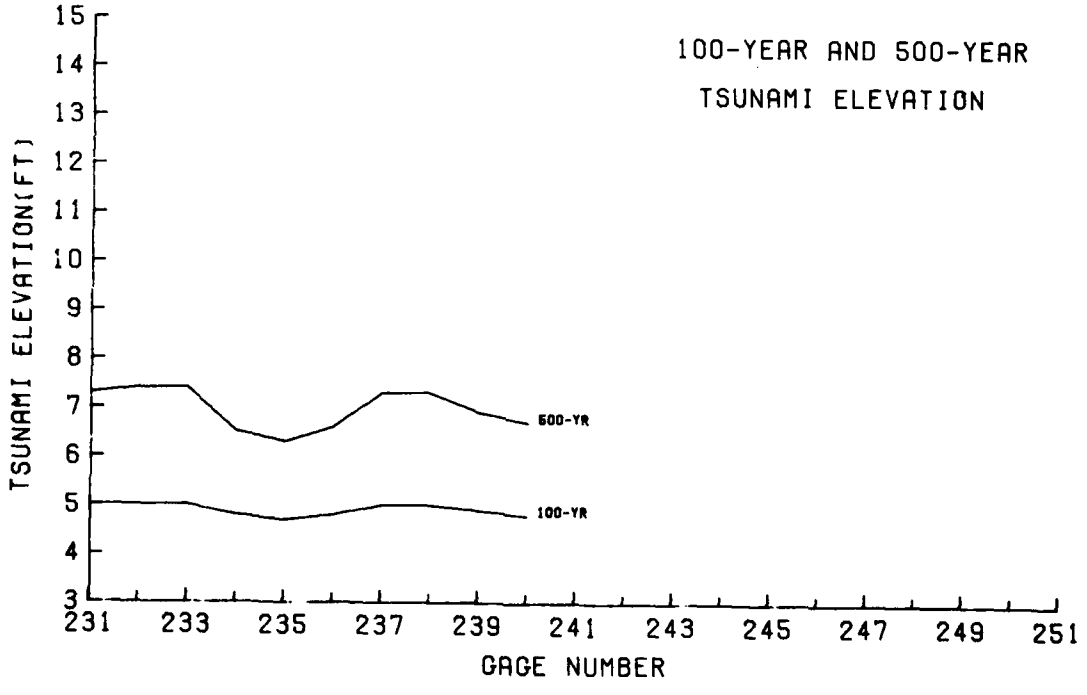

Figure 23. Gage numbers 231-240

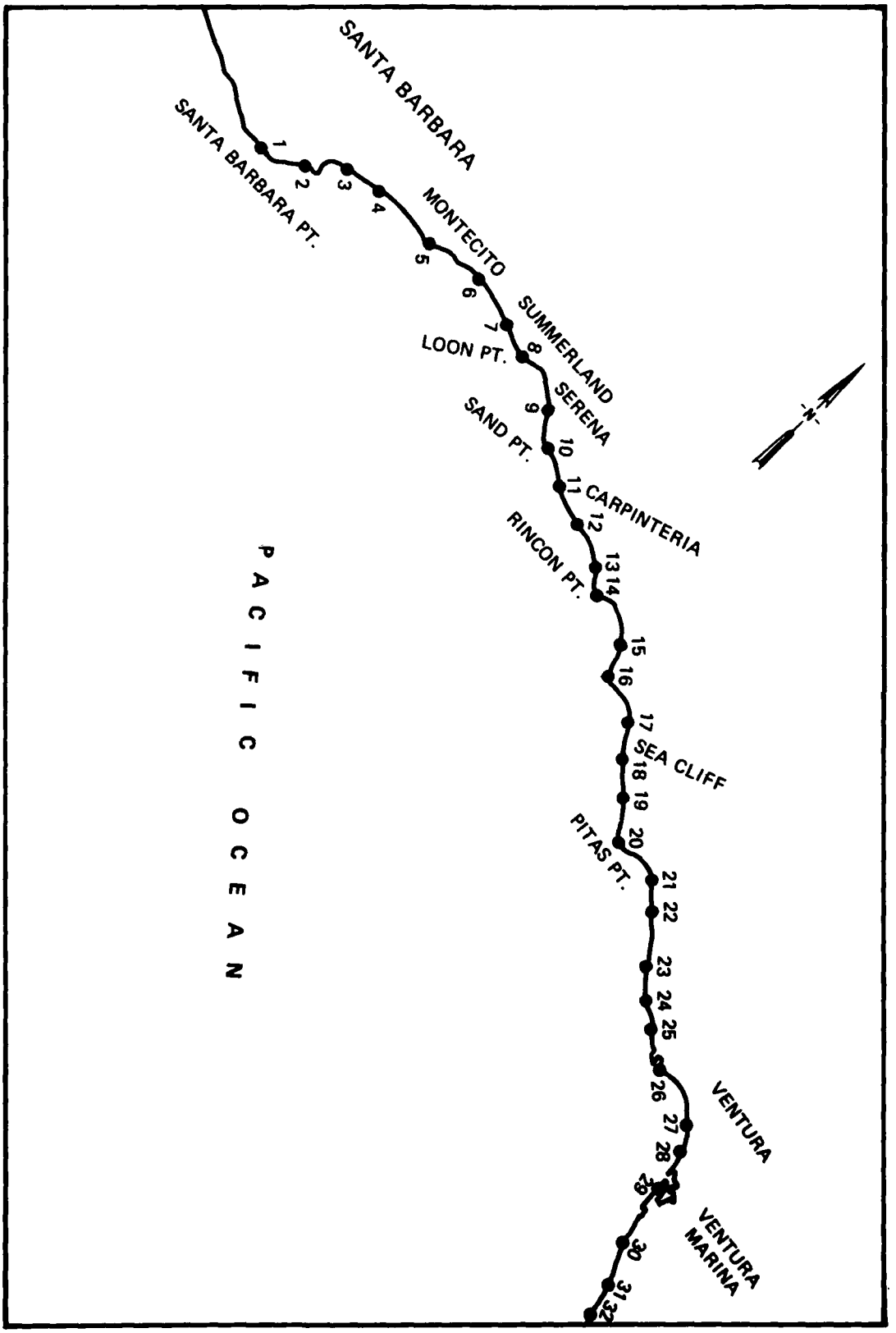

Figure 24. Gage locations 1-32

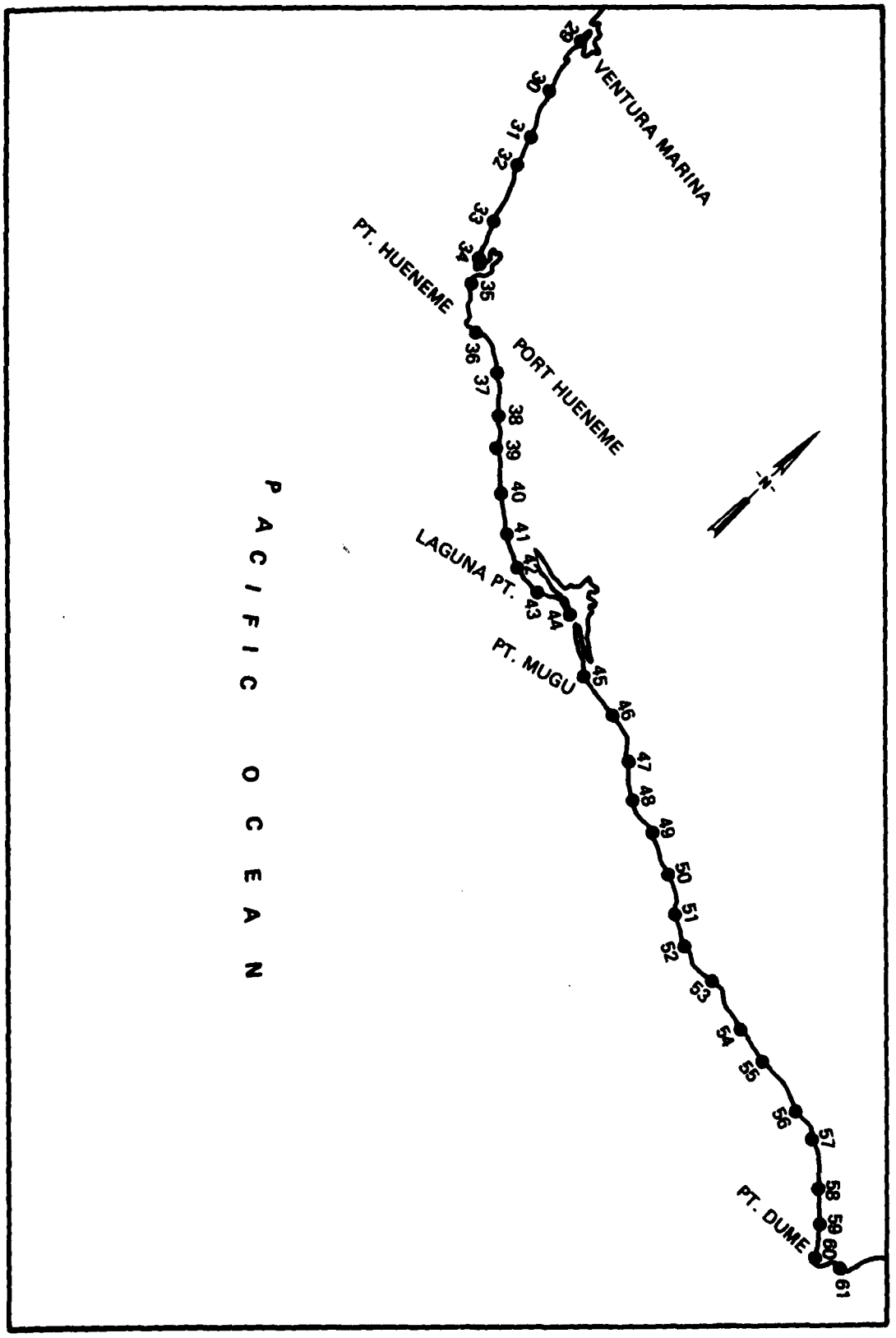

Figure 25. Gage locations 29-61

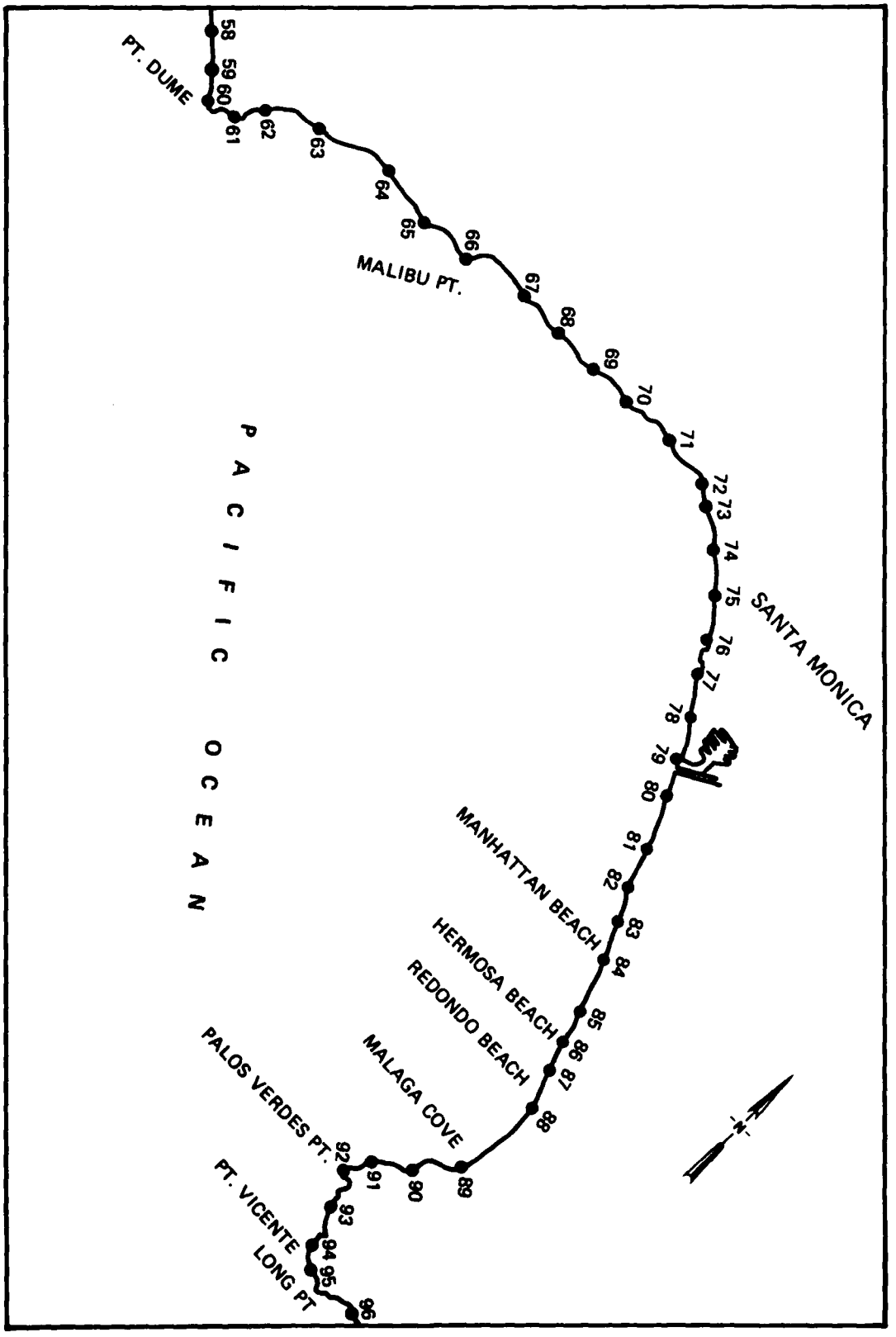

Figure 26. Gage locations 58-96

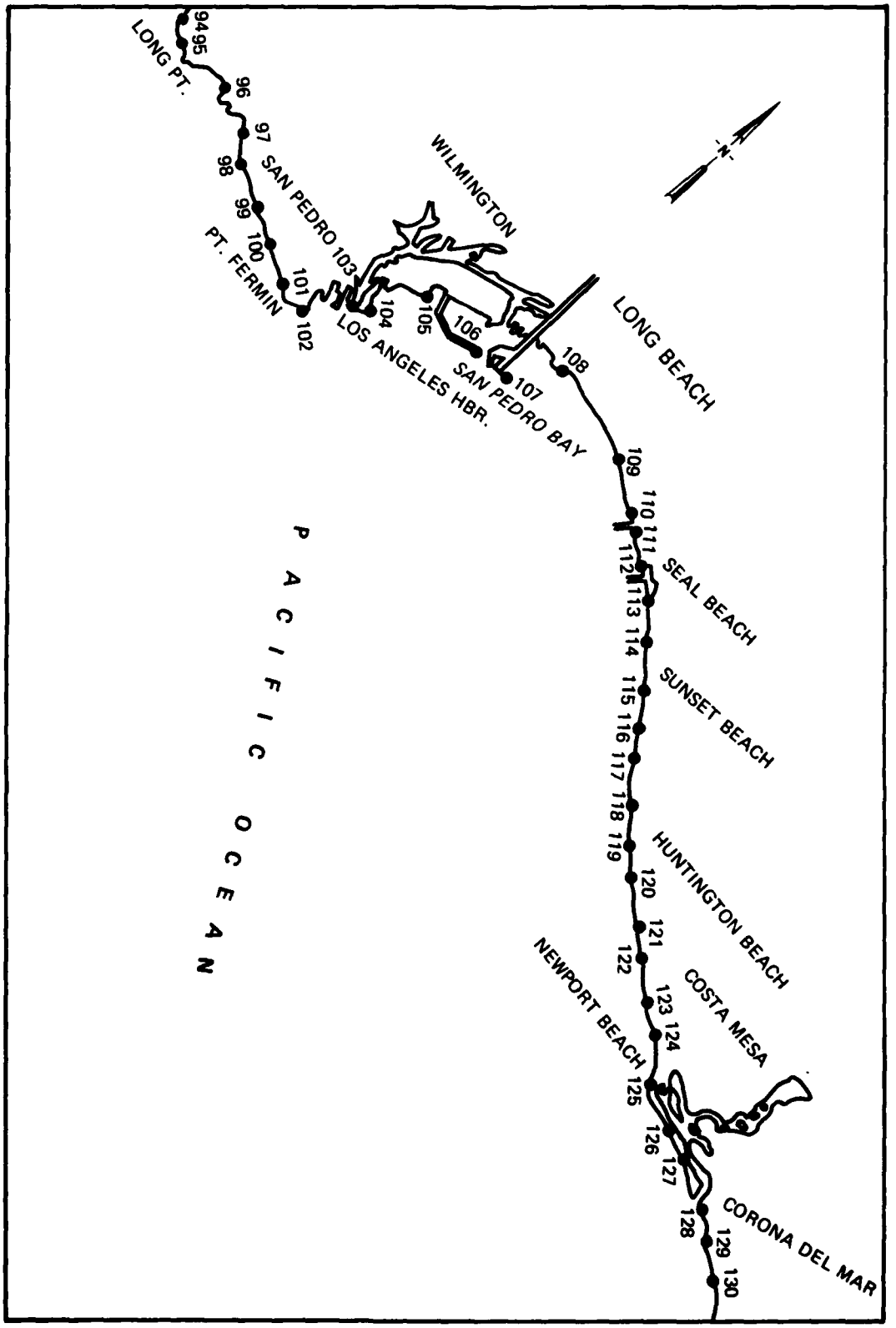

Figure 27. Gage locations 94-130

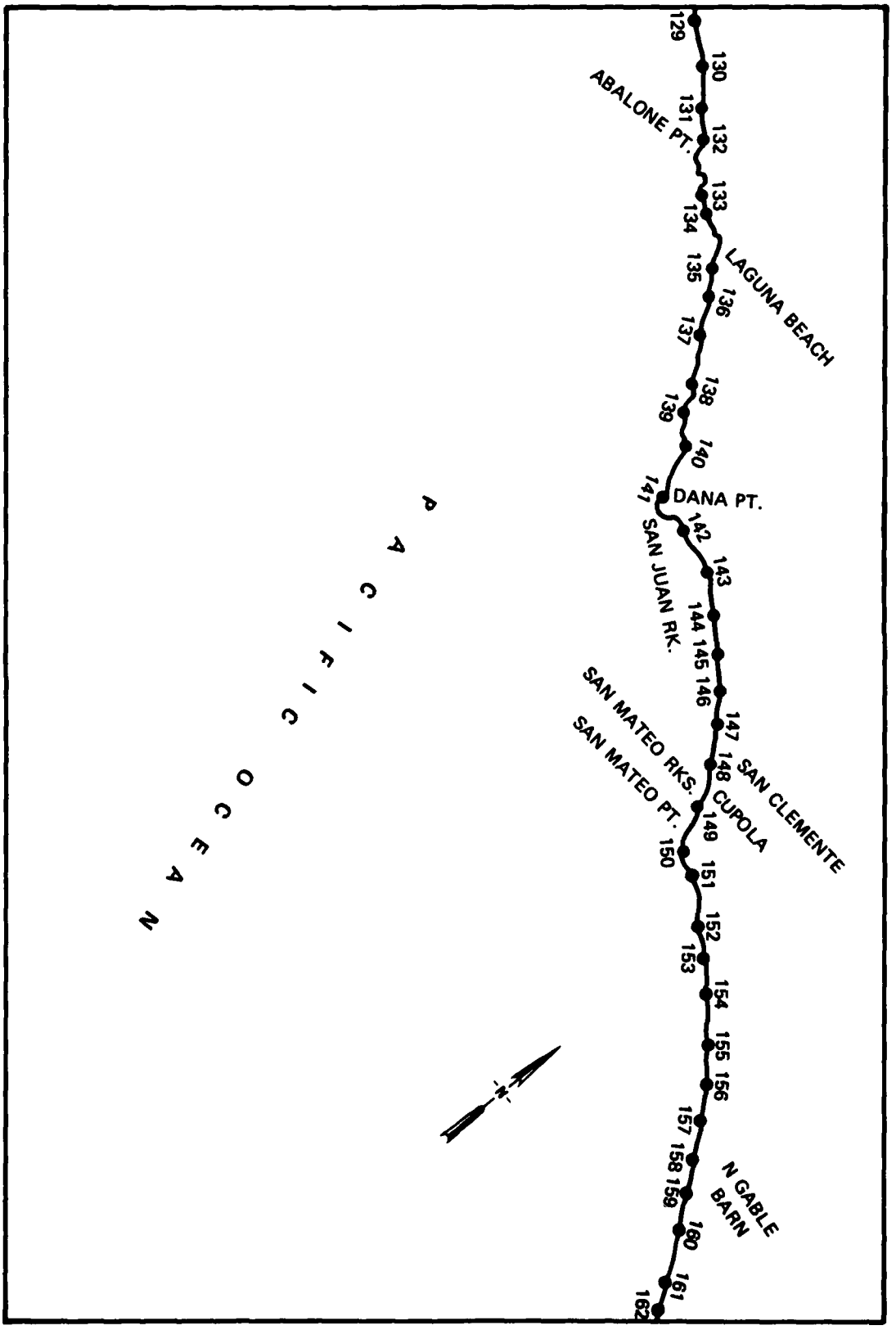

Figure 28. Gage locations 129-162

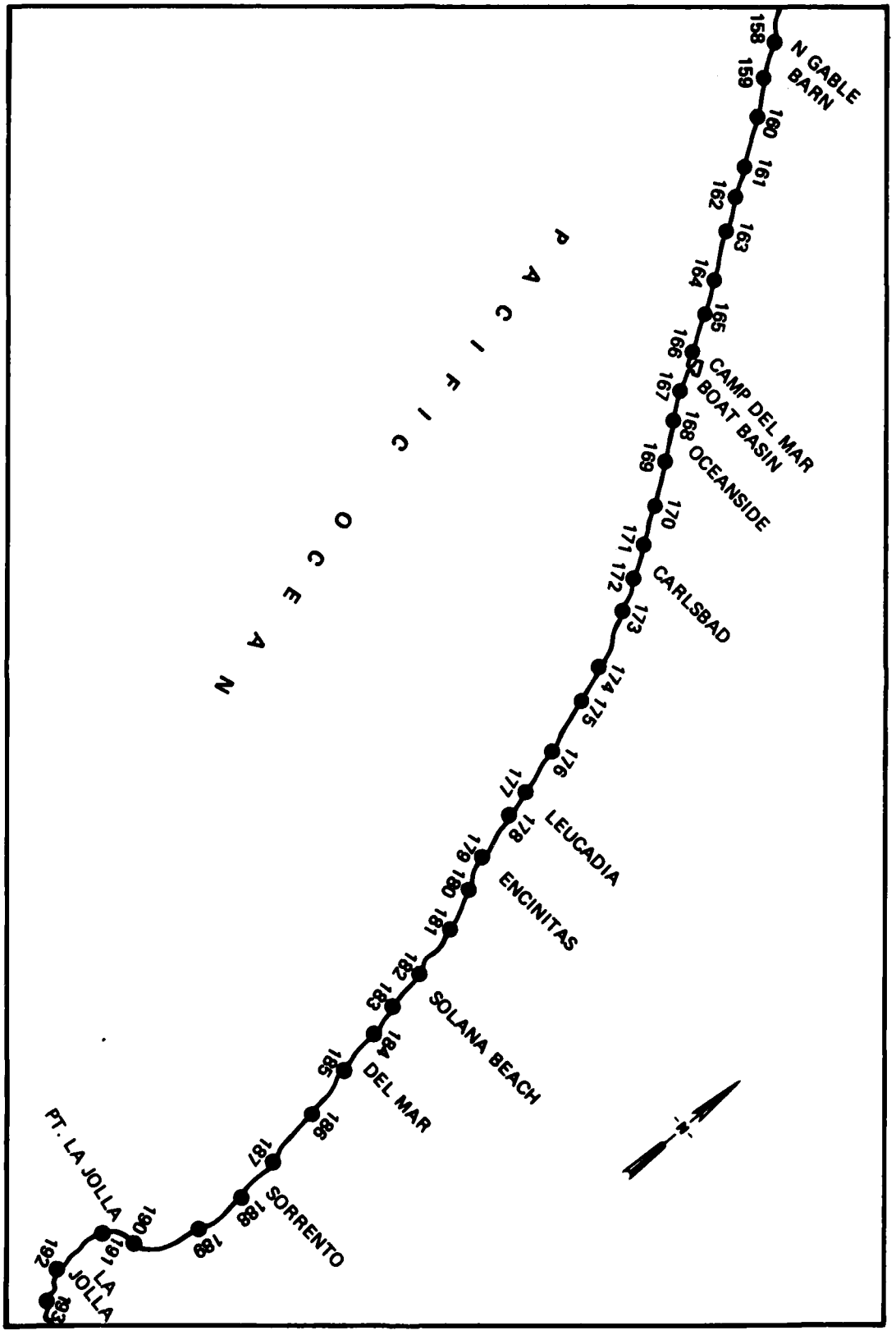

Figure 29. Gage locations 158-193

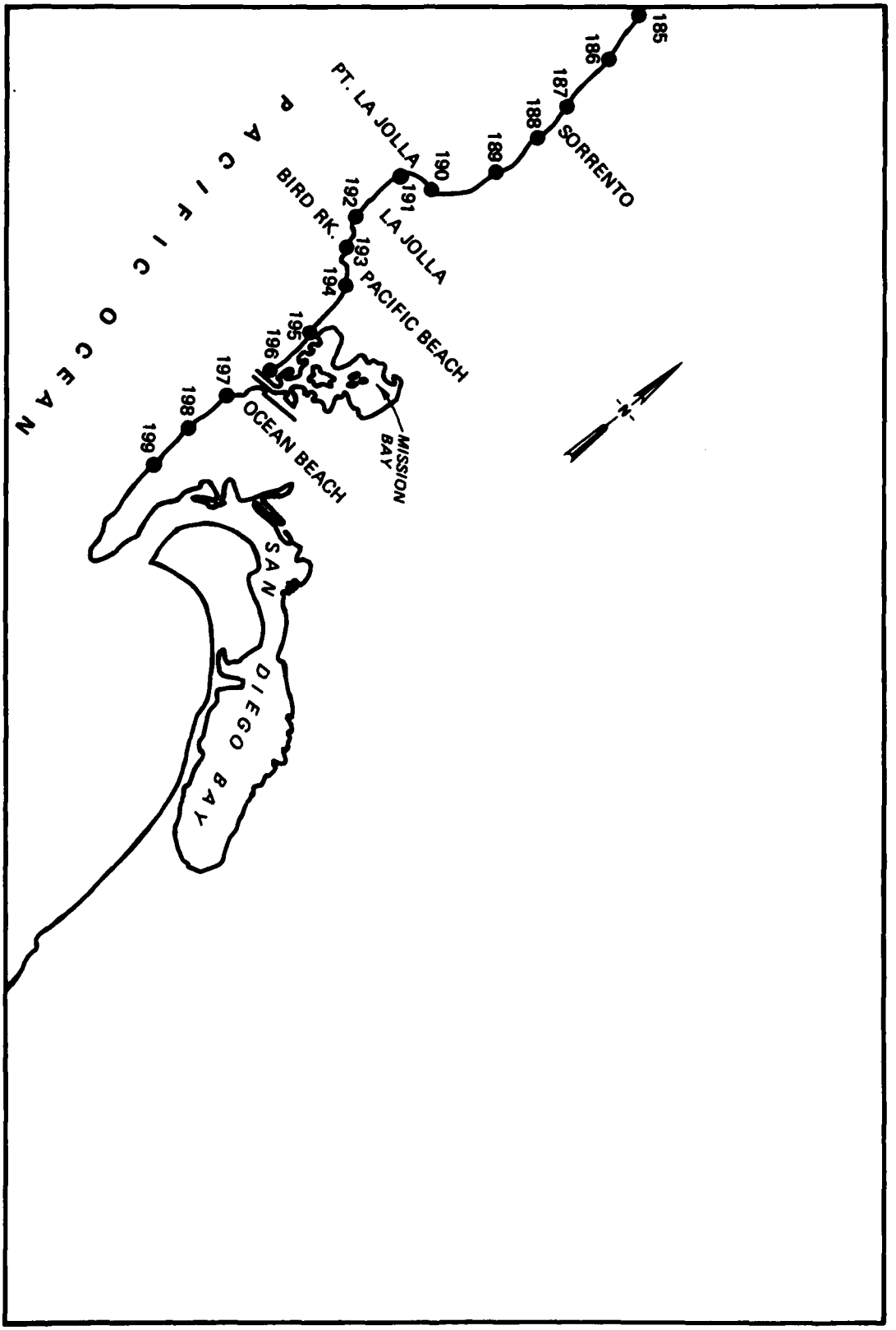

Figure 30. Gage locations 185-199

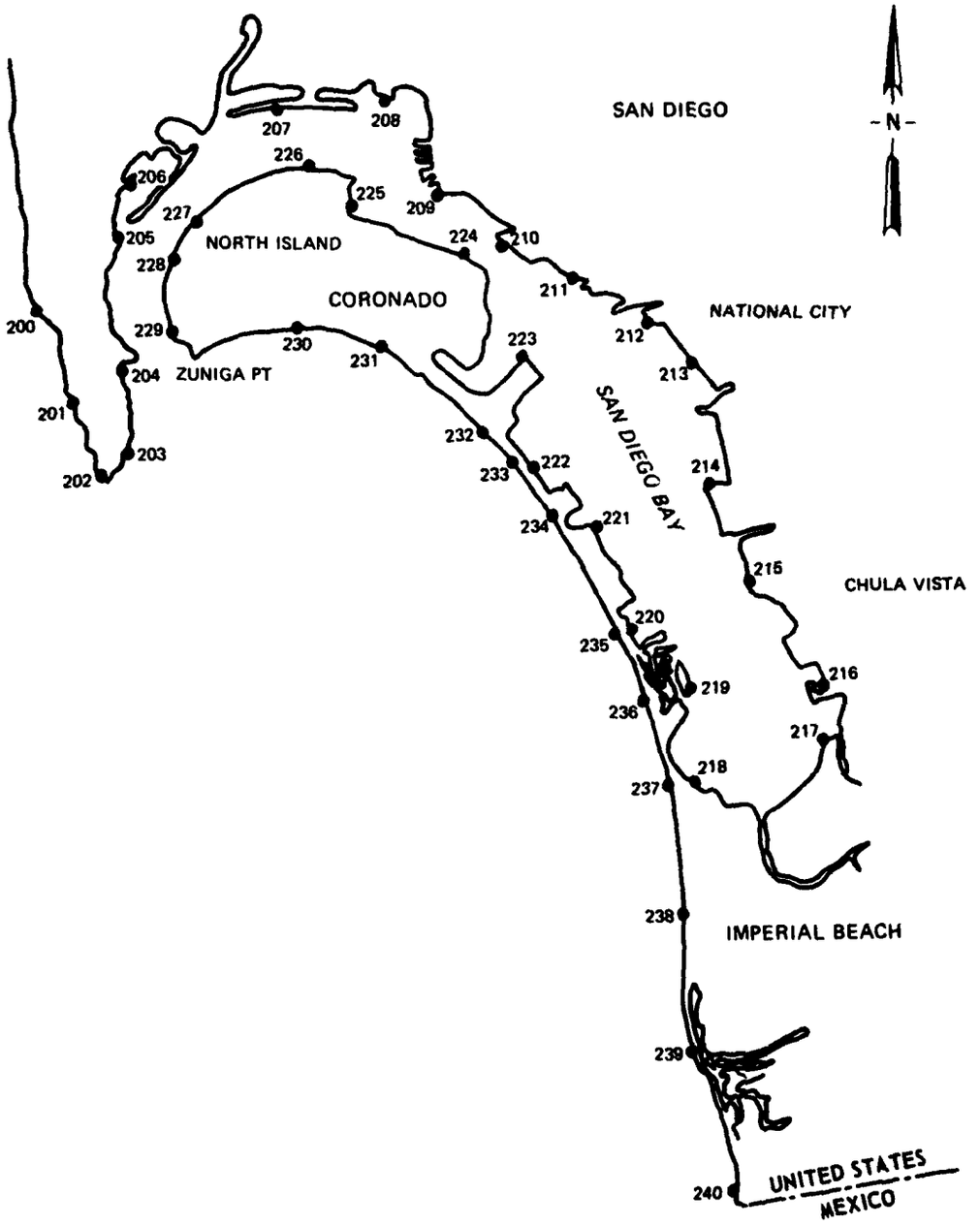

Figure 31. Gage locations 200-240

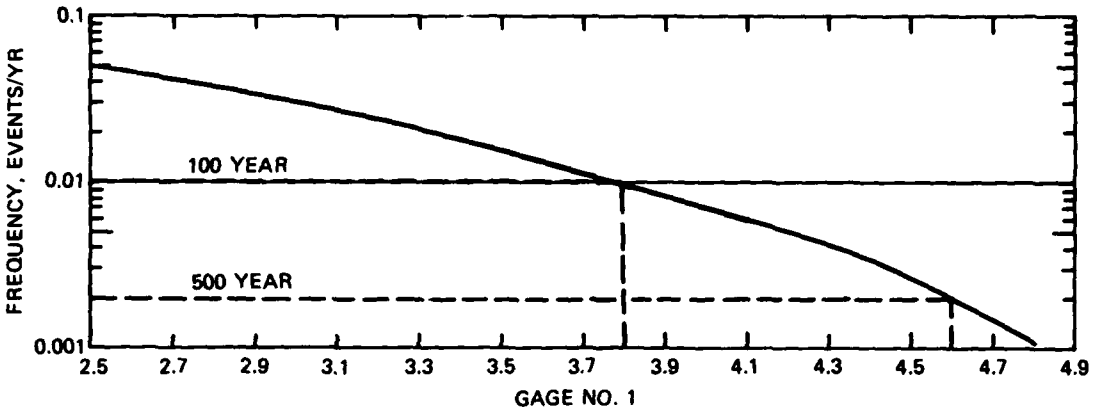

Figure 32. Use of frequency curves

and Garcia (1974) and Houston (1979), runup elevations should be equal to elevations at the shoreline for most locations in southern California. Thus the elevations presented in this report also can be considered to be runup elevations. However, runup elevations may not equal shoreline elevations at locations where dunes prevent flooding except through inlets or if the land is extremely flat and inland flooding is extensive. A land-flooding numerical model (e.g. model presented by Houston and Butler (1979)) can be used to determine runup for such cases.

Discussion

48. The exceedance frequencies presented in Plates 1-120 are for combined tsunami and astronomical tide elevations given the occurrence of a noticeable tsunami in southern California. It is not true that in the limit of a tsunami with an amplitude of zero, the frequency analysis presented determines the maximum possible elevation for the astronomical tide alone over a 100-yr period. It is quite possible that the 100-yr combined tsunami and astronomical tide elevation is less than the maximum possible astronomical tide elevation over a 100-yr period or even less than the maximum astronomical tide elevation that occurs during a typical year. For example, the maximum combined tsunami and astronomical tide

elevation during the last 100 yr at Rincon Island, California, probably occurred during the 1964 Alaskan tsunami (the 1960 Chilean tsunami may have been somewhat larger, but it was not recorded at Rincon Island). The maximum combined elevation was approximately 3.5 ft above msl. This elevation is greater than mean higher high water (2.8 ft) but less than the maximum astronomical tide elevation that typically occurs during the average year at Rincon Island. Thus the fact that the combined tsunami and astronomical tide elevations presented in Plates 1-120 are at some locations less than the maximum possible or even yearly tide elevations that may occur at the locations is a property of the natural phenomenon (tsunami heights are small compared with the tide, and arrival of a tsunami during the maximum astronomical tide of a year is more than a 100-yr event) and not of the methods used to calculate exceedance frequencies.

49. The logarithm of tsunami frequency is plotted versus elevation in Plates 1-120. There are sections of the exceedance frequency distribution curves that are approximately linear. This linear relationship between the logarithm of the tsunami exceedance frequency and tsunami elevations has been noted by many observers (see PART III).

50. The linear relationship between the logarithm of tsunami frequency and tsunami elevations holds only over a certain range of tsunami frequency. Cox (1964)* has shown that tsunami frequencies and elevations are linearly related for frequencies greater than approximately 0.05 to 0.1. Since earthquakes probably only reach certain maximum magnitudes, tsunamis can be expected to have similar upper limits to intensity. Thus the exceedance frequency curves must eventually approach a maximum elevation.

Comparison with Predictions Based on Local Observation

51. Virtually all of the coast of southern California lacks observations of tsunami activity. Only four locations (Alamitos Bay, Los

---

* Cox, D. C. 1964. "Tsunami Height-Frequency Relationship of Hilo" (unpublished paper), Hawaii Institute of Geophysics, University of Hawaii, Honolulu, Hawaii.

Angeles, Santa Monica, and San Diego) have tide gage recordings for both major tsunamis in 1960 and 1964. Since the tide gage at Alamitos Bay malfunctioned during the 1960 tsunami and there is a gap in the recording of approximately 2-1/2 hr, a reasonable determination of exceedance frequency based on observed data cannot be made at Alamitos Bay. The tide gage at Santa Monica also malfunctioned during the 1960 tsunami, but there is a good indication of a lower limit for the maximum elevation.

52. Except at San Diego (where a tide gage has operated since the midnineteenth century), recordings of tsunamis in southern California were not made prior to the twentieth century. Thus the 80-yr period of time from 1900 through 1979 will be used to estimate tsunami exceedance frequencies at Los Angeles, Santa Monica, and San Diego based upon local historical data. The 1960 and 1964 tsunamis produced the largest elevations at all three of these locations during the 80-yr period. By using data for these two tsunamis and assuming that the logarithm of the tsunami exceedance frequency is linearly related to the maximum combined tsunami and astronomical tide elevation (see PART III), the 100- and 500-yr combined tsunami and tide elevation can be estimated. This estimate is quite approximate since the time period is relatively short, there are many locations in source regions where tsunamis can be generated but were not during the time period (the numerical predictions include this effect by considering tsunamis generated all along the source regions), and the effect of tsunami arrival during various tidal stages is not accounted for in the historical data.

53. Using microfiche of tide gage recordings (from the National Oceanic and Atmospheric Administration) of the 1960 and 1964 tsunamis, the 1960 and 1964 tsunamis were found to have produced combined tsunamic and astronomical tide elevations of 4.0 ft and 2.8 ft at Los Angeles, greater than 4.6 ft (tide gage went off scale) and 3.0 ft at Santa Monica, and 3.9 ft and 3.1 ft at San Diego. The tabulation on the following page compares 100- and 500-yr elevations using these data and elevations presented in Plates 52, 38, and 113 for gage locations 104 (Los Angeles), 75 (Santa Monica), and 225 (San Diego) respectively.

Location	Local Historical Data Predictions ft		Predictions Presented in this Report, ft	
	100 yr	500 yr	100 yr	500 yr
Los Angeles	4.4	7.2	5.2	8.2
Santa Monica	>5.2*	>8.9*	5.8	10.2
San Diego	4.2	6.0	4.6	5.7

* Lower limit since tide gage off scale during 1960 tsunami at Santa Monica.

PART V: CONCLUSIONS AND RECOMMENDATIONS

Conclusions

54. The deep-ocean and nearshore numerical models used in this report accurately simulated tsunami generation, deep-ocean and nearshore propagation, and interaction with coastlines. The nearshore numerical model was superior to the analytical techniques used for nearshore propagation in a previous study (Houston and Garcia 1974) because it was two-dimensional and handled arbitrary incident wave forms. The techniques used in this report to predict tsunami elevations provided good estimates of 100- and 500-yr tsunami elevations for southern California. Based upon the techniques presented in this report, 100- and 500-yr predictions at Los Angeles, Santa Monica, and San Diego, California, were shown to agree quite well with predictions based upon historical observations of tsunami activity at these three locations. These were the only locations in southern California which had sufficient local historical data to allow predictions based upon local observations.

Recommendations

55. The elevations predicted in this report are at the shoreline but can be assumed to equal runup elevations for most of southern California. There are locations where time-dependent effects (for example, lack of sufficient time to completely flood extensive low-lying or estuarine areas) or two-dimensional effects (for example, flow divergence or convergence) cause tsunami runup elevations not to be equal to elevations at the shoreline. It is recommended that for these areas inundation limits be determined using a numerical model developed recently at the U. S. Army Engineer Waterways Experiment Station (Houston and Butler 1979). This model is capable of handling land flooding for bays, harbors, developed areas such as cities, large low-lying areas, sand-dune protected areas, and other areas where there are topographical, roughness, or coastline variations.

REFERENCES

Adams, W. M. 1970. "Tsunami Effects and Risk at Kahuku Point, Oahu, Hawaii," Engineering Geology Case Histories, Geological Society of America, No. 8, pp 63-70.

Brown, D. L. 1964. "Tsuanmi Activity Accompanying the Alaskan Earthquake, 27 March 1964," U. S. Army Engineer District, Alaska, CE, Anchorage, Alaska.

Butler, H. L. 1978. "Numerical Simulation of Coos Bay-South Slough Complex," Technical Report H-78-22, U. S. Army Engineer Waterways Experiment Station, CE, Vicksburg, Miss.

Chandrasekhar, S. 1943. Reviews of Modern Physics, Vol 15, pp 1-89.

Eaton, J. P., Richter, D. H., and Ault, W. V. 1964. "The Tsunami of May 23, 1960, on the Island of Hawaii," Bulletin of the Seismological Society of America, Vol 51, No. 2, pp 135-157.

Garcia, A. W. 1976. "Effect of Source Orientation and Location in the Peru-Chile Trench on Tsunami Amplitude Along the Pacific Coast of the Continental United States," Research Report H-76-2, U. S. Army Engineer Waterways Experiment Station, CE, Vicksburg, Miss.

Garcia, A. W., and Houston, J. R. 1975. "Type 16 Flood Insurance Study: Tsunami Predictions for Monterey and San Francisco Bays and Puget Sound," Technical Report H-75-17, U. S. Army Engineer Waterways Experiment Station, CE, Vicksburg, Miss.

Goring, D. G. 1978. "Tsunamis - The Propagation of Long Waves onto a Shelf," Report No. KH-R-38, California Institute of Technology, Pasadena, Calif.

Gutenberg, B., and Richter, C. F. 1965. Seismicity of the Earth and Associated Phenomena, Hafner Publishing Co., New York, N. Y.

Hammack, J. L. 1972. "Tsunamis - A Model of Their Generation and Propagation," Report No. KH-R-28, California Institute of Technology, Pasadena, Calif.

Hammack, J. L., and Segur, H. 1978. "Modeling Criteria for Long Waves," Journal of Fluid Mechanics, Vol 84, Pt. 2.

Hatori, T. 1963. "Directivity of Tsunamis," Bulletin of the Earthquake Research Institute, Tokoyo University, Vol 41, pp 61-81.

Houston, J. R. 1978. "Interaction of Tsunamis with the Hawaiian Islands Calculated by a Finite-Element Numerical Model," Journal of Physical Oceanography, Vol 8, No. 1, pp 93-101.

_____. 1979. "State-of-the-Art for Assessing Earthquake Hazards in the United States; Tsunamis, Seiches, and Landslide-Induced Water Waves," Miscellaneous Paper S-73-1, Report 15, U. S. Army Engineer Waterways Experiment Station, CE, Vicksburg, Miss.

Houston, J. R., and Butler, H. L. 1979. "A Numerical Model for Tsunami Inundation," Technical Report HL-79-2, U. S. Army Engineer Waterways Experiment Station, CE, Vicksburg, Miss.

Houston, J. R., and Garcia, A. W. 1974. "Type 16 Flood Insurance Study: Tsunami Predictions for Pacific Coastal Communities," Technical Report H-74-3, U. S. Army Engineer Waterways Experiment Station, CE, Vicksburg, Miss.

_____. 1978 (Dec). "Type 16 Flood Insurance Study: Tsunami Predictions for the West Coast of the Continental United States," Technical Report H-78-26, U. S. Army Engineer Waterways Experiment Station, CE, Vicksburg, Miss.

Houston, J. R., et al. 1975. "Effect of Source Orientation and Location in the Aleutian Trench on Tsunami Amplitude Along the Pacific Coast of the Continental United States," Research Report H-75-4, U. S. Army Engineer Waterways Experiment Station, CE, Vicksburg, Miss.

Hwang, L. S., Butler, H. L., and Divoky, H. L. 1972. "Tsunami Model: Generation and Open-Sea Characteristics," Bulletin of the Seismological Society of America, Vol 62, No. 6, pp 1579-1594.

Joy, J. W. 1968. "Tsunamis and Their Occurrence Along the San Diego County Coast" (unpublished report), Unified San Diego County Civil Defense and Disaster Organization, San Diego, Calif.

Kelleher, J., et al. 1974. "Why and Where Great Thrust Earthquakes Occur Along Island Arc," Journal of Geophysical Research, Vol 79, No. 32, pp 4889-4899.

McGarr, A. 1976. "Upper Limit to Earthquake Size," Nature, Vol 262, pp 378-379.

Perkins, D. 1972. "The Search for Maximum Magnitude," National Oceanic and Atmospheric Administration Earthquake Information Bulletin, pp 18-23.

Plafker, G. 1964. "Tectonics of the March 27, 1964, Alaska Earthquake," U. S. Geological Survey Professional Paper 543-I, pp 11-174.

Rascon, O. A., and Villarreal, A. G. 1975. "On a Stochastic Model to Estimate Tsunami Risk," Journal, Hydraulic Research, Vol 13, No. 4, pp 383-403.

Schureman, P. 1948. Manual of Harmonic Analysis and Prediction of Tides, Spec. Pub. No. 98, U. S. Coast and Geodetic Survey.

Soloviev, S. L. 1970. "Recurrence of Tsunamis in the Pacific," Tsunamis in the Pacific Ocean, W. M. Adams, ed., East-West Center Press, Honolulu, Hawaii.

Soloviev, S. L., and Go, Ch. N. 1969. "Catalog of Tsunamis in the Pacific (Main Data)," Union of Soviet Socialist Republics, Moscow.

Tuck, E. O. 1979. "Models for Predicting Tsunami Propagation," Tsunamis, Proceedings of the National Science Foundation Workshop, Coto de Caza, Calif., pp 43-48.

Wanstrath, J. J. 1976. "Storm Surge Simulation in Transformed Coordinates; Vol. 1; Theory and Application," Technical Report 76-3, U. S. Army Coastal Engineering Research Center, Fort Belvoir, Va.

Weber, H. F., and Kiessling, E. W. 1978. "Historic Earthquakes Effects in Ventura County," California Geology, California Division of Mines and Geology, Vol 39, No. 5, pp 103-107.

Wiegel, R. L. 1965. "Protection of Crescent City, California, from Tsunami Waves," prepared for the Redevelopment Agency of the City of Crescent City, Berkeley, Calif.

Wilson, B. W. 1969. "Earthquake Occurrence and Effects in Ocean Areas," CR 69.027, Naval Civil Engineering Laboratory, Port Hueneme, Calif.

Wood, H. O., and Heck, N. H. 1966. "Earthquake History of the United States; Part II, Stronger Earthquakes of California and Nevada," U. S. Coast and Geodetic Survey, Washington, D. C.

Table 1

Location of Gages

GAGE LOCATIONS
IN DEGREES, MINUTES, SECONDS (SEC WITH ONE DECIMAL PLACE)

GAGE NUMBER	LONGITUDE	LATITUDE	GAGE NUMBER	LONGITUDE	LATITUDE
1	119 43 4.8	34 23 45.6	61	118 47 38.4	34 [illegible] 25.2
2	119 41 49.2	34 24 3.6	62	118 47 13.2	34 1 1.2
3	119 41 9.6	34 24 39.6	63	118 46 4.8	34 1 22.8
4	119 40 8.4	34 25 1.2	64	118 43 51.6	34 2 6.0
5	119 38 2[illegible].4	34 25 1.2	65	118 42 28.8	34 1 55.2
6	119 36 54.0	34 25 8.4	66	118 40 58.8	34 1 58.8
7	119 35 13.2	34 25 4.8	67	118 39 21.6	34 2 31.2
8	119 34 19.2	34 24 43.2	68	118 37 58.8	34 2 20.4
9	119 33 .0	34 24 36.0	69	118 36 36.0	34 2 20.4
10	119 32 16.8	34 23 56.4	70	118 35 9.6	34 2 27.6
11	119 31 15.6	34 23 34.8	71	118 33 32.4	34 2 31.2
12	119 30 21.6	34 23 6.0	72	118 32 27.6	34 2 16.8
13	119 29 6.0	34 22 55.2	73	118 31 3[illegible].0	34 1 58.8
14	119 28 26.4	34 22 22.8	74	118 30 36.0	34 1 30.0
15	119 27 10.8	34 22 12.0	75	118 29 49.2	34 [illegible] 54.0
16	119 26 38.4	34 21 36.0	76	118 29 9.6	34 [illegible] 10.8
17	119 25 33.6	34 21 10.8	77	118 28 22.8	33 59 34.8
18	119 24 57.6	34 20 34.8	78	118 27 36.0	33 59 2.4
19	119 24 7.2	34 19 58.8	79	118 27 14.4	33 58 4.8
20	119 23 27.6	34 19 19.2	80	118 26 38.4	33 57 18.0
21	119 22 12.0	34 19 8.4	81	118 26 6.0	33 56 24.0
22	119 21 25.2	34 18 36.0	82	118 25 40.8	33 55 30.0
23	119 20 38.4	34 17 60.0	83	118 25 12.0	33 54 39.6
24	119 19 58.8	34 17 20.4	84	118 24 46.8	33 53 45.6
25	119 19 8.4	34 16 51.6	85	118 24 21.6	33 52 51.6
26	119 18 18.0	34 16 19.2	86	118 23 56.4	33 51 54.0
27	119 16 58.8	34 16 12.0	87	118 23 38.4	33 51 10.8
28	119 16 22.8	34 15 39.6	88	118 23 9.6	33 50 16.8
29	119 15 57.6	34 14 31.2	89	118 23 38.4	33 48 21.6
30	119 15 43.2	34 13 30.0	90	118 24 25.2	33 47 42.0
31	119 15 18.0	34 12 32.4	91	118 25 15.6	33 47 13.2
32	119 14 49.2	34 11 52.8	92	118 25 26.4	33 46 37.2
33	119 14 16.8	34 10 55.2	93	118 25 1.2	33 45 54.0
34	119 13 44.4	34 10 12.0	94	118 24 39.6	33 45 0.0
35	119 13 15.6	34 9 18.0	95	118 24 10.8	33 44 38.4
36	119 12 28.8	34 8 42.0	96	118 22 37.2	33 44 45.6
37	119 11 16.8	34 8 24.0	97	118 21 32.4	33 44 24.0
38	119 10 33.6	34 7 58.8	98	118 20 42.0	33 43 58.8
39	119 9 46.8	34 7 22.8	99	118 19 44.4	33 43 30.0
40	119 8 56.4	34 6 50.4	100	118 18 39.6	33 43 12.0
41	119 8 13.2	34 6 21.6	101	118 17 52.8	33 42 50.4
42	119 7 15.6	34 5 49.2	102	118 16 58.8	33 43 19.2
43	119 6 3.6	34 5 42.0	103	118 16 8.4	33 43 48.0
44	119 4 48.8	34 5 45.6	104	118 15 36.0	33 44 38.4
45	119 3 5[illegible].4	34 5 16.8	105	118 15 9.0	33 45 21.6
46	119 2 3[illegible].8	34 5 6.0	106	118 13 4.8	33 44 56.4
47	119 1 37.2	34 4 40.8	107	118 11 24.0	33 45 54.0
48	119 0 5[illegible].4	34 4 8.4	108	118 11 16.8	33 46 1.2
49	118 59 38.4	34 3 50.4	109	118 8 45.6	33 45 39.6
50	118 58 33.6	34 3 36.[illegible]	110	118 7 40.8	33 45 18.0
51	118 57 5[illegible].4	34 3 10.8	111	118 7 1.2	33 44 45.6
52	118 56 52.8	34 2 45.6	112	118 6 10.8	33 44 24.[illegible]
53	118 55 26.4	34 2 49.2	113	118 5 9.6	33 43 51.6
54	118 54 18.0	34 2 27.6	114	118 4 30.0	33 43 19.2
55	118 53 9.6	34 2 20.4	115	118 3 46.8	33 42 39.6
56	118 51 57.6	34 2 6.0	116	118 3 7.2	33 42 .0
57	118 50 52.8	34 1 55.2	117	118 2 24.0	33 41 20.4
58	118 49 55.2	34 1 26.4	118	118 1 40.8	33 4 [illegible]0.8
59	118 49 15.6	34 [illegible]50.4	119	118 1 1.2	33 4 4.8
60	118 48 32.4	34 [illegible] 10.8	120	118 0 14.4	33 39 25.2

(Continued)

Table 1 (Concluded)

GAGE NUMBER	LONGITUDE	LATITUDE	GAGE NUMBER	LONGITUDE	LATITUDE
121	117 59 27.6	33 38 56.4	181	117 16 48.0	33 [illegible] 54.0
122	117 58 37.2	33 38 27.6	182	117 16 26.4	32 59 52.8
123	117 57 43.2	33 37 51.6	183	117 16 12.0	32 58 48.0
124	117 56 49.2	33 37 30.0	184	117 15 54.0	32 57 50.4
125	117 55 55.2	33 36 43.2	185	117 15 39.6	32 56 45.6
126	117 54 50.4	33 36 18.0	186	117 15 21.6	32 55 37.2
127	117 53 49.2	33 36 3.6	187	117 15 13.8	32 54 32.4
128	117 52 37.2	33 35 49.2	188	117 15 [illegible]0	32 53 31.2
129	117 51 54.0	33 35 20.4	189	117 15 [illegible]0	32 52 12.[illegible]
130	117 51 7.2	33 34 48.0	190	117 15 46.8	32 5[illegible] 52.8
131	117 50 6.0	33 34 19.2	191	117 16 [illegible].8	32 50 38.4
132	117 49 19.2	33 33 50.4	192	117 16 33.6	32 49 22.8
133	117 48 36.0	33 33 14.4	193	117 16 4.8	32 48 39.6
134	117 47 49.2	33 34 19.2	194	117 15 25.2	32 48 7.2
135	117 46 51.6	33 32 20.4	195	117 15 7.2	32 46 58.8
136	117 46 [illegible].4	33 31 44.4	196	117 15 3.6	32 45 43.2
137	117 45 32.4	33 31 1.2	197	117 15 [illegible].8	32 44 27.6
138	117 44 49.2	33 3 25.2	198	117 15 18.0	32 43 33.6
139	117 44 [illegible].4	33 29 38.4	199	117 15 25.2	32 42 21.6
140	117 43 [illegible].8	33 28 48.0	200	117 15 [illegible].8	32 41 45.6
141	117 43 8.4	33 28 1.2	201	117 14 52.8	32 41 40.8
142	117 42 7.2	33 27 43.2	202	117 14 34.8	32 39 57.6
143	117 40 48.0	33 27 32.4	203	117 14 6.0	32 40 4.8
144	117 39 57.6	33 27 3.6	204	117 14 16.8	32 41 31.2
145	117 39 [illegible].8	33 26 34.8	205	117 14 9.6	32 42 36.0
146	117 38 2.4	33 26 2.4	206	117 13 26.4	32 43 8.4
147	117 37 [illegible].8	33 25 26.4	207	117 12 14.4	32 43 44.4
148	117 36 54.0	33 24 46.8	208	117 10 48.0	32 43 33.6
149	117 36 18.0	33 24 3.6	209	117 10 12.0	32 42 39.6
150	117 35 38.4	33 23 16.8	210	117 9 28.8	32 42 3.6
151	117 34 4.8	33 22 55.2	211	117 8 38.4	32 41 34.8
152	117 33 54.0	33 22 30.0	212	117 7 44.4	32 41 58.8
153	117 33 3.6	33 22 1.2	213	117 7 12.0	32 40 30.0
154	117 32 16.8	33 21 21.6	214	117 7 1.2	32 39 28.8
155	117 31 3.0	33 21 45.6	215	117 6 36.0	32 38 9.6
156	117 30 36.0	33 20 20.4	216	117 5 49.2	32 37 12.0
157	117 29 56.4	33 19 40.8	217	117 5 45.6	32 36 36.0
158	117 29 13.2	33 19 4.8	218	117 7 26.4	32 36 18.0
159	117 28 37.2	33 18 14.4	219	117 7 44.4	32 37 12.0
160	117 27 57.6	33 17 34.8	220	117 8 16.8	32 38 9.6
161	117 27 18.0	33 16 51.6	221	117 8 34.8	32 39 3.6
162	117 26 42.0	33 16 12.0	222	117 9 14.4	32 39 46.8
163	117 26 6.0	33 15 28.8	223	117 9 36.0	32 40 55.2
164	117 25 26.4	33 14 42.0	224	117 10 1.2	32 41 52.8
165	117 24 50.4	33 14 2.4	225	117 10 44.4	32 42 14.4
166	117 24 21.6	33 13 15.6	226	117 11 27.6	32 42 50.4
167	117 23 42.0	33 12 26.8	227	117 12 54.0	32 42 39.6
168	117 23 9.6	33 11 49.2	228	117 13 30.0	32 42 7.2
169	117 22 33.6	33 11 9.6	229	117 13 22.8	32 41 6.0
170	117 21 57.6	33 1 26.4	230	117 11 52.8	32 41 13.2
171	117 21 14.4	33 9 39.6	231	117 10 48.0	32 41 51.6
172	117 20 45.6	33 9 3.6	232	117 10 8.4	32 40 30.0
173	117 20 9.6	33 8 9.6	233	117 9 32.4	32 39 32.4
174	117 19 [illegible].8	33 7 19.2	234	117 8 56.4	32 38 42.0
175	117 19 8.4	33 6 21.6	235	117 8 31.2	32 37 55.2
176	117 18 50.4	33 5 24.0	236	117 8 9.6	32 36 50.4
177	117 18 [illegible].4	33 4 12.0	237	117 7 58.8	32 35 42.0
178	117 18 [illegible].0	33 3 39.6	238	117 7 51.6	32 34 44.4
179	117 17 52.8	33 2 27.6	239	117 7 44.4	32 33 28.8
180	117 17 9.6	33 1 51.6	240	117 7 30.0	32 32 31.2

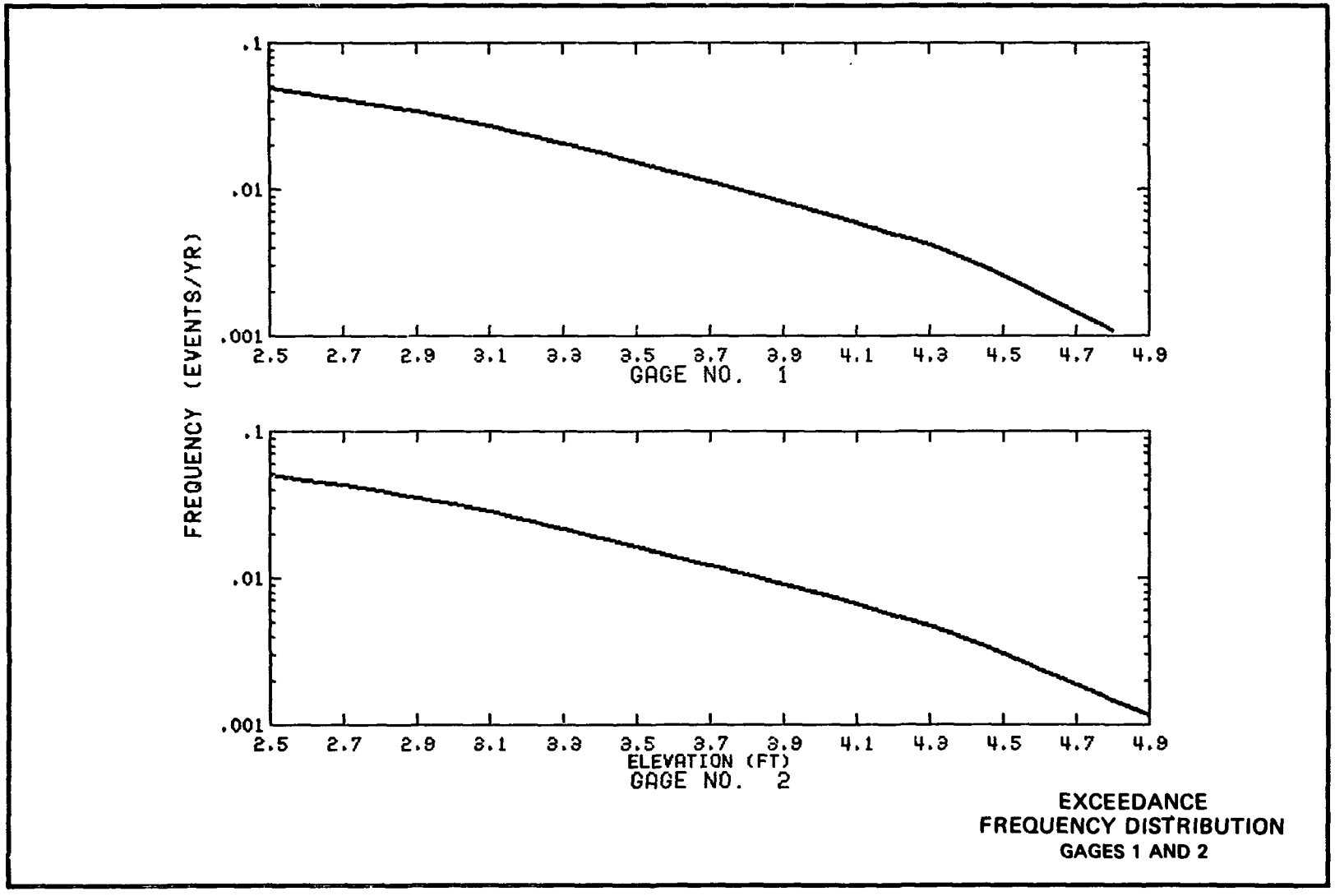

EXCEEDANCE FREQUENCY DISTRIBUTION
GAGES 1 AND 2

PLATE 1

PLATE 2

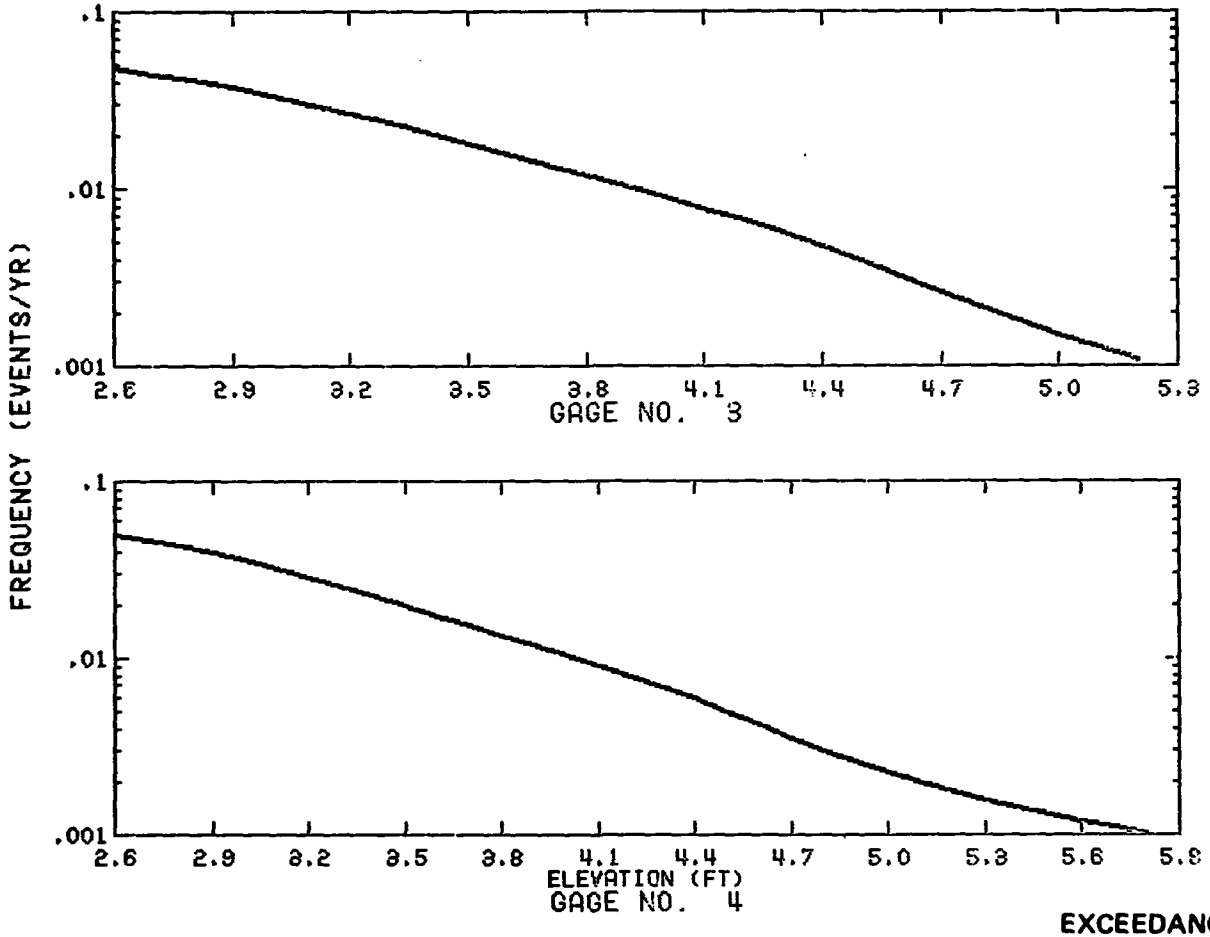

EXCEEDANCE FREQUENCY DISTRIBUTION
GAGES 3 AND 4

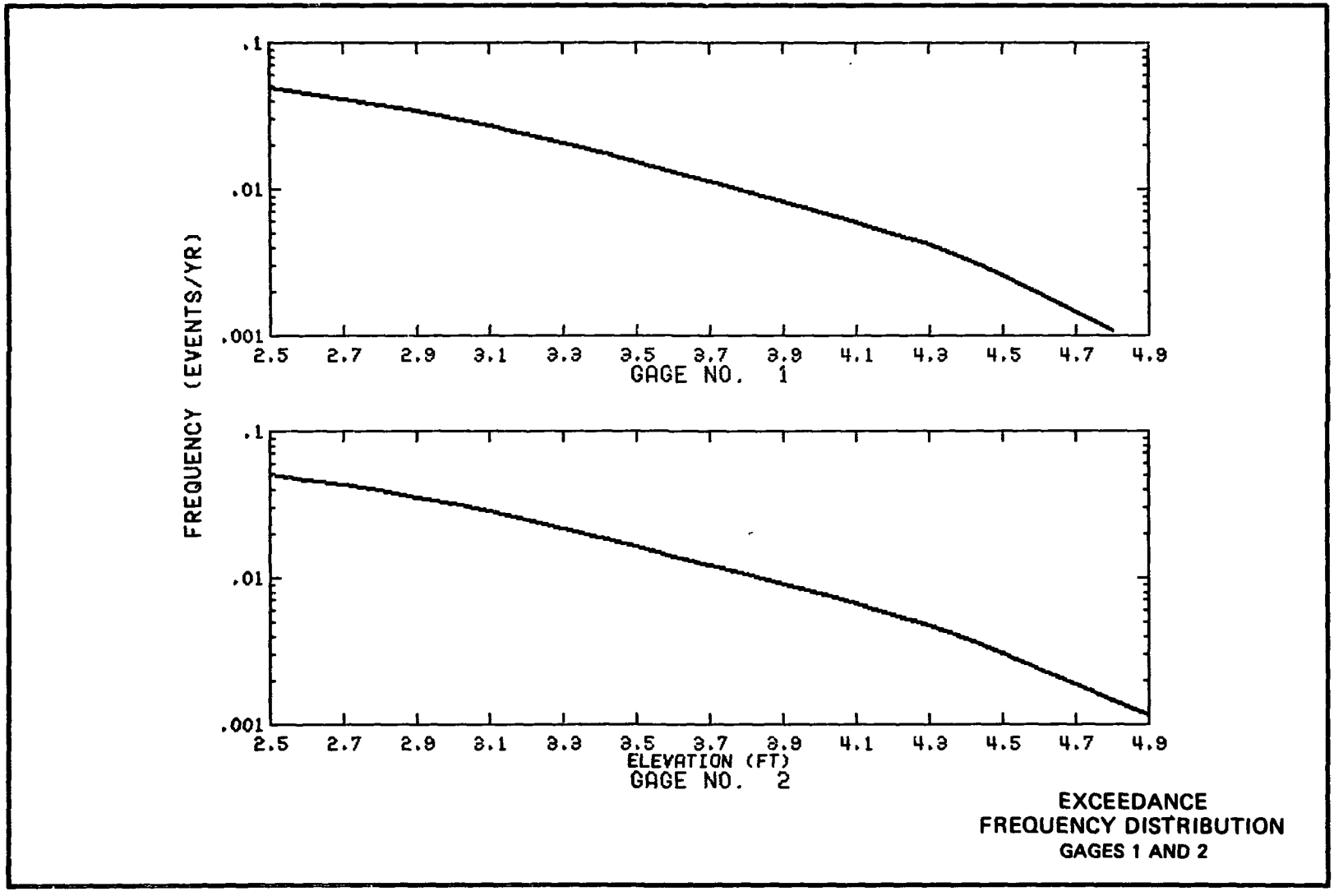

EXCEEDANCE FREQUENCY DISTRIBUTION
GAGES 1 AND 2

PLATE 1

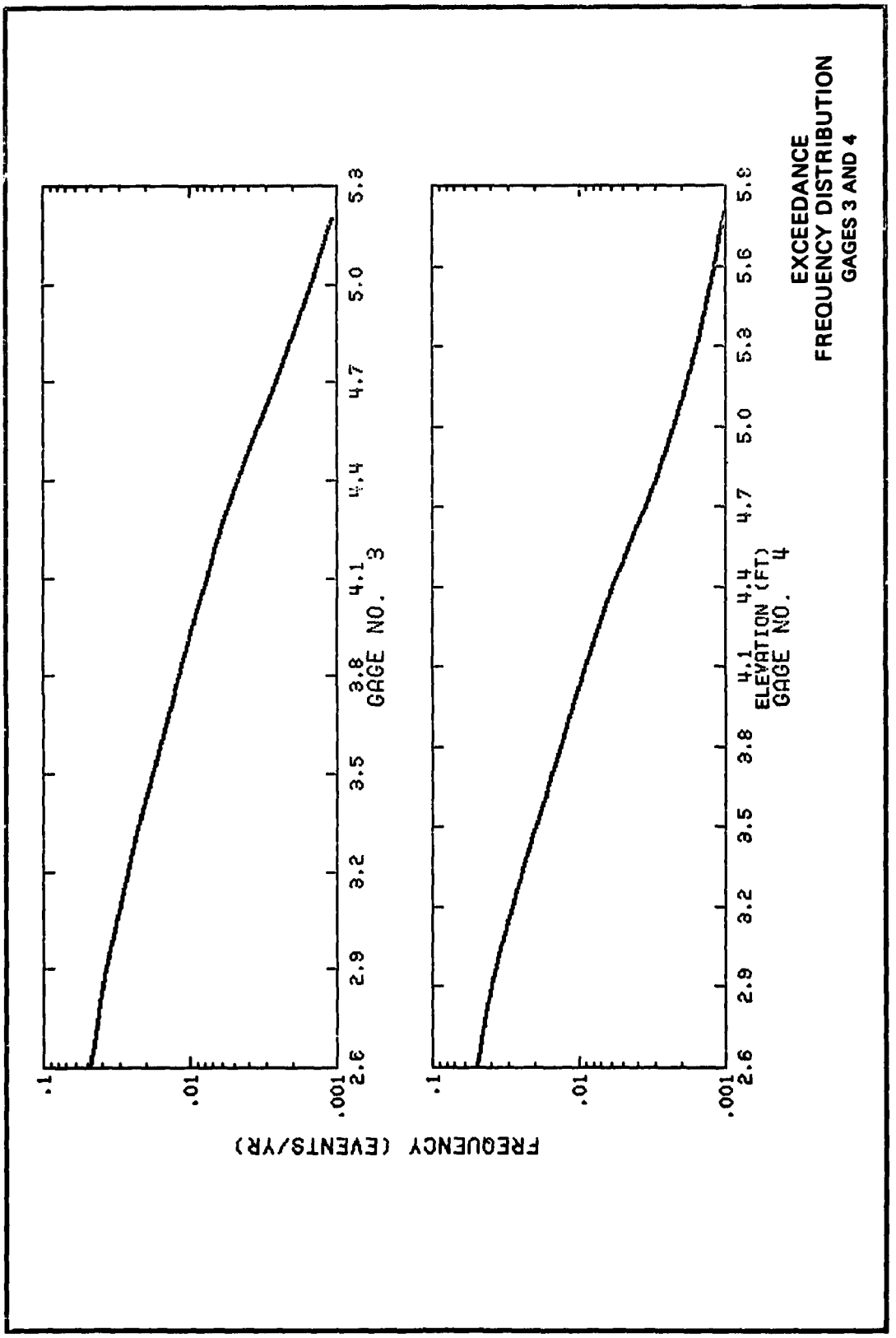
EXCEEDANCE
FREQUENCY DISTRIBUTION
GAGES 3 AND 4
FREQUENCY (EVENTS/YR)
.1
.01
.001
2.6
2.9
3.2
3.5
3.8
4.1
4.4
4.7
5.0
5.3
5.6
5.8
ELEVATION (FT)
GAGE NO. 3
GAGE NO. 4

PLATE 2

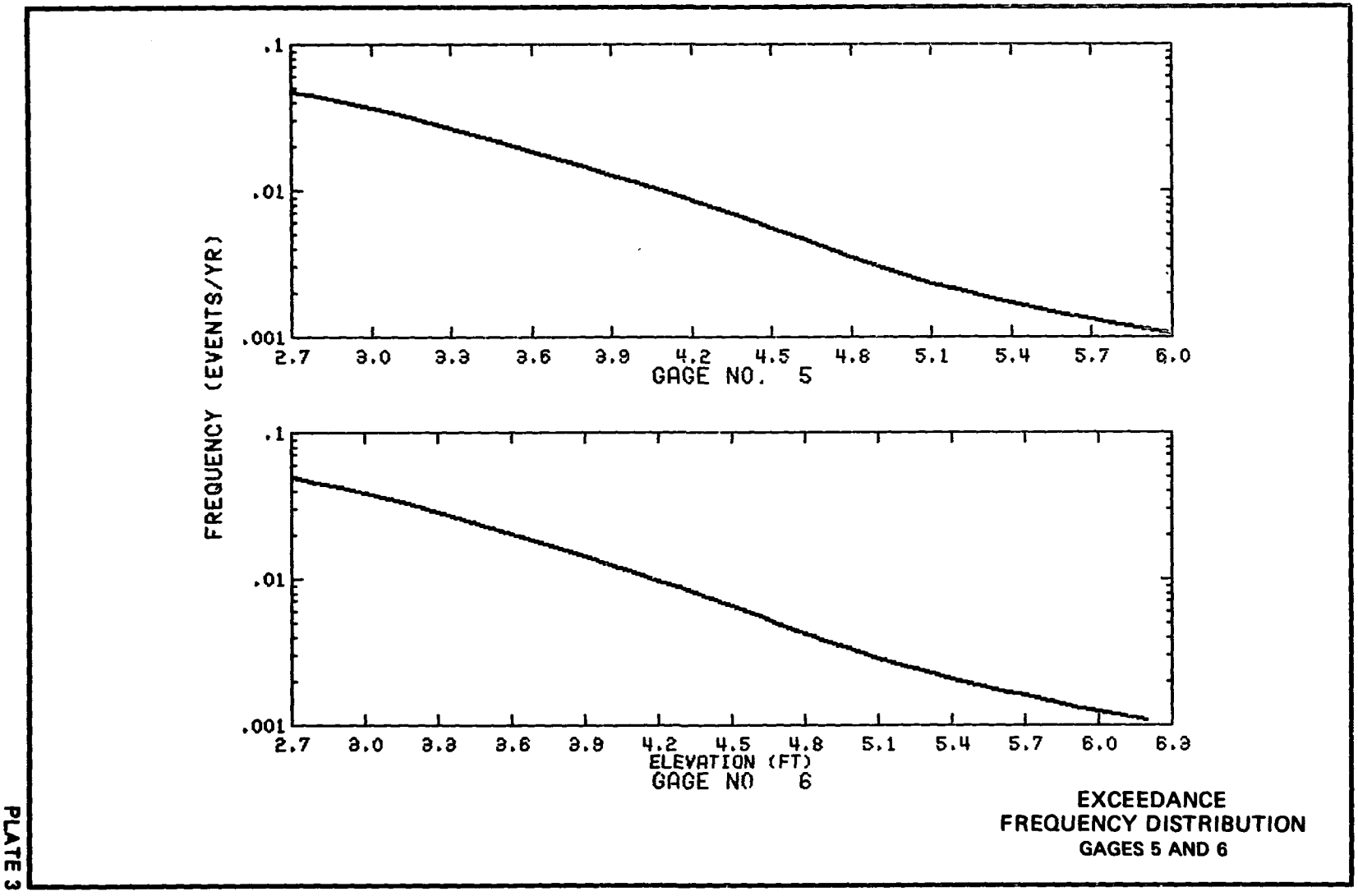

EXCEEDANCE FREQUENCY DISTRIBUTION
GAGES 5 AND 6

PLATE 3

PLATE 4

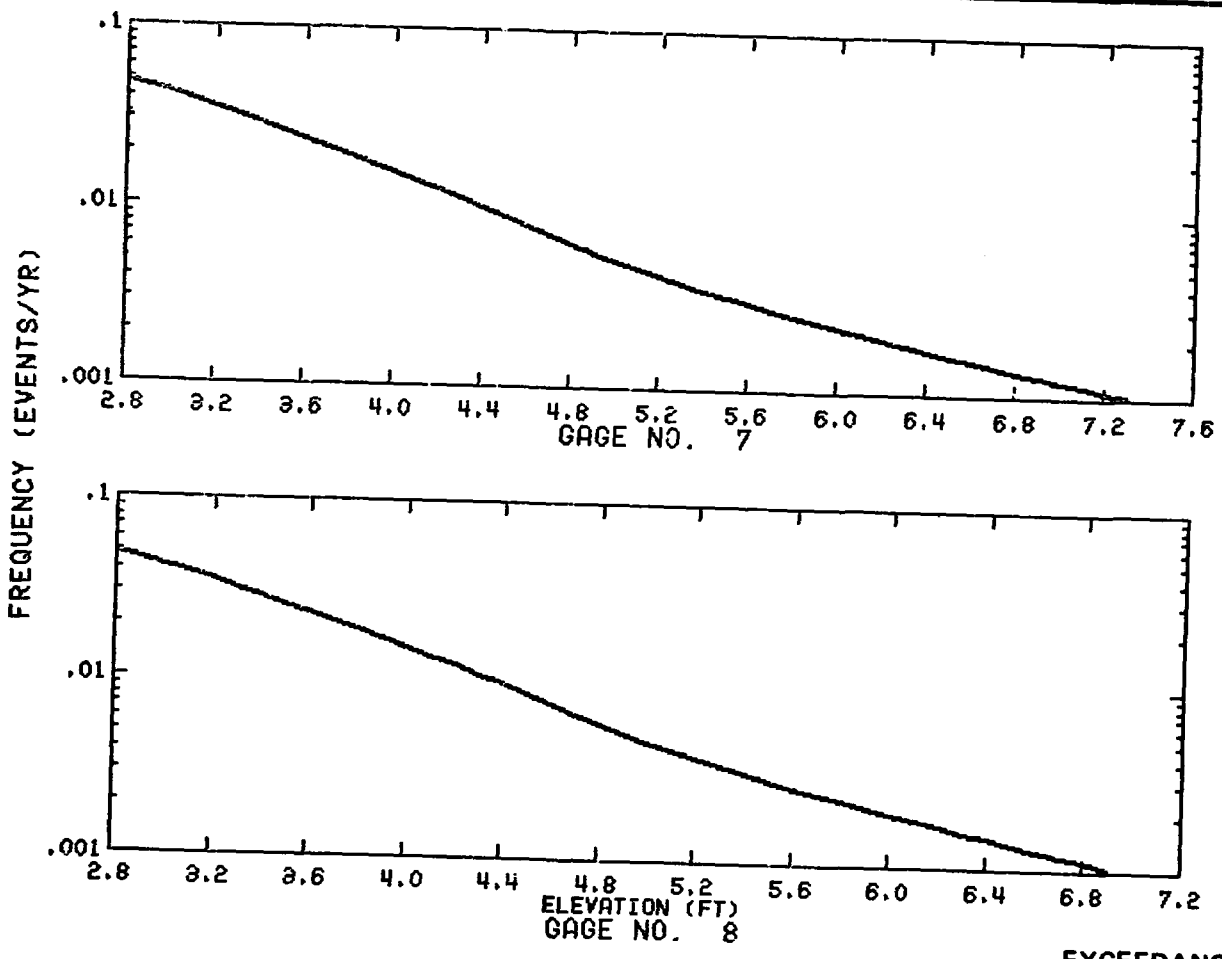

EXCEEDANCE FREQUENCY DISTRIBUTION
GAGES 7 AND 8

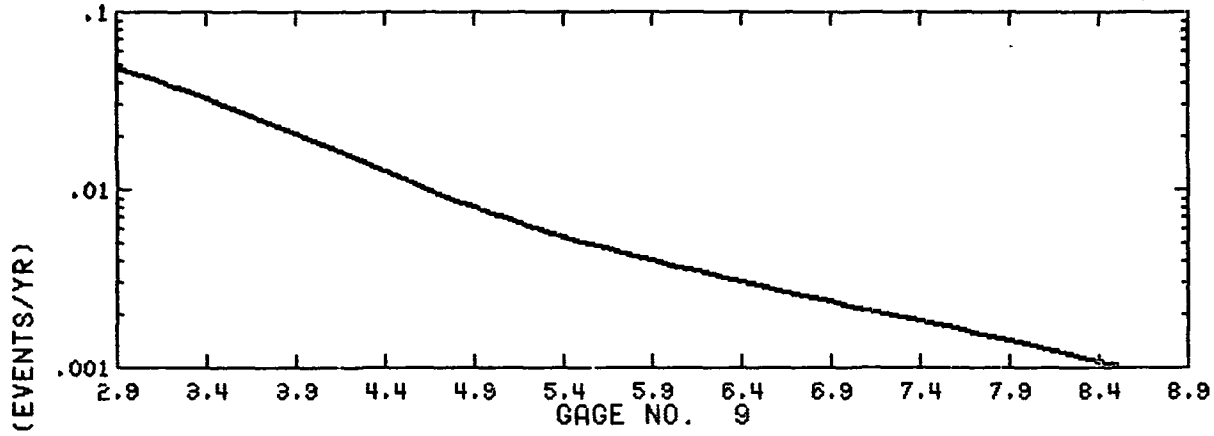

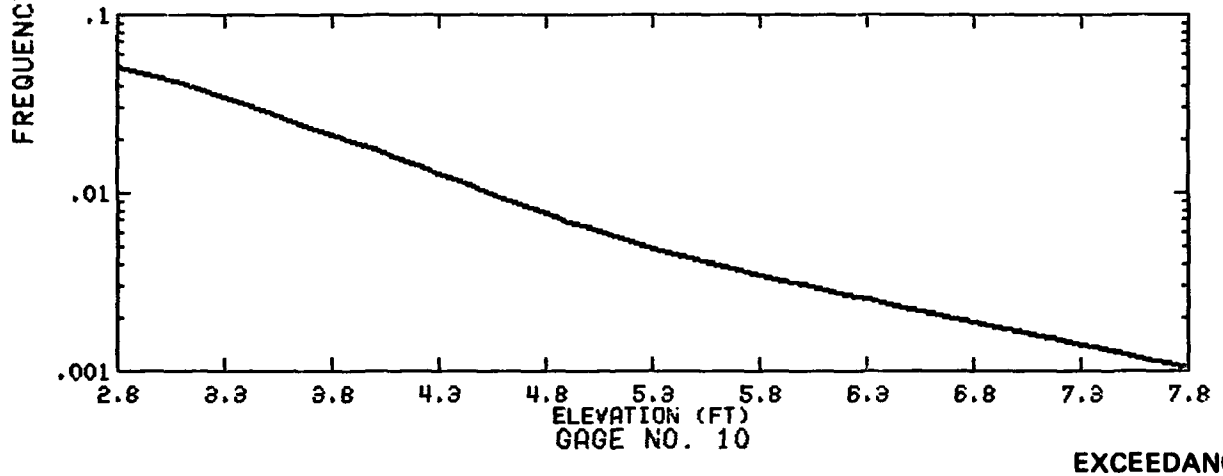

EXCEEDANCE FREQUENCY DISTRIBUTION
GAGES 9 AND 10

PLATE 5

PLATE 6

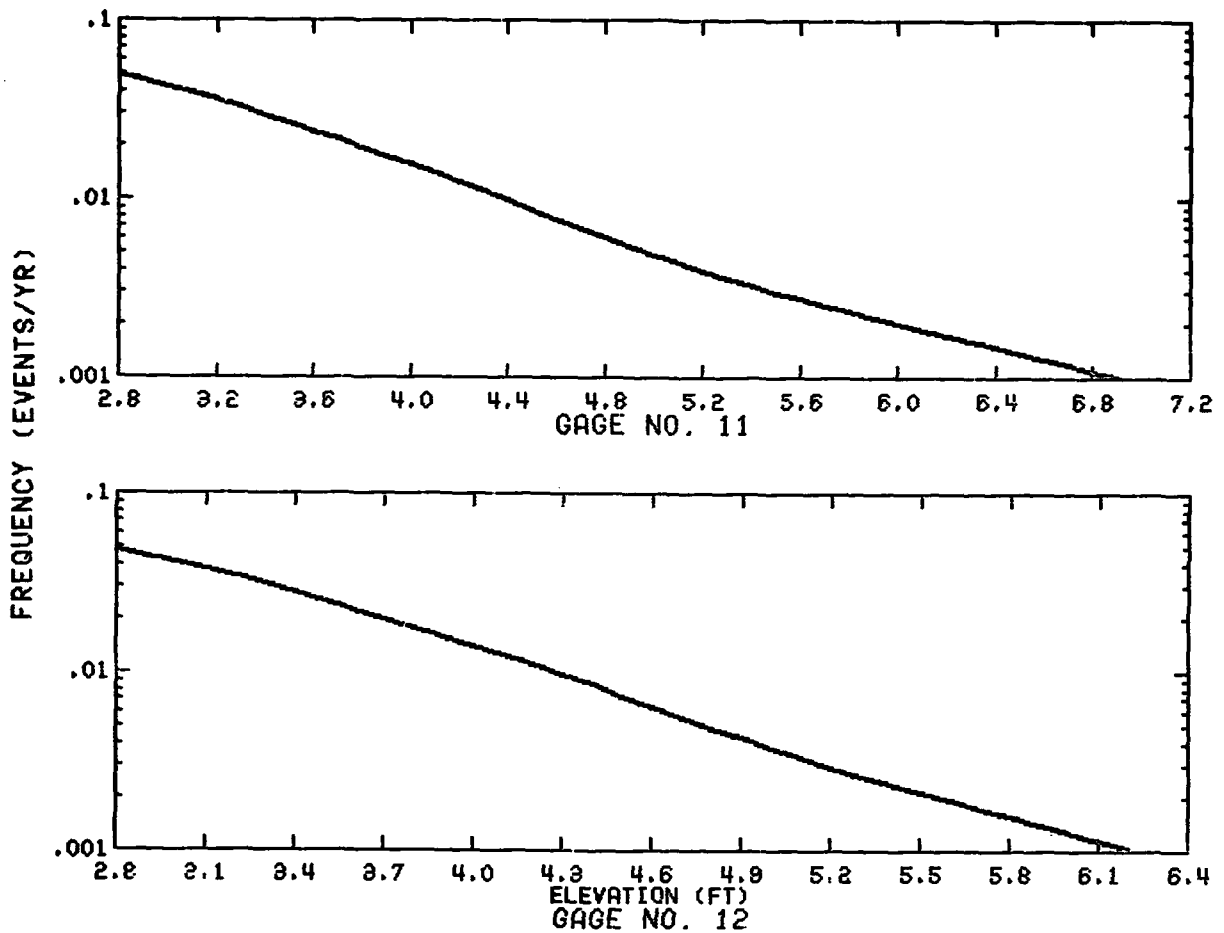

EXCEEDANCE FREQUENCY DISTRIBUTION
GAGES 11 AND 12

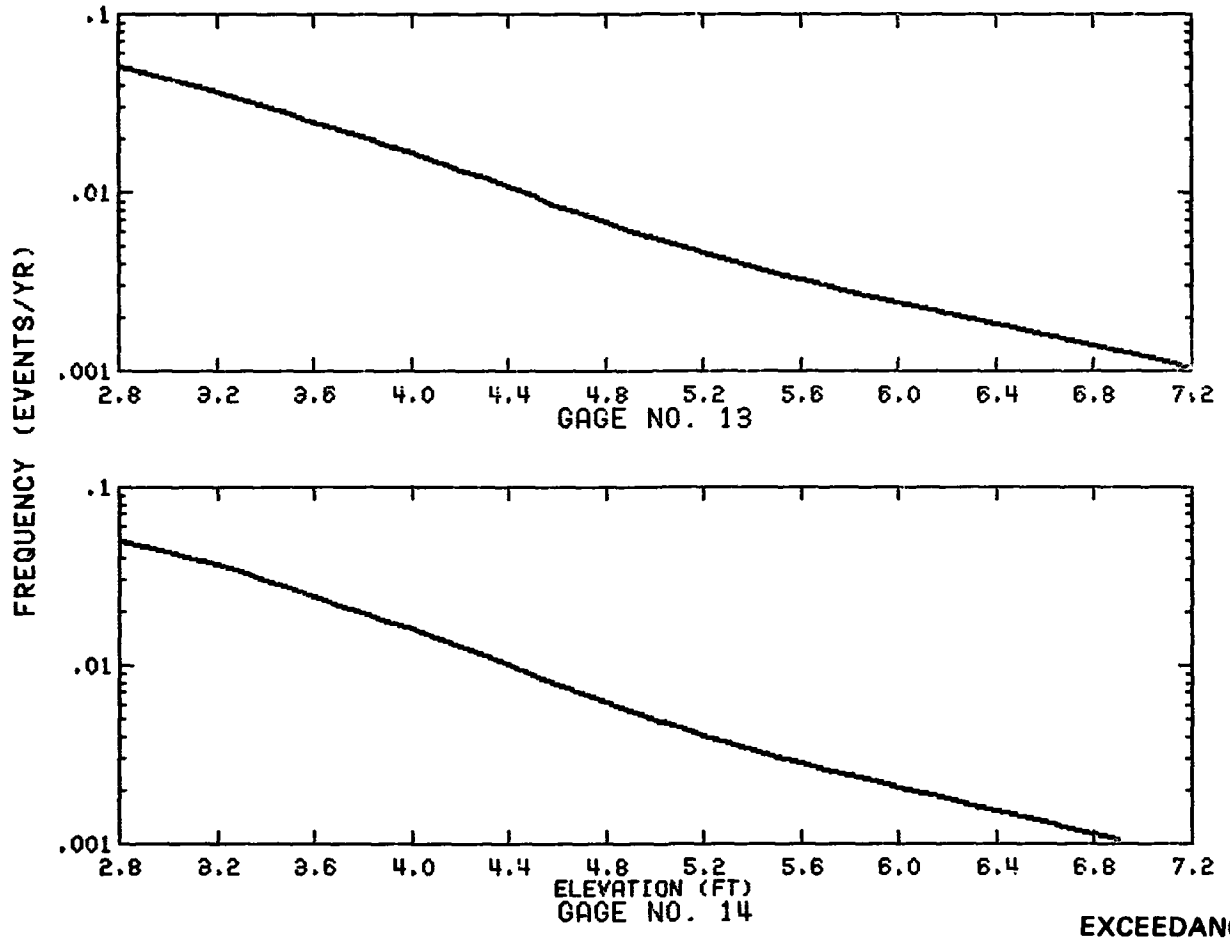

EXCEEDANCE FREQUENCY DISTRIBUTION
GAGES 13 AND 14

PLATE 7

PLATE 8

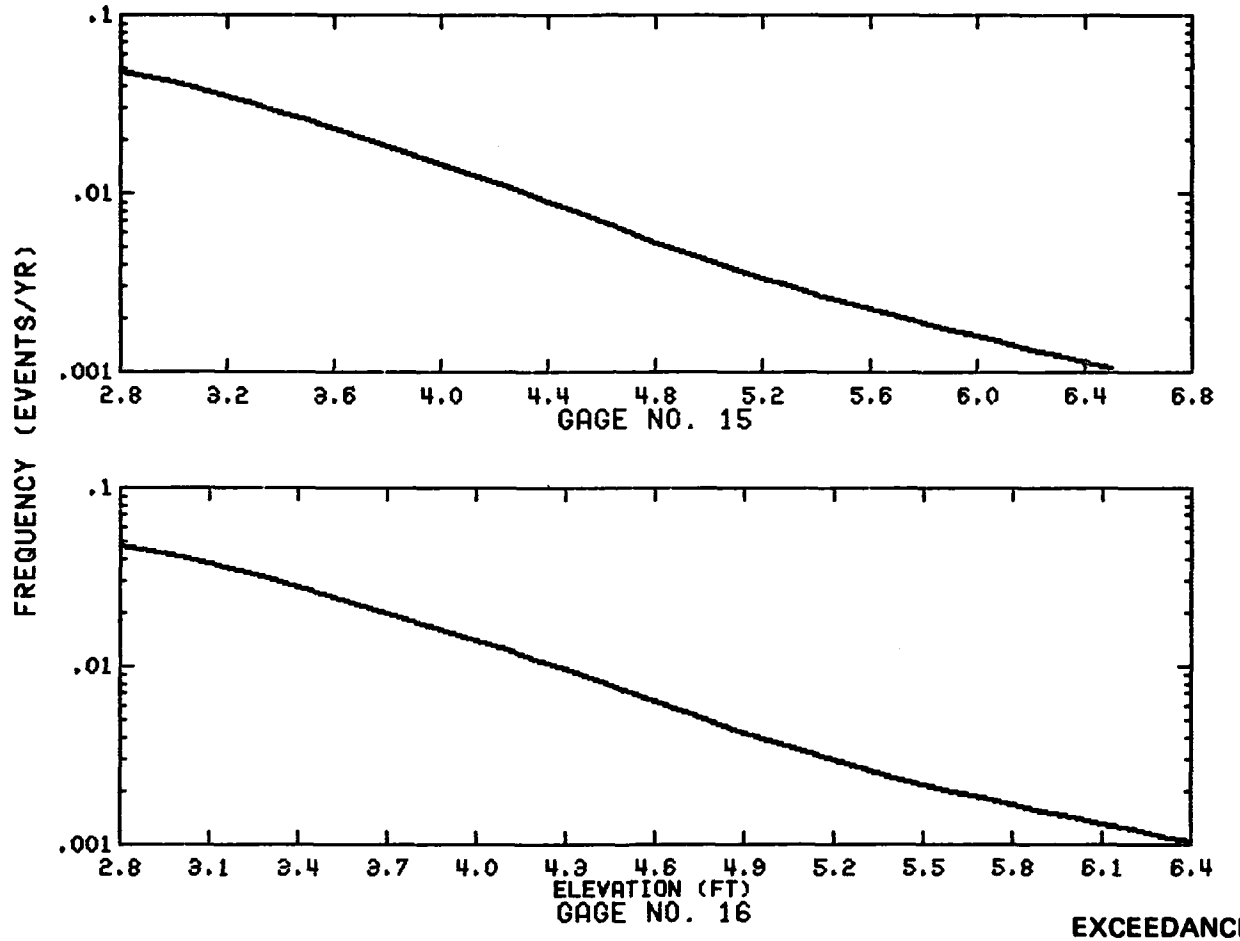

EXCEEDANCE FREQUENCY DISTRIBUTION
GAGES 15 AND 16

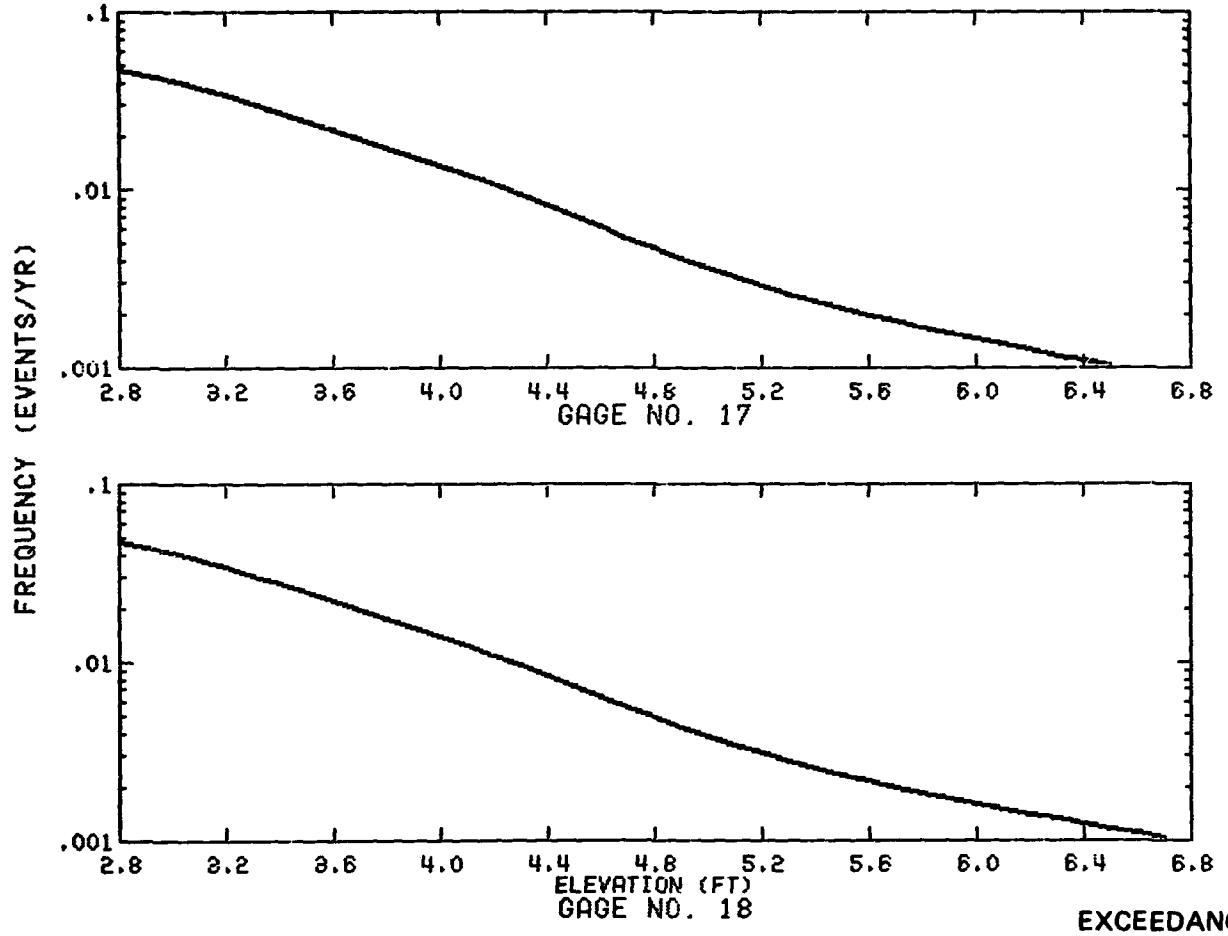

EXCEEDANCE FREQUENCY DISTRIBUTION
GAGES 17 AND 18

PLATE 9

PLATE 10

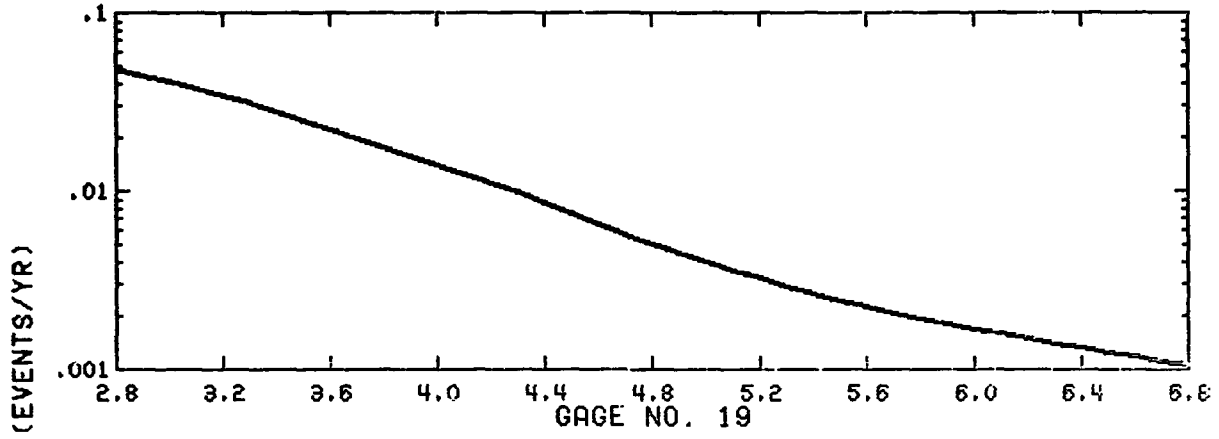

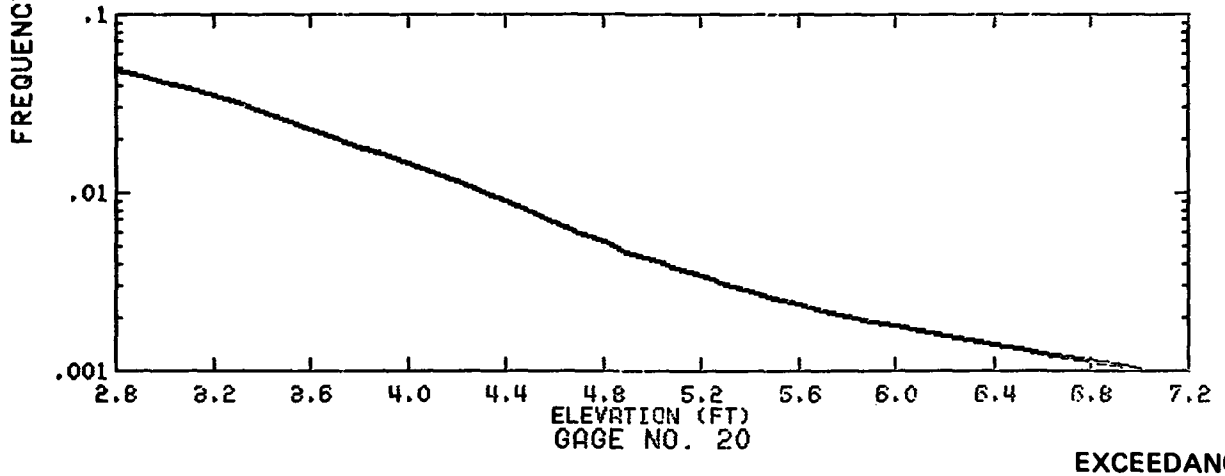

EXCEEDANCE FREQUENCY DISTRIBUTION
GAGES 19 AND 20

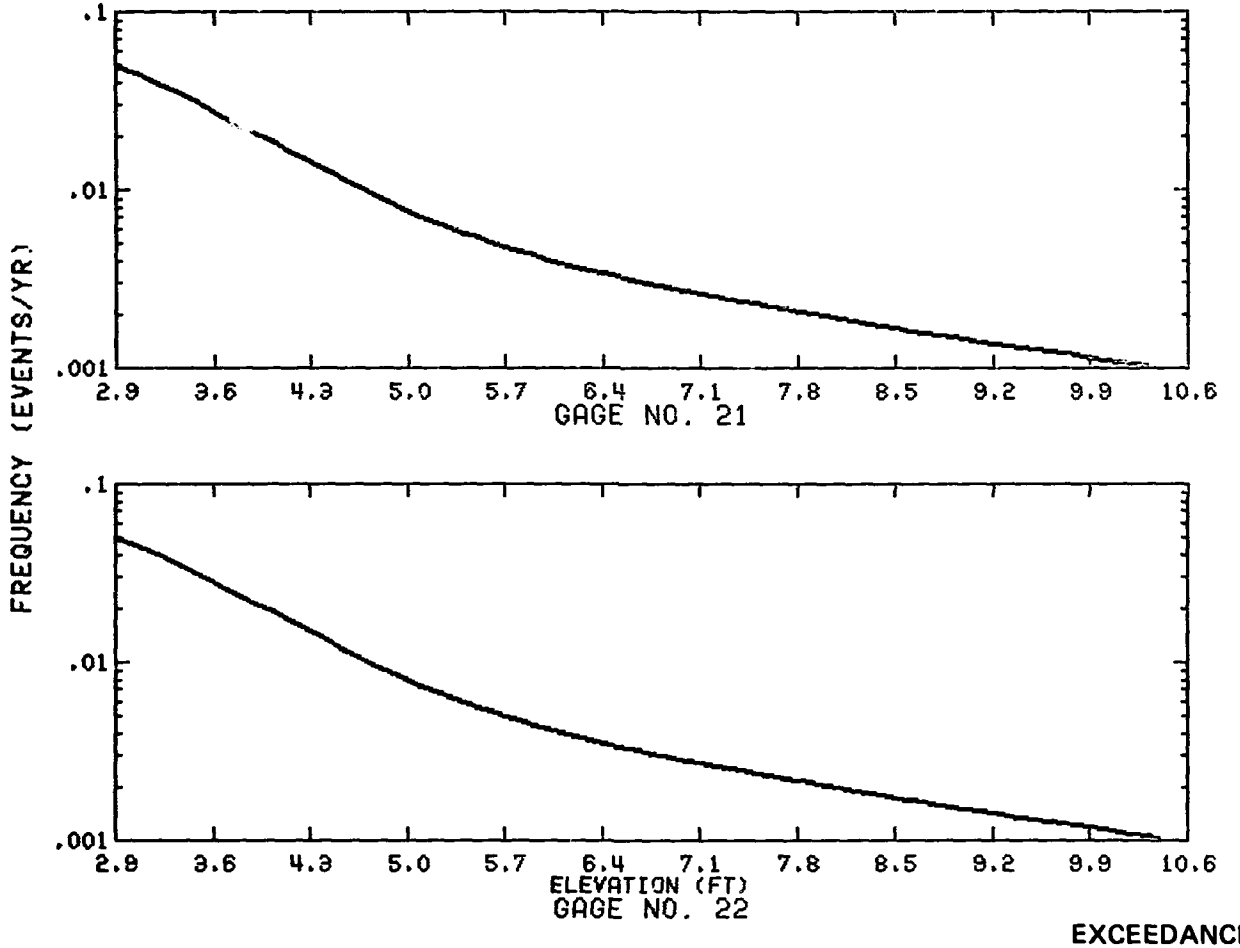

PLATE 11

EXCEEDANCE FREQUENCY DISTRIBUTION
GAGES 21 AND 22

PLATE 12

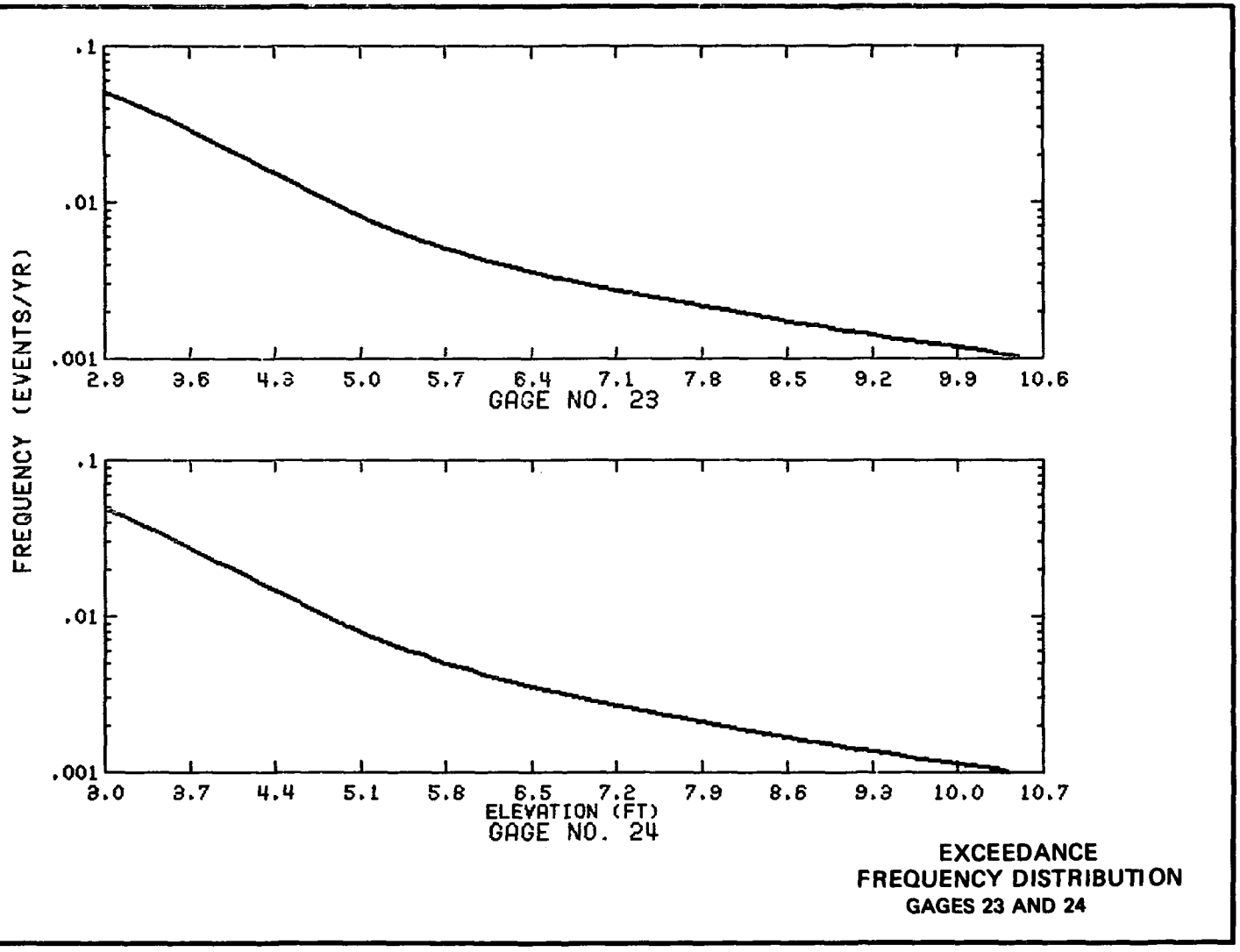

EXCEEDANCE FREQUENCY DISTRIBUTION
GAGES 23 AND 24

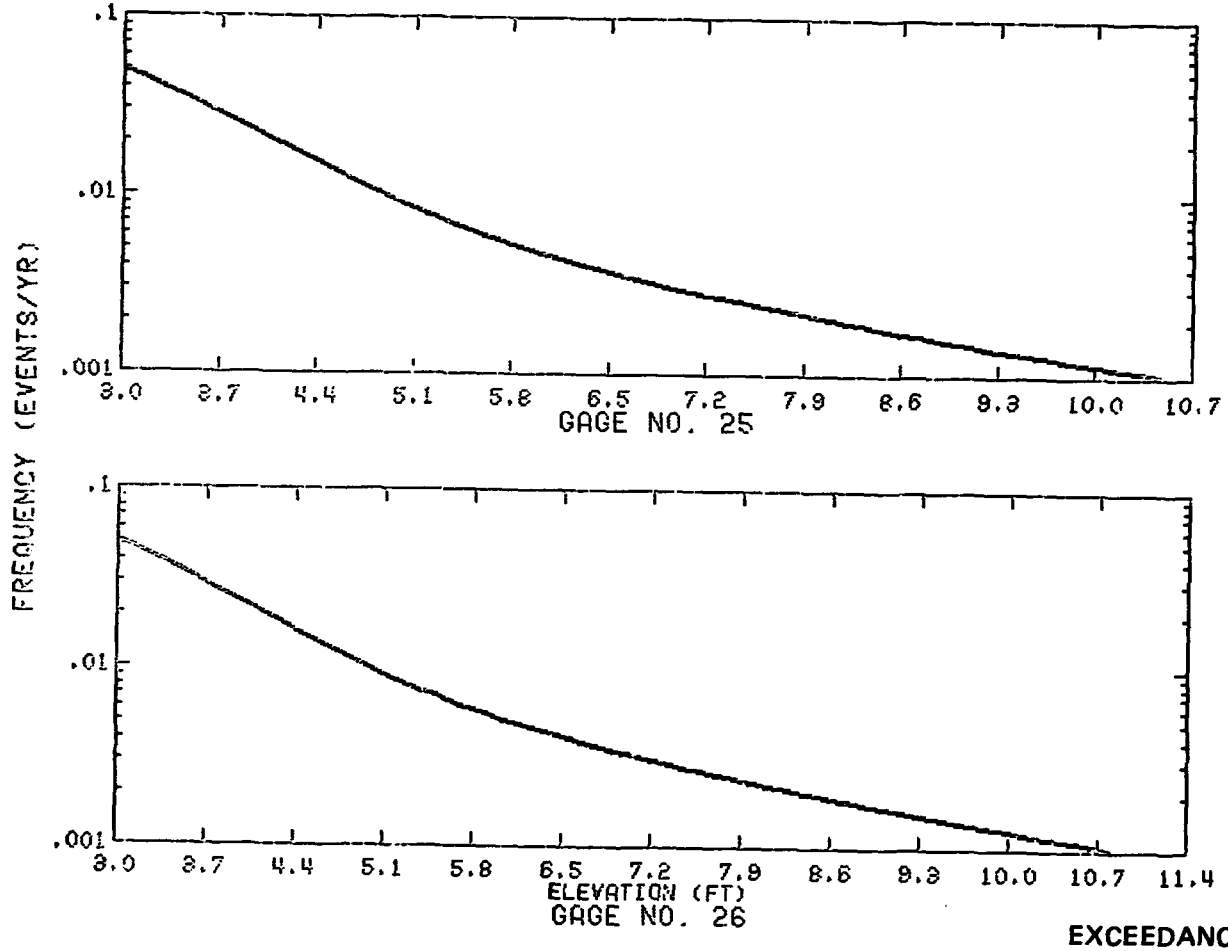

EXCEEDANCE FREQUENCY DISTRIBUTION
GAGES 25 AND 26

PLATE 13

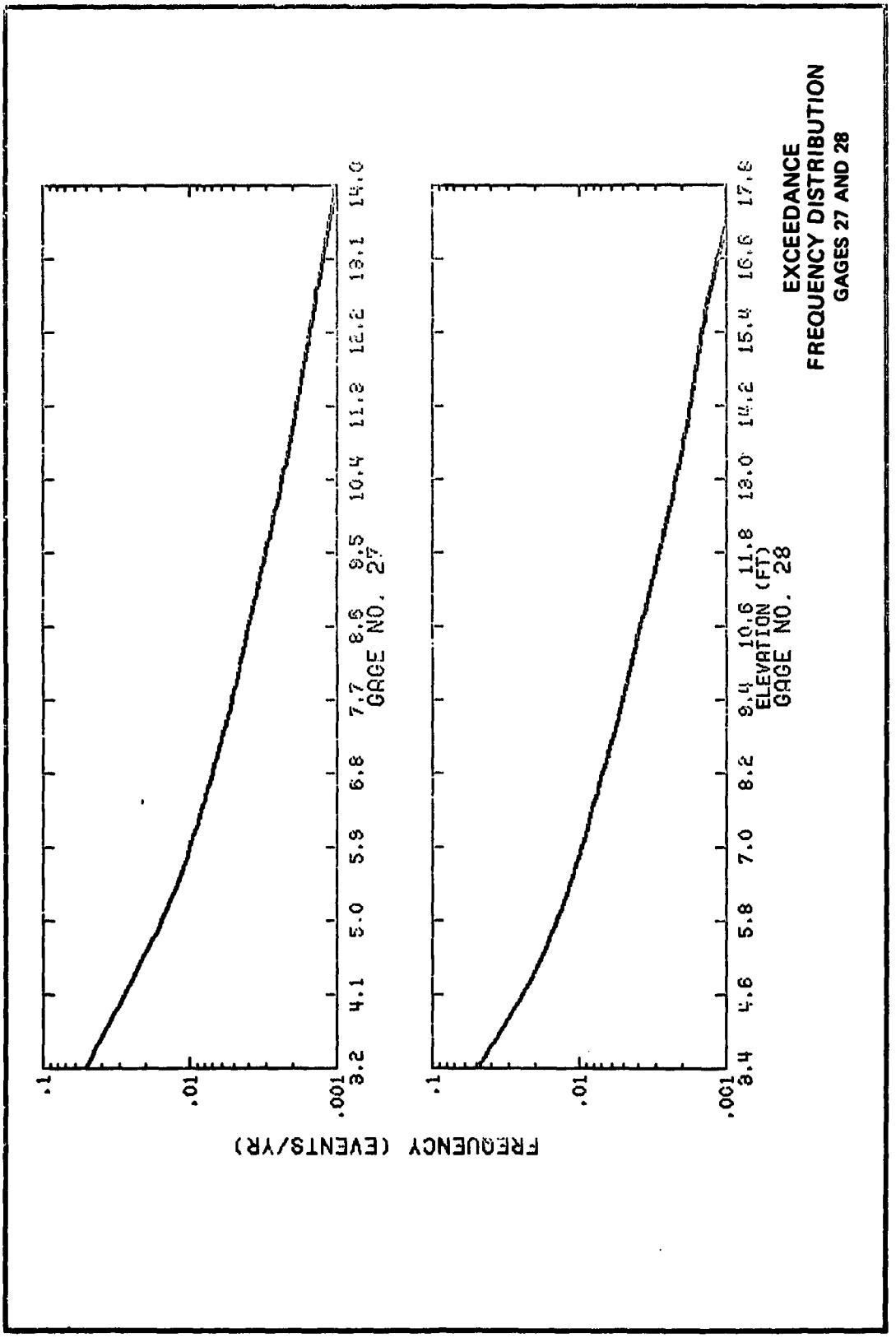
EXCEEDANCE
FREQUENCY DISTRIBUTION
GAGES 27 AND 28
FREQUENCY (EVENTS/YR)
.1
.01
.001
3.2
4.1
5.0
5.9
6.8
7.7
8.6
9.5
10.4
11.3
12.2
13.1
14.0
GAGE NO. 27
.1
.01
.001
3.4
4.6
5.8
7.0
8.2
9.4
10.6
11.8
13.0
14.2
15.4
16.6
17.8
ELEVATION (FT)
GAGE NO. 28

PLATE 14

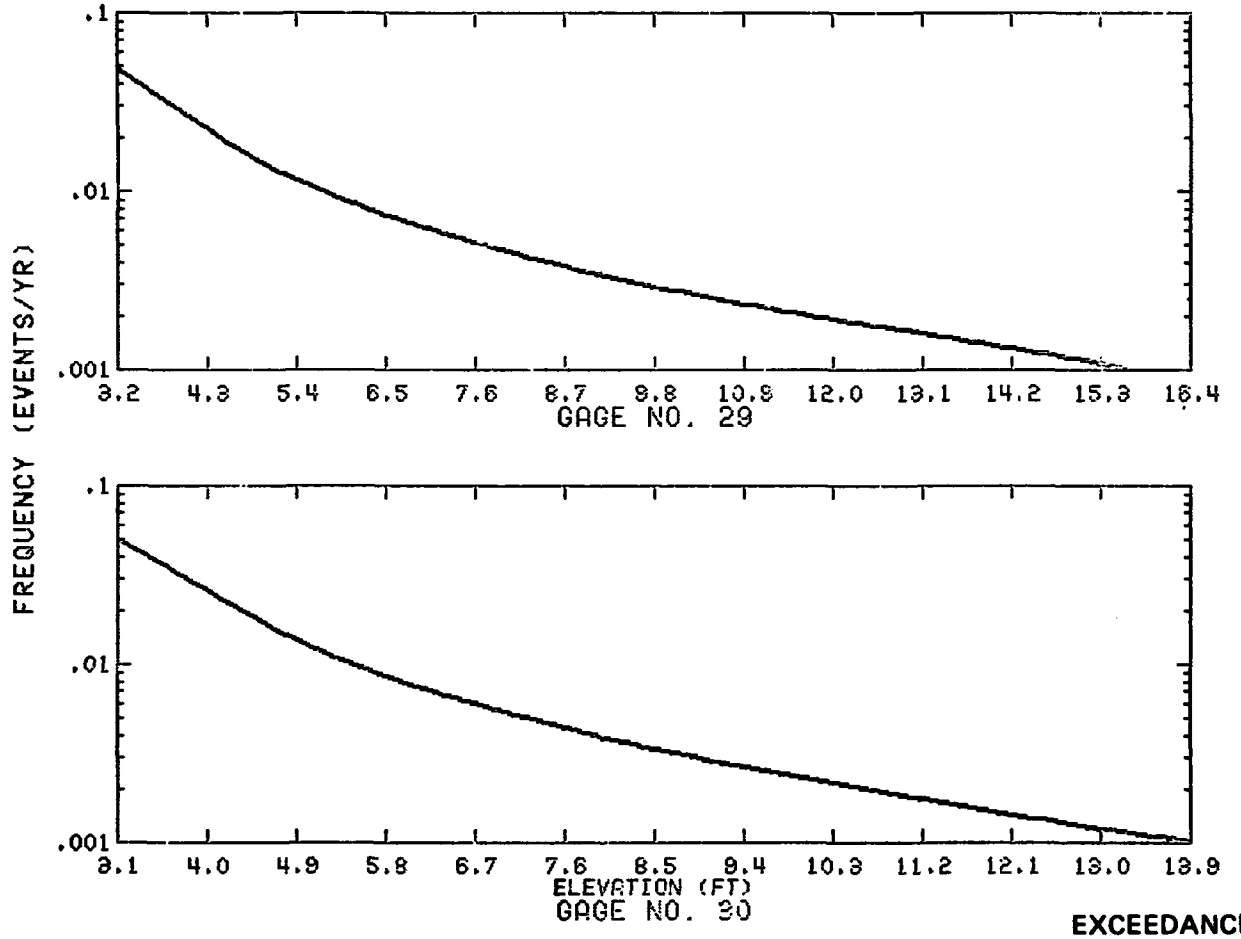

EXCEEDANCE FREQUENCY DISTRIBUTION
GAGES 29 AND 30

PLATE 15

PLATE 16

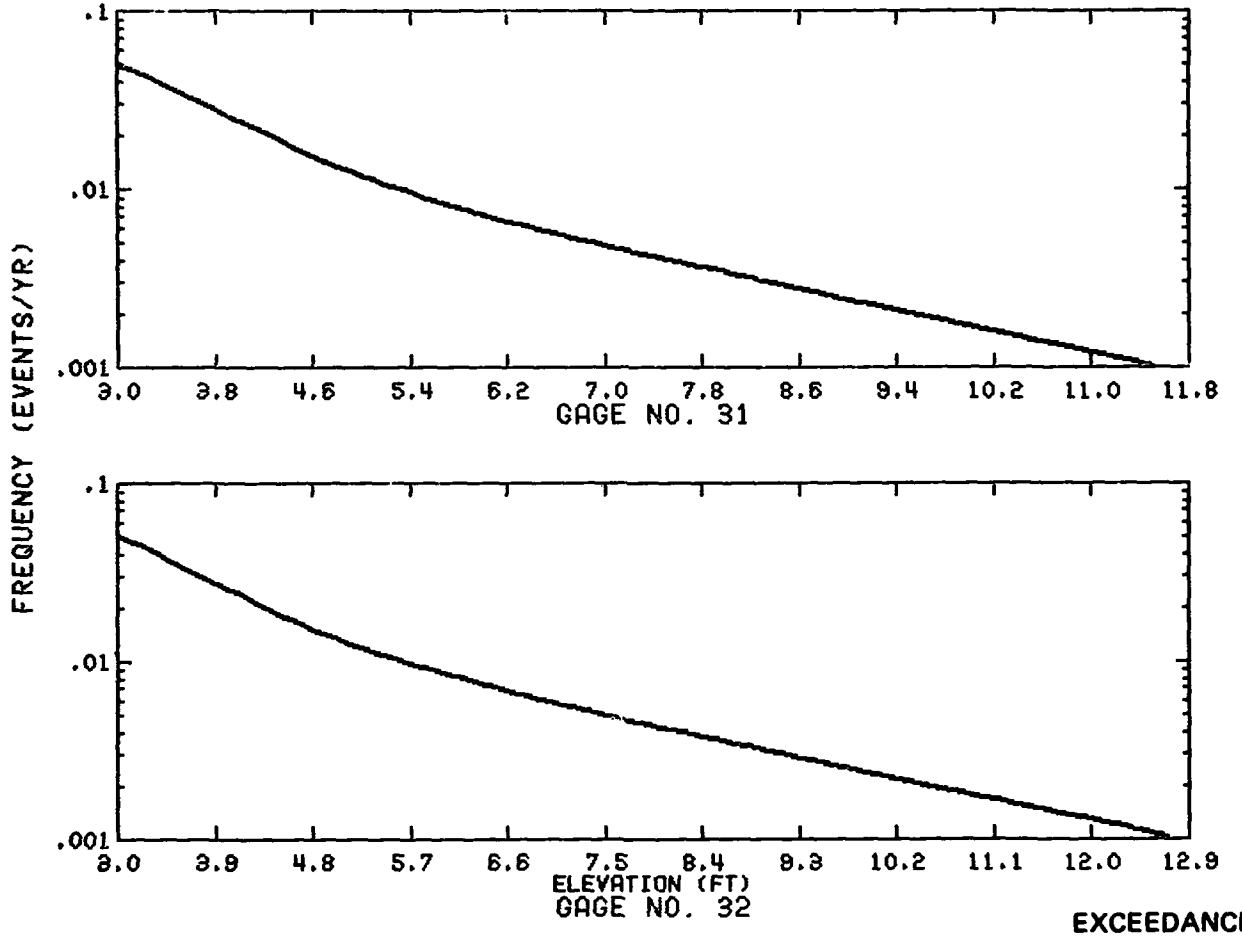

EXCEEDANCE FREQUENCY DISTRIBUTION
GAGES 31 AND 32

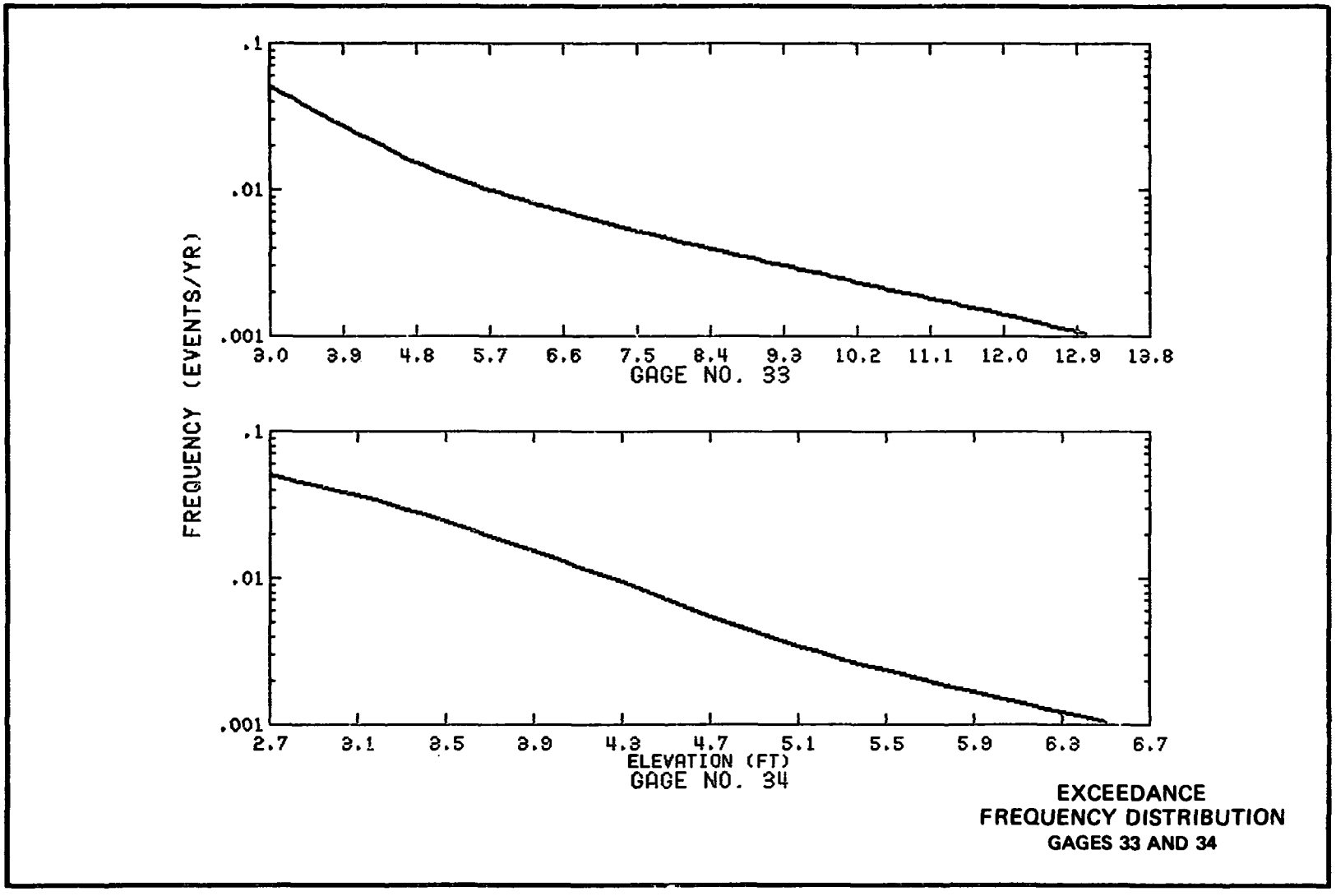

EXCEEDANCE FREQUENCY DISTRIBUTION
GAGES 33 AND 34

PLATE 17

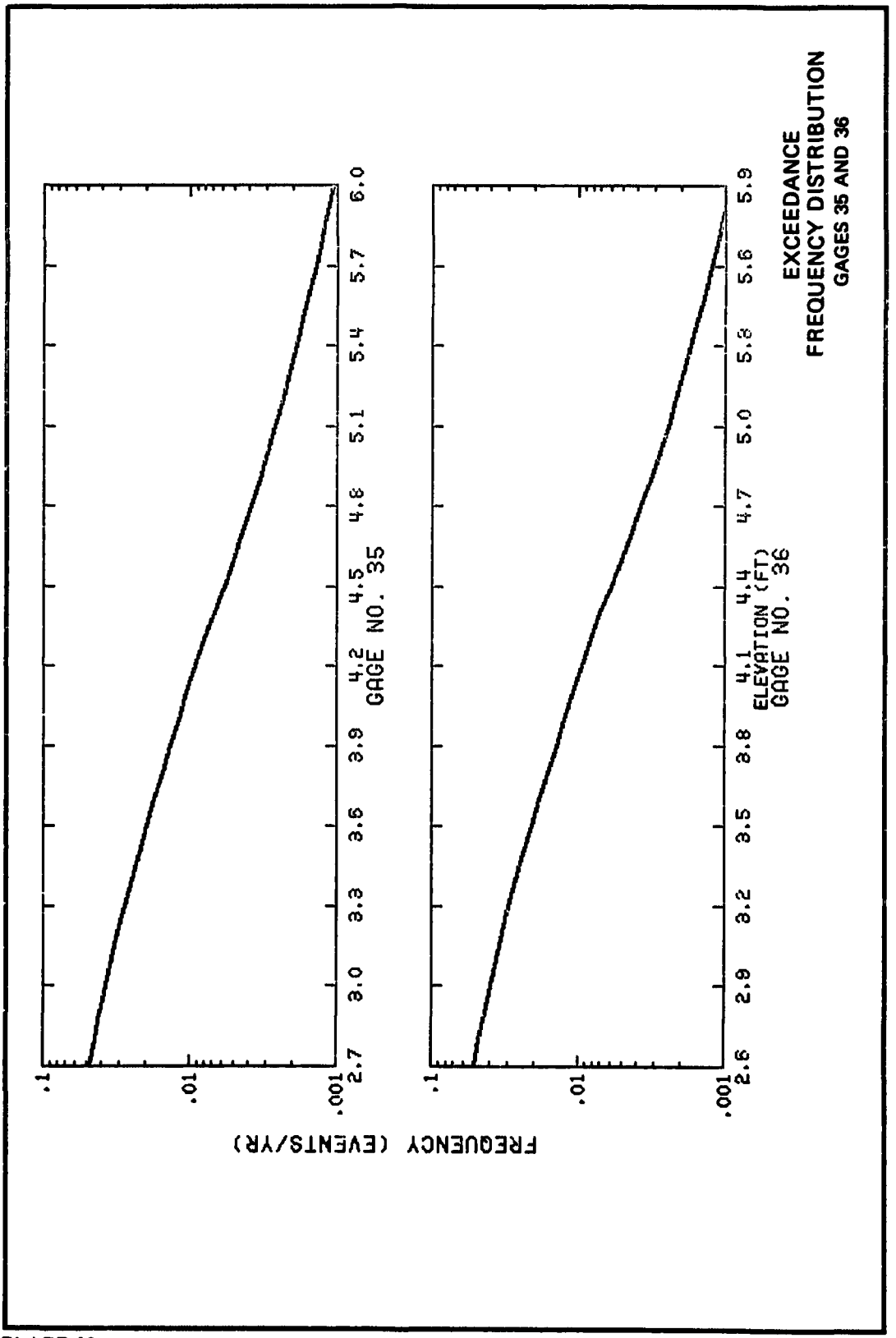
EXCEEDANCE
FREQUENCY DISTRIBUTION
GAGES 35 AND 36
FREQUENCY (EVENTS/YR)
.1
.01
.001
2.7
3.0
3.3
3.6
3.9
4.2
4.5
4.8
5.1
5.4
5.7
6.0
GAGE NO. 35
2.6
2.9
3.2
3.5
3.8
4.1
4.4
4.7
5.0
5.3
5.6
5.9
ELEVATION (FT)
GAGE NO. 36

PLATE 18

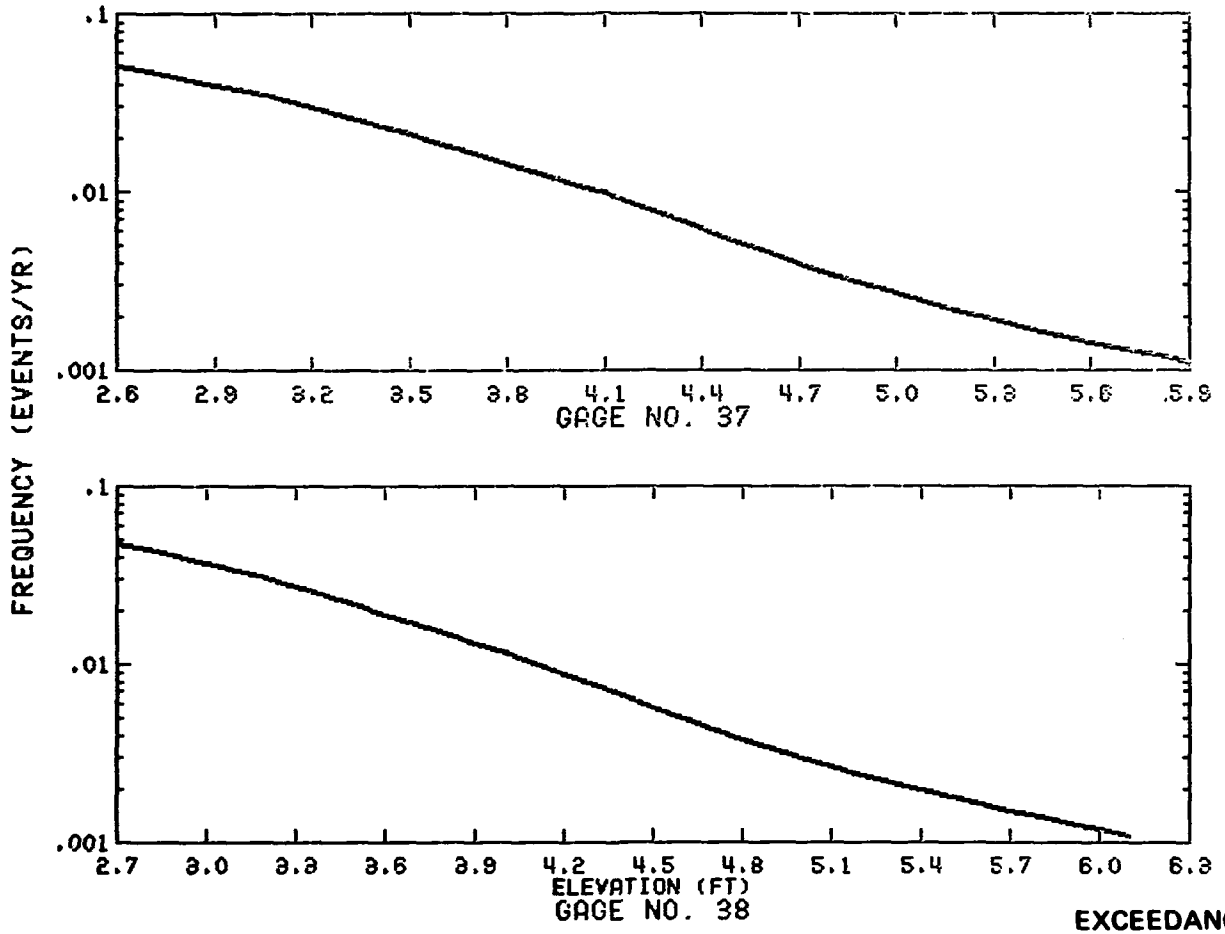

EXCEEDANCE FREQUENCY DISTRIBUTION
GAGES 37 AND 38

PLATE 19

PLATE 20

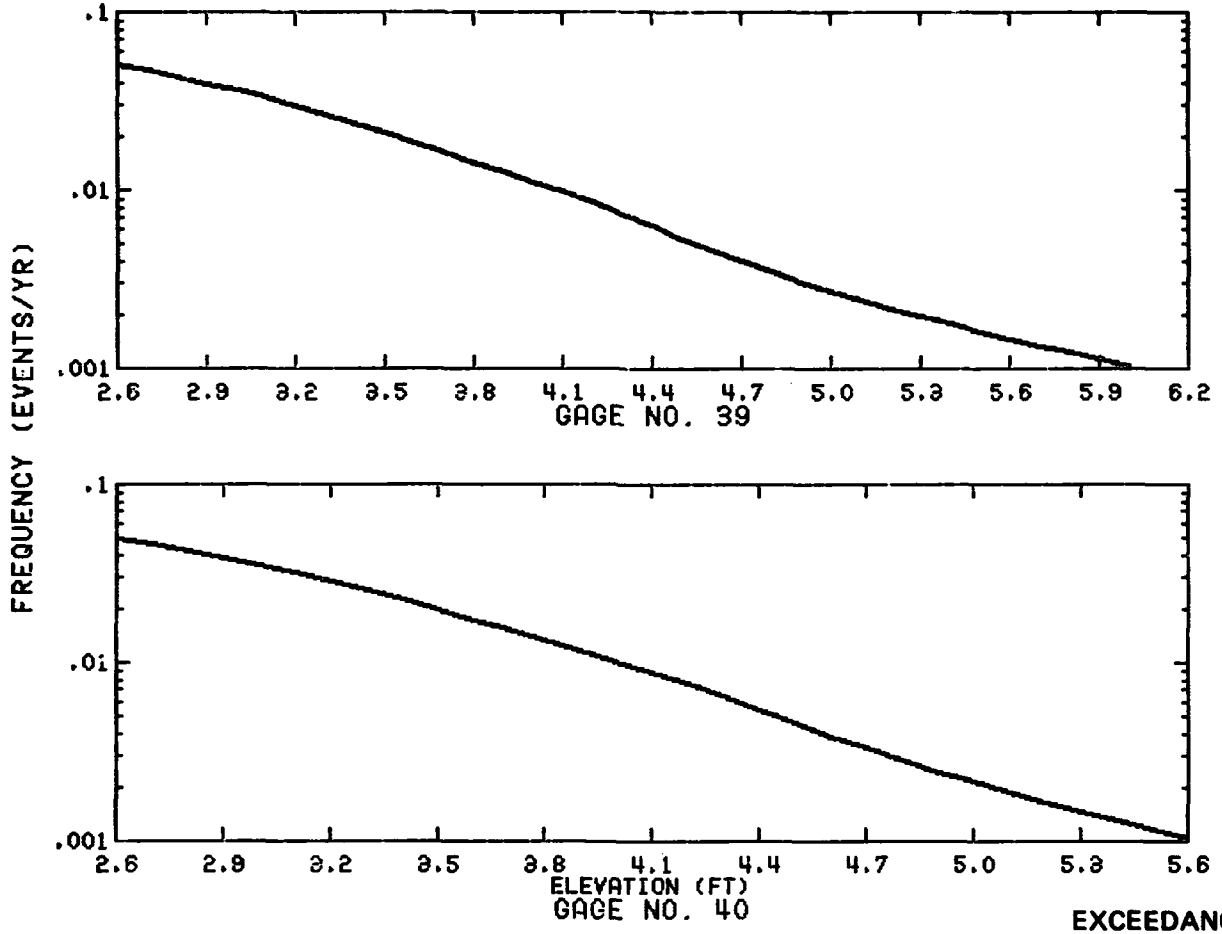

EXCEEDANCE FREQUENCY DISTRIBUTION
GAGES 39 AND 40

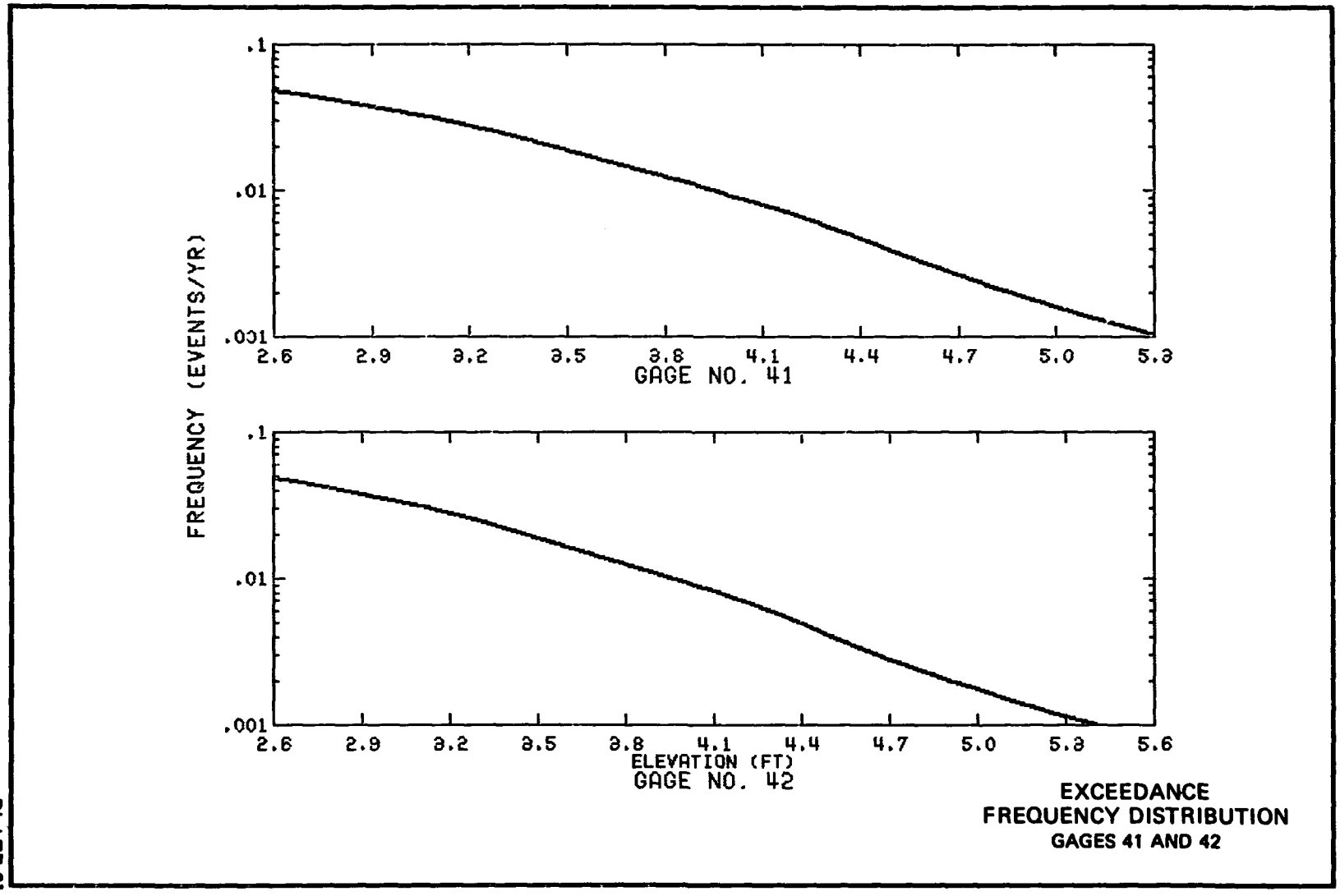

EXCEEDANCE FREQUENCY DISTRIBUTION
GAGES 41 AND 42

PLATE 21

PLATE 22

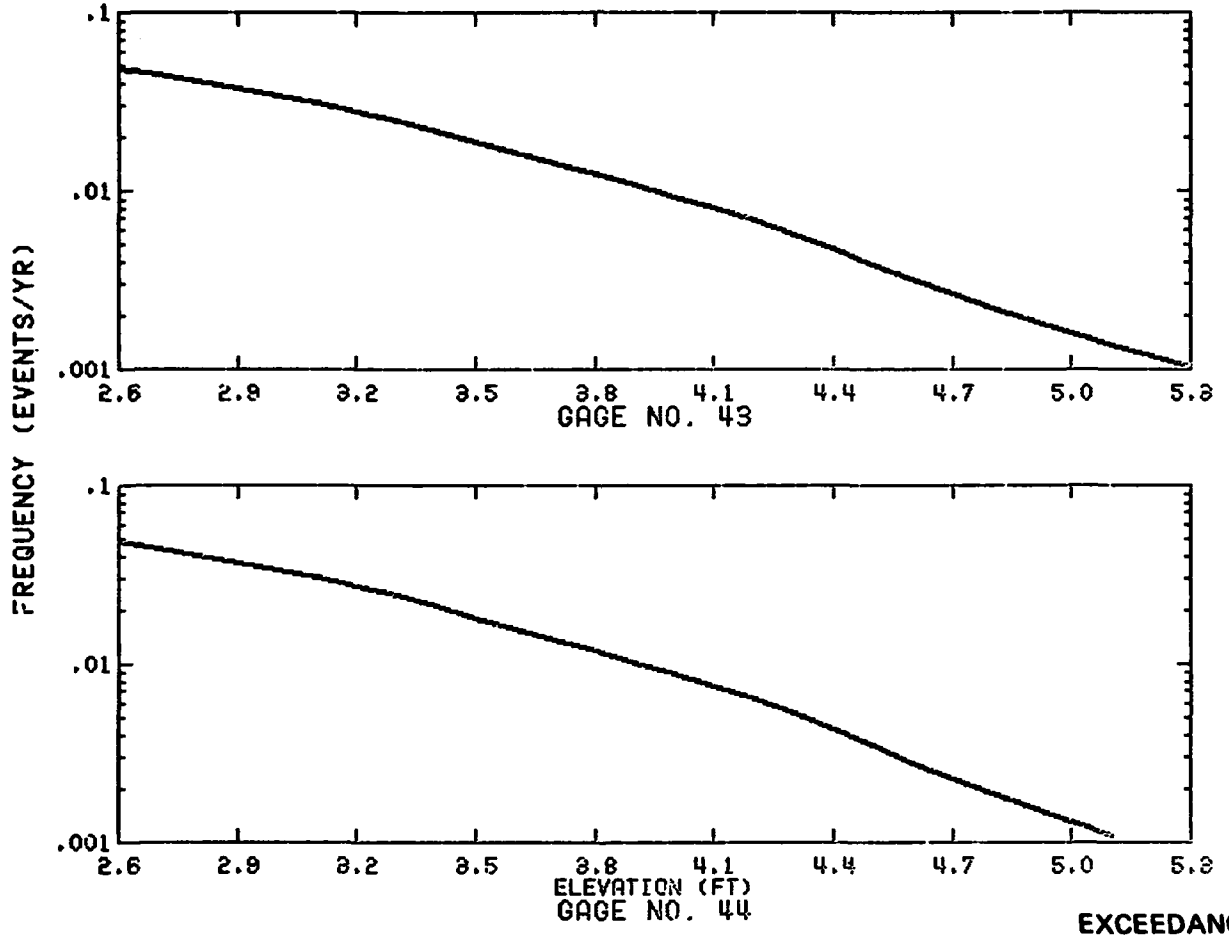

EXCEEDANCE FREQUENCY DISTRIBUTION
GAGES 43 AND 44

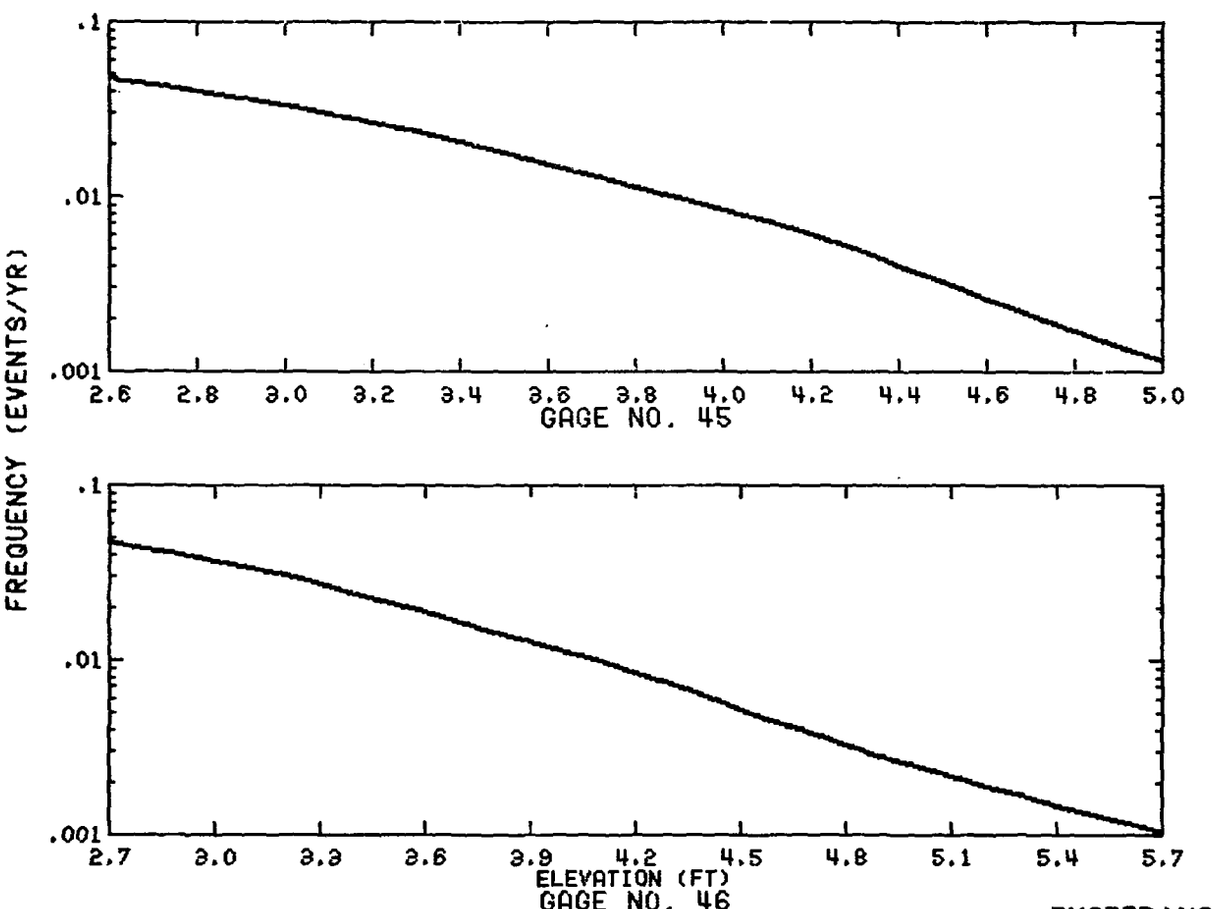

EXCEEDANCE FREQUENCY DISTRIBUTION
GAGES 45 AND 46

PLATE 23

PLATE 24

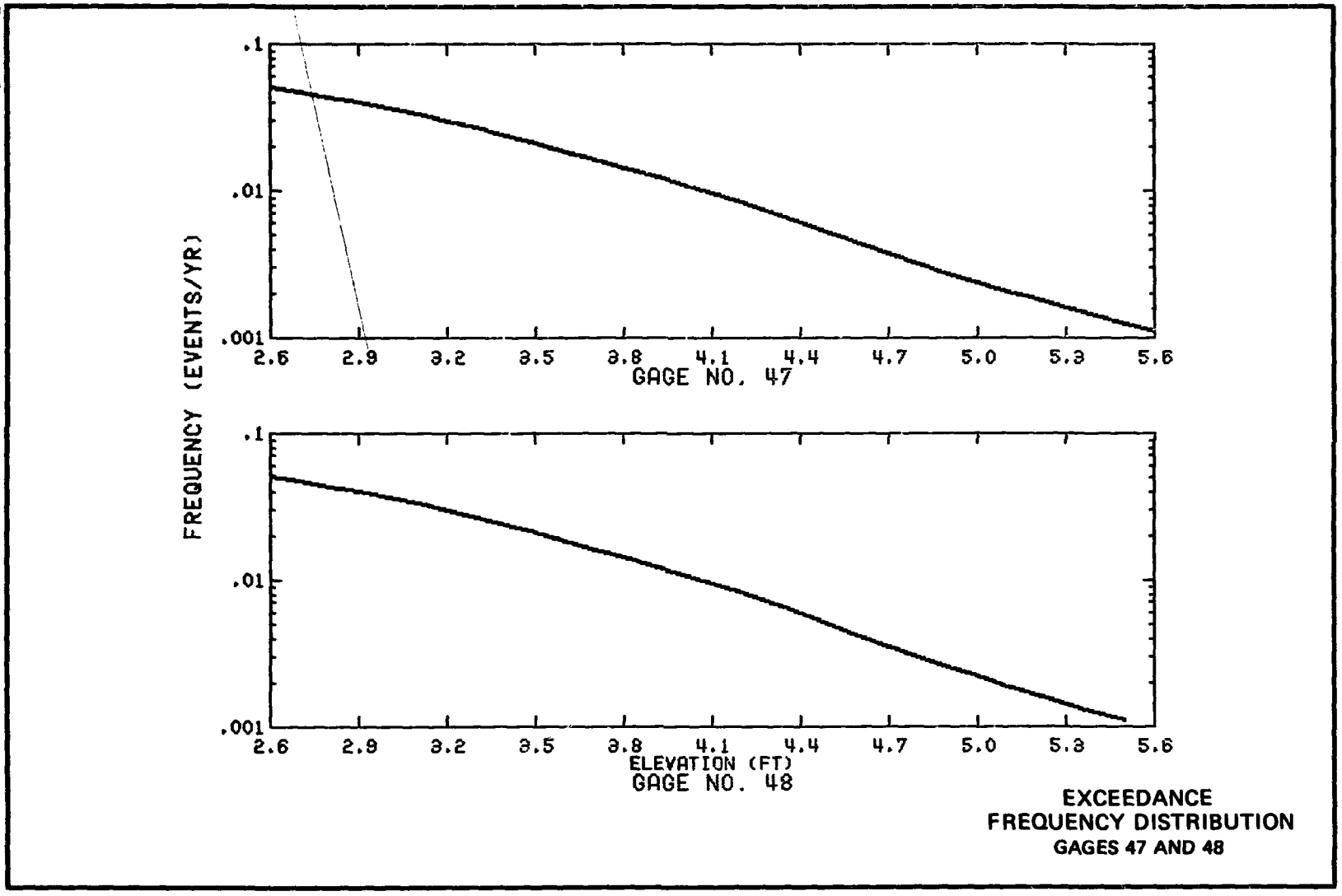

EXCEEDANCE FREQUENCY DISTRIBUTION
GAGES 47 AND 48

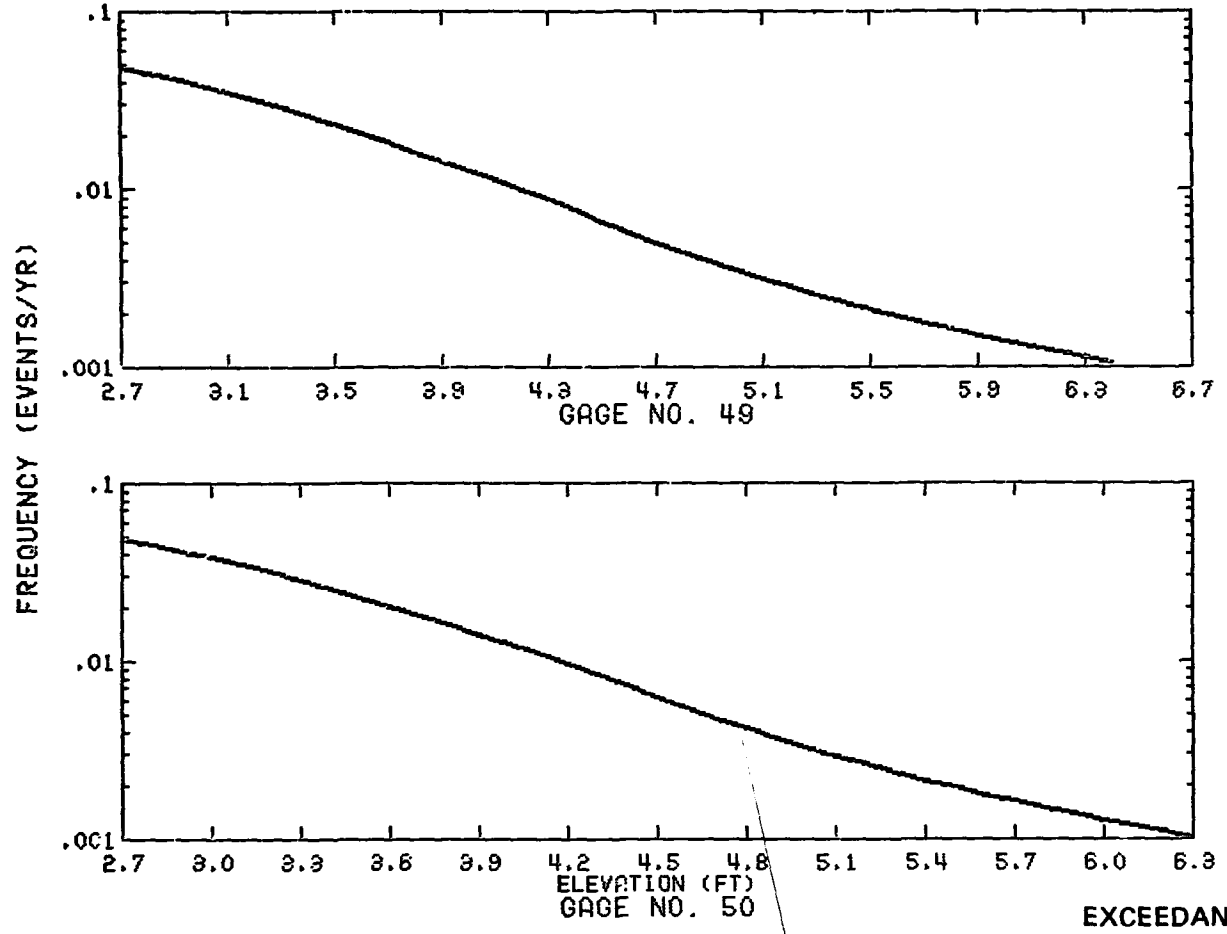

EXCEEDANCE FREQUENCY DISTRIBUTION
GAGES 49 AND 50

PLATE 25

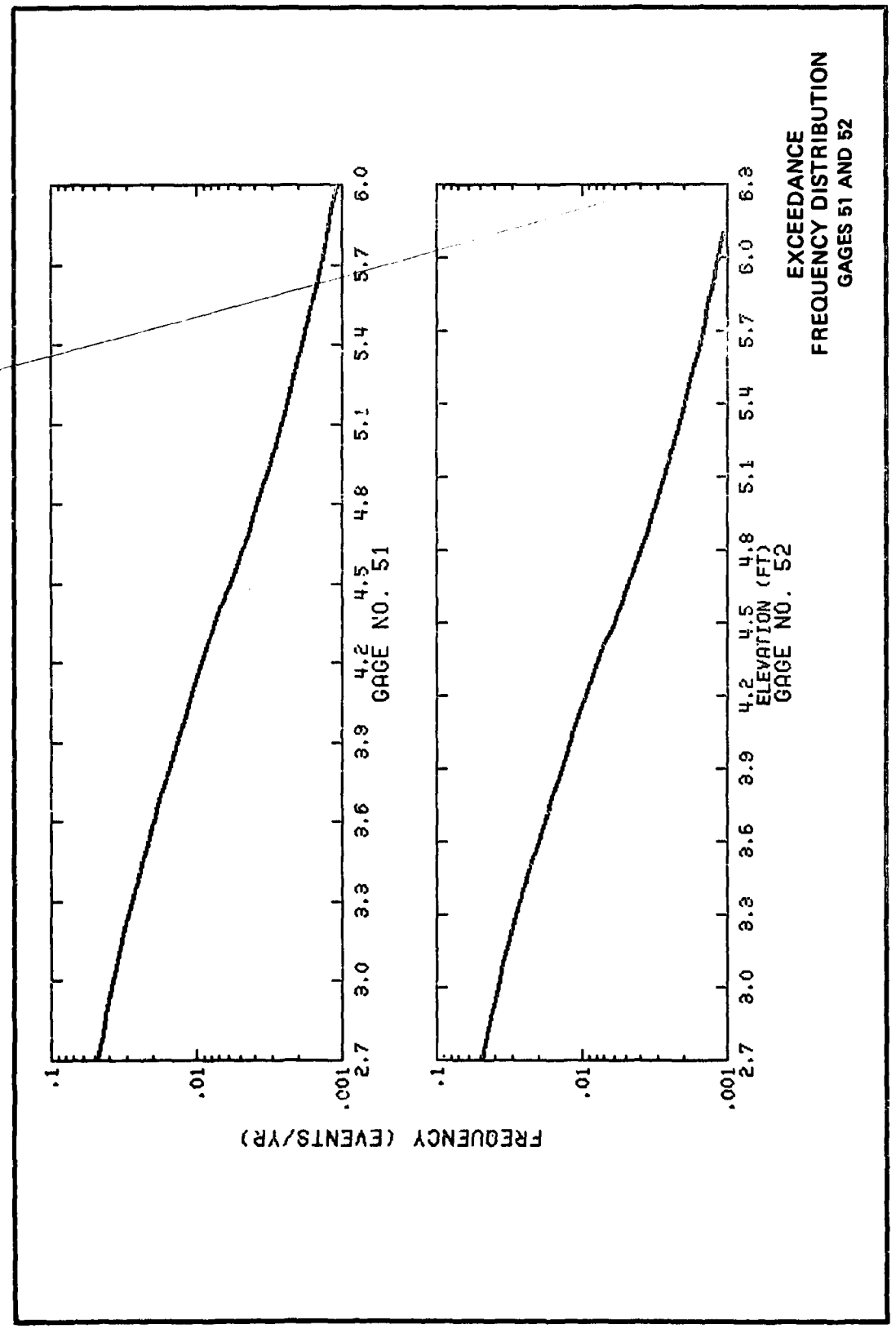
EXCEEDANCE
FREQUENCY DISTRIBUTION
GAGES 51 AND 52
FREQUENCY (EVENTS/YR)
.1
.01
.001
2.7
3.0
3.3
3.6
3.9
4.2
4.5
4.8
5.1
5.4
5.7
6.0
6.3
ELEVATION (FT)
GAGE NO. 51
GAGE NO. 52

PLATE 26

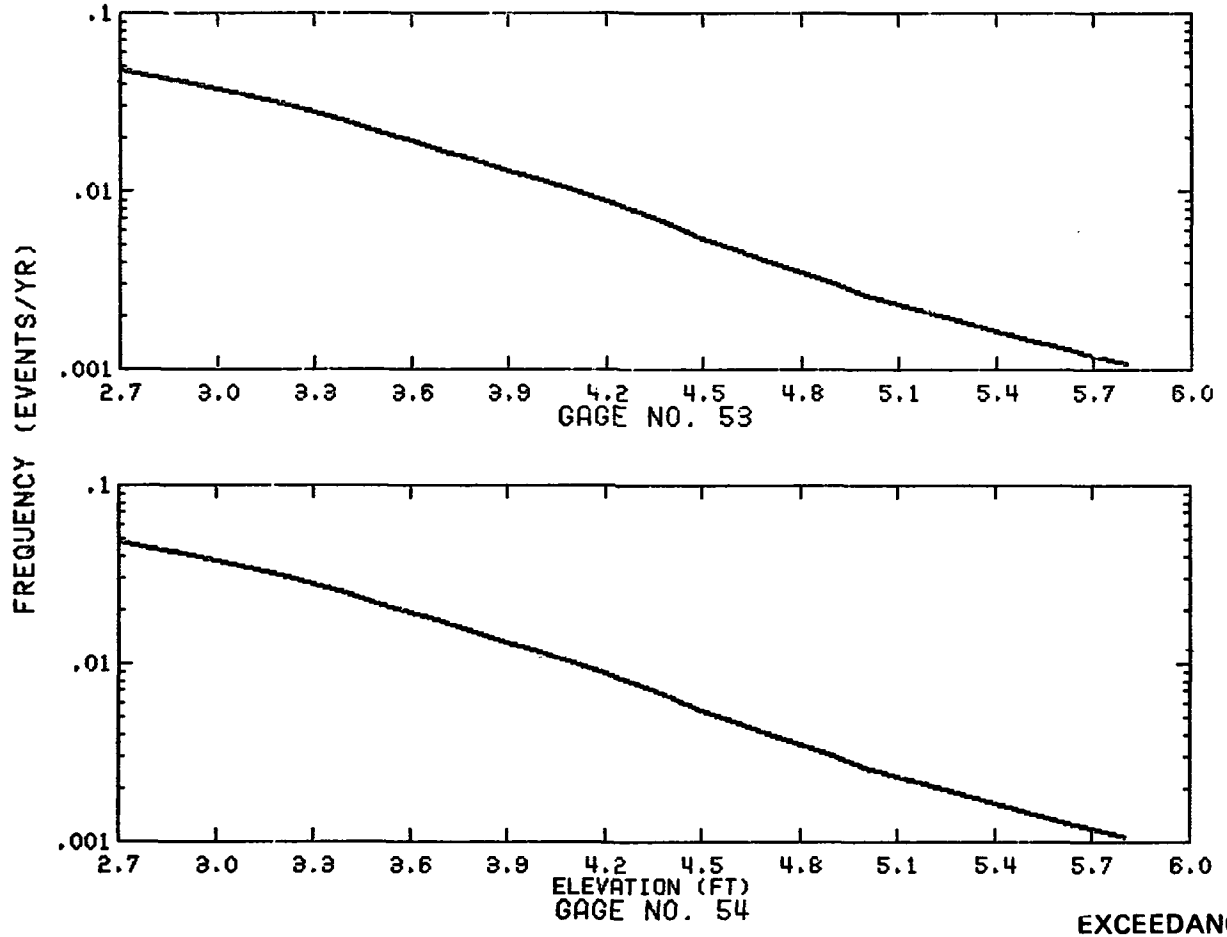

EXCEEDANCE FREQUENCY DISTRIBUTION
GAGES 53 AND 54

PLATE 27

PLATE 28

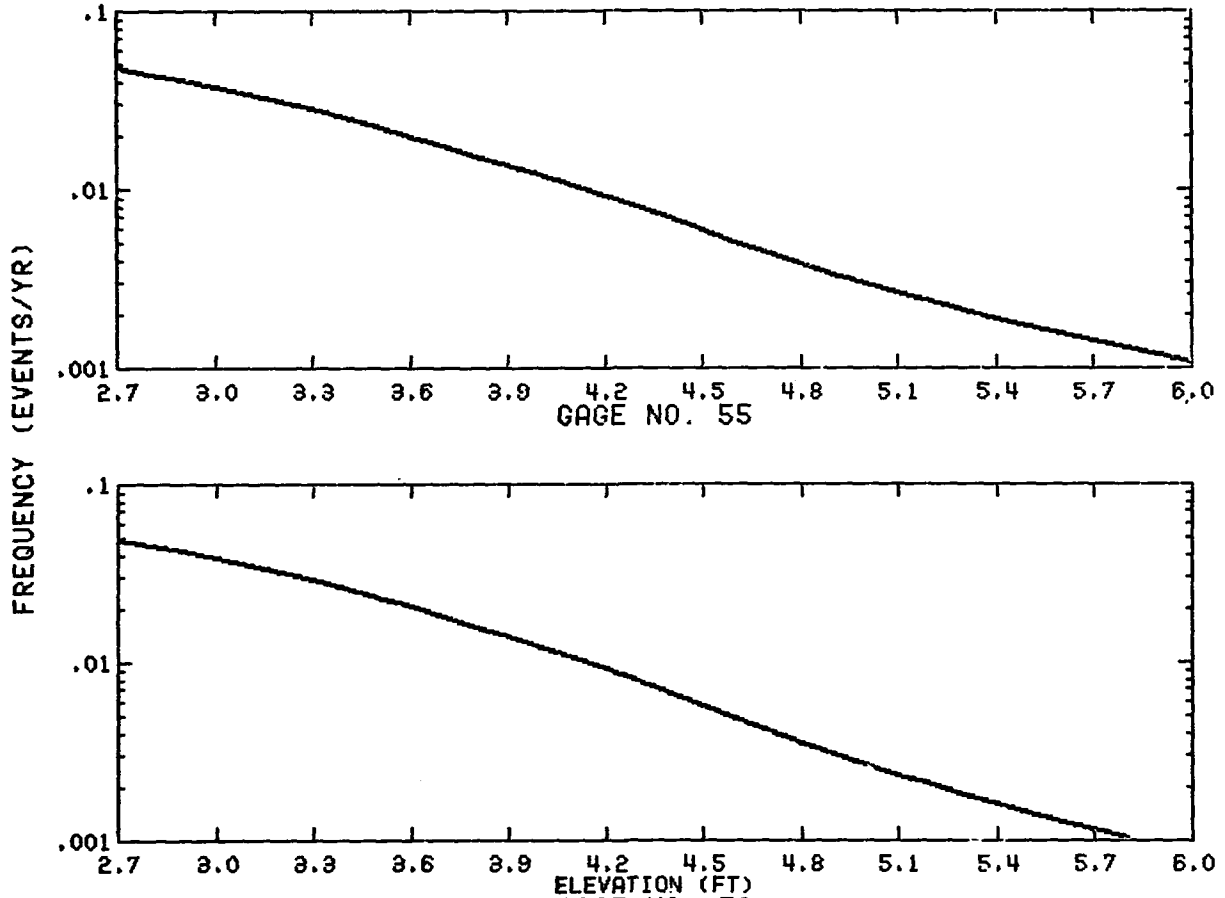

EXCEEDANCE FREQUENCY DISTRIBUTION
GAGES 55 AND 56

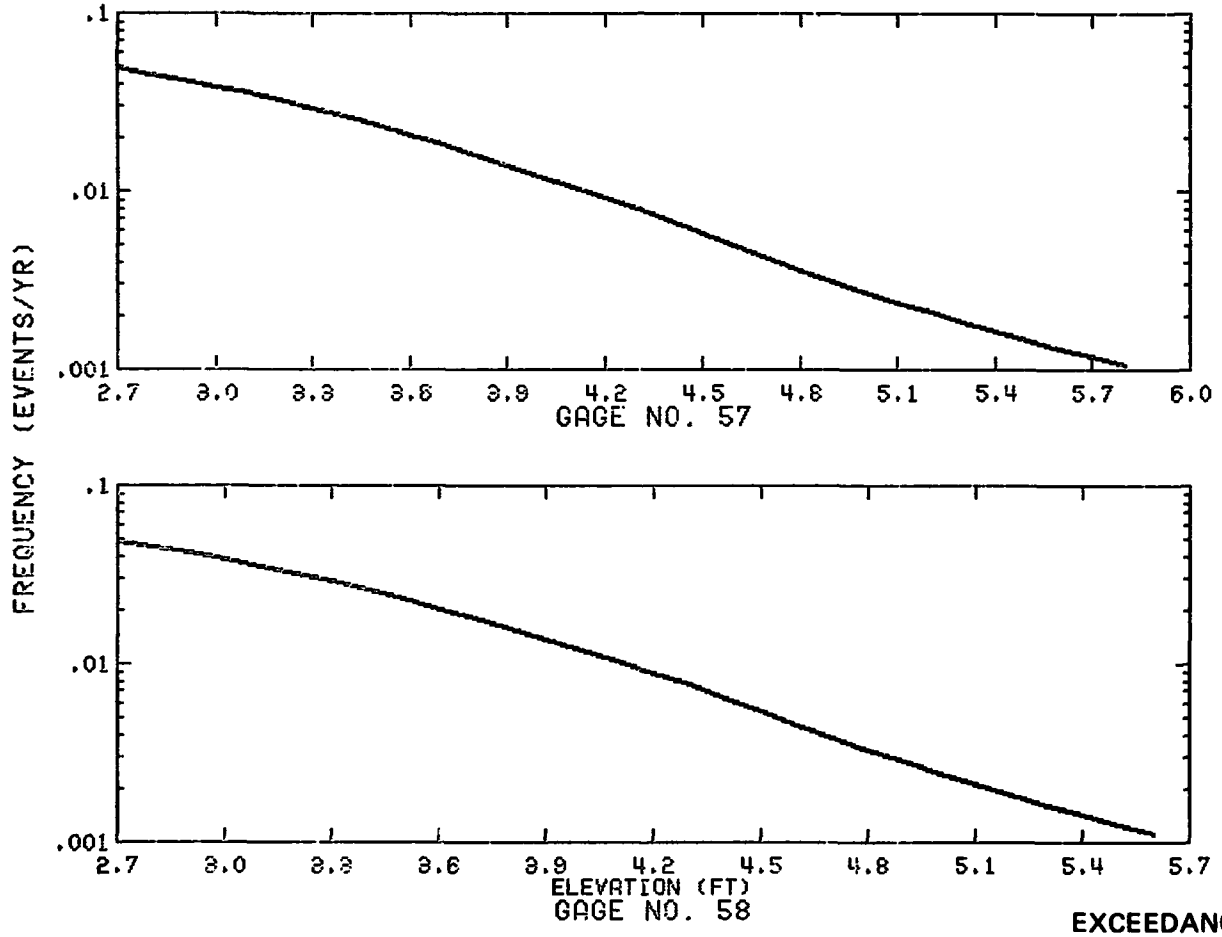

EXCEEDANCE FREQUENCY DISTRIBUTION
GAGES 57 AND 58

PLATE 29

PLATE 30

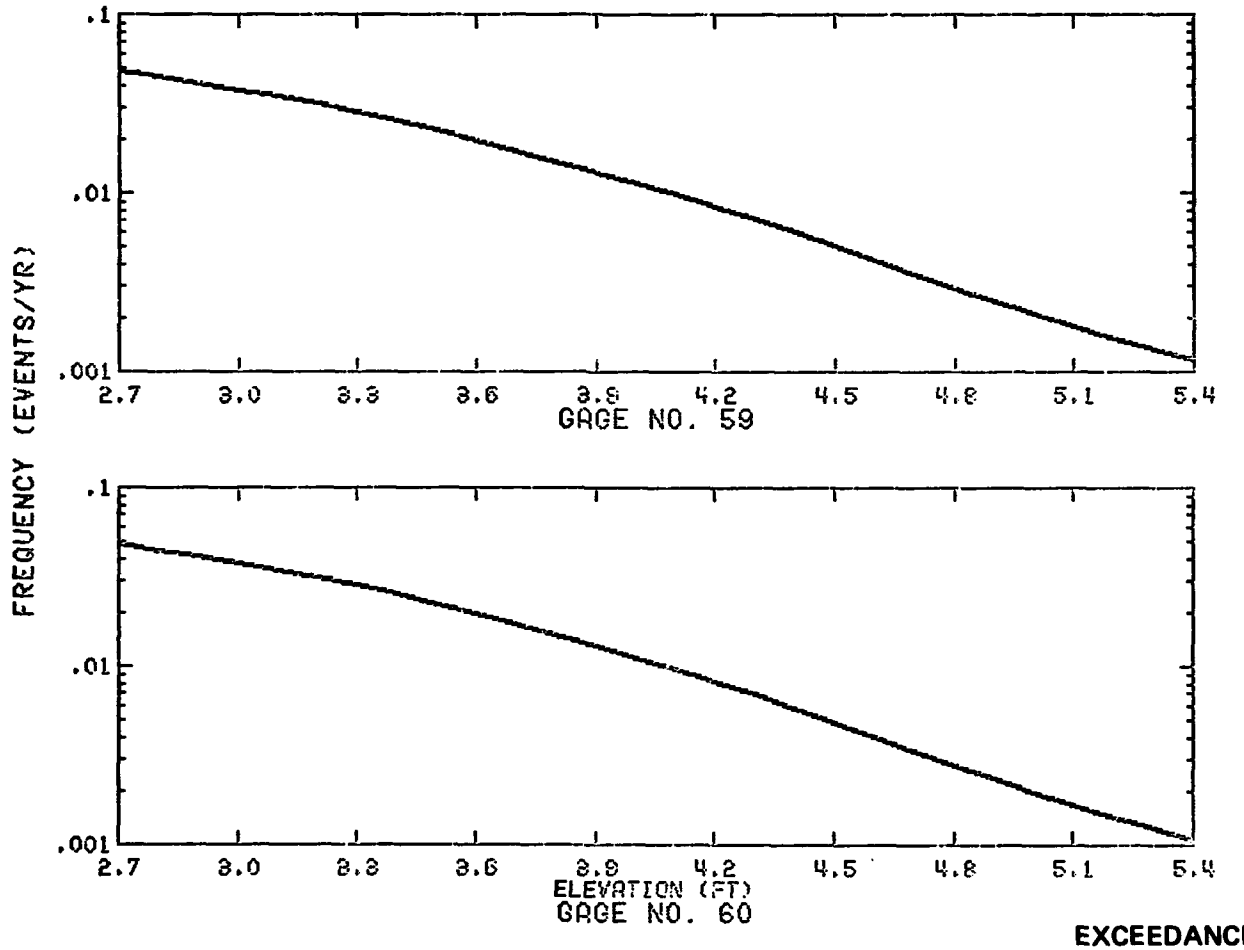

EXCEEDANCE FREQUENCY DISTRIBUTION
GAGES 59 AND 60

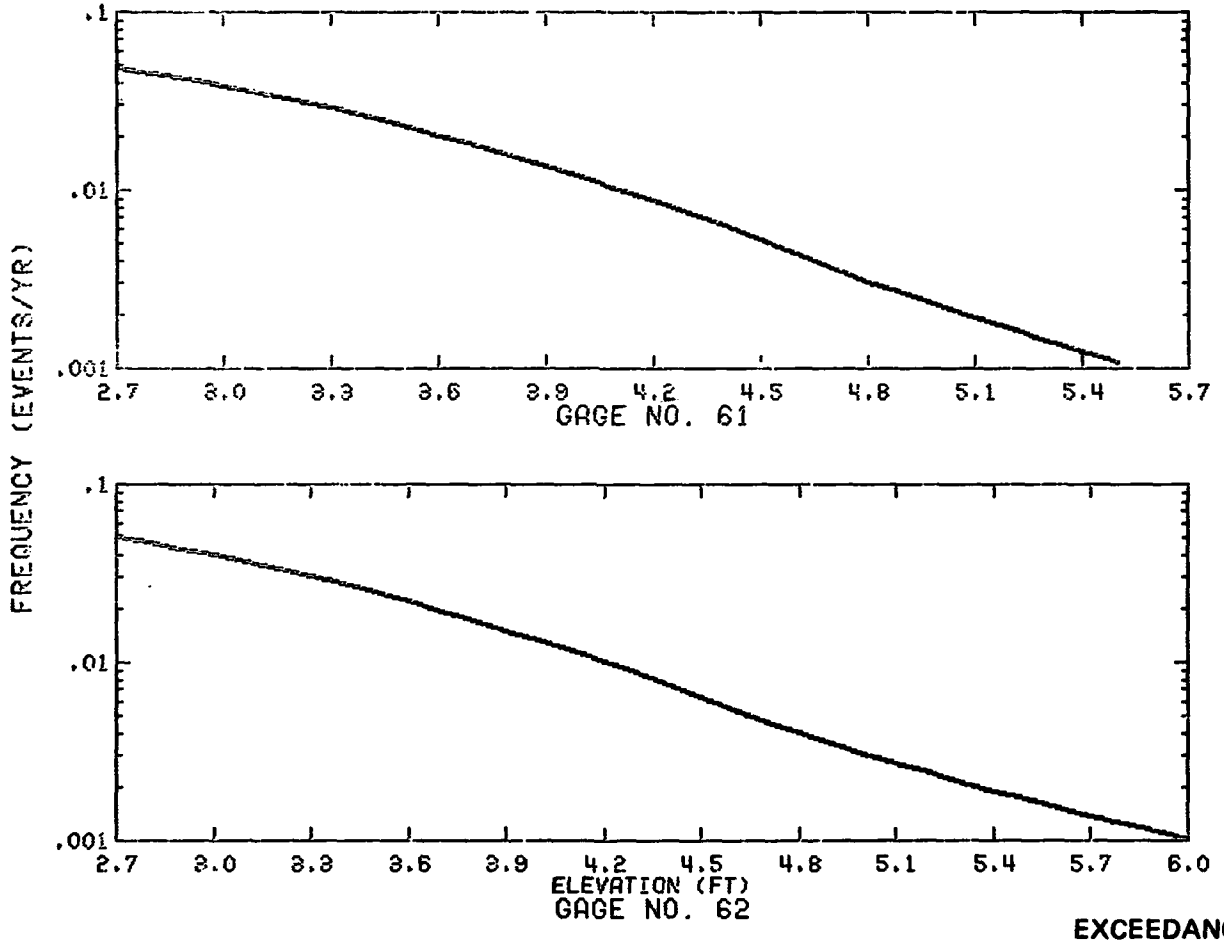

EXCEEDANCE FREQUENCY DISTRIBUTION
GAGES 61 AND 62

PLATE 31

PLATE 32

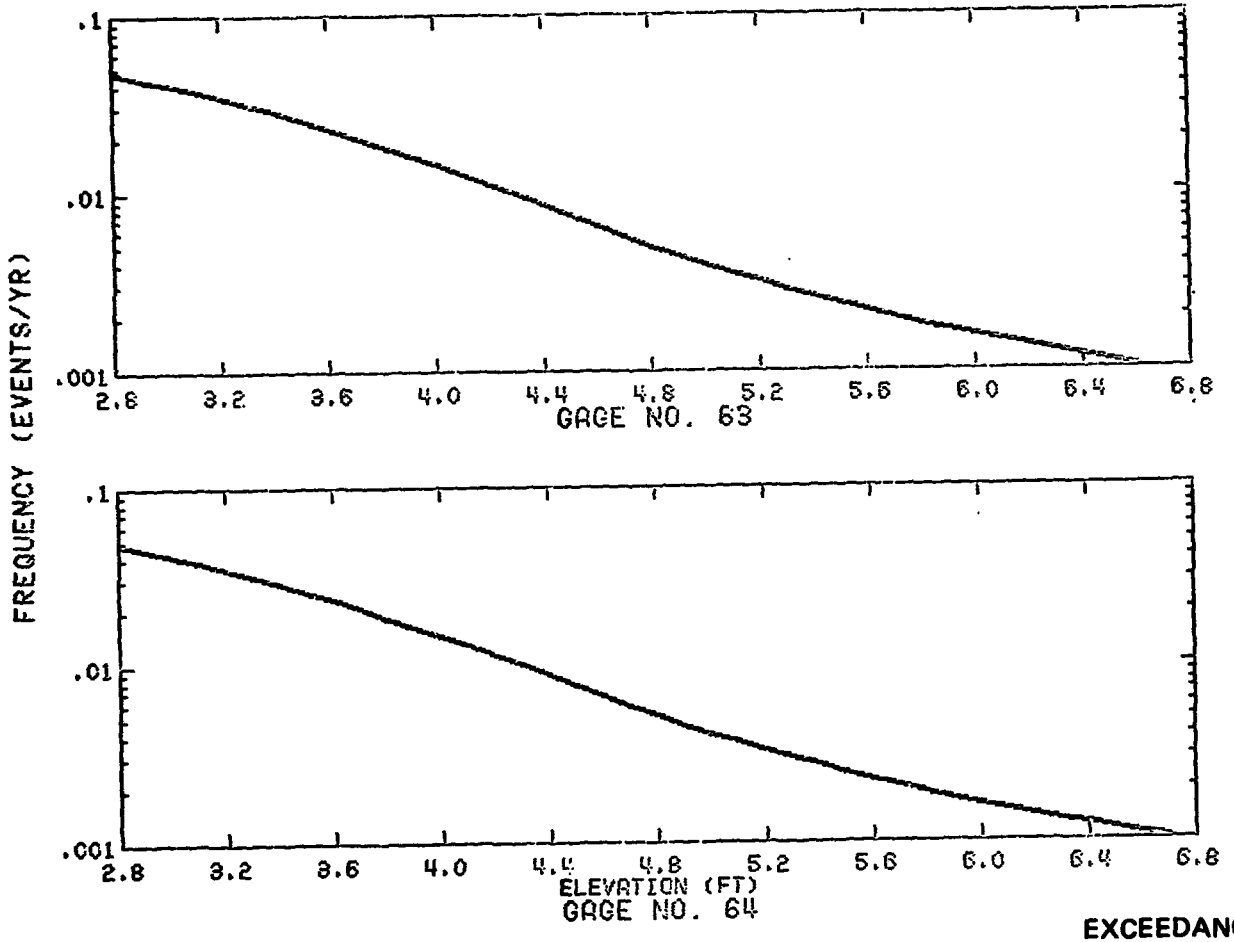

EXCEEDANCE FREQUENCY DISTRIBUTION
GAGES 63 AND 64

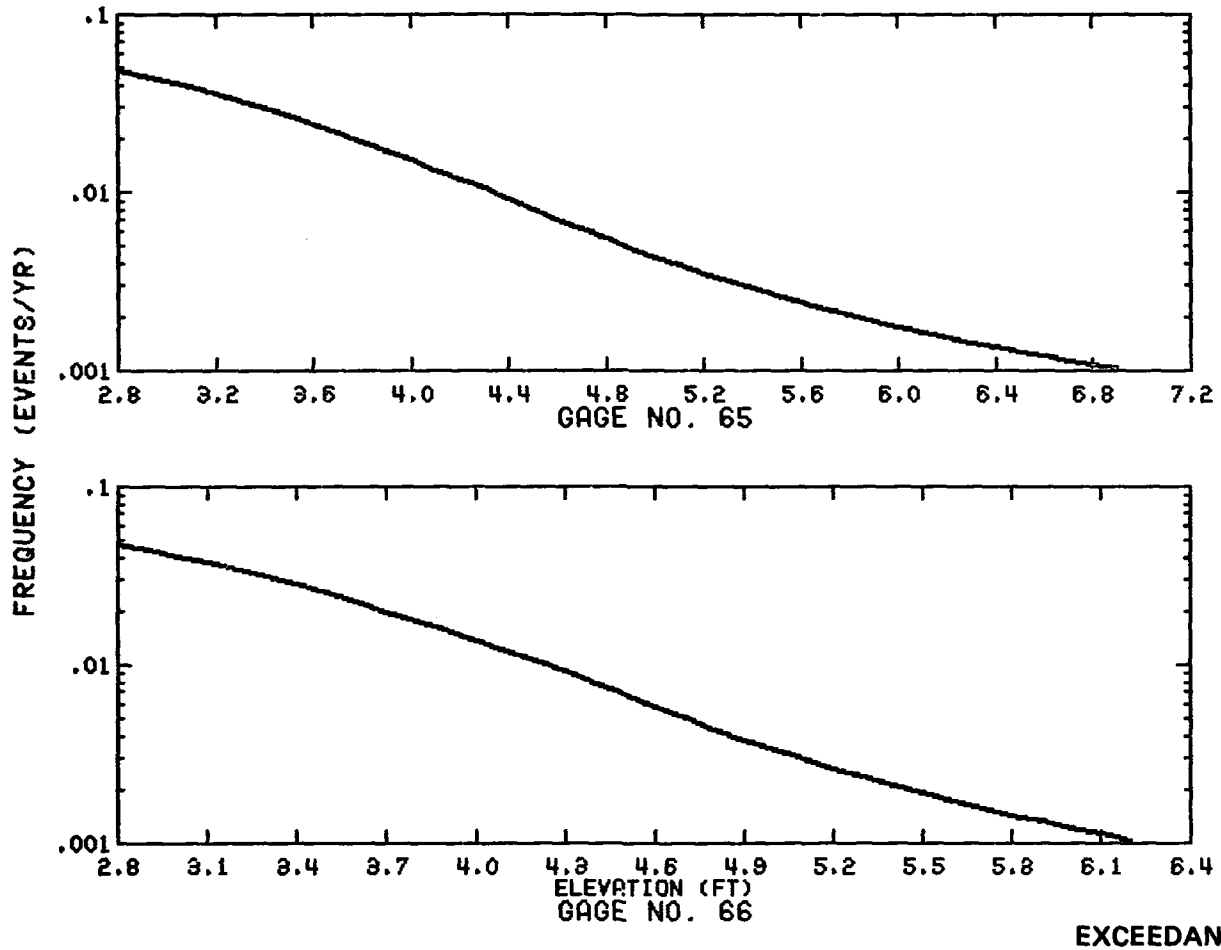

EXCEEDANCE FREQUENCY DISTRIBUTION
GAGES 65 AND 66

PLATE 33

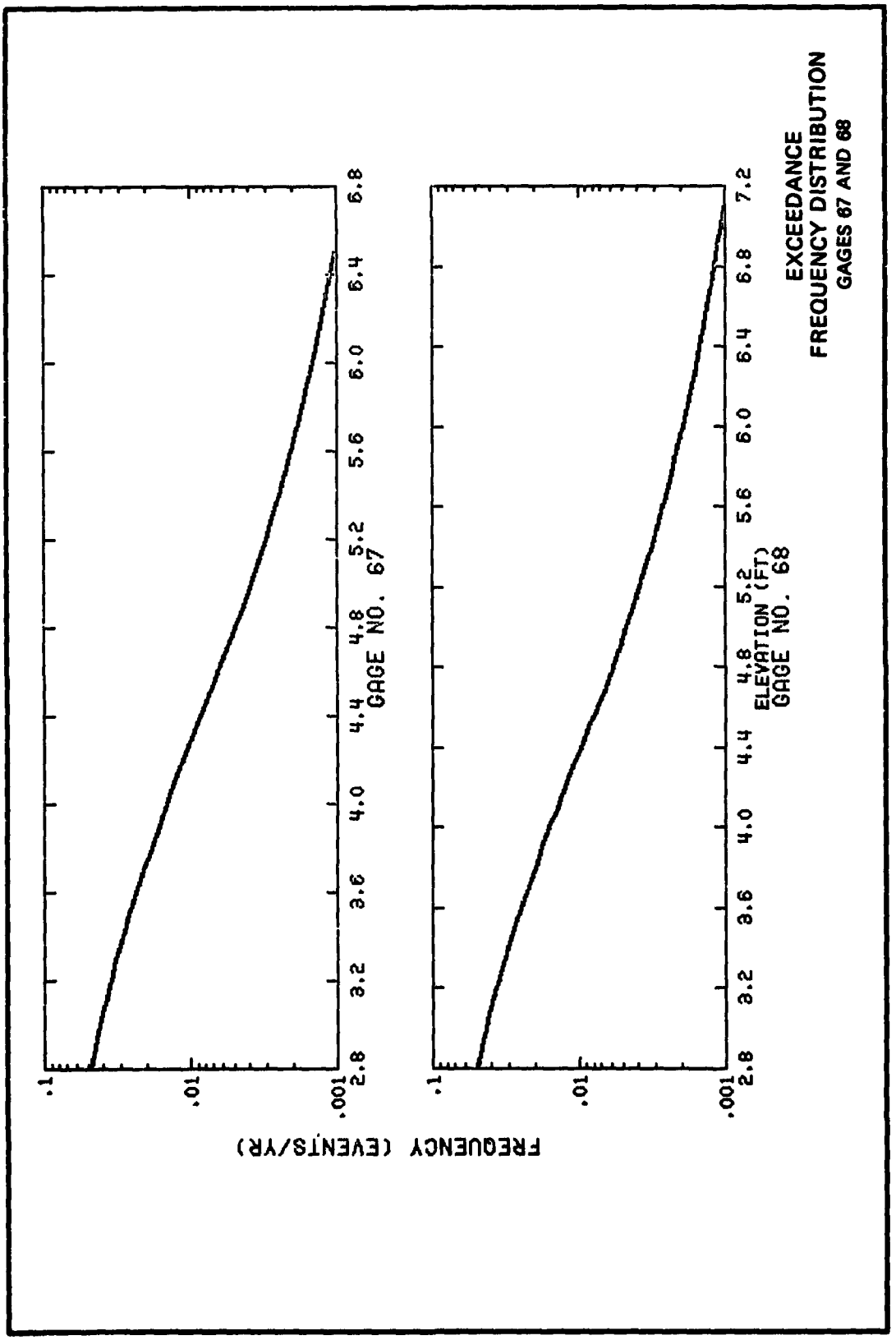
EXCEEDANCE
FREQUENCY DISTRIBUTION
GAGES 67 AND 68
FREQUENCY (EVENTS/YR)
.1
.01
.001
2.8
3.2
3.6
4.0
4.4
4.8
5.2
5.6
6.0
6.4
6.8
7.2
GAGE NO. 67
ELEVATION (FT)
GAGE NO. 68

PLATE 34

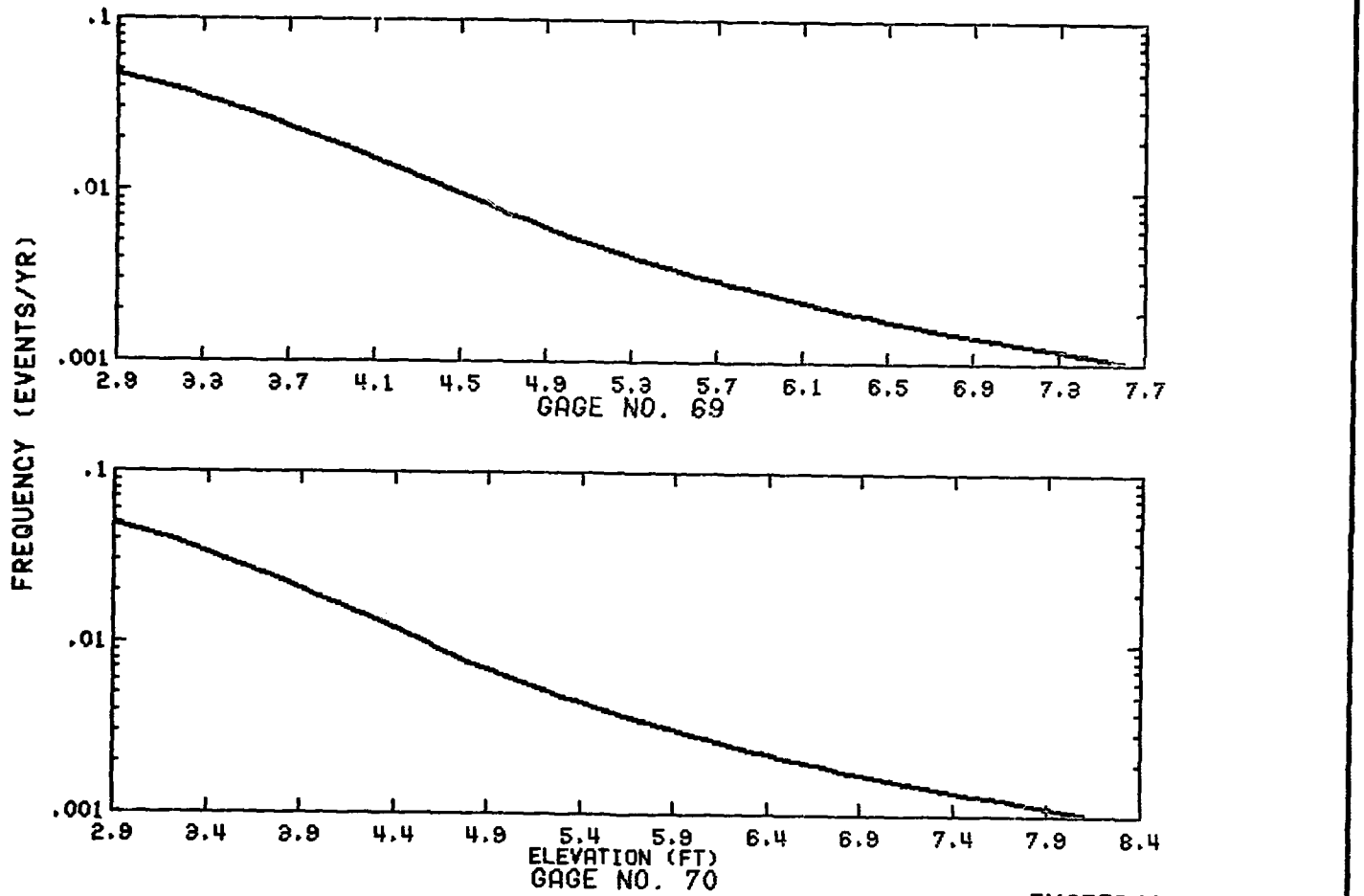

EXCEEDANCE FREQUENCY DISTRIBUTION
GAGES 69 AND 70

PLATE 35

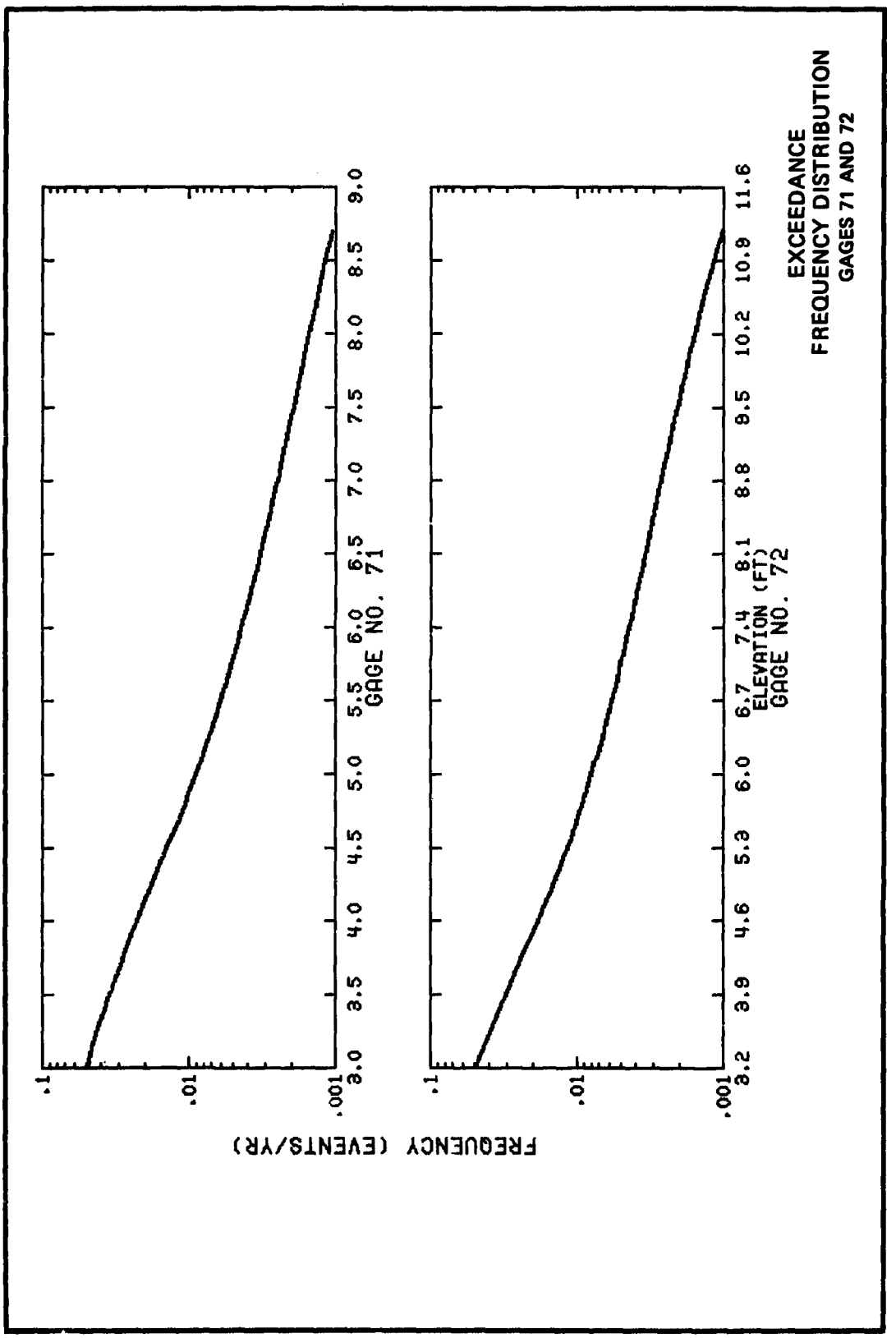
EXCEEDANCE
FREQUENCY DISTRIBUTION
GAGES 71 AND 72
FREQUENCY (EVENTS/YR)
.1
.01
.001
3.0 3.5 4.0 4.5 5.0 5.5 6.0 6.5 7.0 7.5 8.0 8.5 9.0
GAGE NO. 71
3.2 3.9 4.6 5.3 6.0 6.7 7.4 8.1 8.8 9.5 10.2 10.9 11.6
ELEVATION (FT)
GAGE NO. 72

PLATE 36

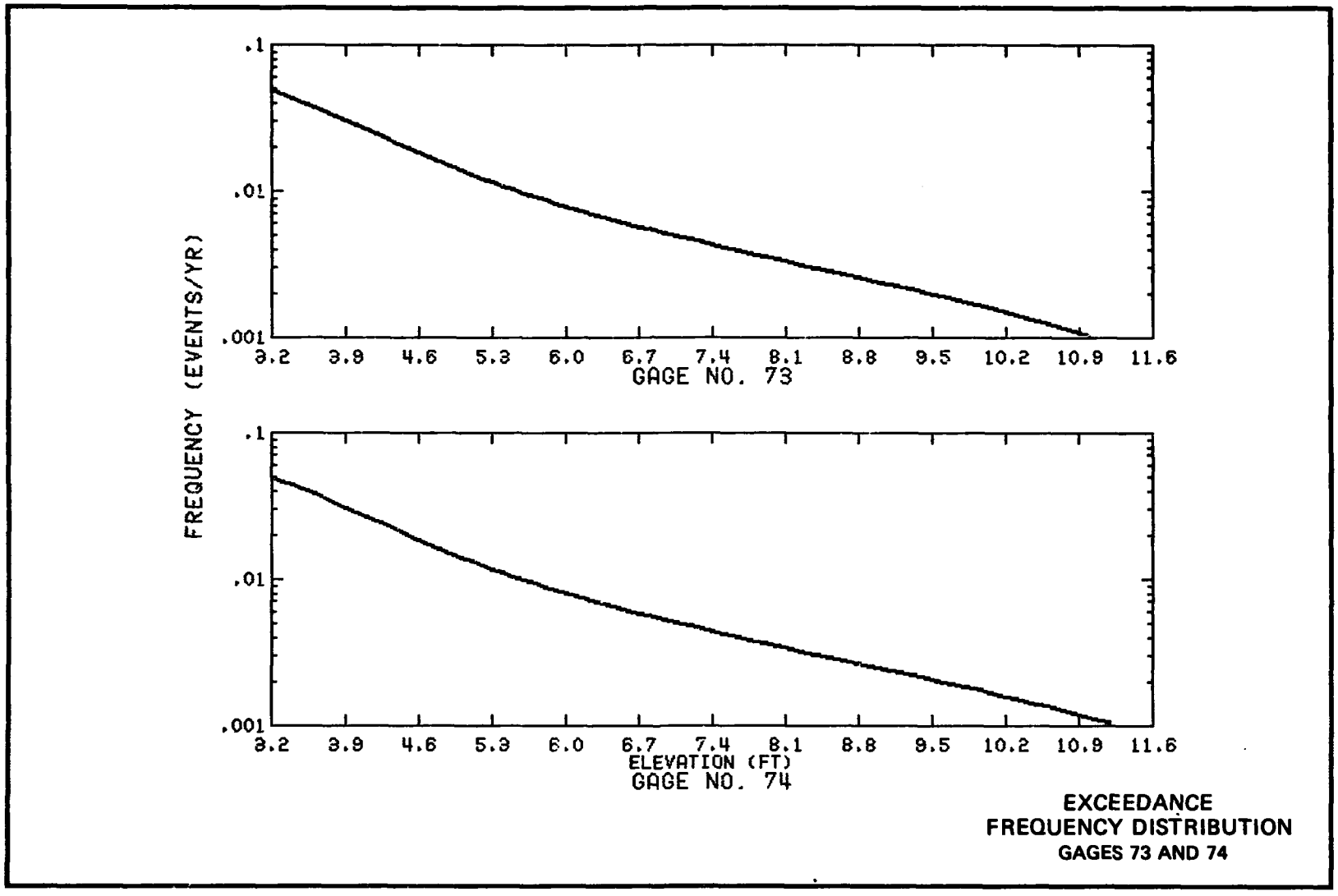

EXCEEDANCE FREQUENCY DISTRIBUTION
GAGES 73 AND 74

PLATE 37

PLATE 38

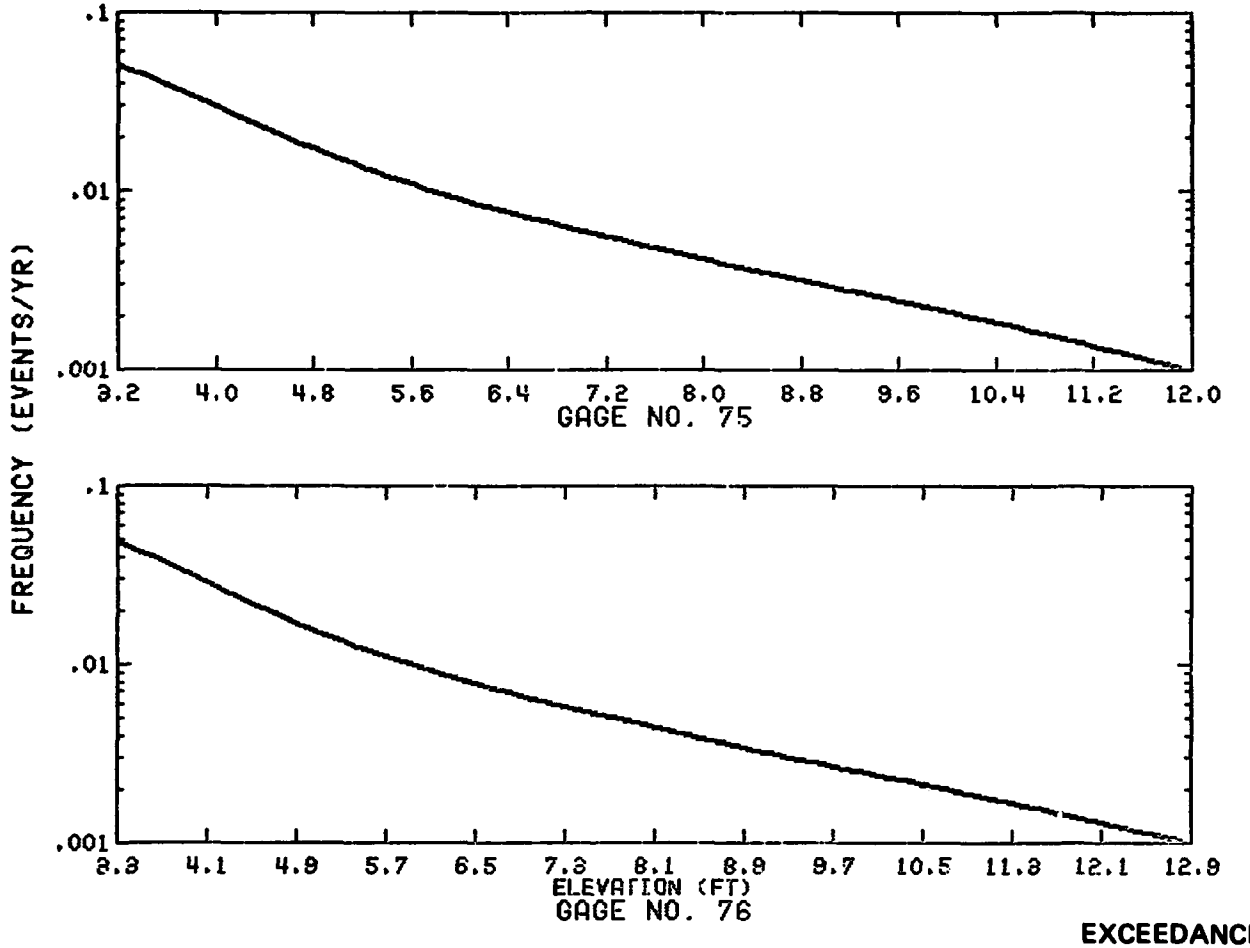

EXCEEDANCE FREQUENCY DISTRIBUTION
GAGES 75 AND 76

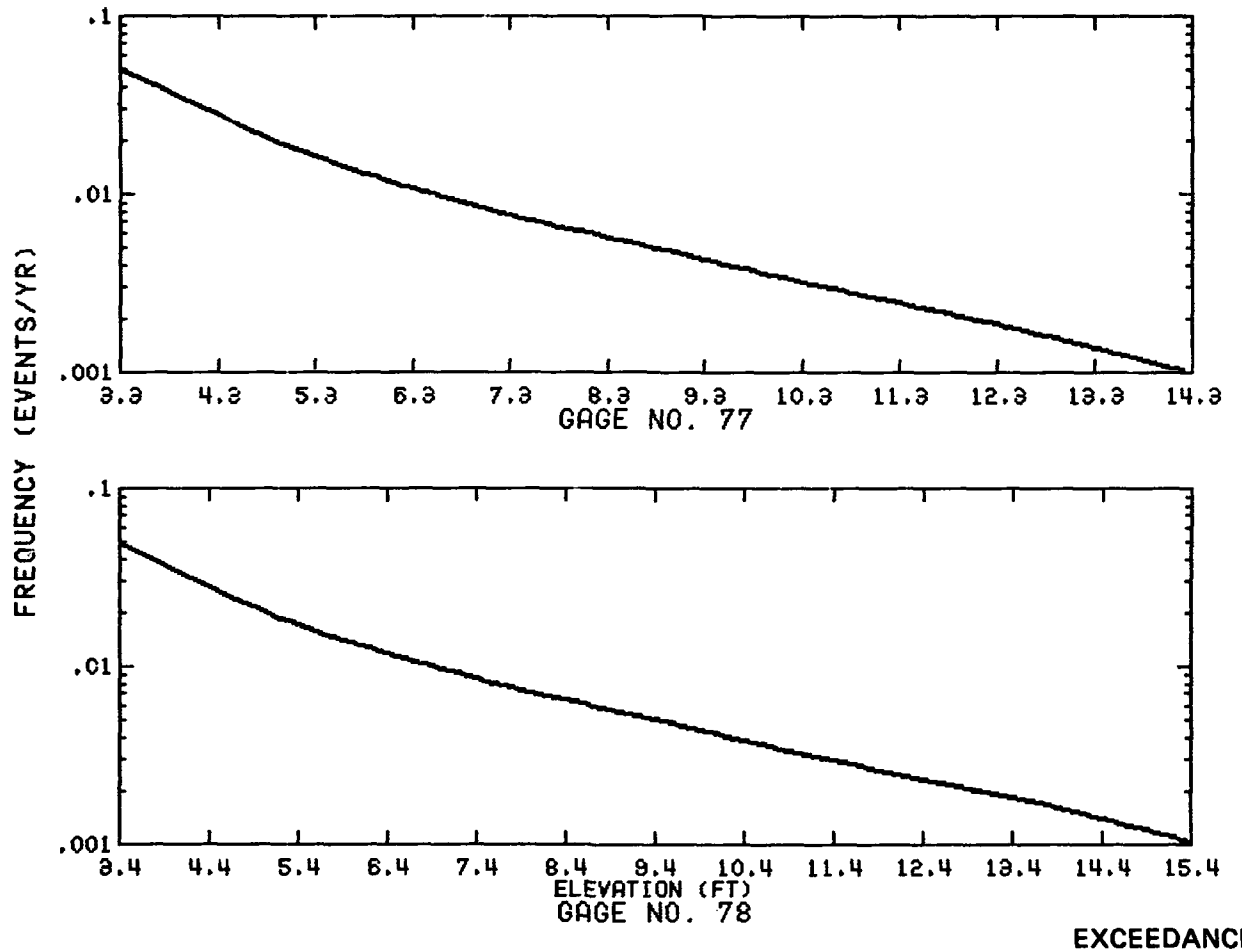

EXCEEDANCE FREQUENCY DISTRIBUTION
GAGES 77 AND 78

PLATE 39

PLATE 40

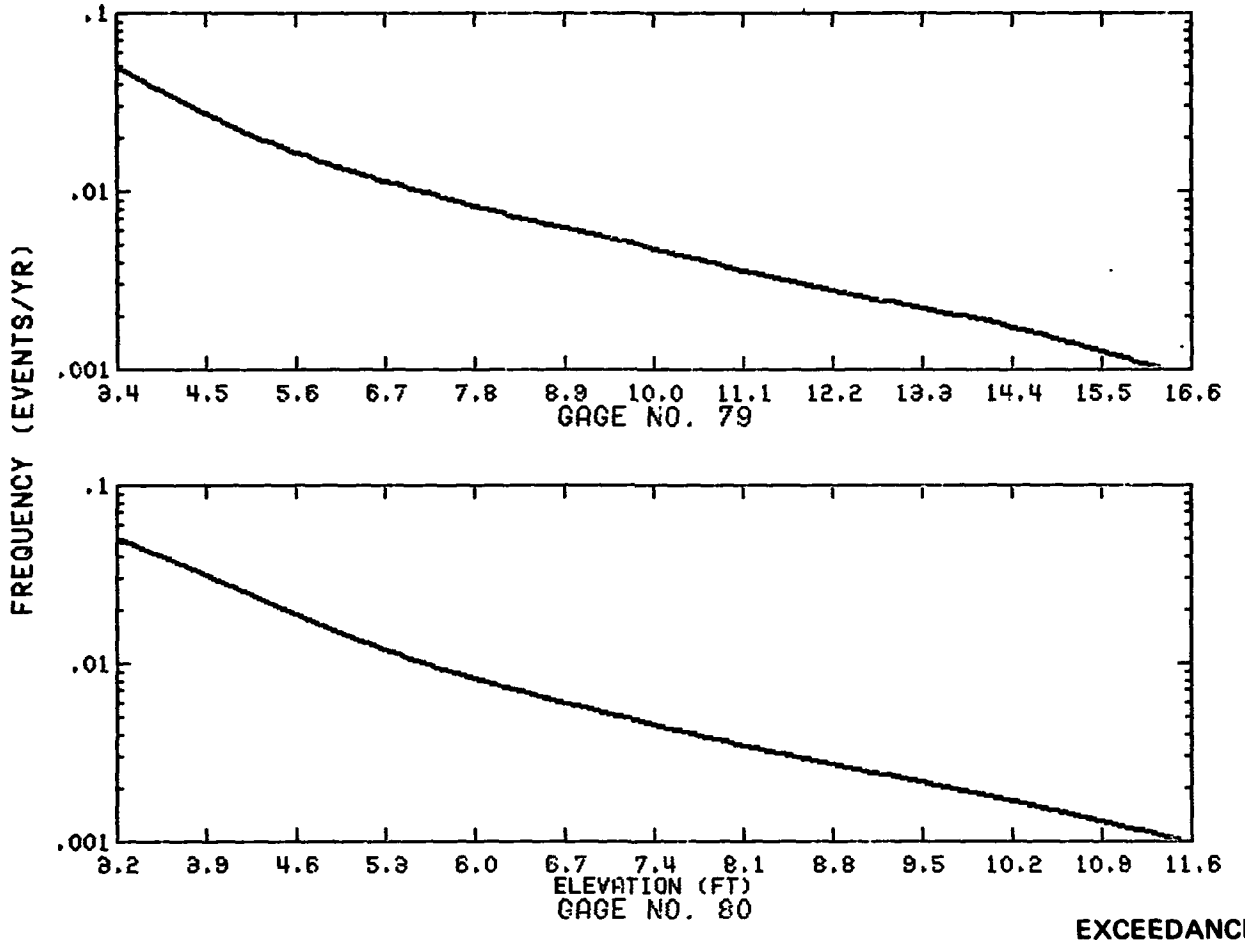

EXCEEDANCE FREQUENCY DISTRIBUTION
GAGES 79 AND 80

AD-A091 657 ARMY ENGINEER WATERWAYS EXPERIMENT STATION VICKSBURG--ETC F/G 8/3
TYPE 19 FLOOD INSURANCE STUDY: TSUNAMI PREDICTIONS FOR SOUTHERN--ETC(U)
SEP 80 J R HOUSTON FEMA-IAA-H-9-79
UNCLASSIFIED WES/TR/HL-80-18 NL

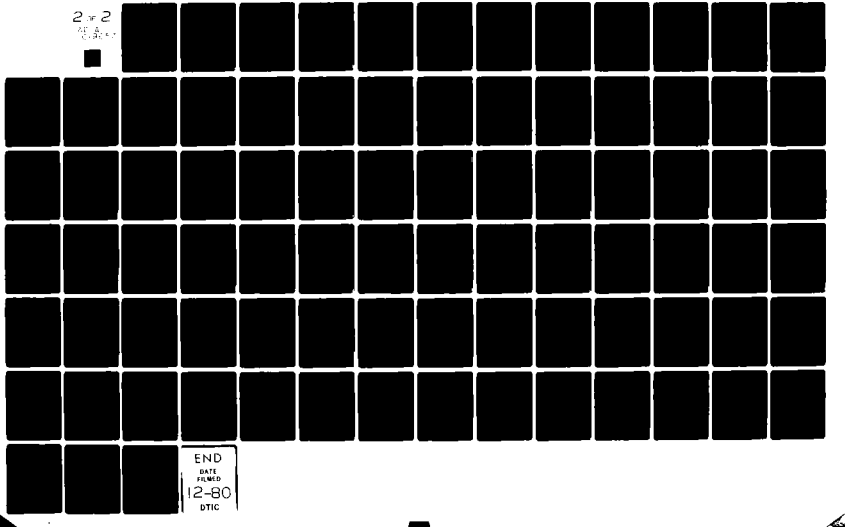

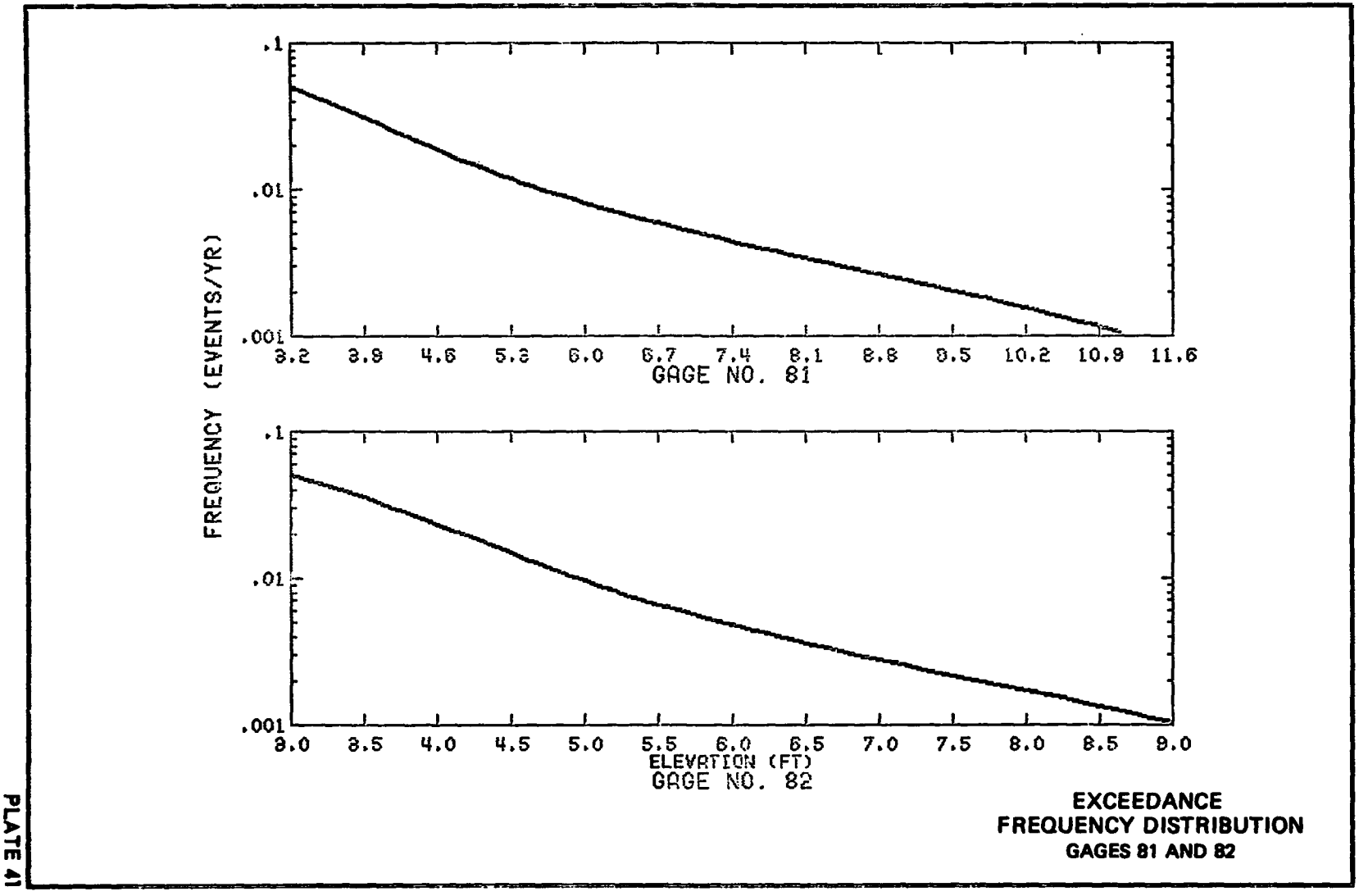

EXCEEDANCE FREQUENCY DISTRIBUTION
GAGES 81 AND 82

PLATE 41

PLATE 42

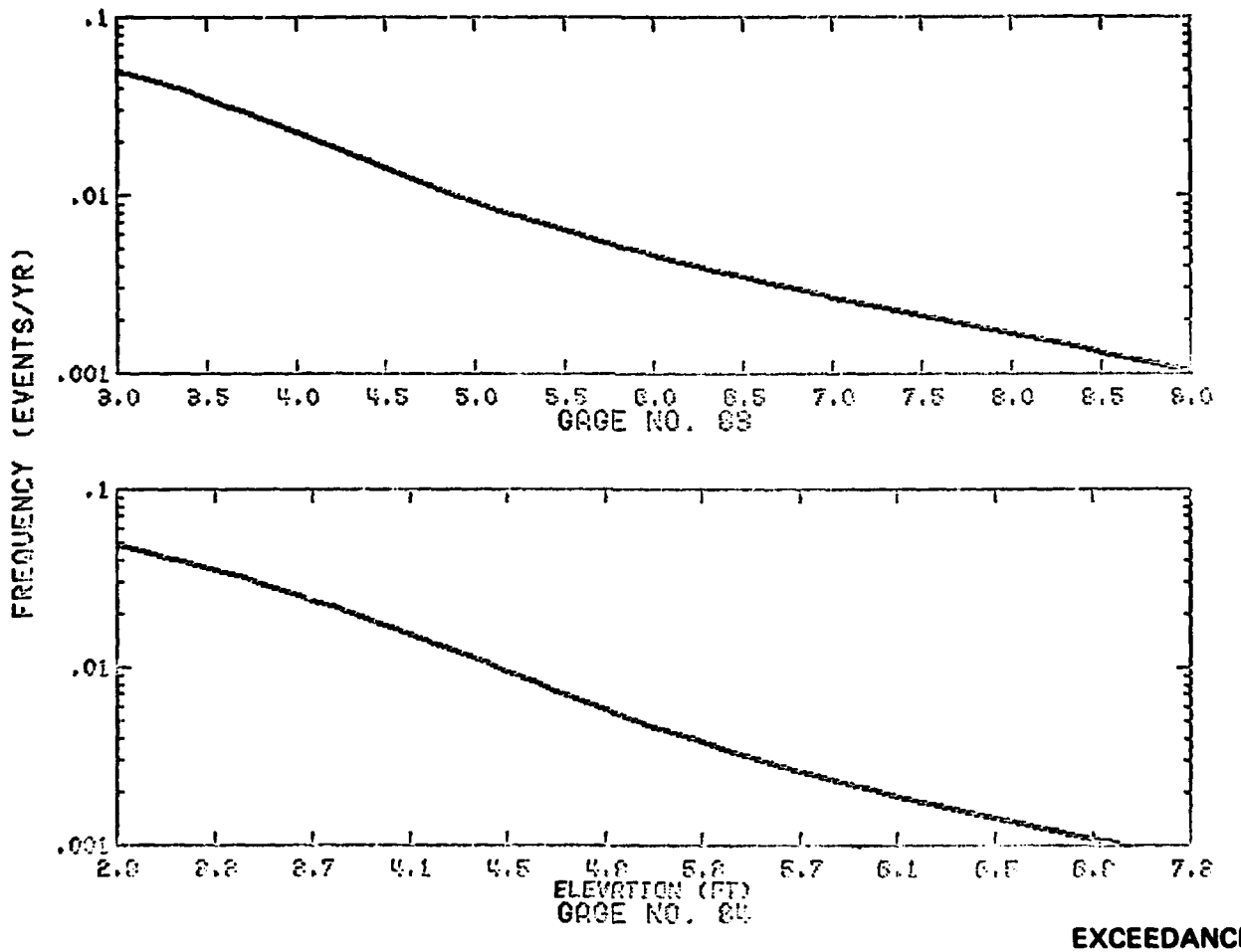

EXCEEDANCE FREQUENCY DISTRIBUTION
GAGES 83 AND 84

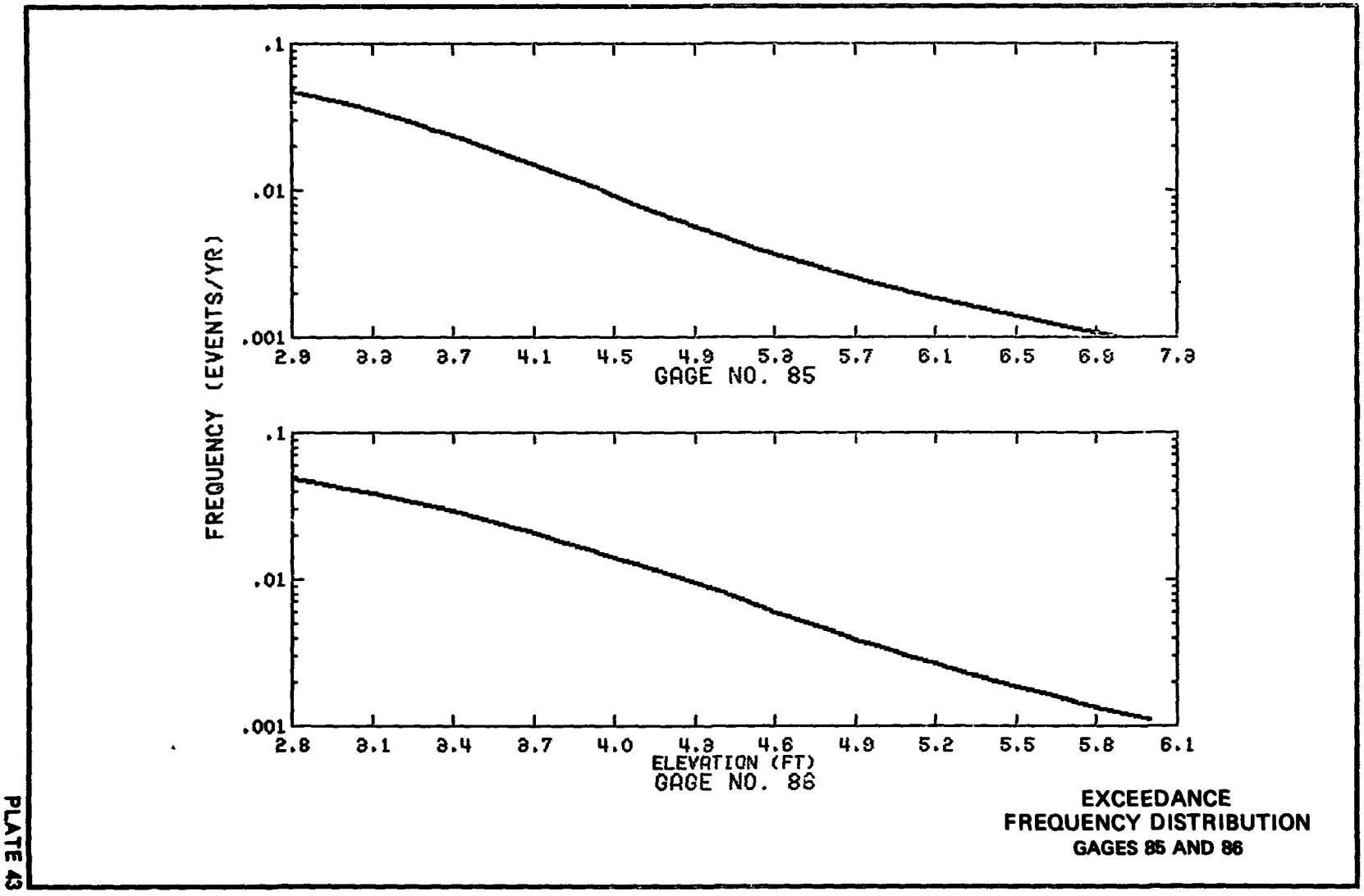

EXCEEDANCE FREQUENCY DISTRIBUTION
GAGES 85 AND 86

PLATE 43

PLATE 44

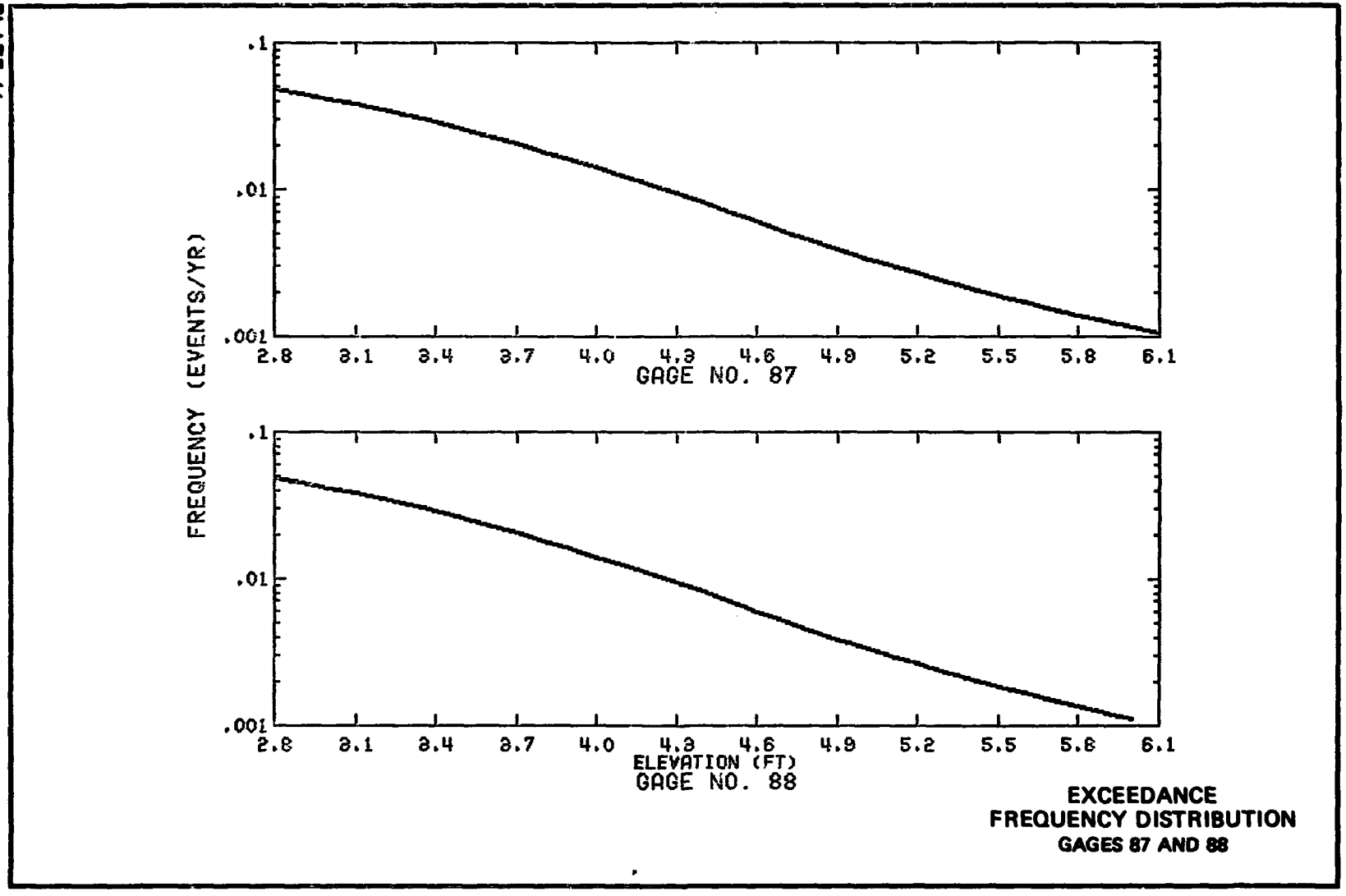

EXCEEDANCE FREQUENCY DISTRIBUTION
GAGES 87 AND 88

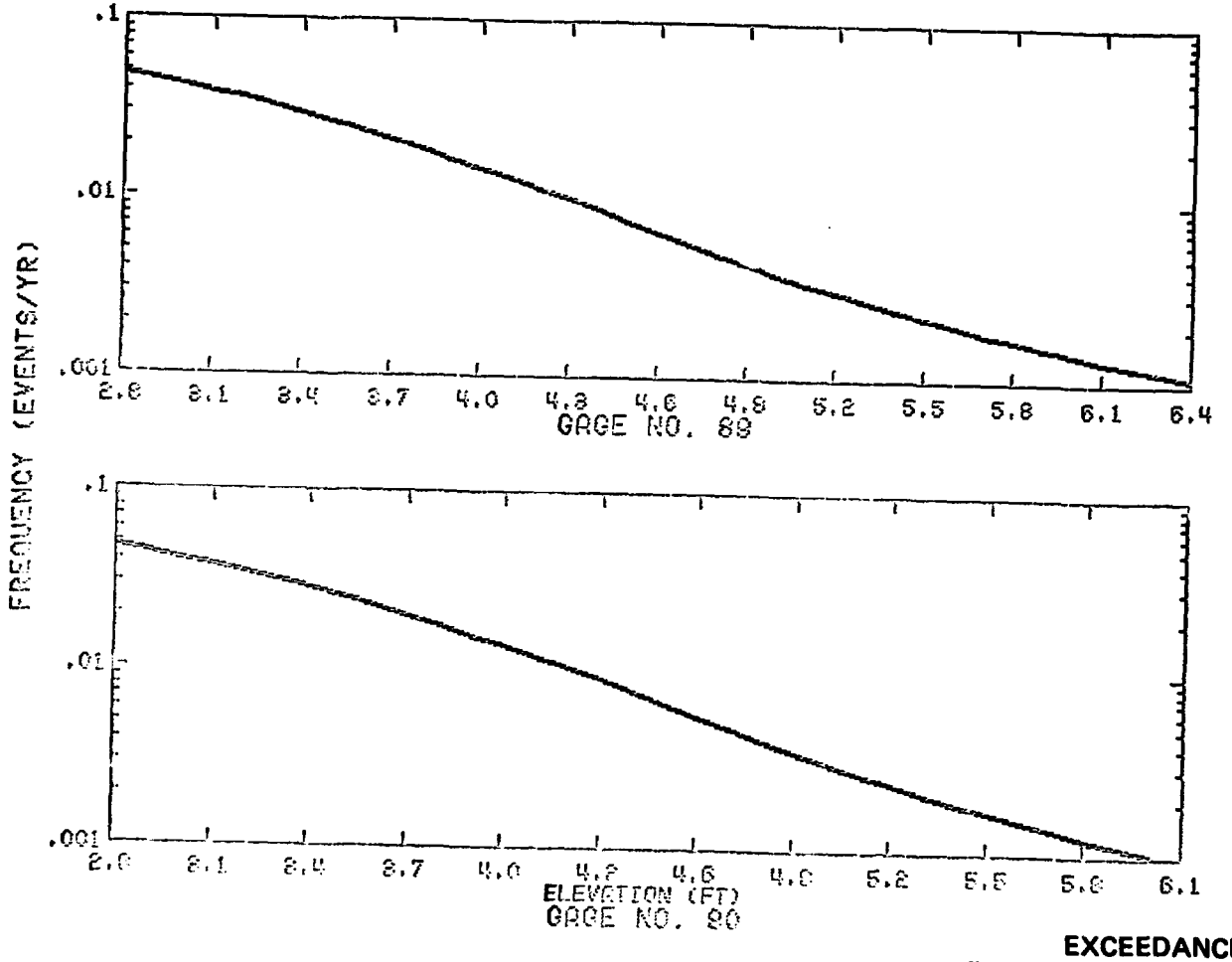

EXCEEDANCE FREQUENCY DISTRIBUTION
GAGES 89 AND 90

PLATE 45

PLATE 46

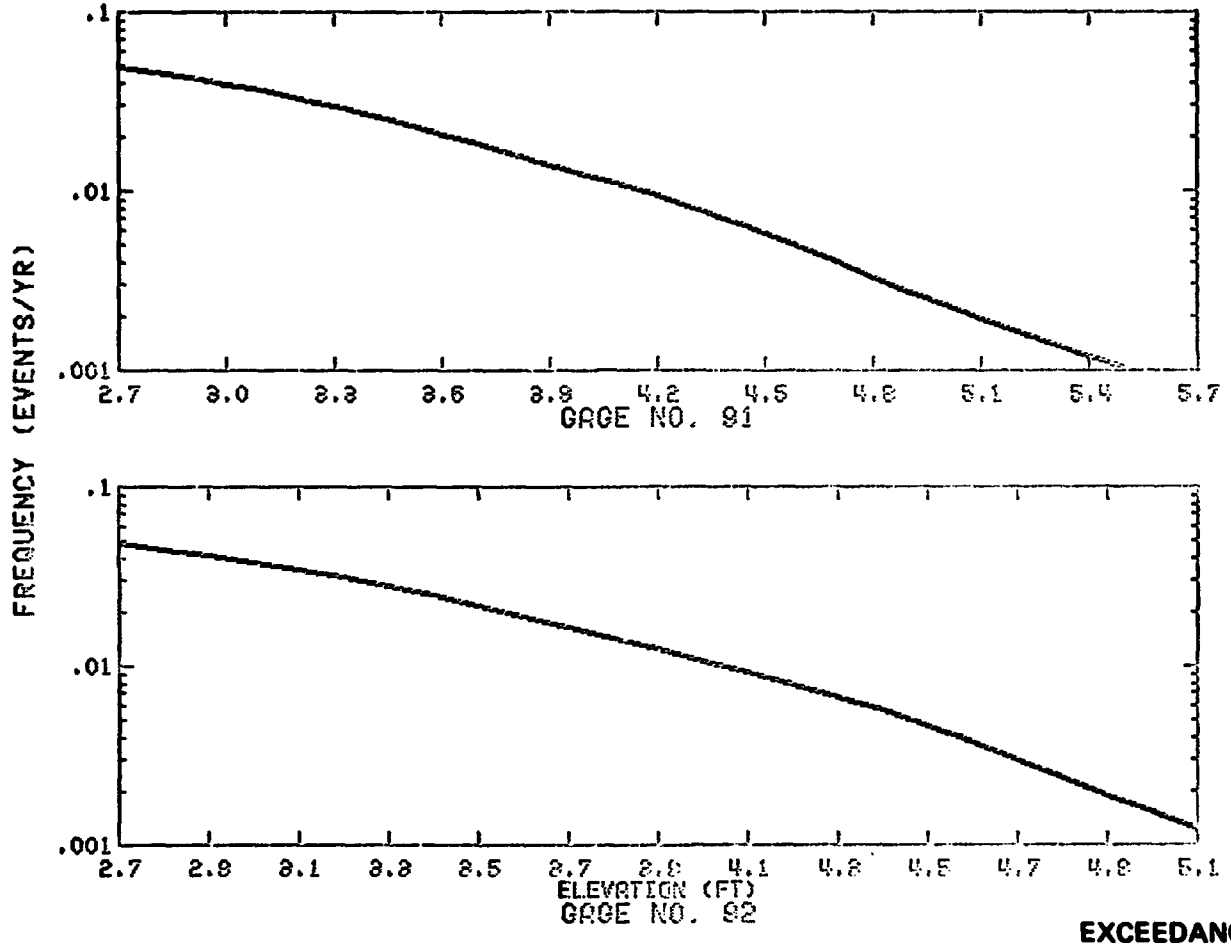

EXCEEDANCE FREQUENCY DISTRIBUTION
GAGES 91 AND 92

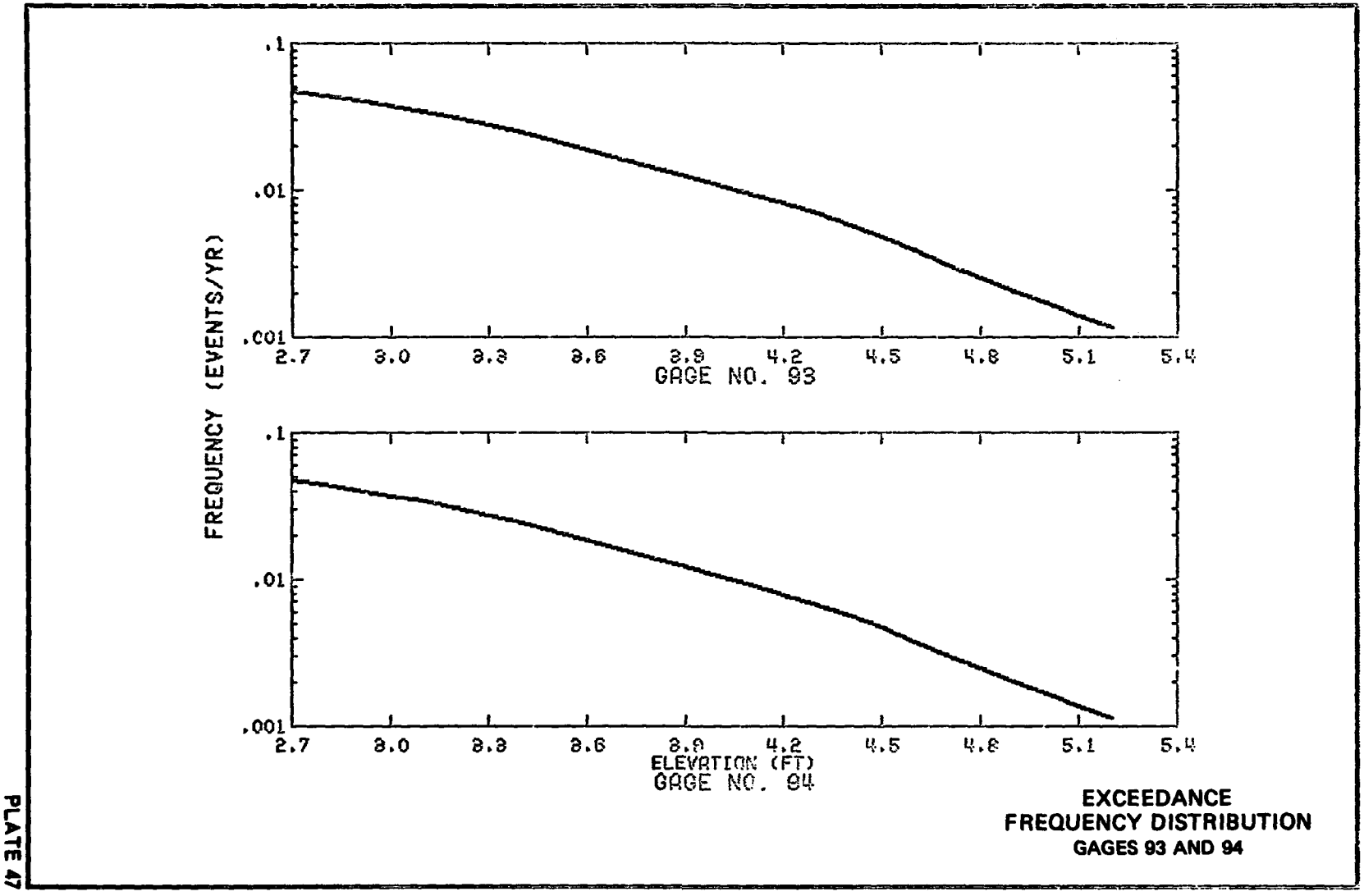

PLATE 47

EXCEEDANCE FREQUENCY DISTRIBUTION
GAGES 93 AND 94

PLATE 48

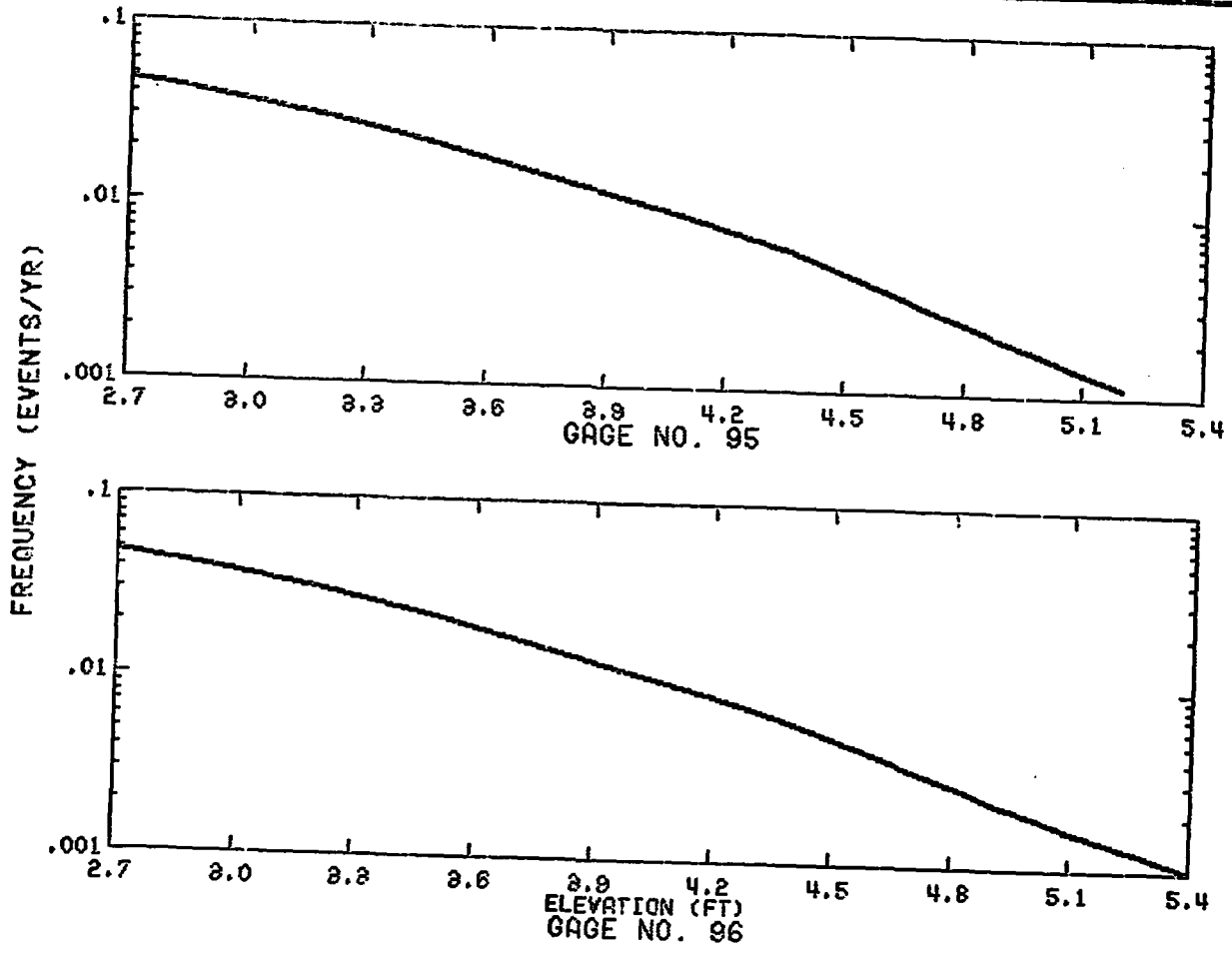

EXCEEDANCE FREQUENCY DISTRIBUTION
GAGES 95 AND 96

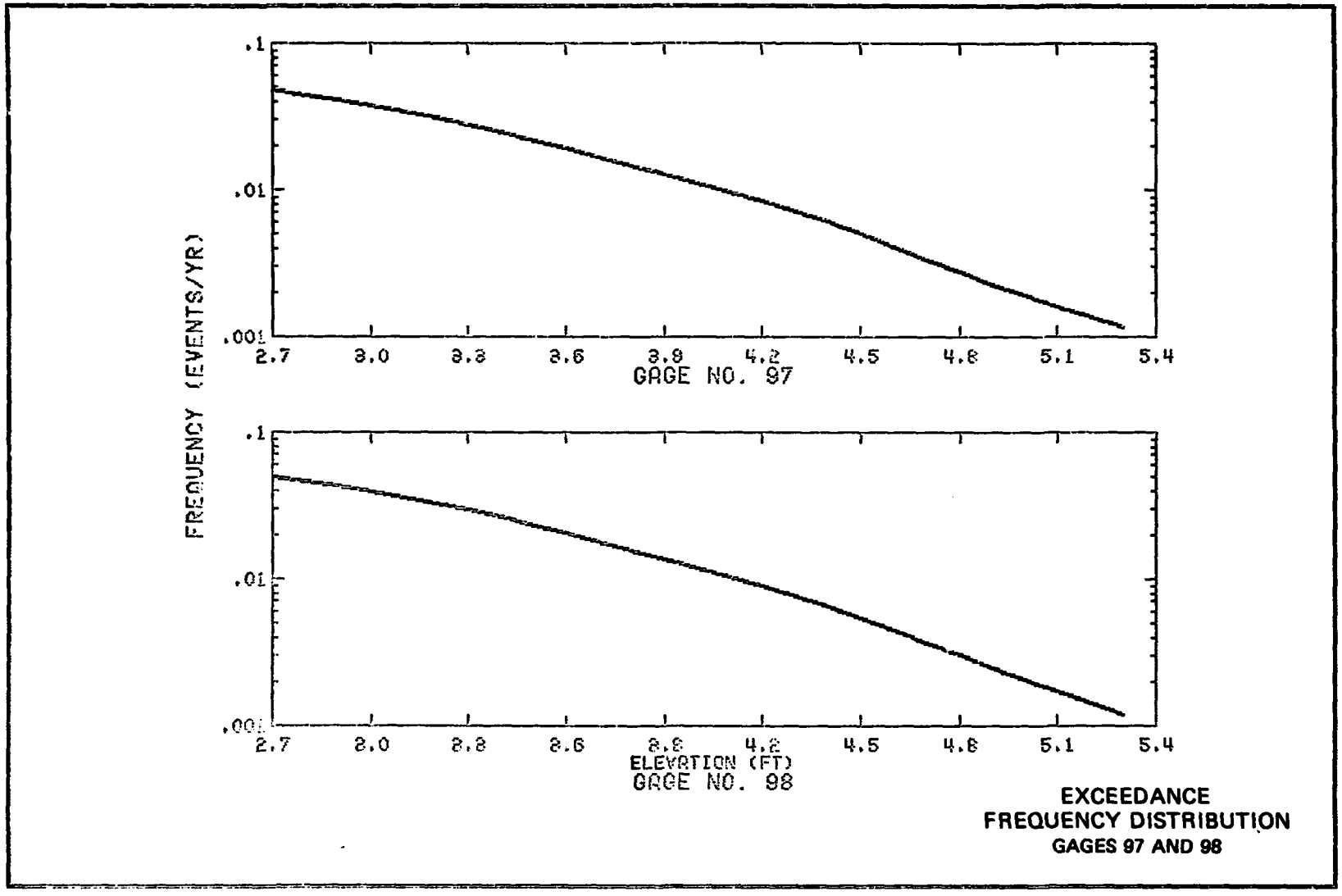

EXCEEDANCE FREQUENCY DISTRIBUTION
GAGES 97 AND 98

PLATE 49

PLATE 50

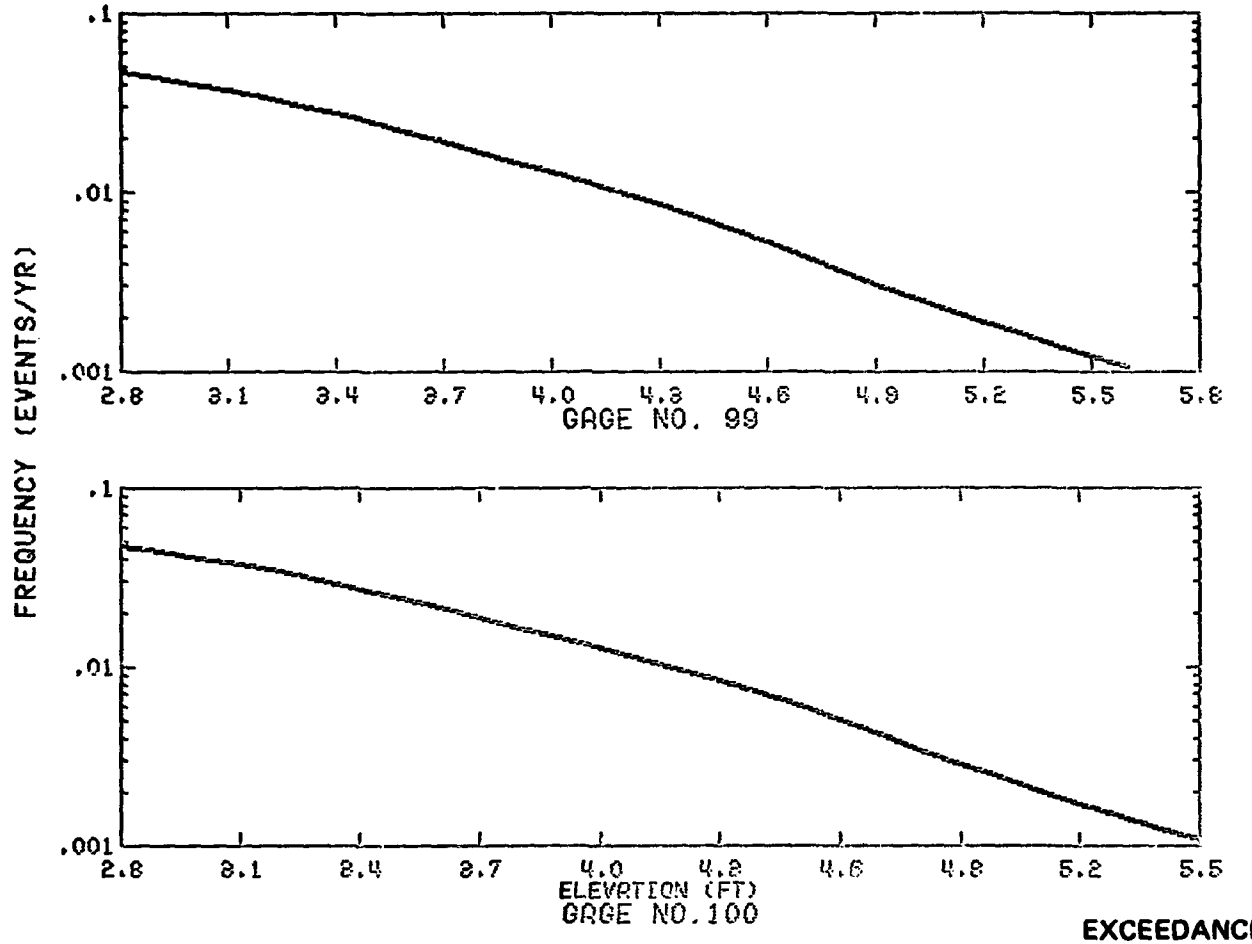

EXCEEDANCE FREQUENCY DISTRIBUTION
GAGES 99 AND 100

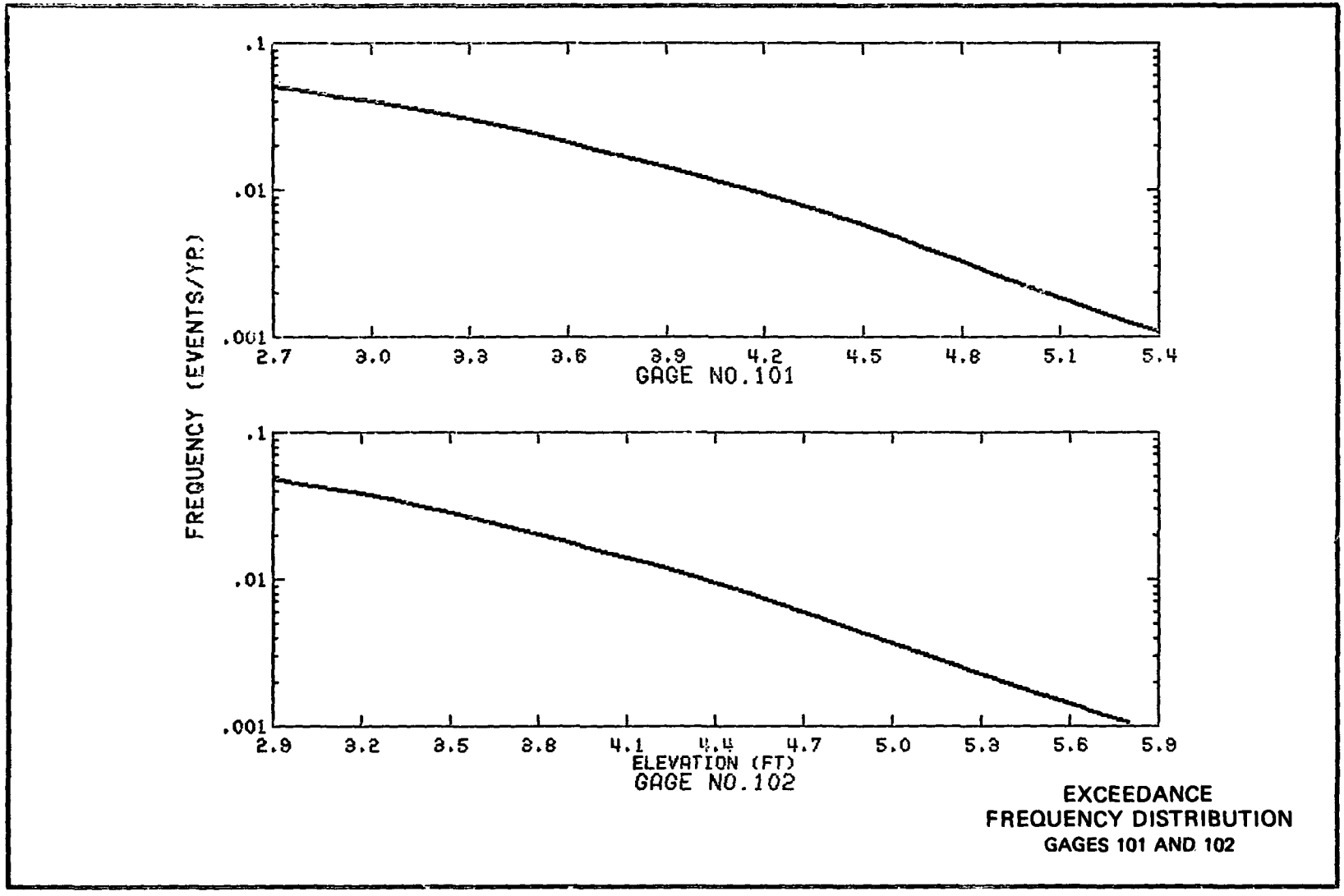

EXCEEDANCE FREQUENCY DISTRIBUTION
GAGES 101 AND 102

PLATE 51

PLATE 52

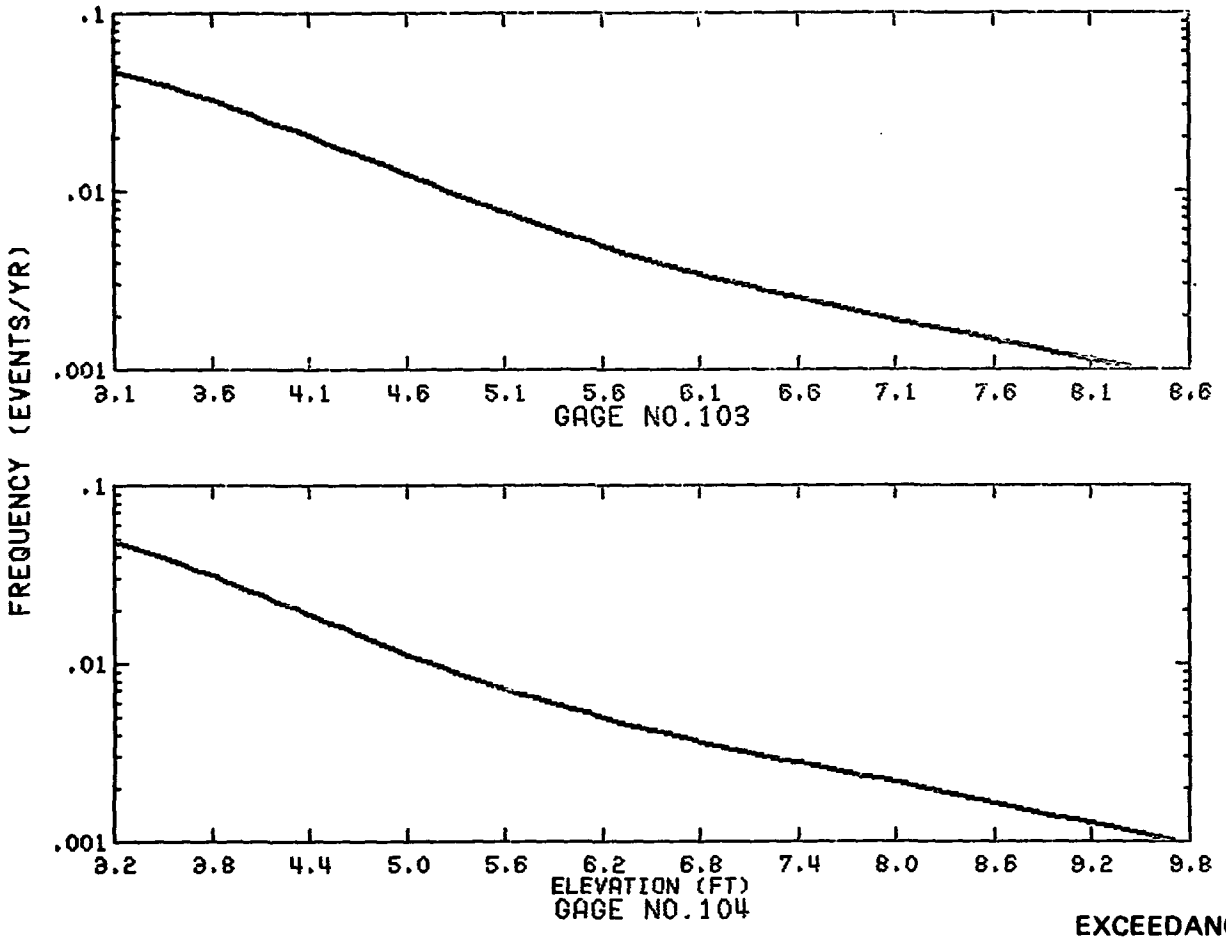

EXCEEDANCE FREQUENCY DISTRIBUTION
GAGES 103 AND 104

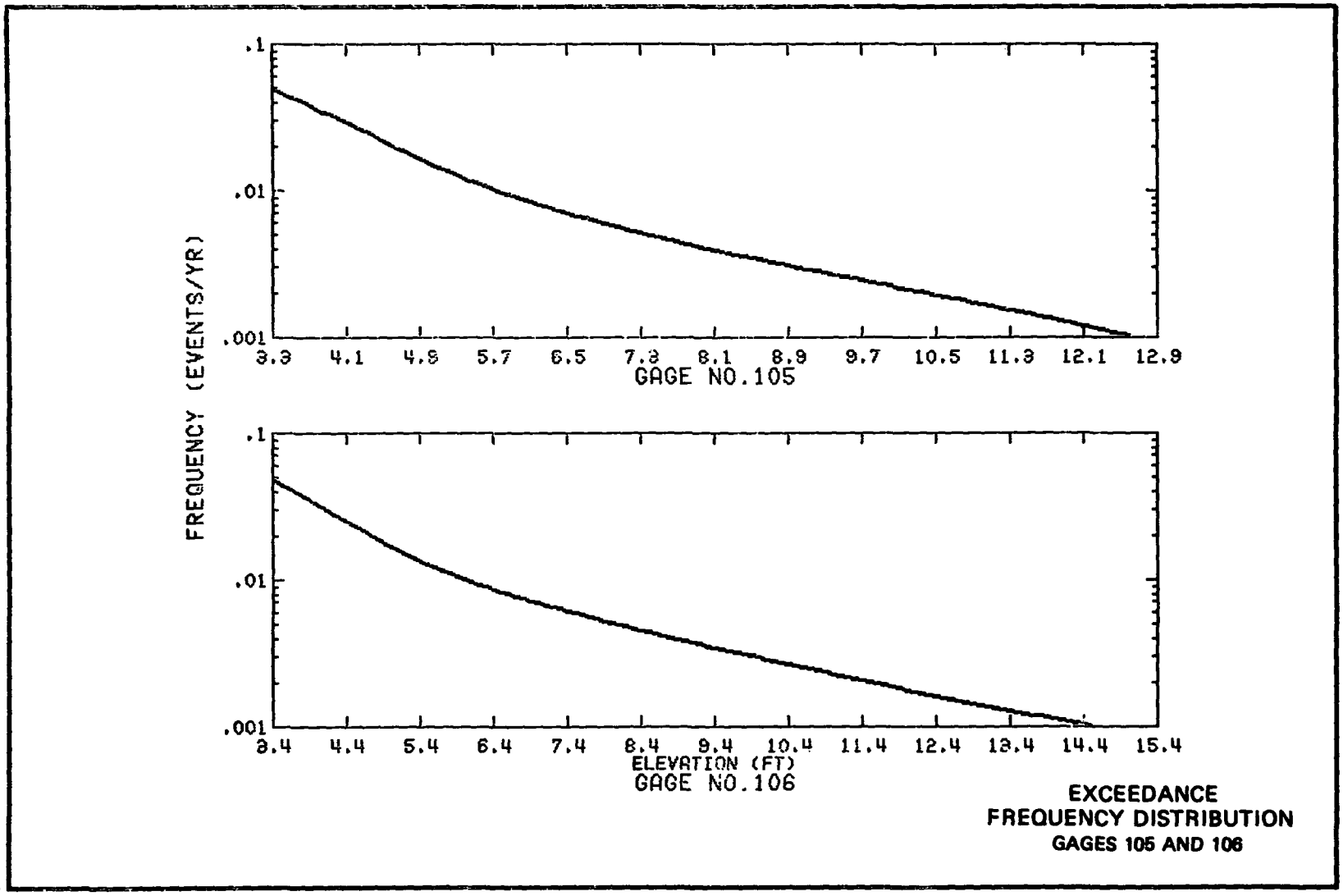

EXCEEDANCE FREQUENCY DISTRIBUTION
GAGES 105 AND 106

PLATE 53

PLATE 54

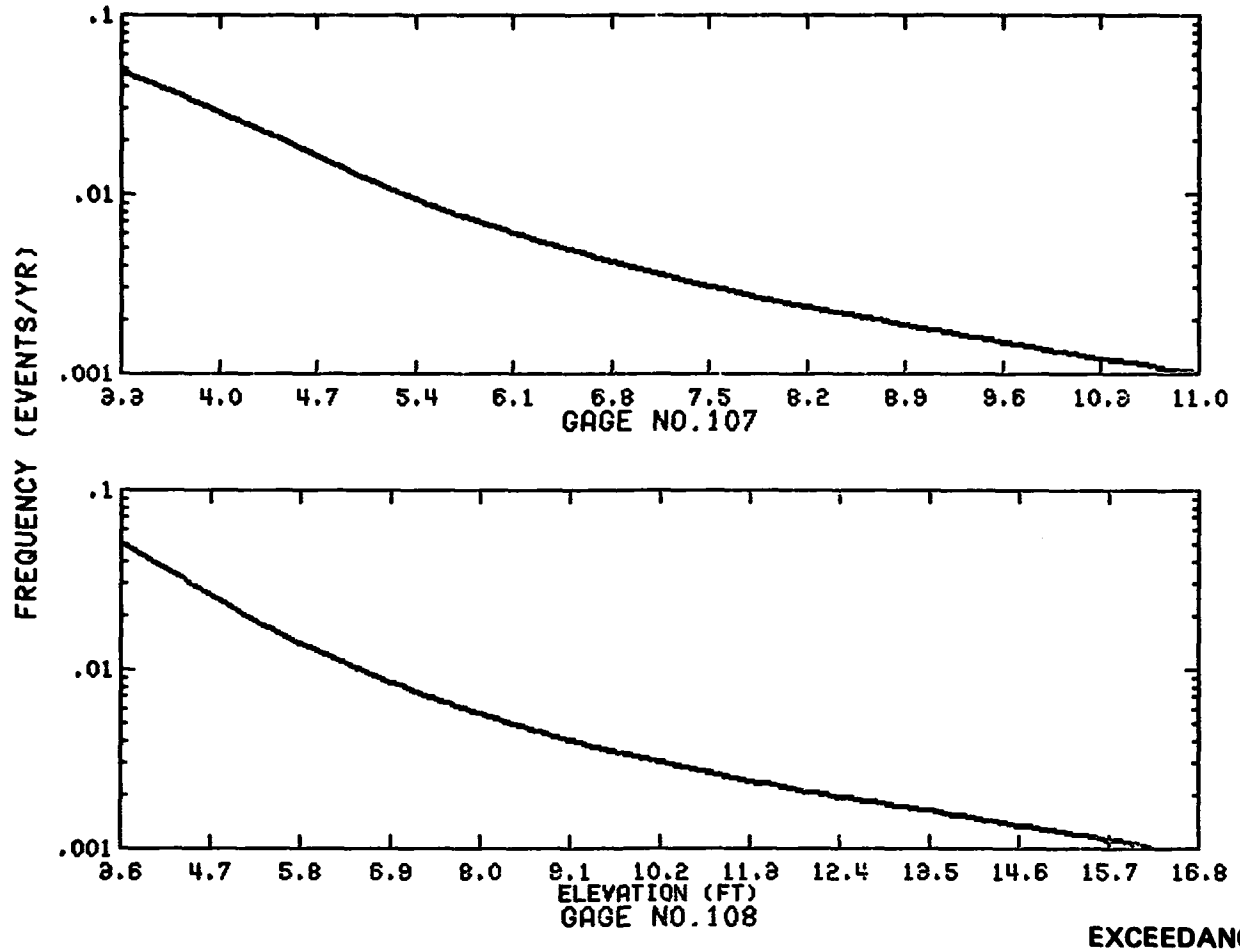

EXCEEDANCE FREQUENCY DISTRIBUTION
GAGES 107 AND 108

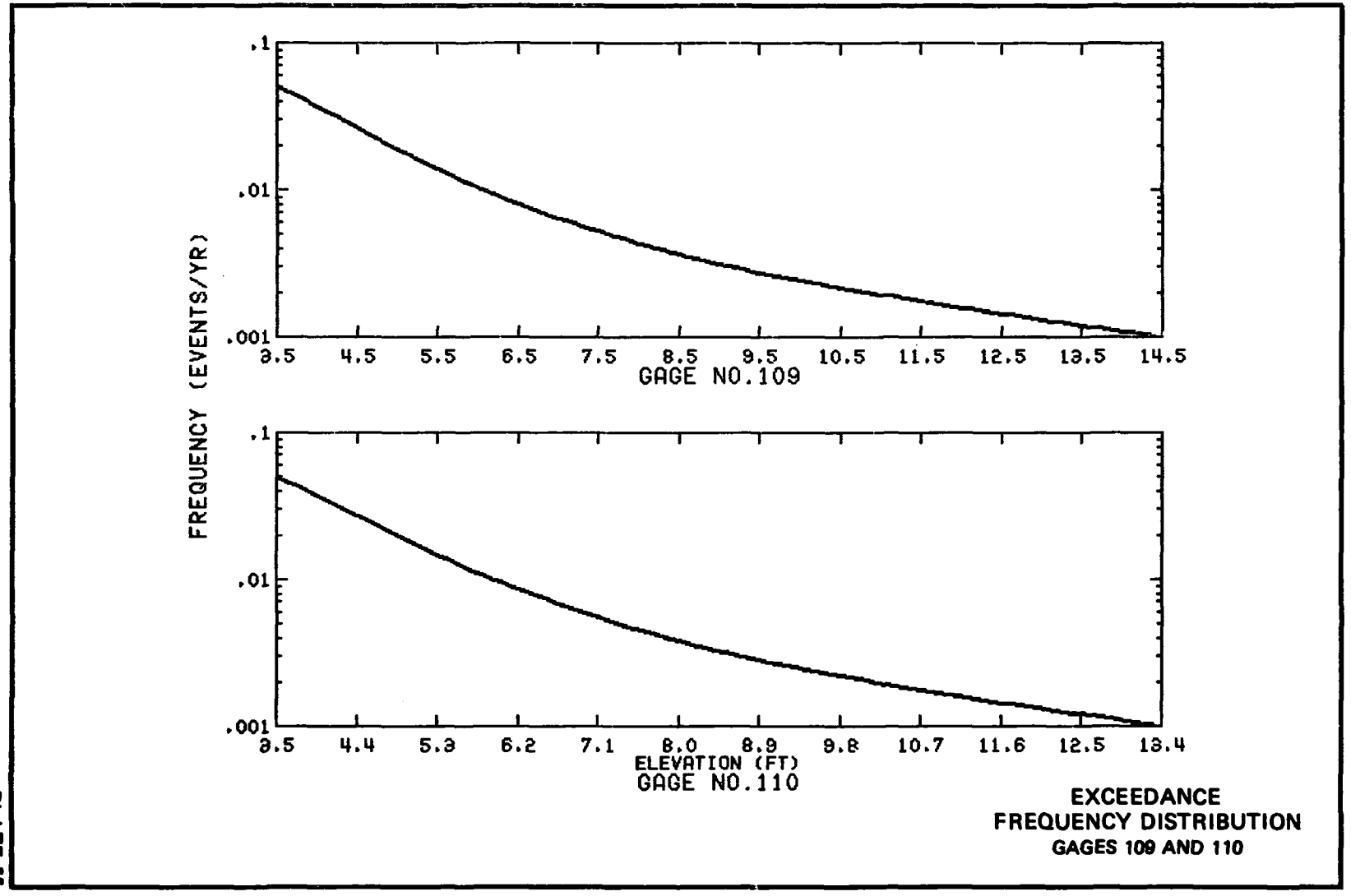

EXCEEDANCE FREQUENCY DISTRIBUTION
GAGES 109 AND 110

PLATE 55

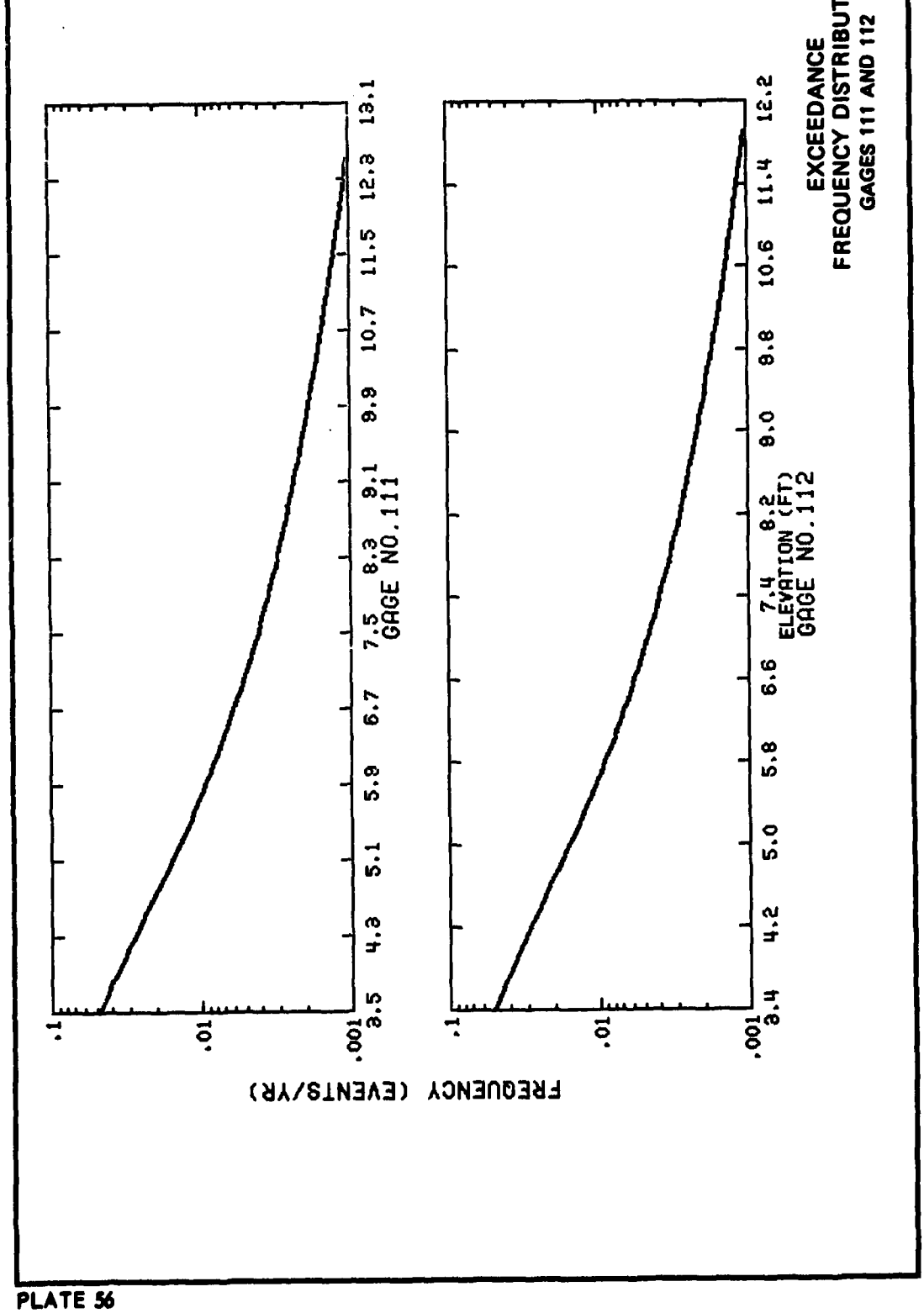
EXCEEDANCE
FREQUENCY DISTRIBUTION
GAGES 111 AND 112
FREQUENCY (EVENTS/YR)
.1
.01
.001
3.5
4.3
5.1
5.9
6.7
7.5
8.3
8.9
9.9
10.7
11.5
12.3
13.1
GAGE NO.111
3.4
4.2
5.0
5.8
6.6
7.4
8.2
9.0
9.8
10.6
11.4
12.2
ELEVATION (FT)
GAGE NO.112

PLATE 56

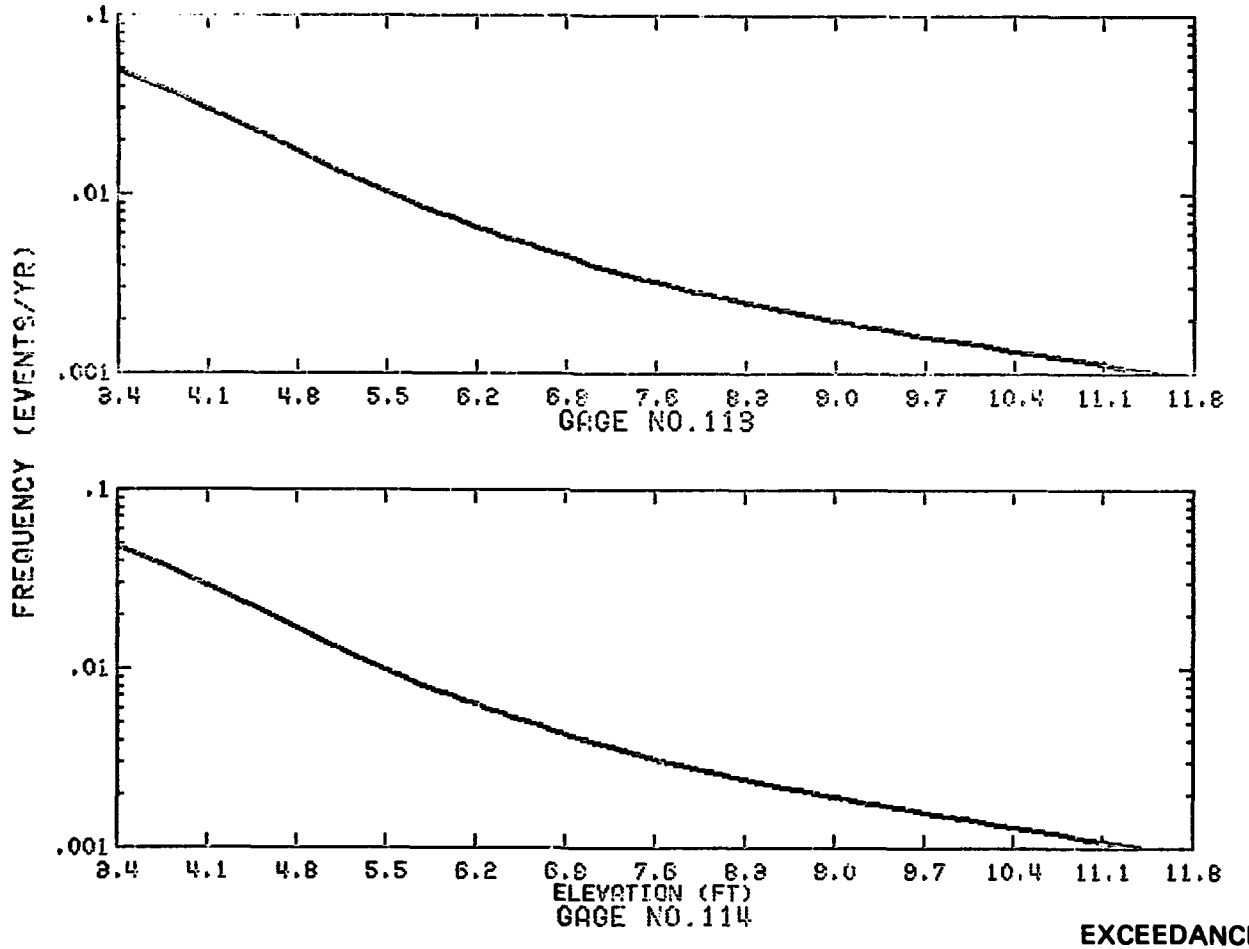

EXCEEDANCE FREQUENCY DISTRIBUTION
GAGES 113 AND 114

PLATE 57

PLATE 58

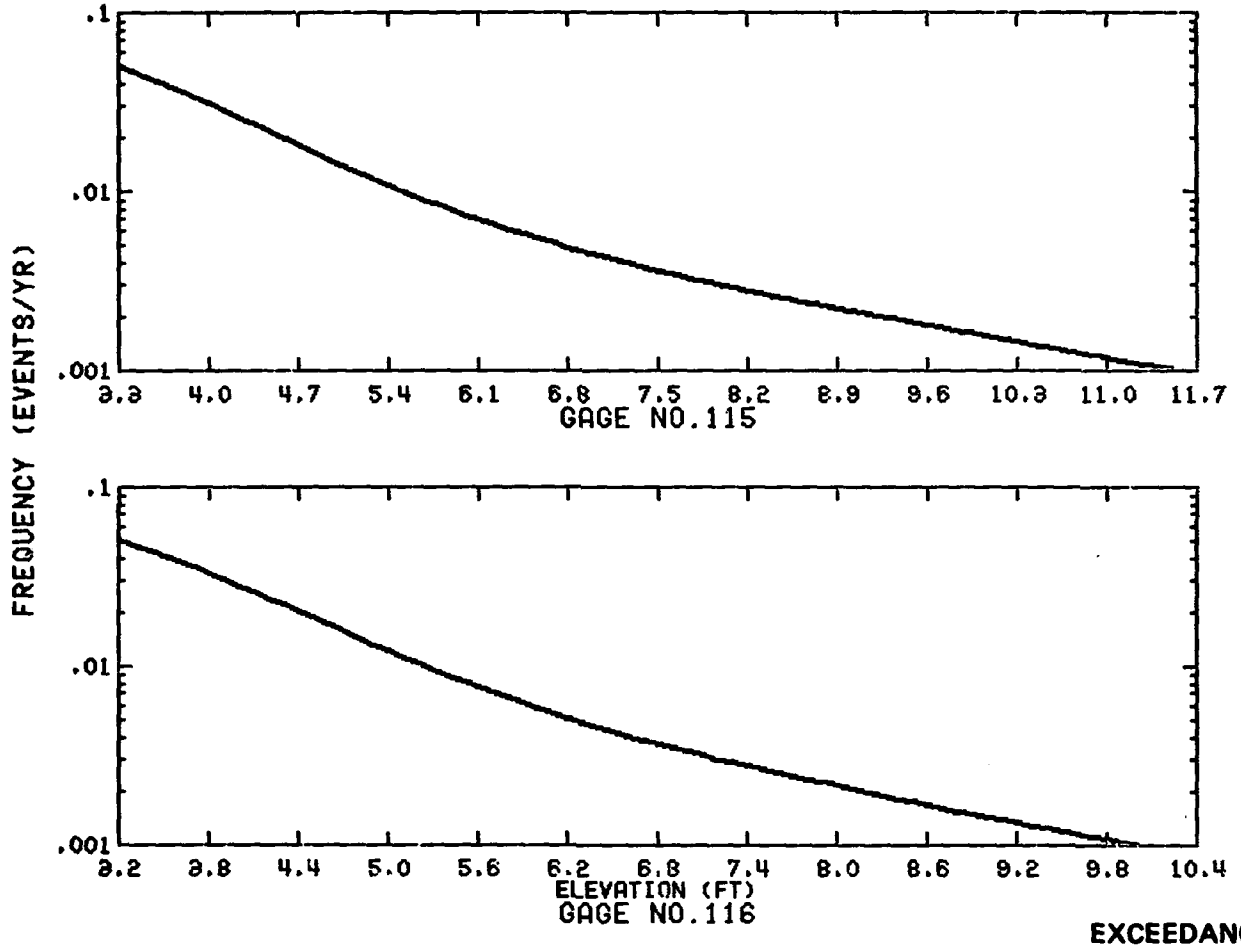

EXCEEDANCE FREQUENCY DISTRIBUTION
GAGES 115 AND 116

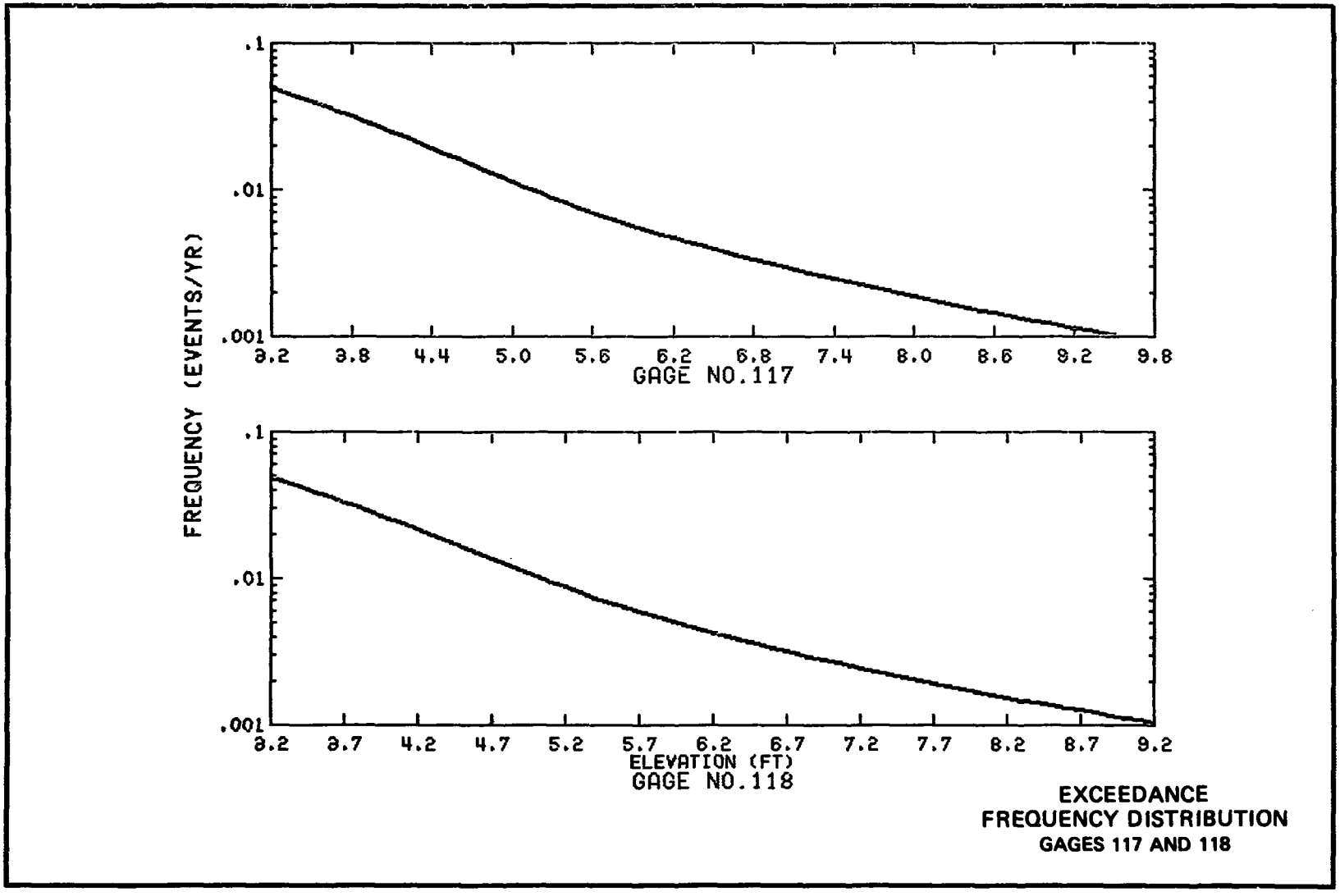

EXCEEDANCE FREQUENCY DISTRIBUTION
GAGES 117 AND 118

PLATE 59

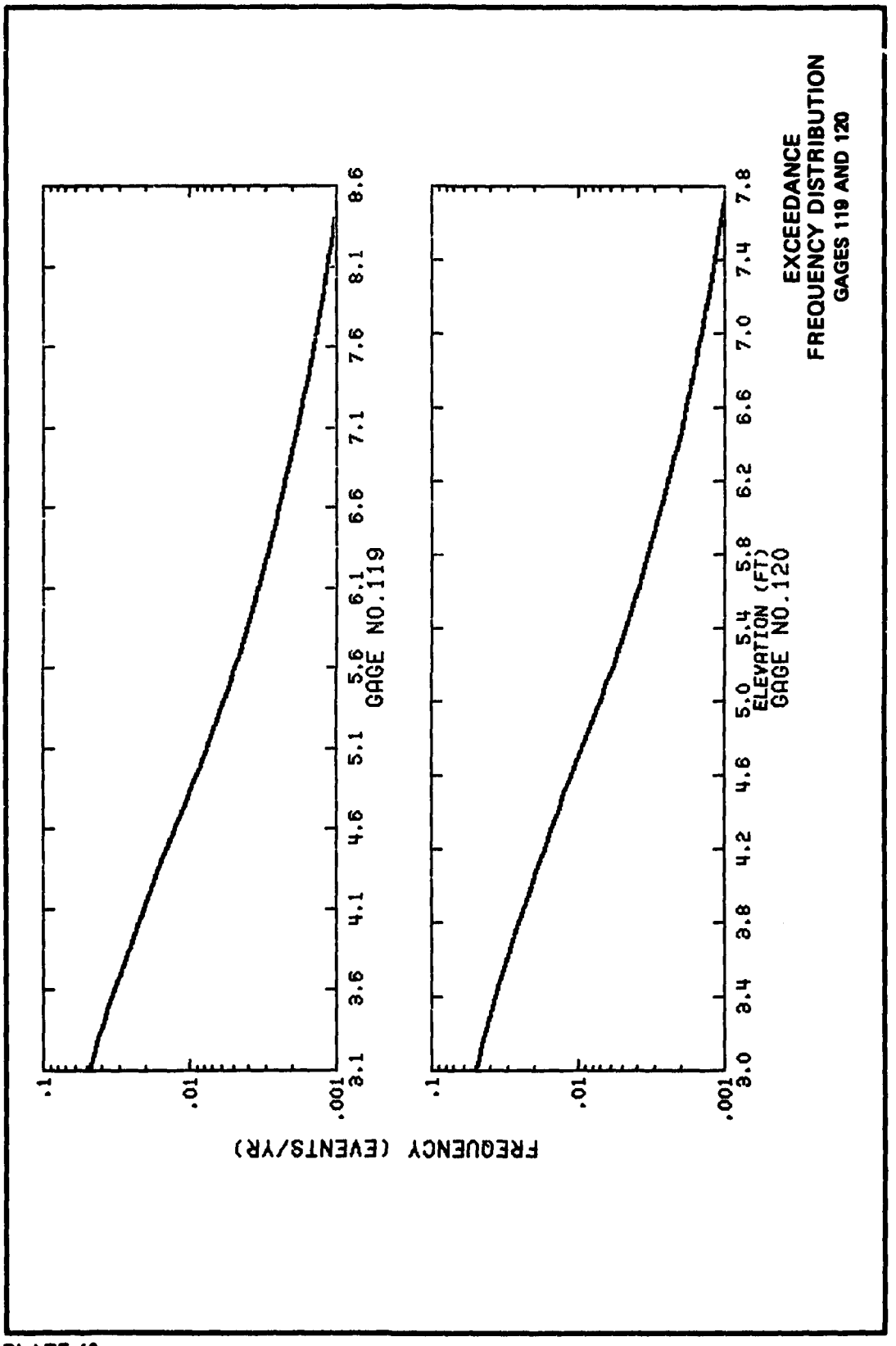
EXCEEDANCE
FREQUENCY DISTRIBUTION
GAGES 119 AND 120
FREQUENCY (EVENTS/YR)
.1
.01
.001
3.1
3.6
4.1
4.6
5.1
5.6
6.1
6.6
7.1
7.6
8.1
8.6
GAGE NO.119
3.0
3.4
3.8
4.2
4.6
5.0
5.4
5.8
6.2
6.6
7.0
7.4
7.8
ELEVATION (FT)
GAGE NO.120

PLATE 60

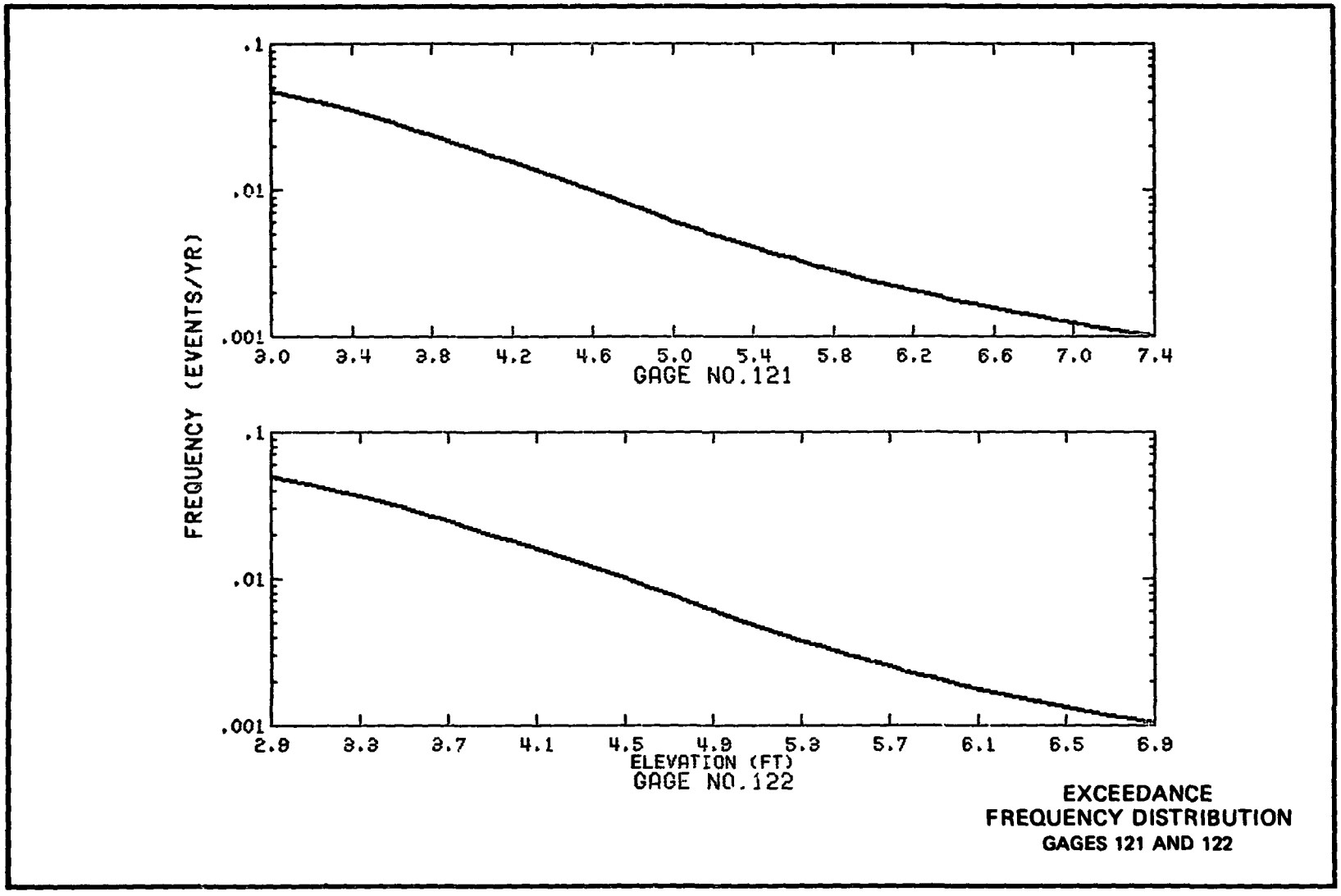

EXCEEDANCE FREQUENCY DISTRIBUTION
GAGES 121 AND 122

PLATE 61

PLATE 62

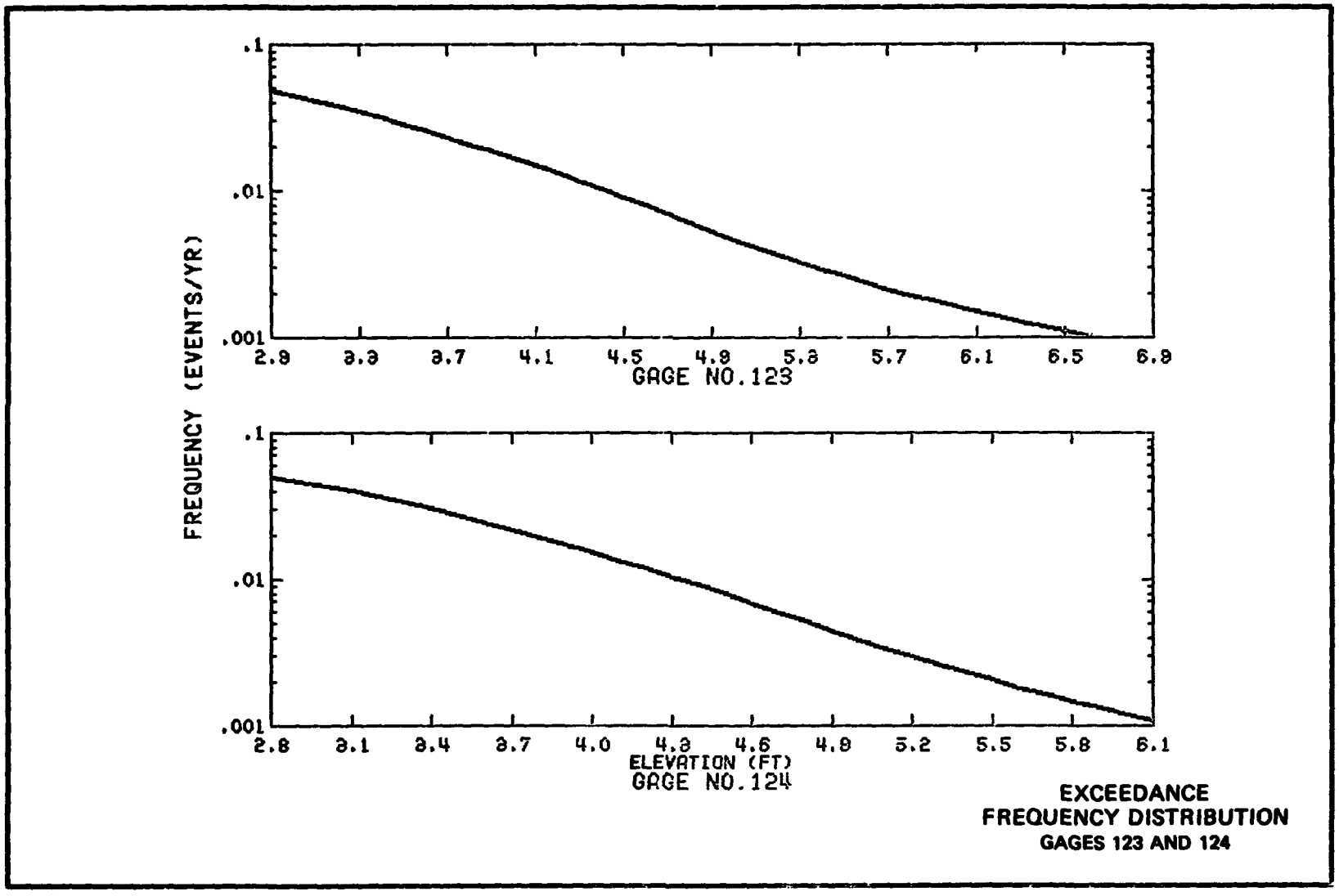

EXCEEDANCE FREQUENCY DISTRIBUTION
GAGES 123 AND 124

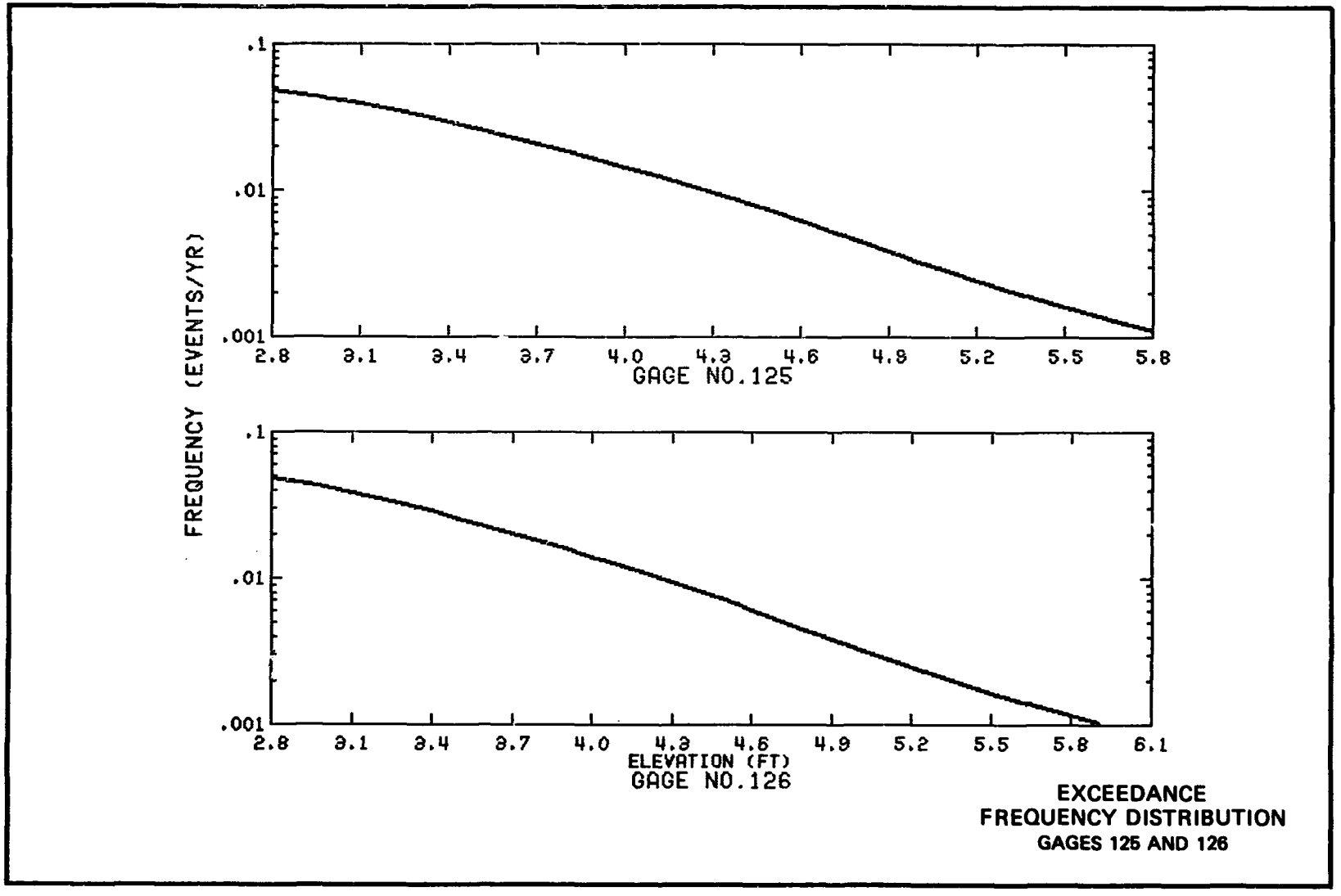

EXCEEDANCE FREQUENCY DISTRIBUTION
GAGES 125 AND 126

PLATE 63

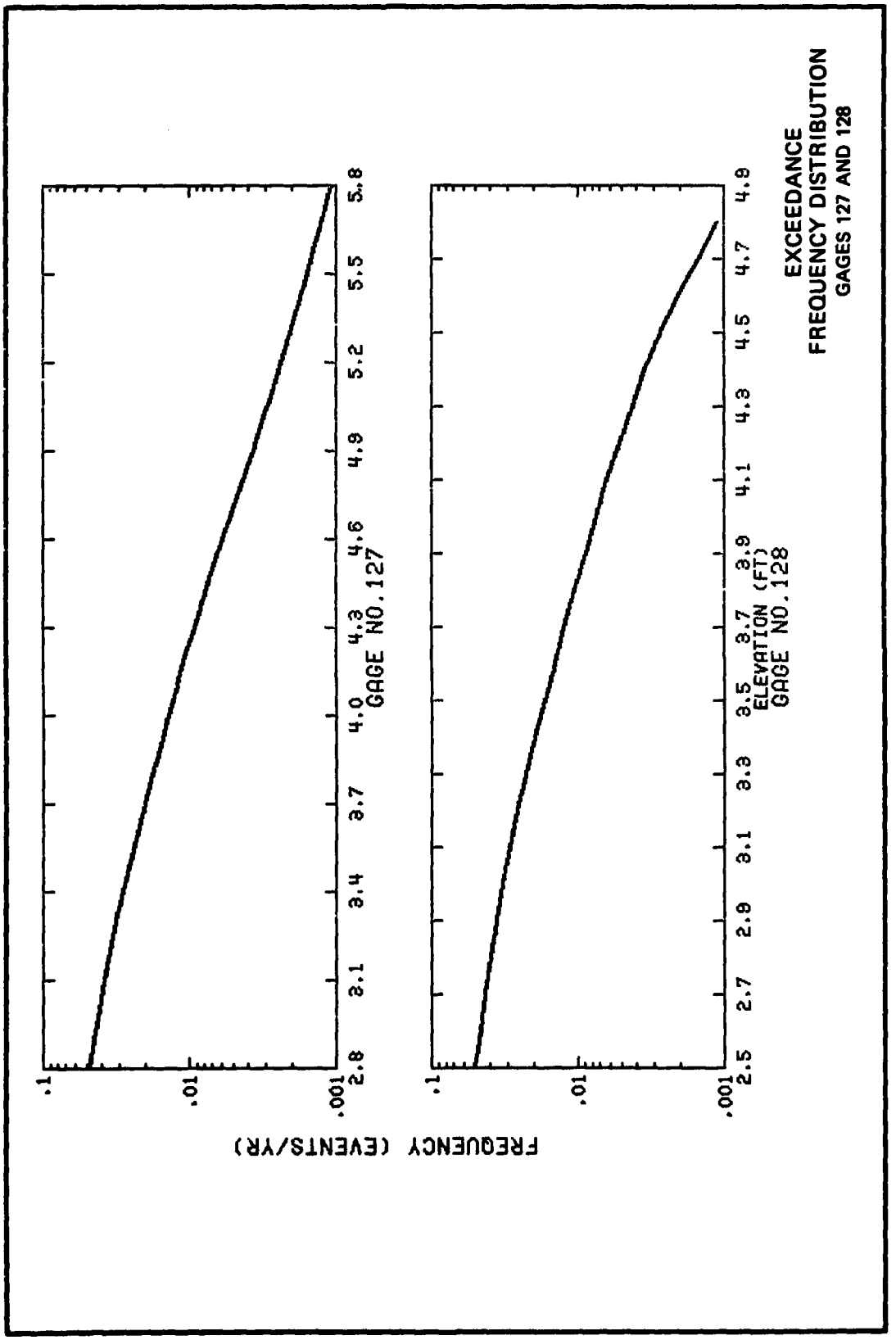
EXCEEDANCE
FREQUENCY DISTRIBUTION
GAGES 127 AND 128
FREQUENCY (EVENTS/YR)
.1
.01
.001
GAGE NO.127
2.8 3.1 3.4 3.7 4.0 4.3 4.6 4.9 5.2 5.5 5.8
GAGE NO.128
2.5 2.7 2.9 3.1 3.3 3.5 3.7 3.9 4.1 4.3 4.5 4.7 4.9
ELEVATION (FT)

PLATE 64

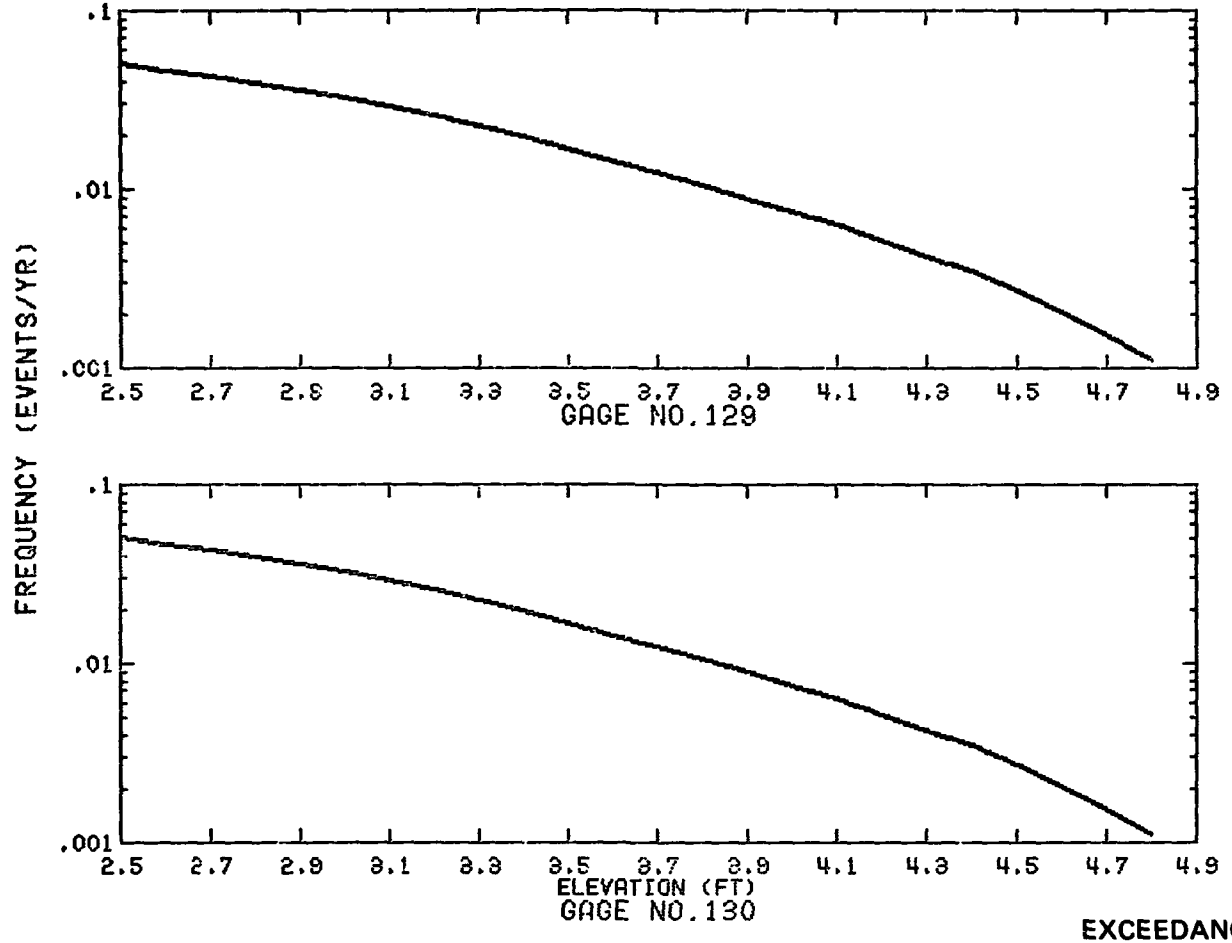

EXCEEDANCE FREQUENCY DISTRIBUTION
GAGES 129 AND 130

PLATE 65

PLATE 66

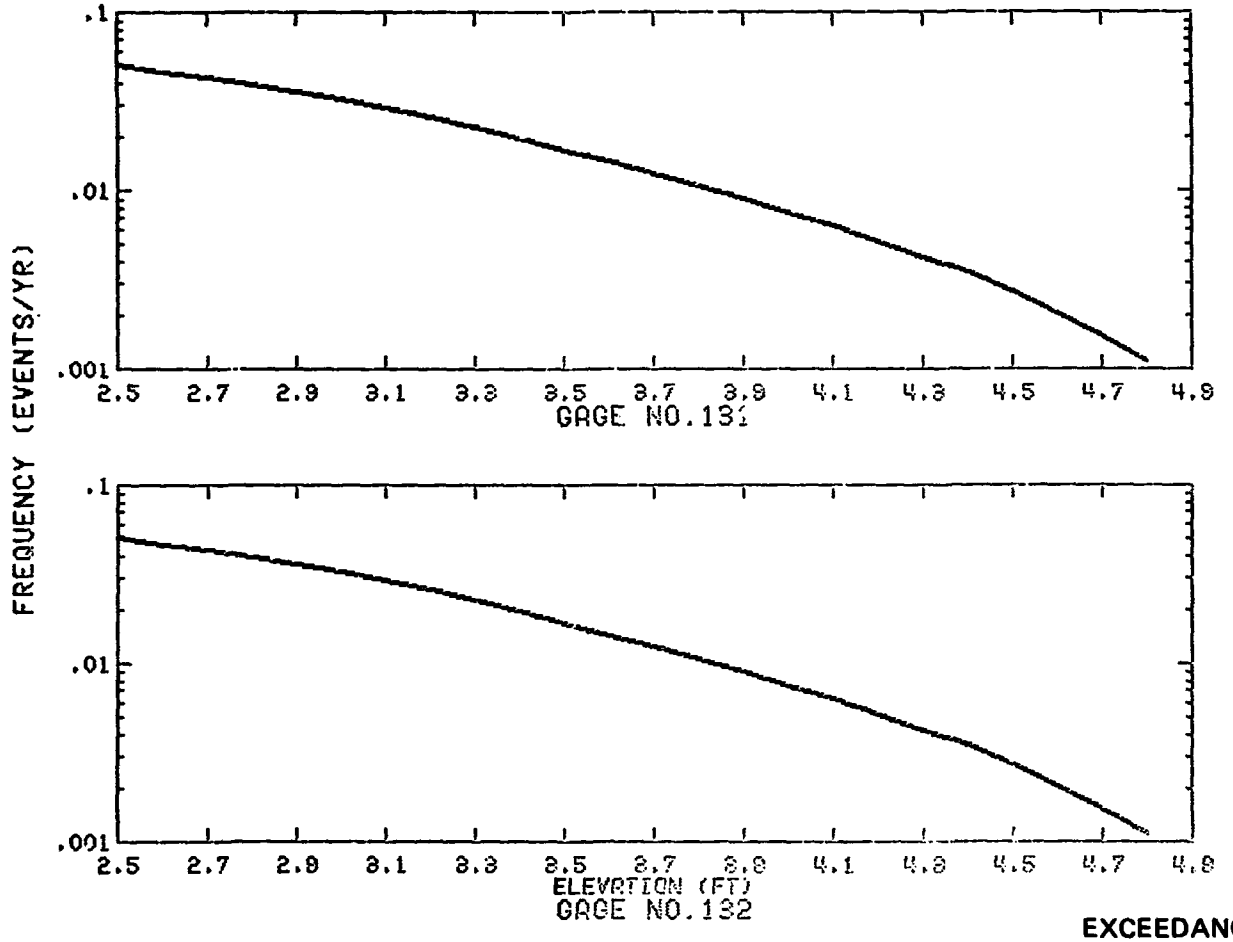

EXCEEDANCE FREQUENCY DISTRIBUTION
GAGES 131 AND 132

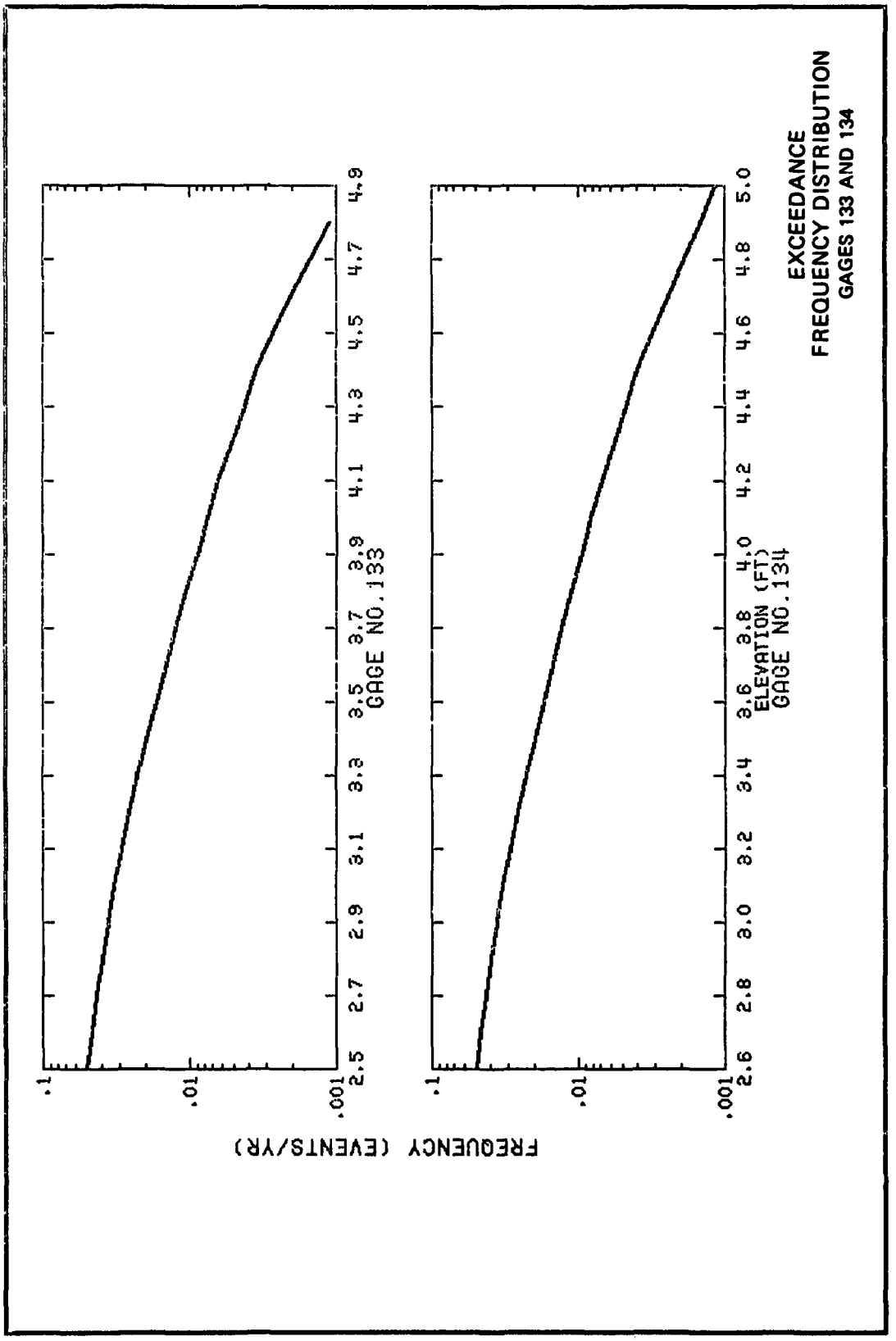
EXCEEDANCE
FREQUENCY DISTRIBUTION
GAGES 133 AND 134
FREQUENCY (EVENTS/YR)
.1
.01
.001
2.5 2.7 2.9 3.1 3.3 3.5 3.7 3.9 4.1 4.3 4.5 4.7 4.9
GAGE NO.133
2.6 2.8 3.0 3.2 3.4 3.6 3.8 4.0 4.2 4.4 4.6 4.8 5.0
ELEVATION (FT)
GAGE NO.134

PLATE 67

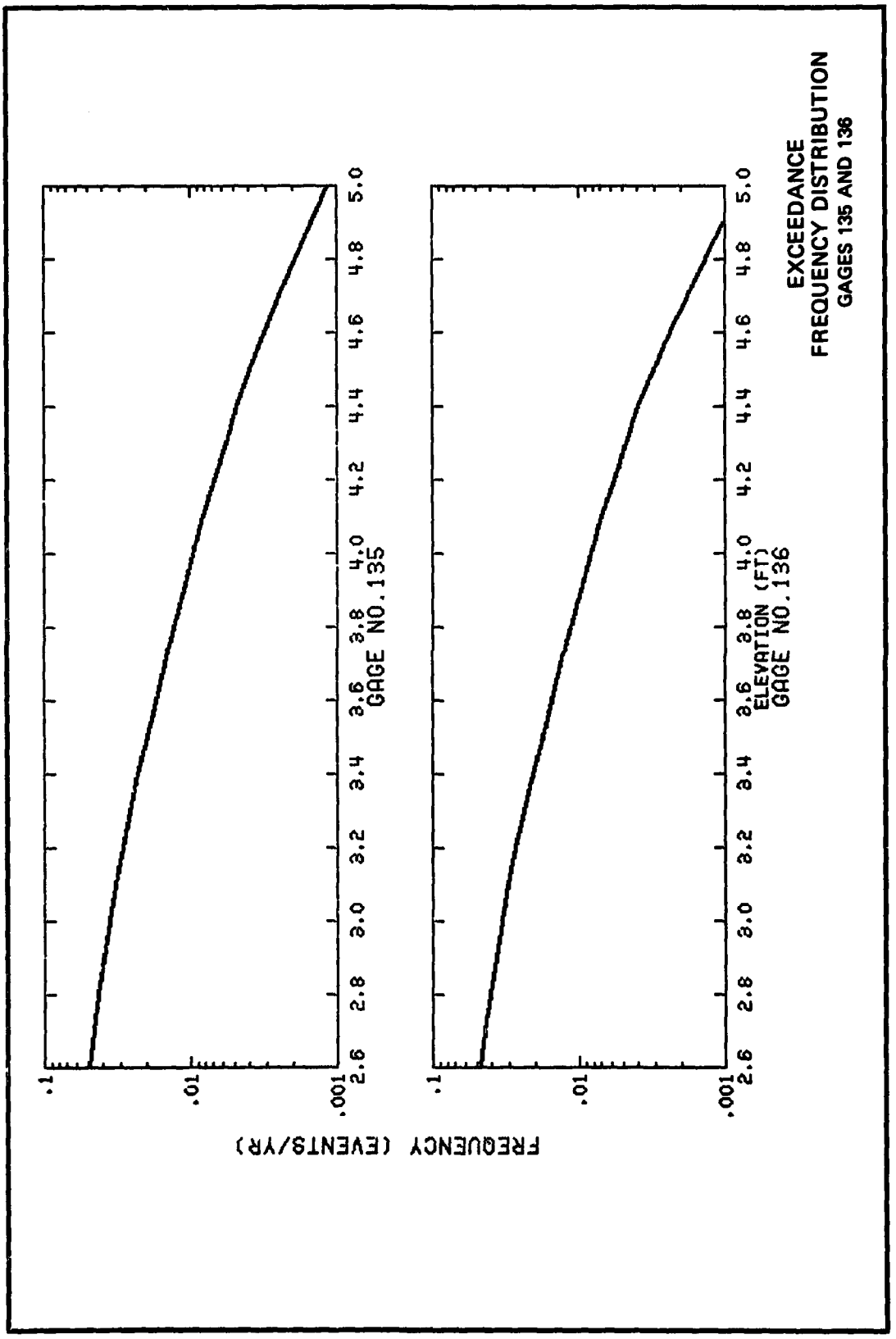
EXCEEDANCE
FREQUENCY DISTRIBUTION
GAGES 135 AND 136
FREQUENCY (EVENTS/YR)
.1
.01
.001
2.6
2.8
3.0
3.2
3.4
3.6
3.8
4.0
4.2
4.4
4.6
4.8
5.0
ELEVATION (FT)
GAGE NO.135
GAGE NO.136

PLATE 68

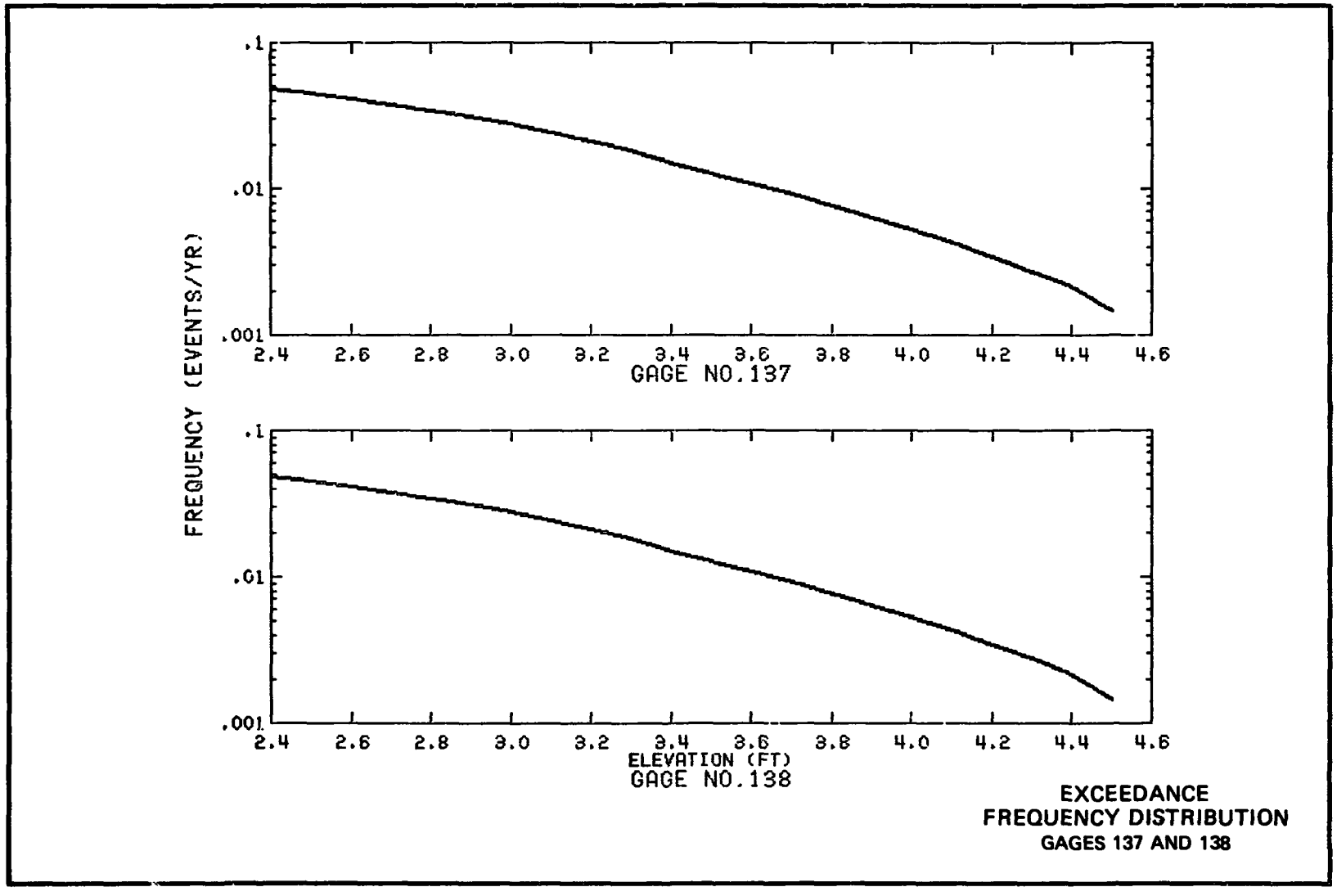

EXCEEDANCE FREQUENCY DISTRIBUTION
GAGES 137 AND 138

PLATE 69

PLATE 70

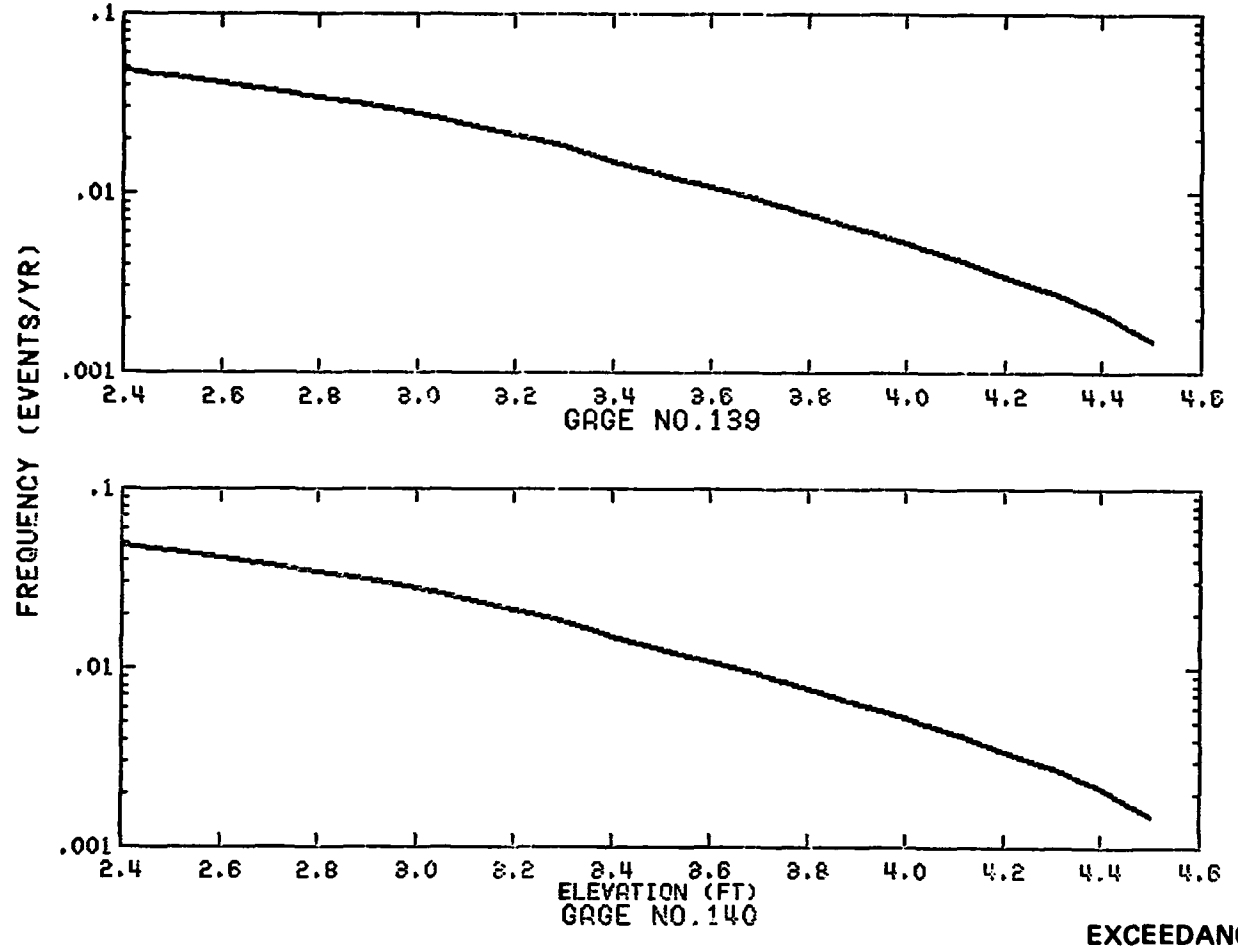

EXCEEDANCE FREQUENCY DISTRIBUTION
GAGES 139 AND 140

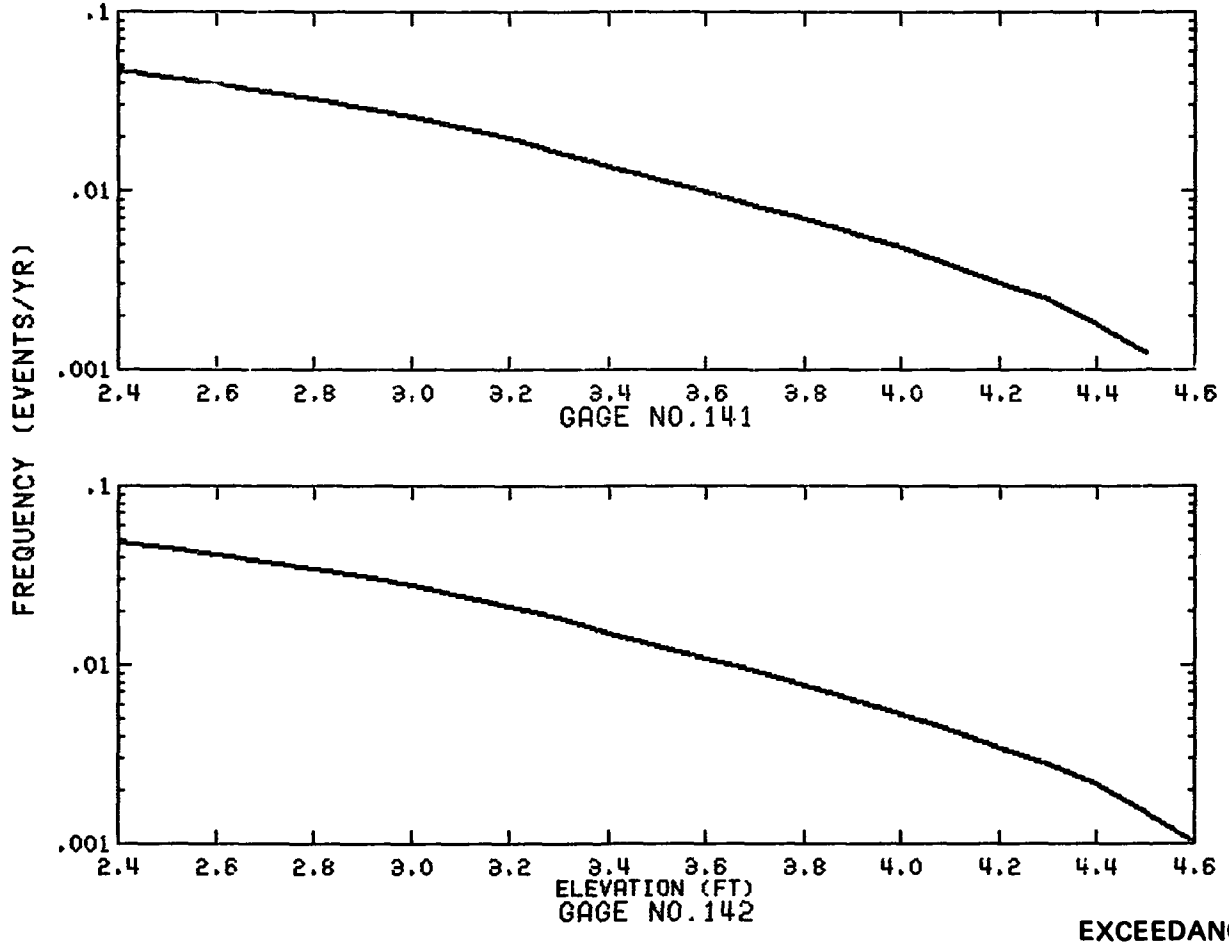

EXCEEDANCE FREQUENCY DISTRIBUTION
GAGES 141 AND 142

PLATE 71

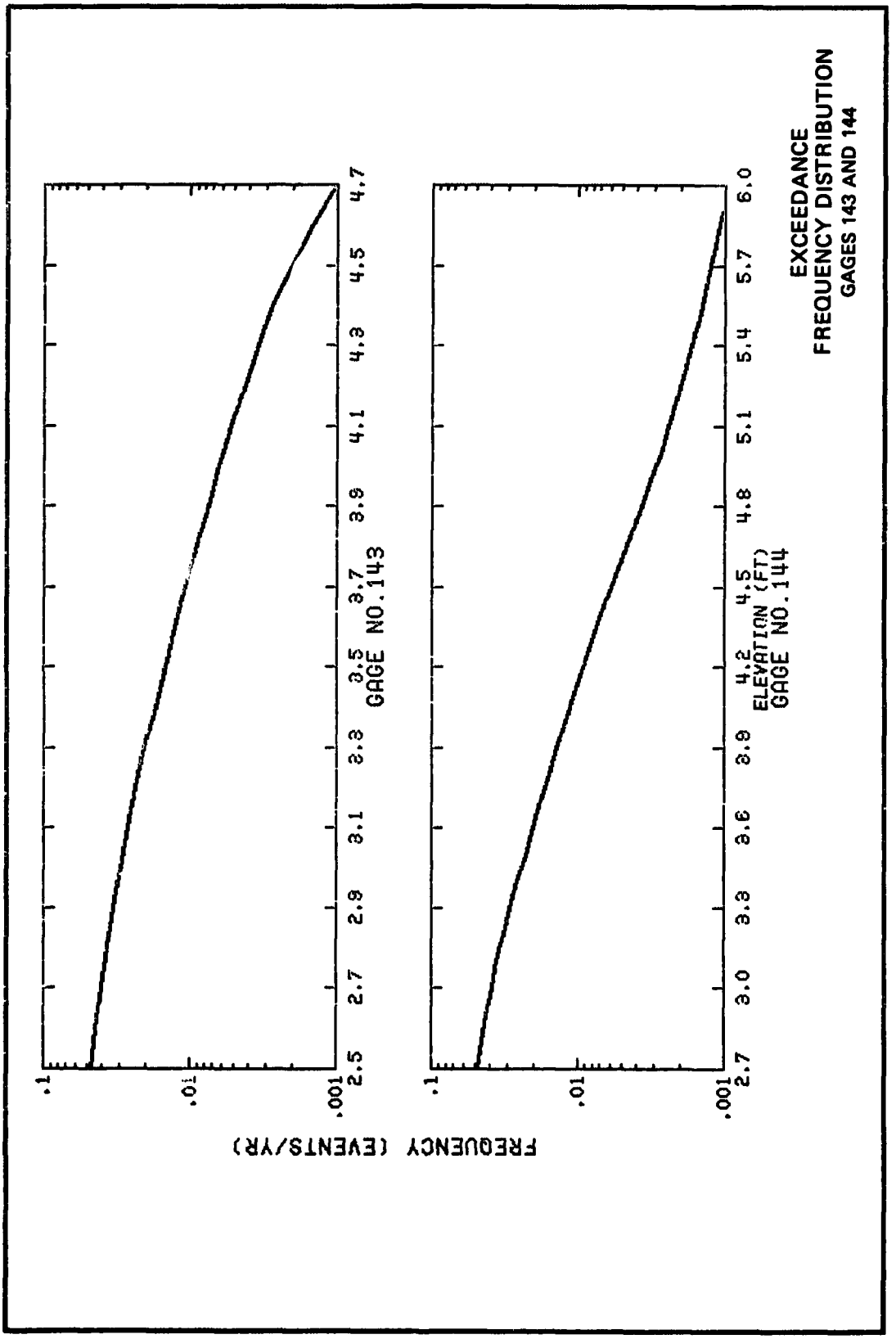
EXCEEDANCE
FREQUENCY DISTRIBUTION
GAGES 143 AND 144
FREQUENCY (EVENTS/YR)
.1
.01
.001
2.5
2.7
2.9
3.1
3.3
3.5
3.7
3.9
4.1
4.3
4.5
4.7
GAGE NO.143
ELEVATION (FT)
2.7
3.0
3.3
3.6
3.9
4.2
4.5
4.8
5.1
5.4
5.7
6.0
GAGE NO.144

PLATE 72

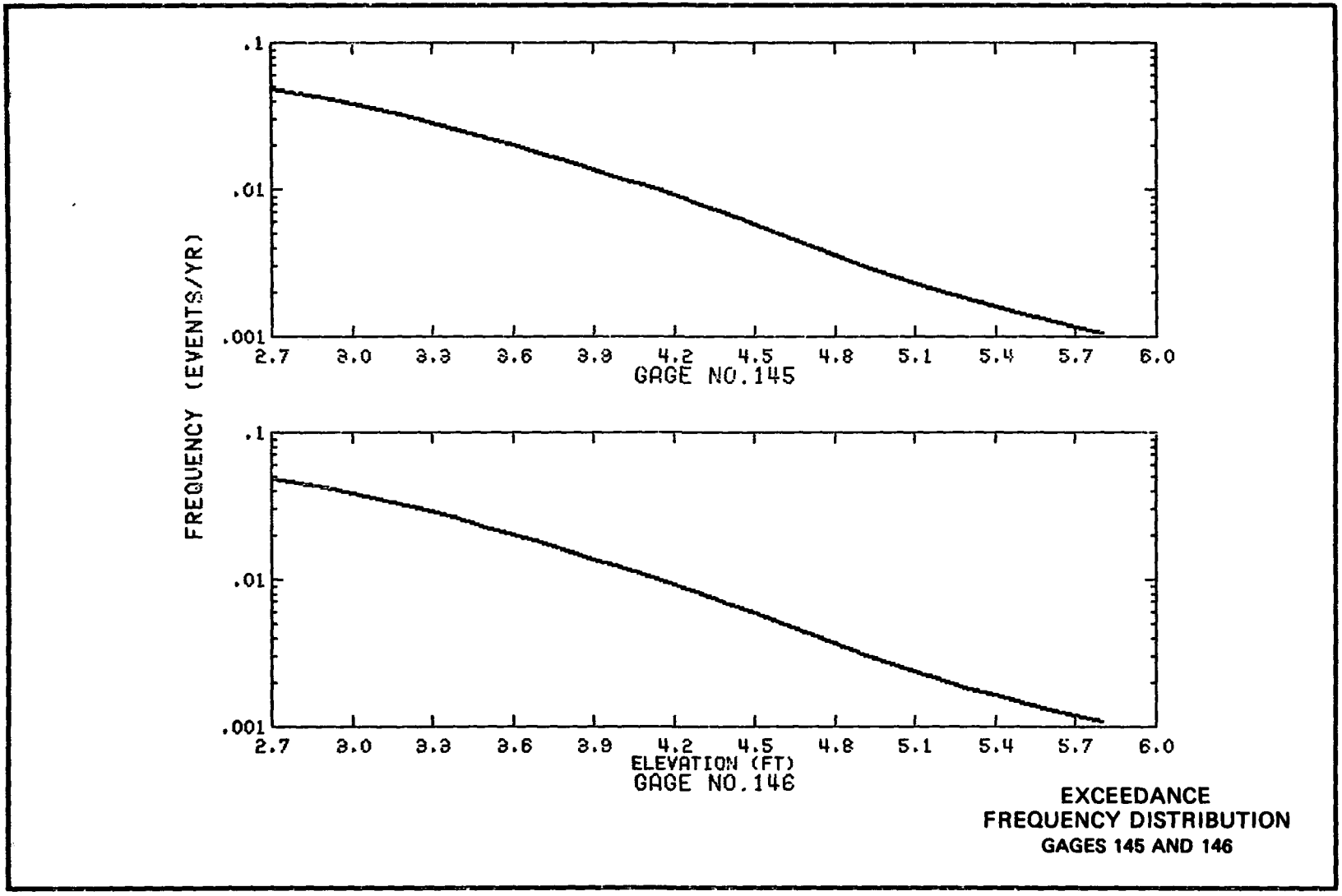

EXCEEDANCE FREQUENCY DISTRIBUTION
GAGES 145 AND 146

PLATE 73

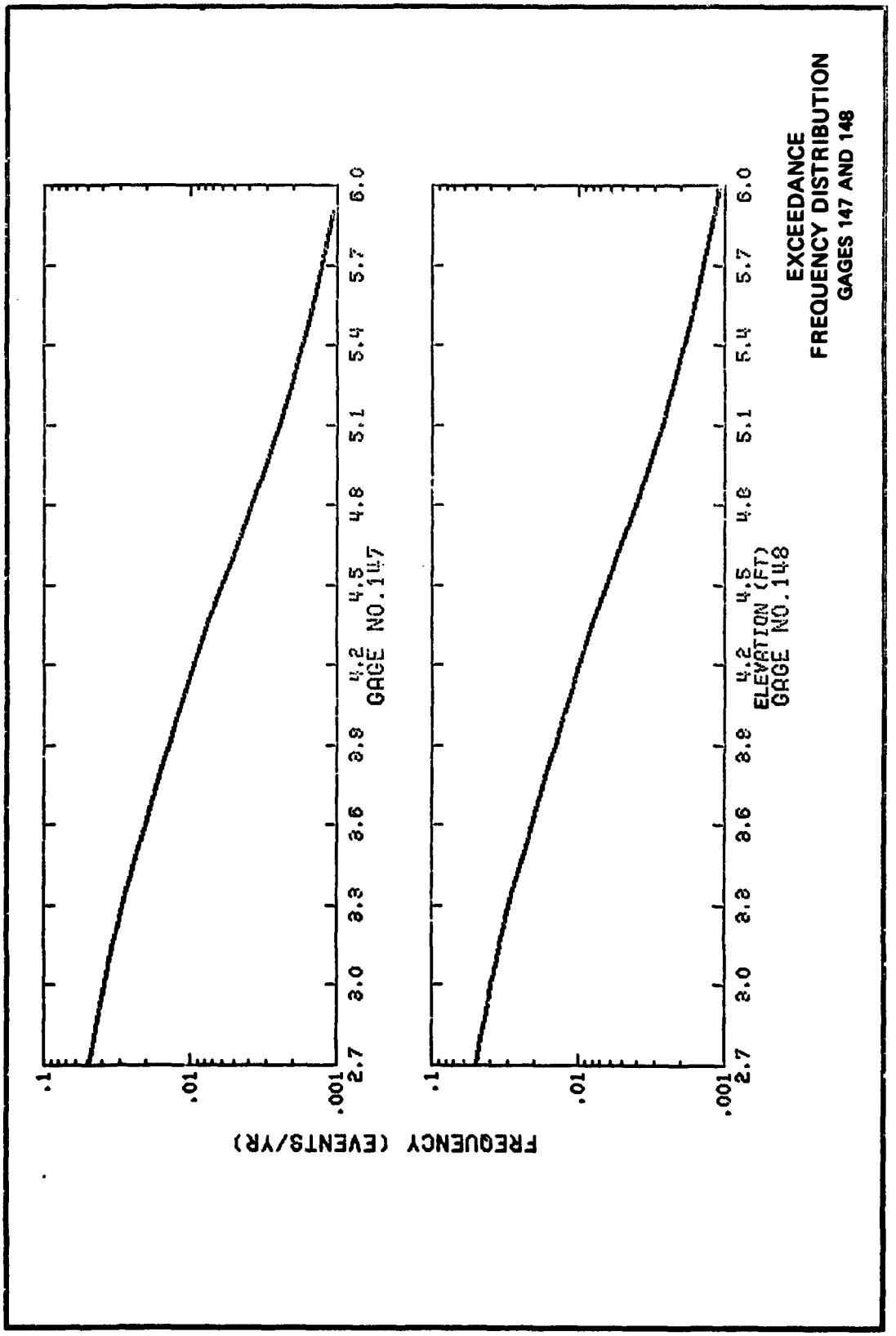
EXCEEDANCE
FREQUENCY DISTRIBUTION
GAGES 147 AND 148
FREQUENCY (EVENTS/YR)
.1
.01
.001
2.7
3.0
3.3
3.6
3.9
4.2
4.5
4.8
5.1
5.4
5.7
6.0
ELEVATION (FT)
GAGE NO.147
GAGE NO.148

PLATE 74

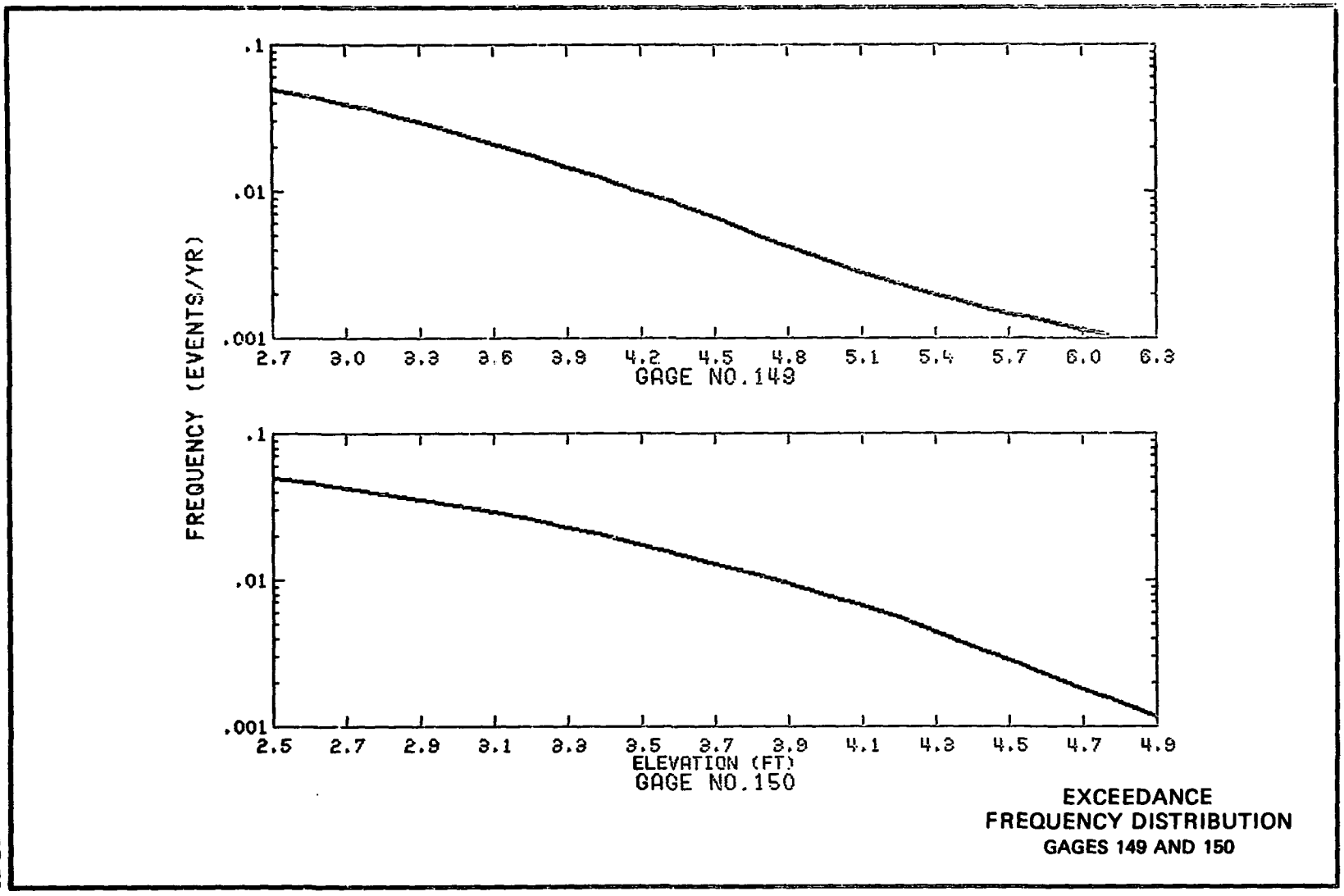

EXCEEDANCE FREQUENCY DISTRIBUTION
GAGES 149 AND 150

PLATE 75

PLATE 76

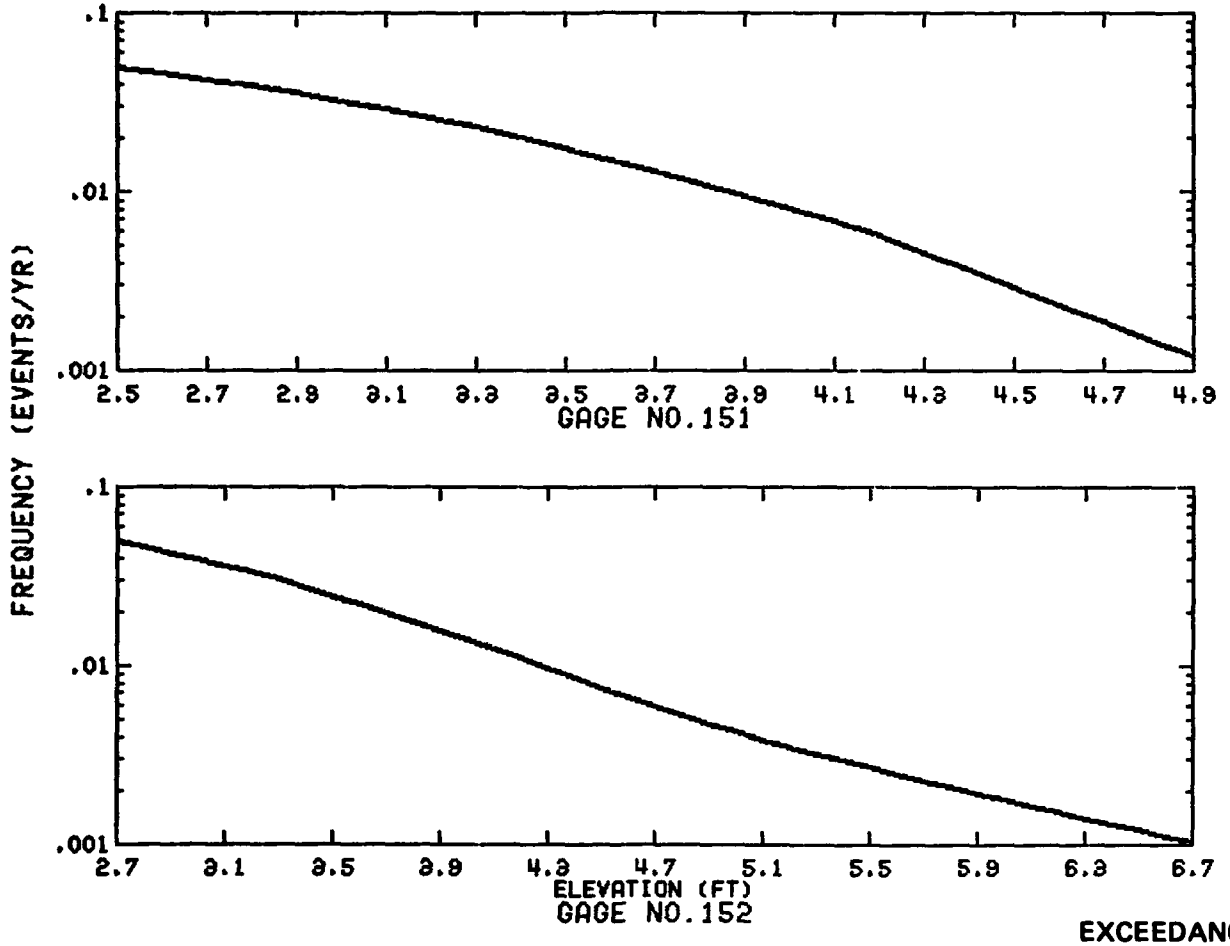

EXCEEDANCE FREQUENCY DISTRIBUTION
GAGES 151 AND 152

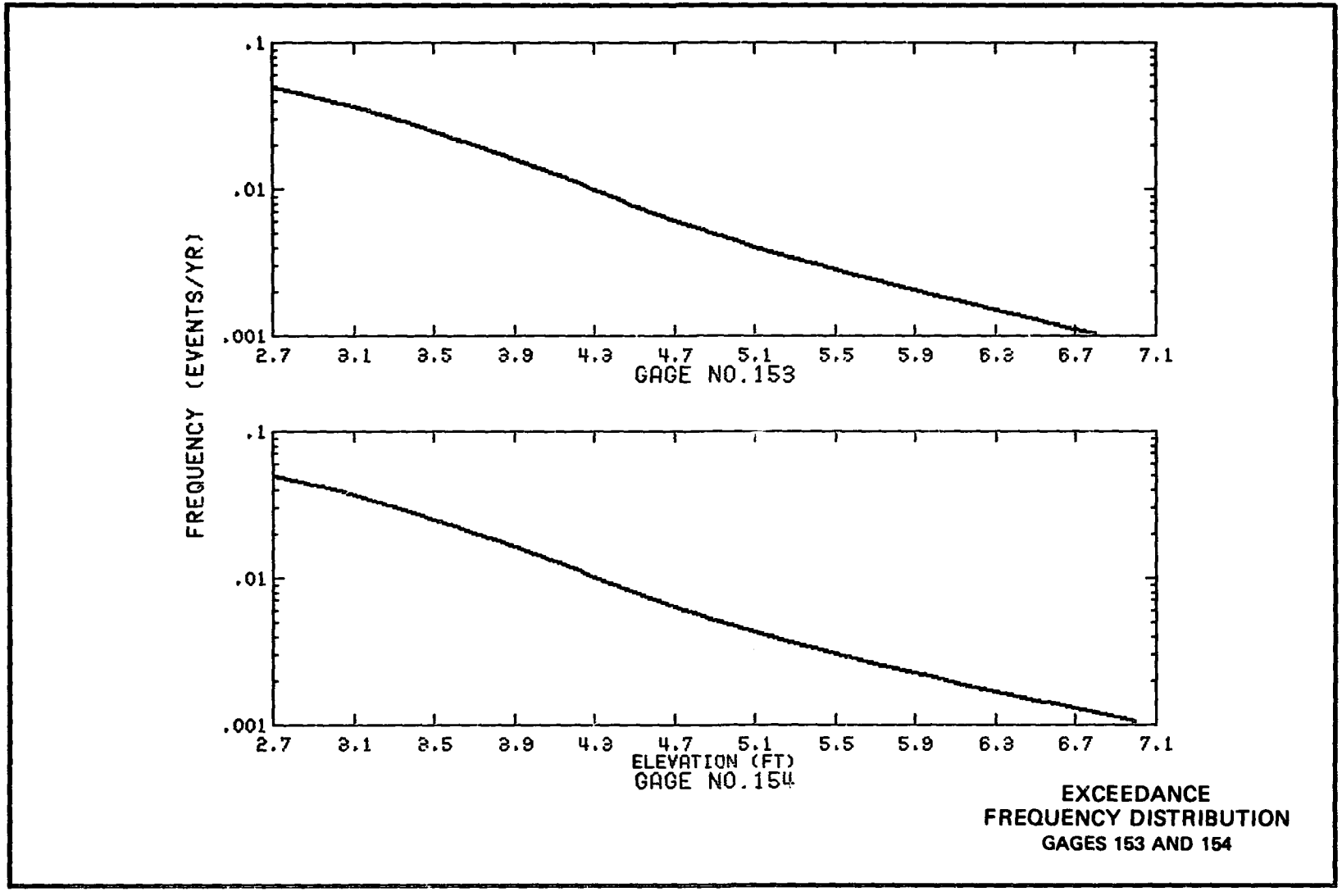

EXCEEDANCE FREQUENCY DISTRIBUTION
GAGES 153 AND 154

PLATE 77

PLATE 78

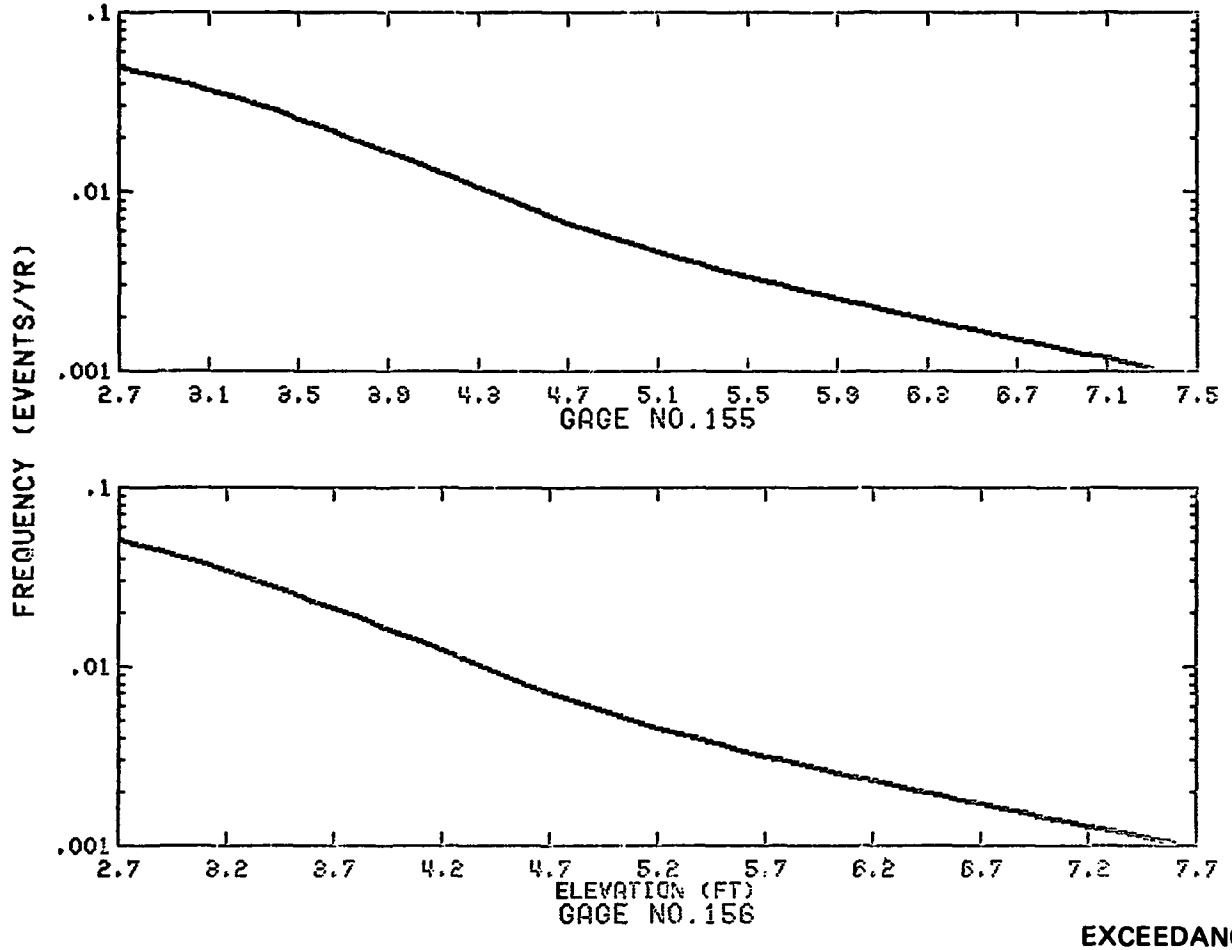

EXCEEDANCE FREQUENCY DISTRIBUTION
GAGES 155 AND 156

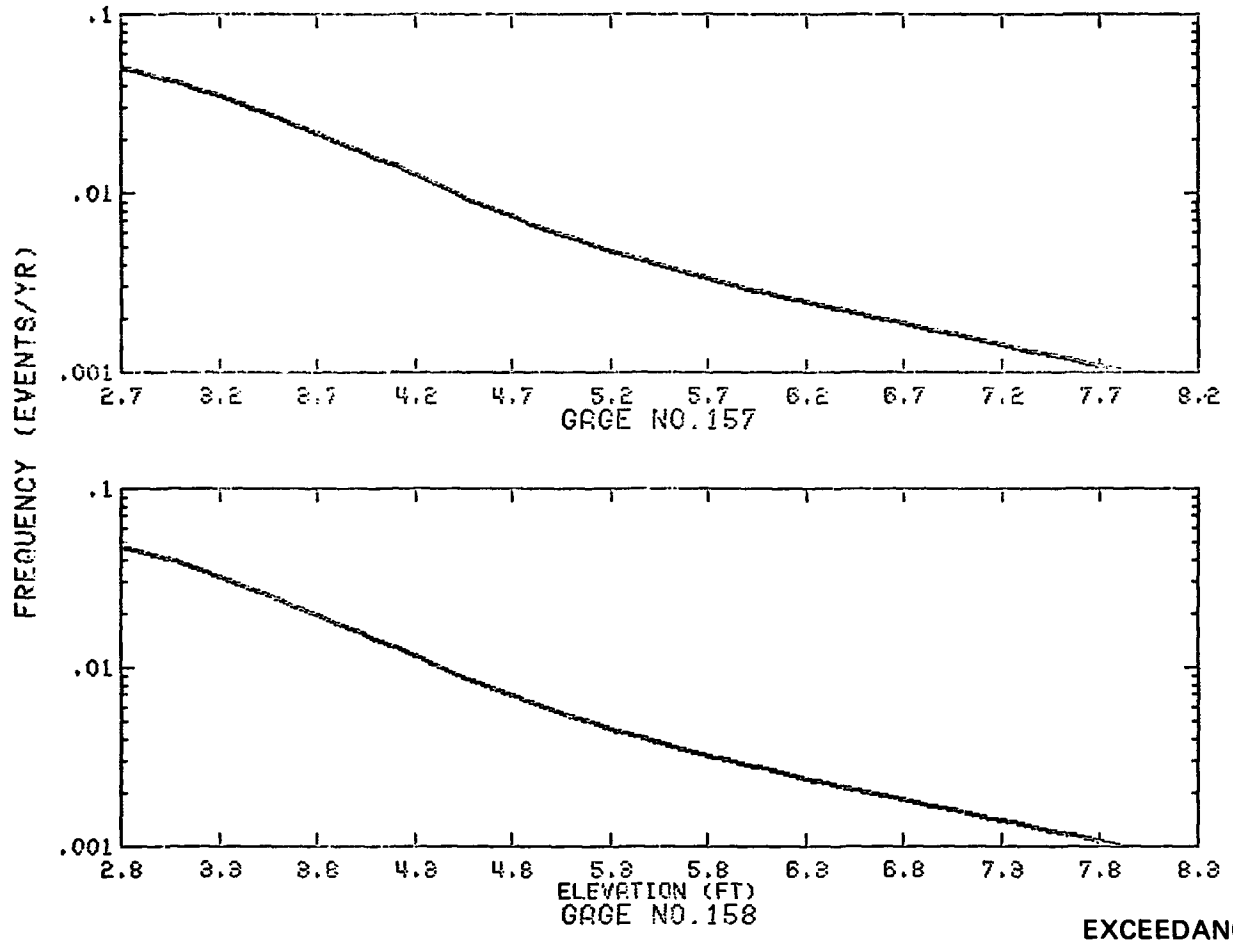

EXCEEDANCE FREQUENCY DISTRIBUTION
GAGES 157 AND 158

PLATE 79

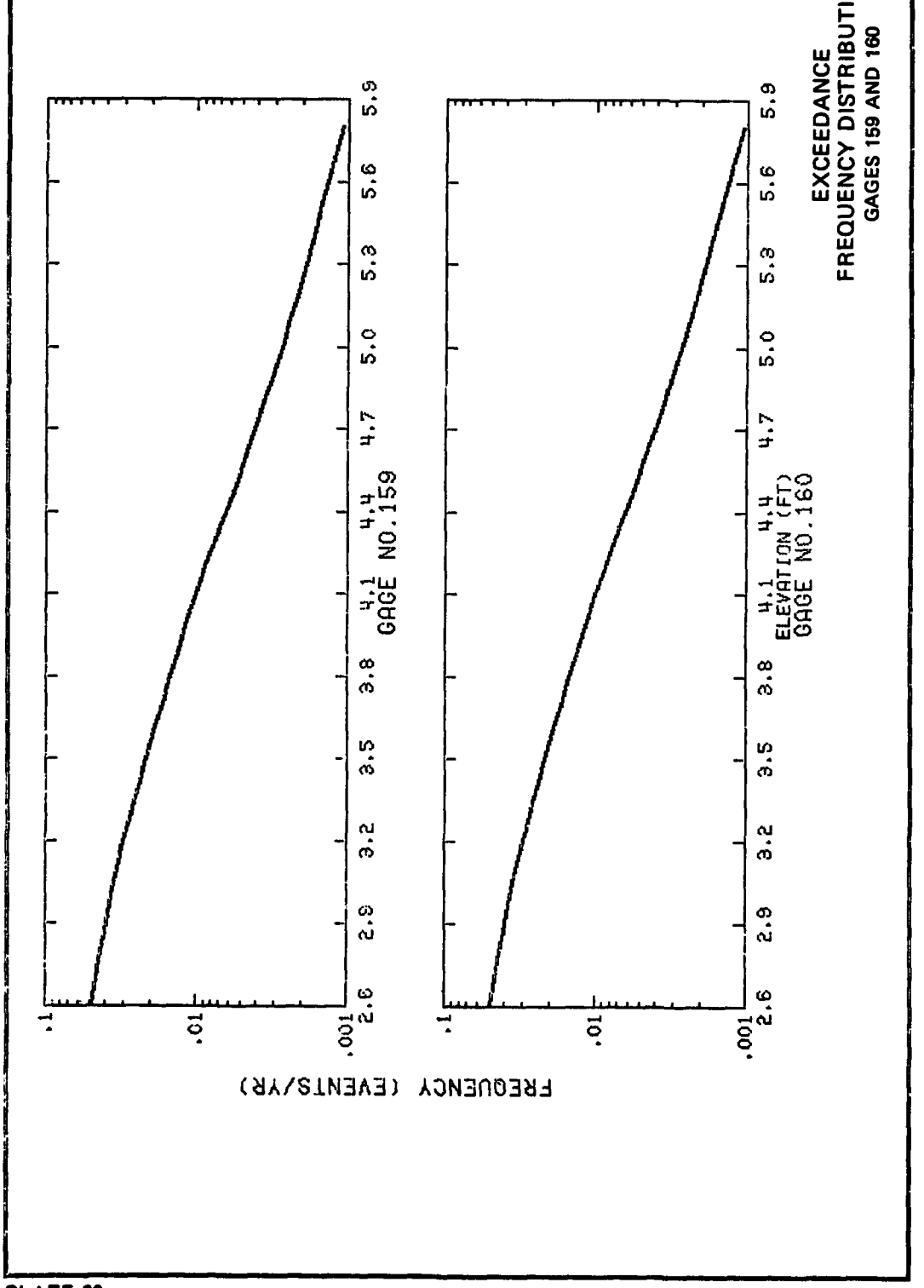
EXCEEDANCE
FREQUENCY DISTRIBUTION
GAGES 159 AND 160
FREQUENCY (EVENTS/YR)
.1
.01
.001
2.6
2.9
3.2
3.5
3.8
4.1
4.4
4.7
5.0
5.3
5.6
5.9
ELEVATION (FT)
GAGE NO.159
GAGE NO.160

PLATE 80

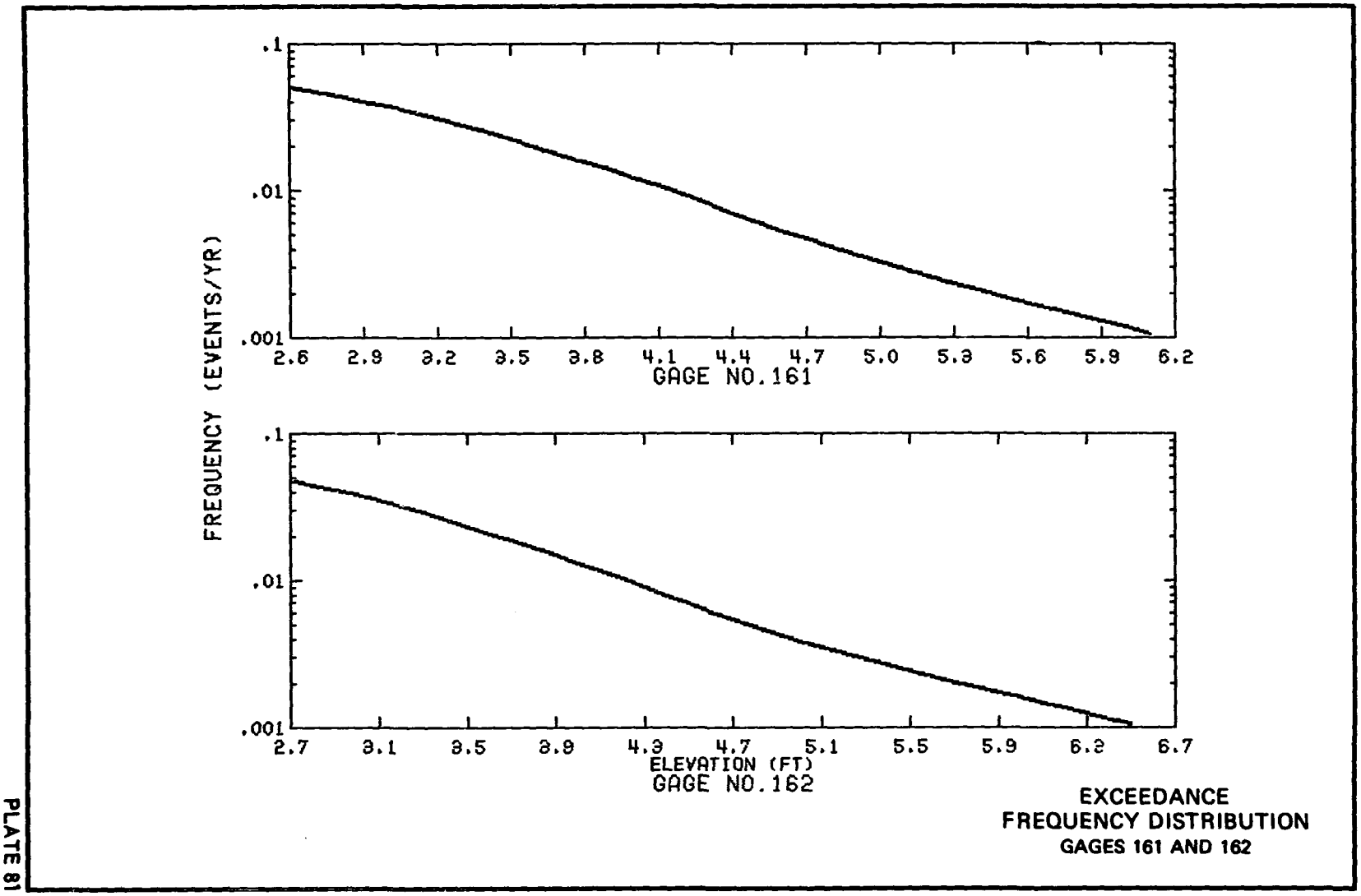

EXCEEDANCE FREQUENCY DISTRIBUTION
GAGES 161 AND 162

PLATE 81

PLATE 82

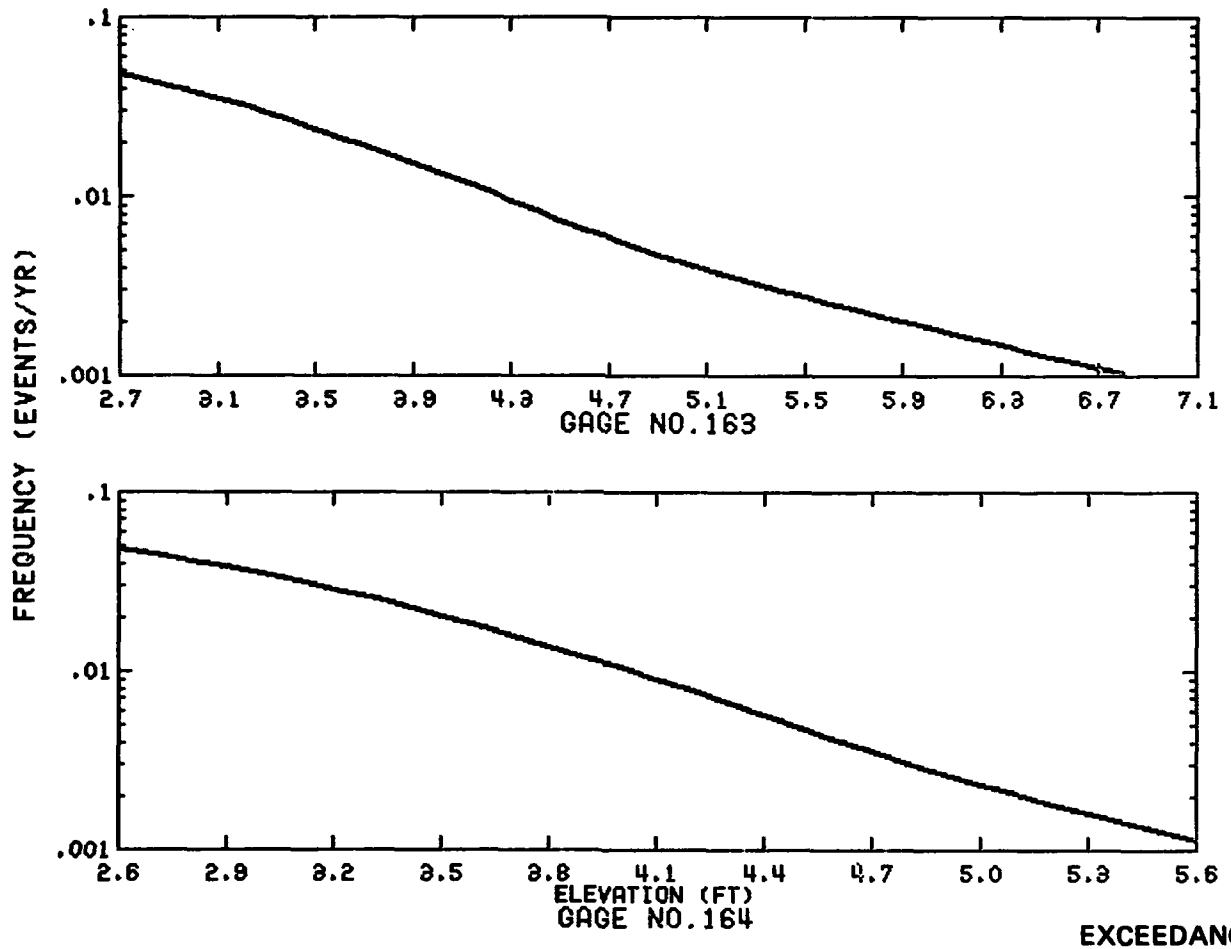

EXCEEDANCE FREQUENCY DISTRIBUTION

GAGES 163 AND 164

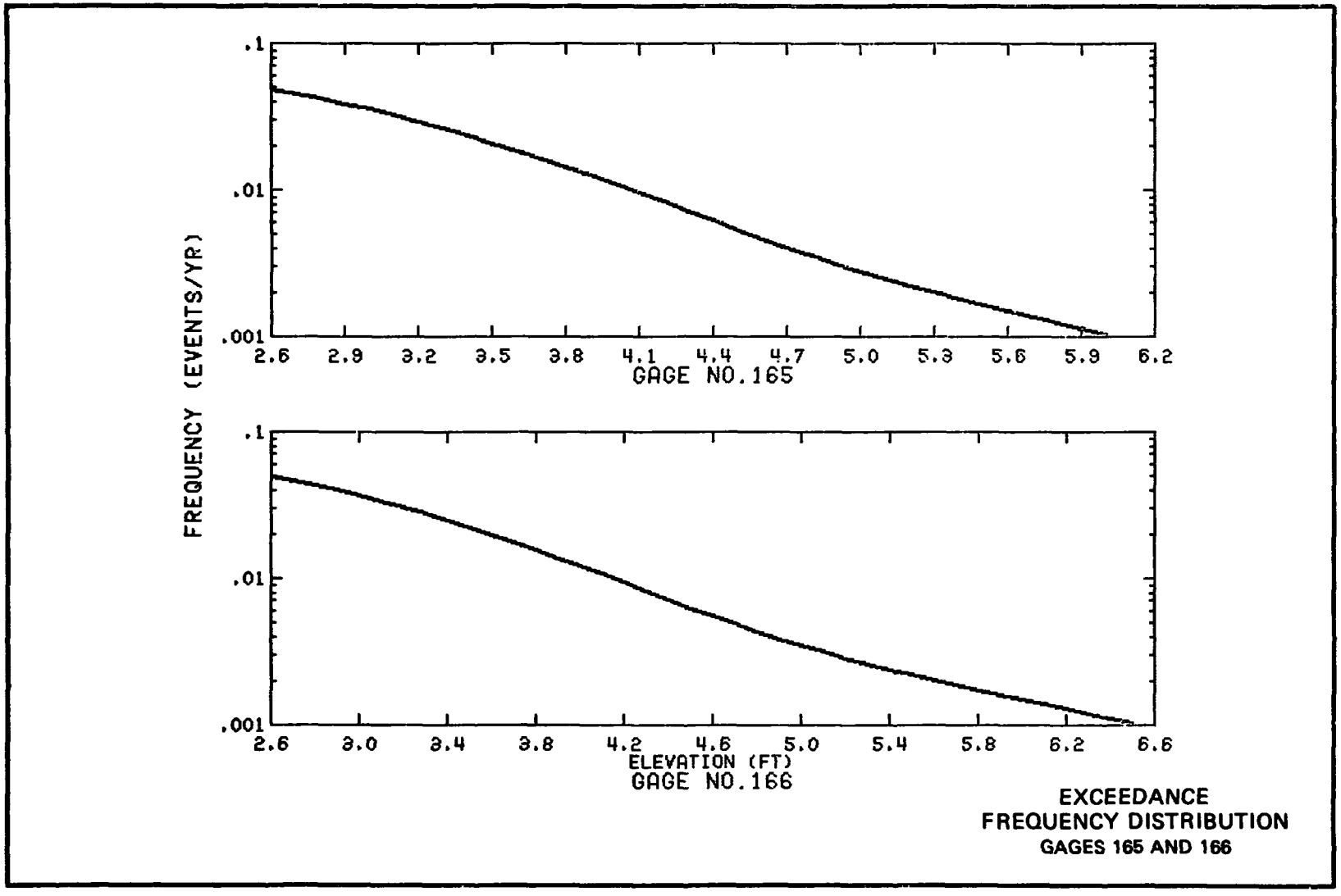

EXCEEDANCE FREQUENCY DISTRIBUTION
GAGES 165 AND 166

PLATE 83

PLATE 84

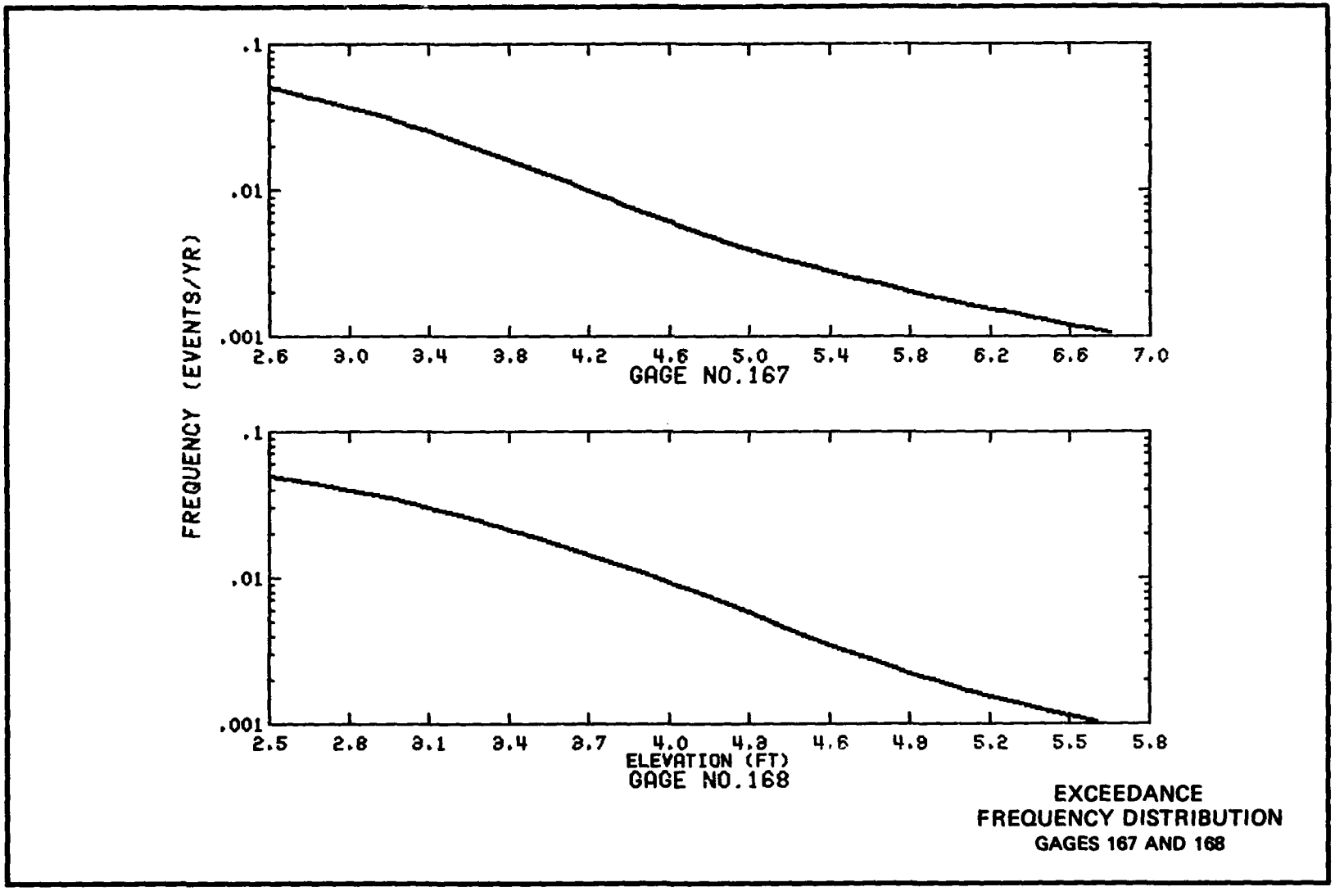

EXCEEDANCE FREQUENCY DISTRIBUTION
GAGES 167 AND 168

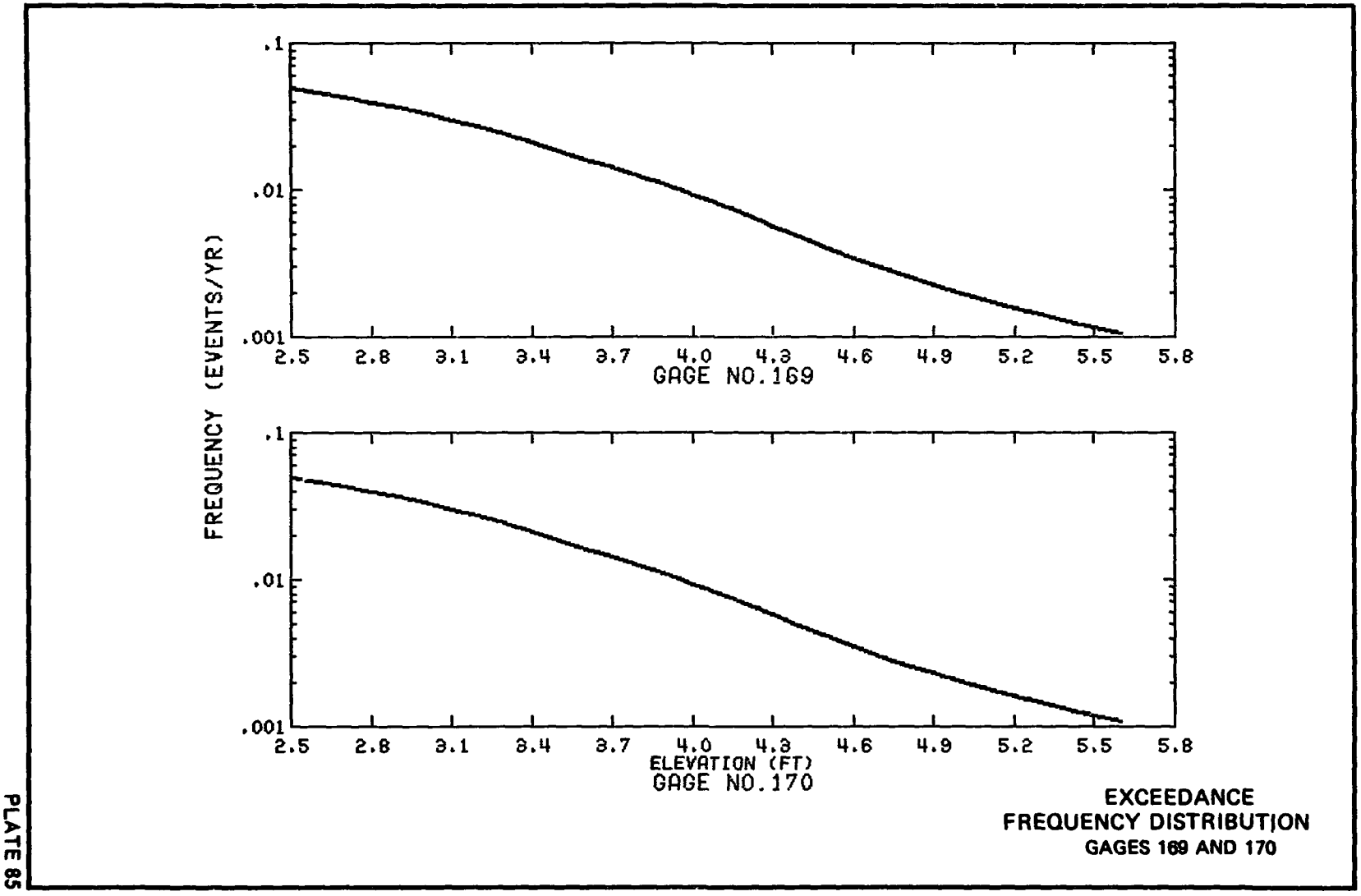

EXCEEDANCE FREQUENCY DISTRIBUTION
GAGES 169 AND 170

PLATE 85

PLATE 86

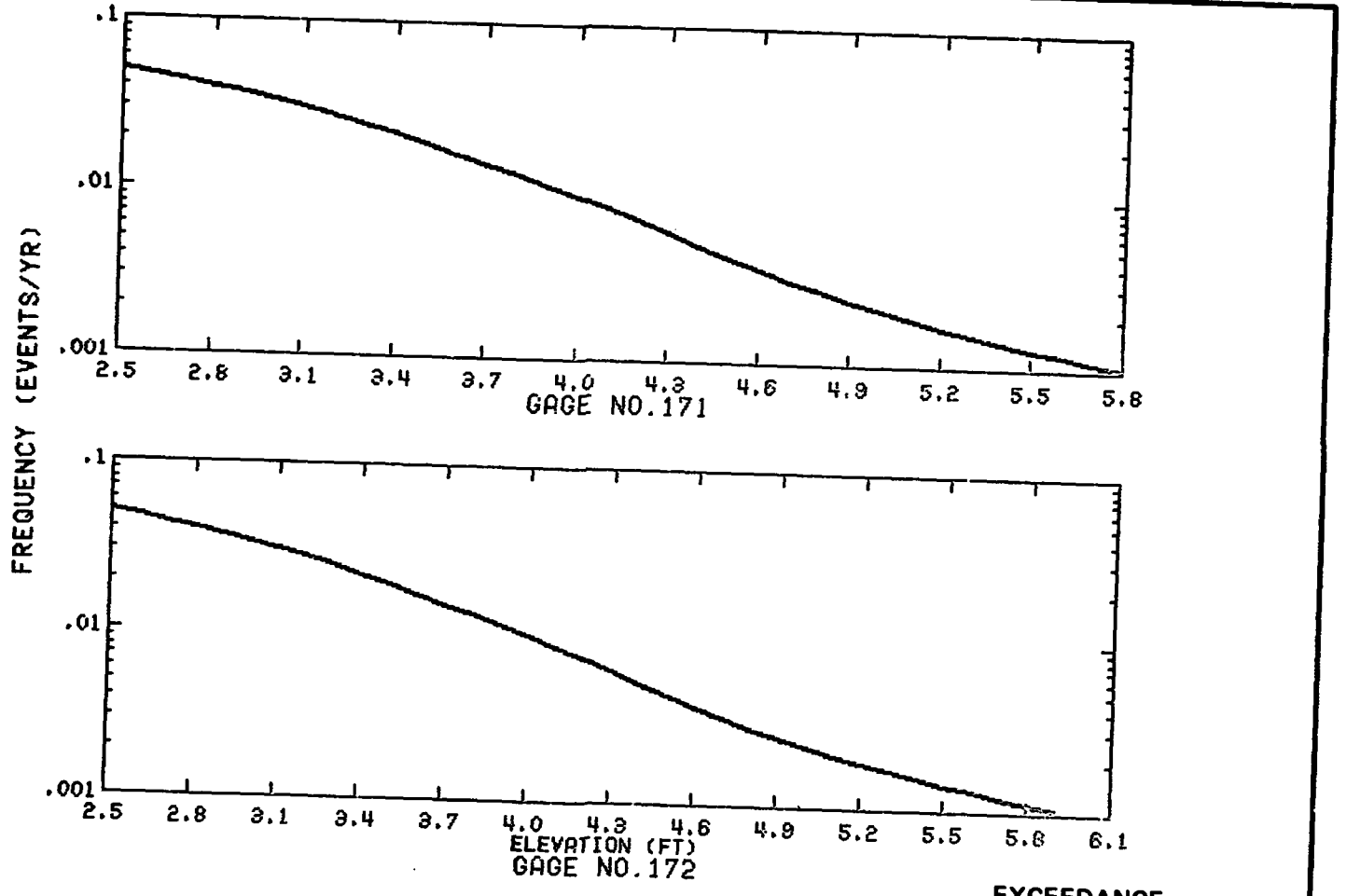

EXCEEDANCE FREQUENCY DISTRIBUTION
GAGES 171 AND 172

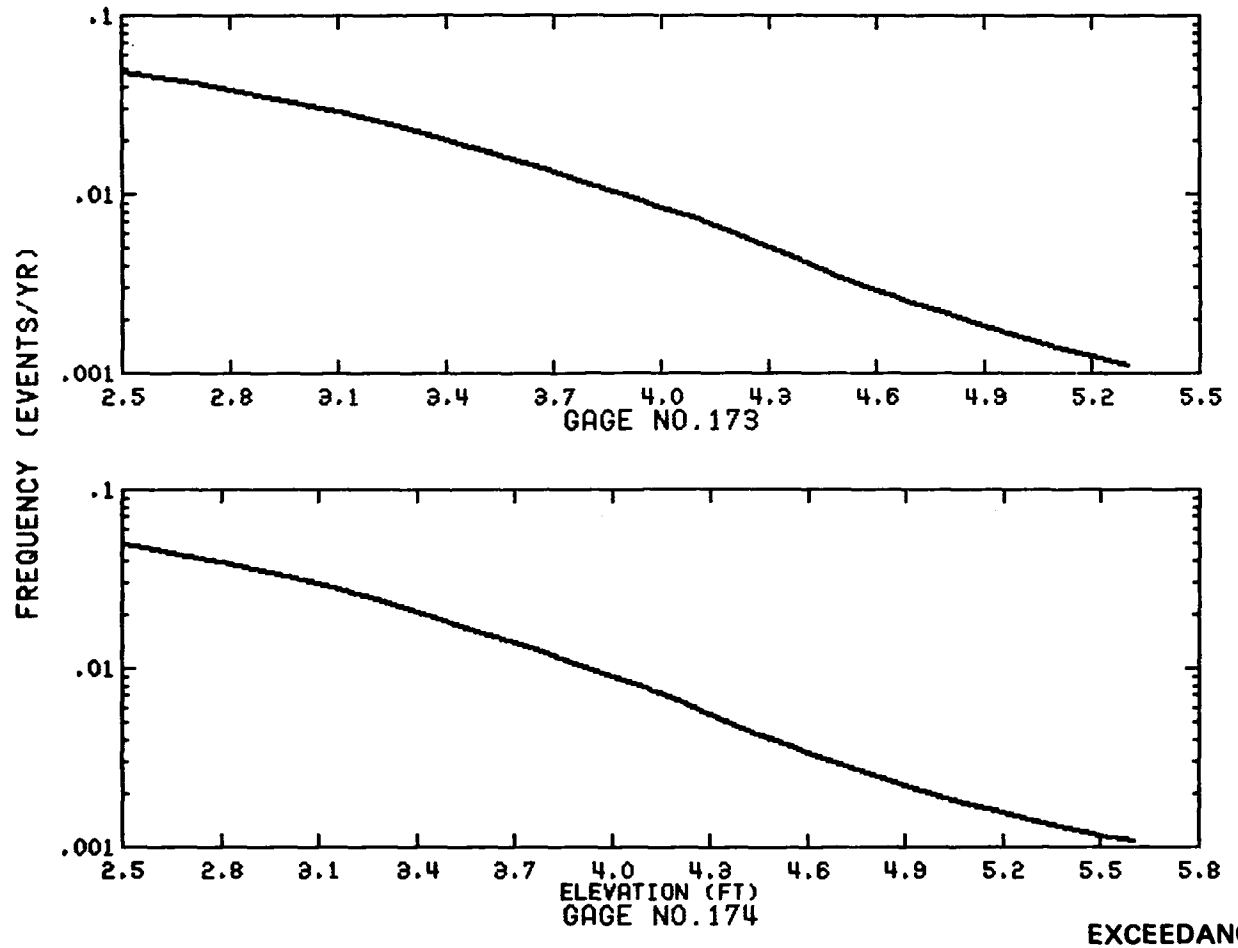

EXCEEDANCE FREQUENCY DISTRIBUTION
GAGES 173 AND 174

PLATE 87

PLATE 88

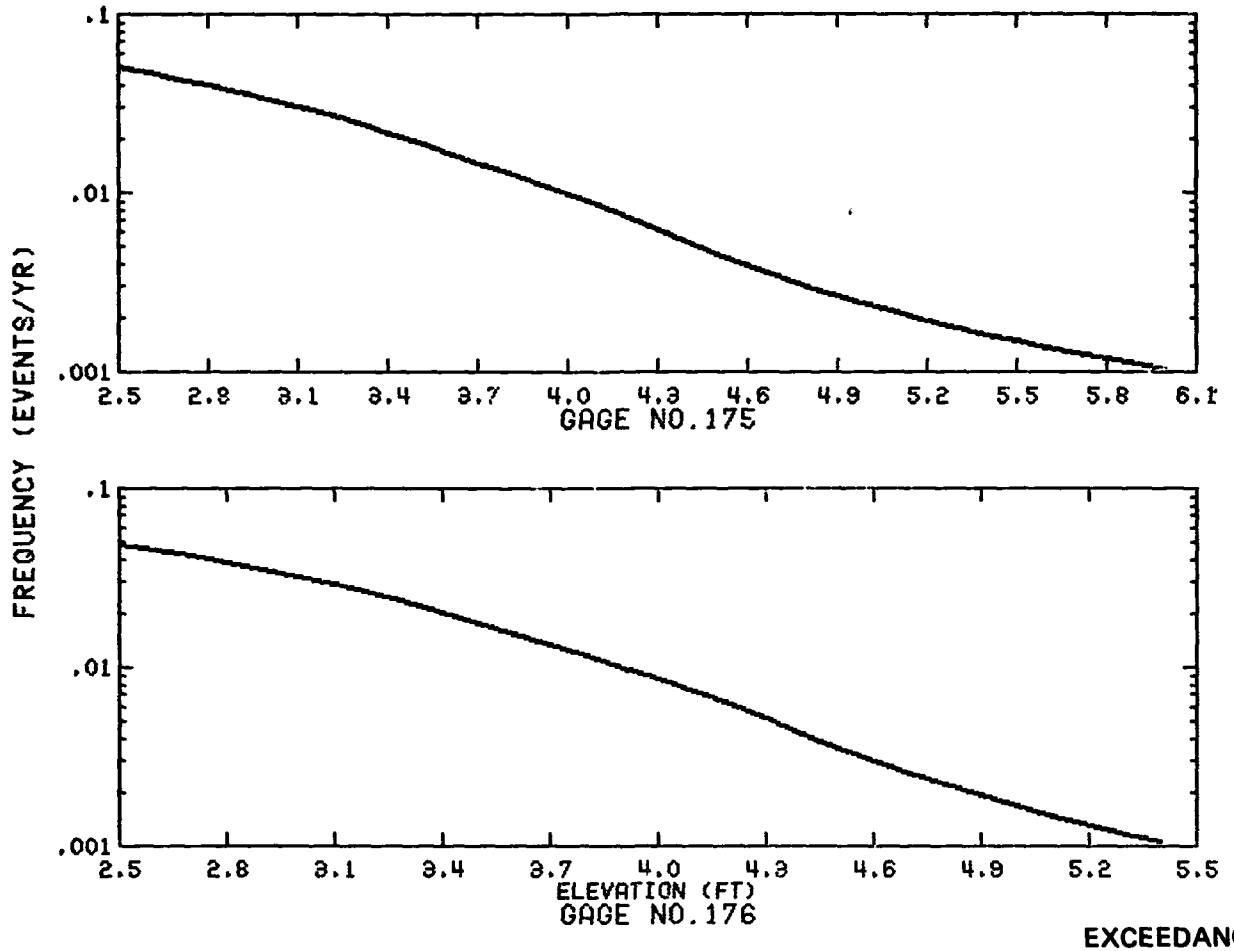

EXCEEDANCE FREQUENCY DISTRIBUTION
GAGES 175 AND 176

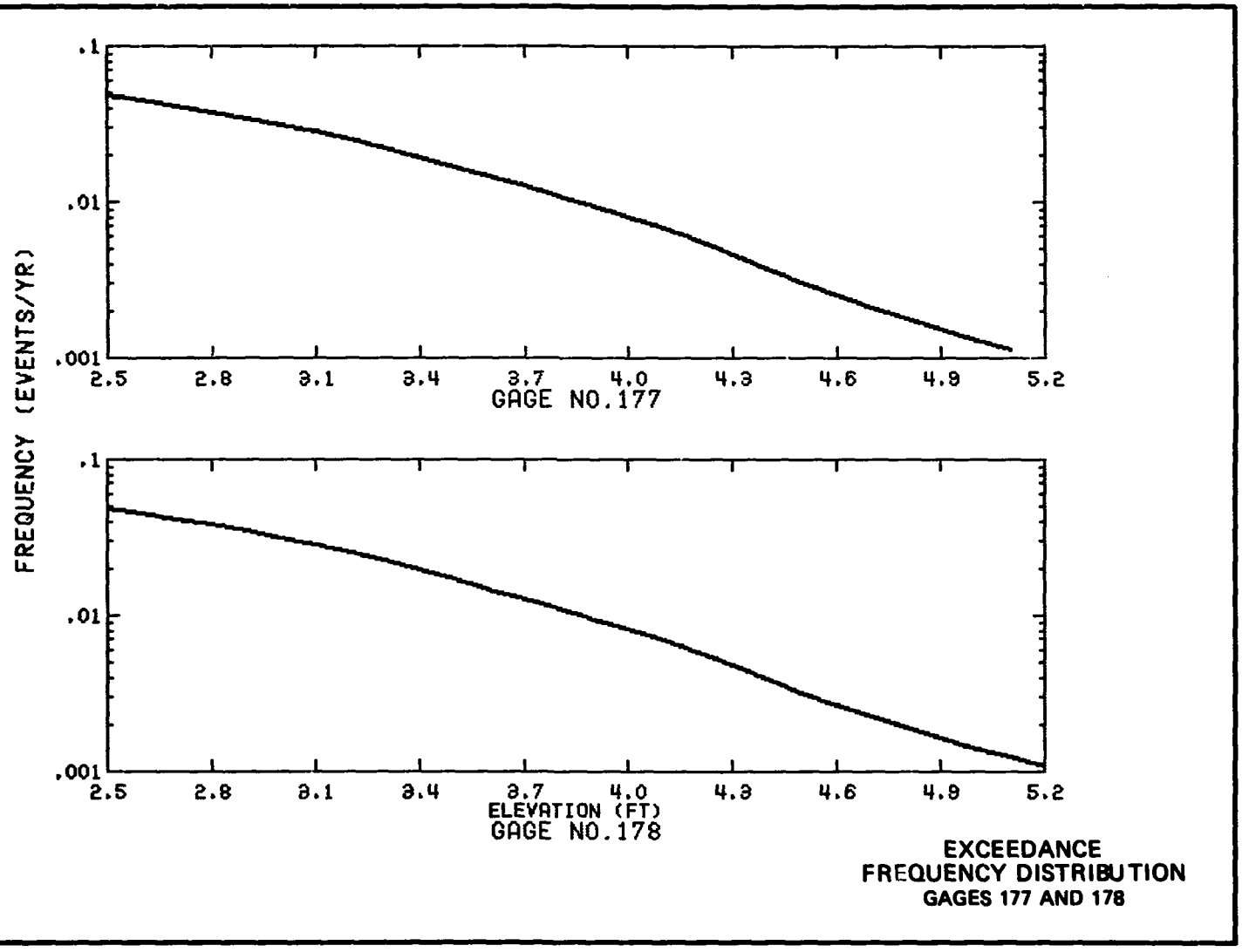

EXCEEDANCE FREQUENCY DISTRIBUTION
GAGES 177 AND 178

PLATE 89

PLATE 90

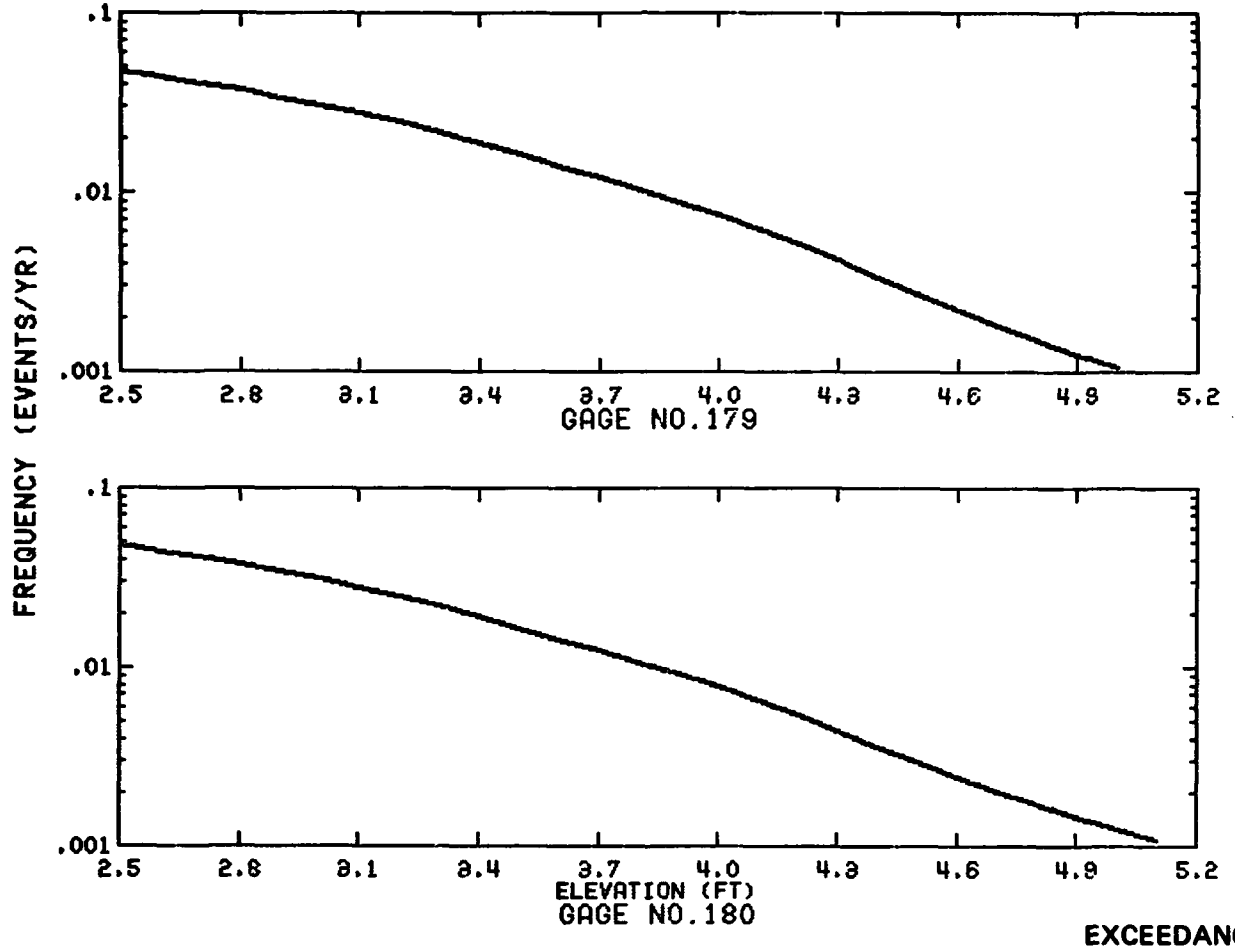

EXCEEDANCE FREQUENCY DISTRIBUTION
GAGES 179 AND 180

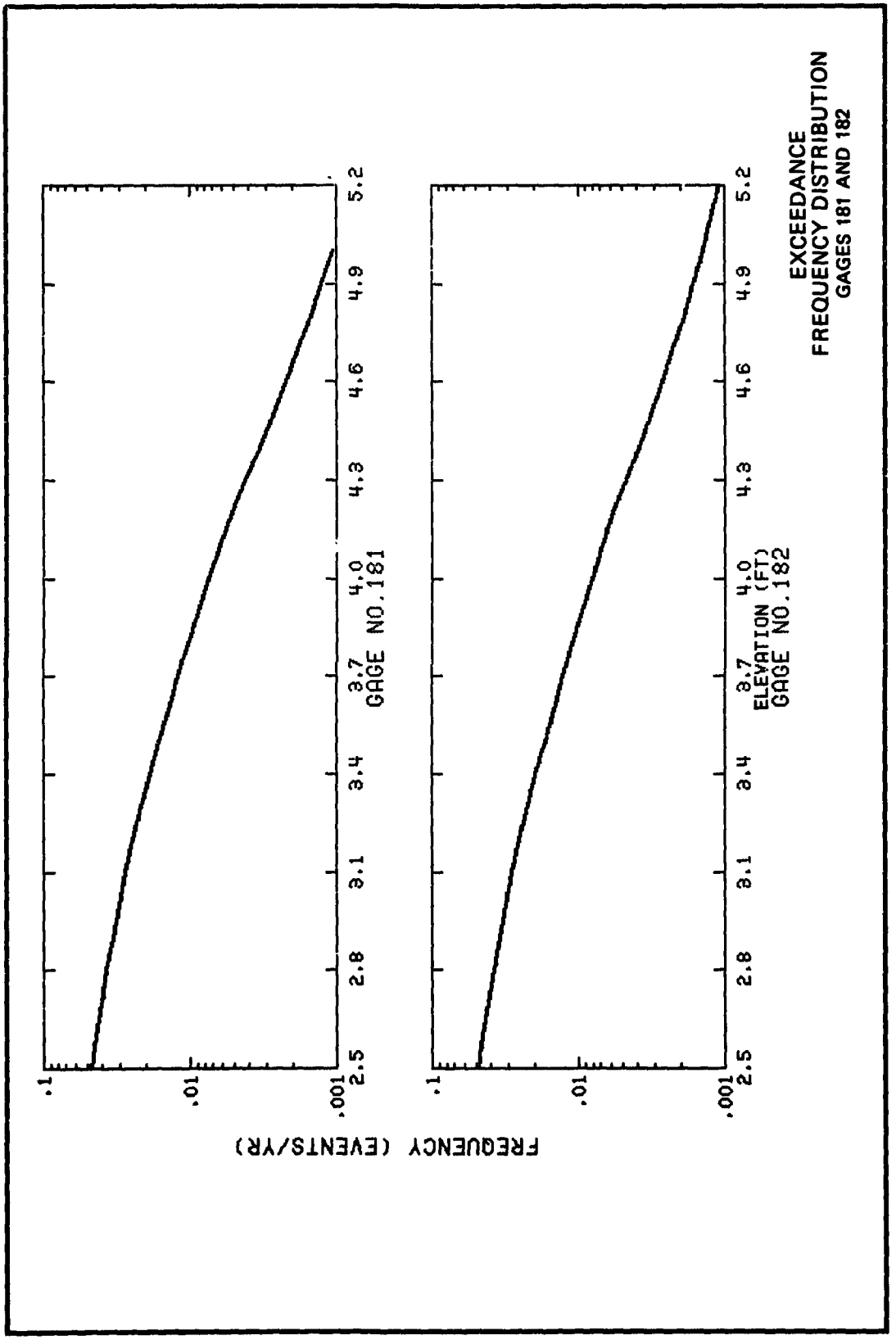
EXCEEDANCE
FREQUENCY DISTRIBUTION
GAGES 181 AND 182
FREQUENCY (EVENTS/YR)
.1
.01
.001
2.5
2.8
3.1
3.4
3.7
4.0
4.3
4.6
4.9
5.2
ELEVATION (FT)
GAGE NO.181
GAGE NO.182

PLATE 91

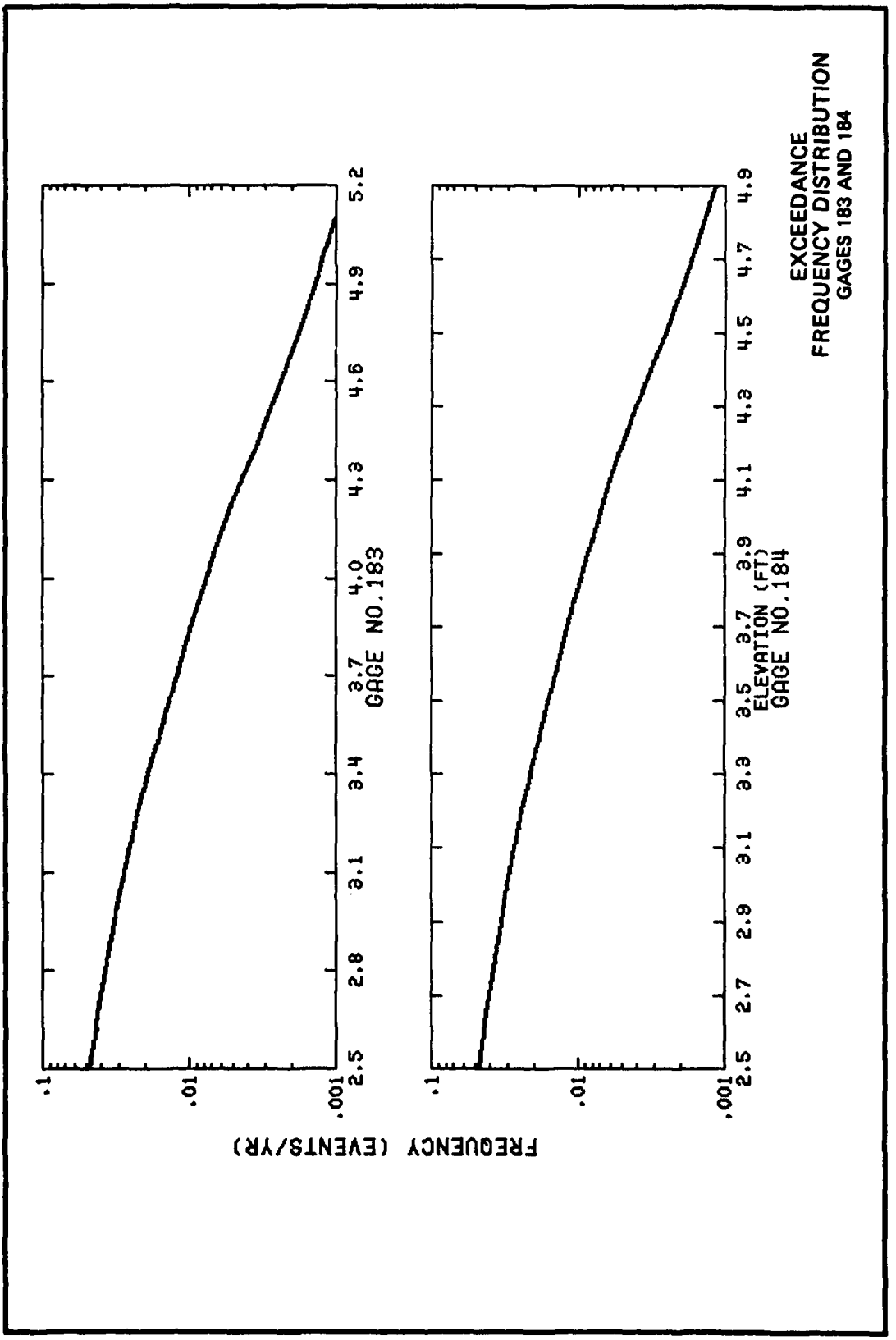
EXCEEDANCE
FREQUENCY DISTRIBUTION
GAGES 183 AND 184
FREQUENCY (EVENTS/YR)
.1
.01
.001
2.5
2.8
3.1
3.4
3.7
4.0
4.3
4.6
4.9
5.2
ELEVATION (FT)
GAGE NO.183
2.5
2.7
2.9
3.1
3.3
3.5
3.7
3.9
4.1
4.3
4.5
4.7
4.9
ELEVATION (FT)
GAGE NO.184

PLATE 92

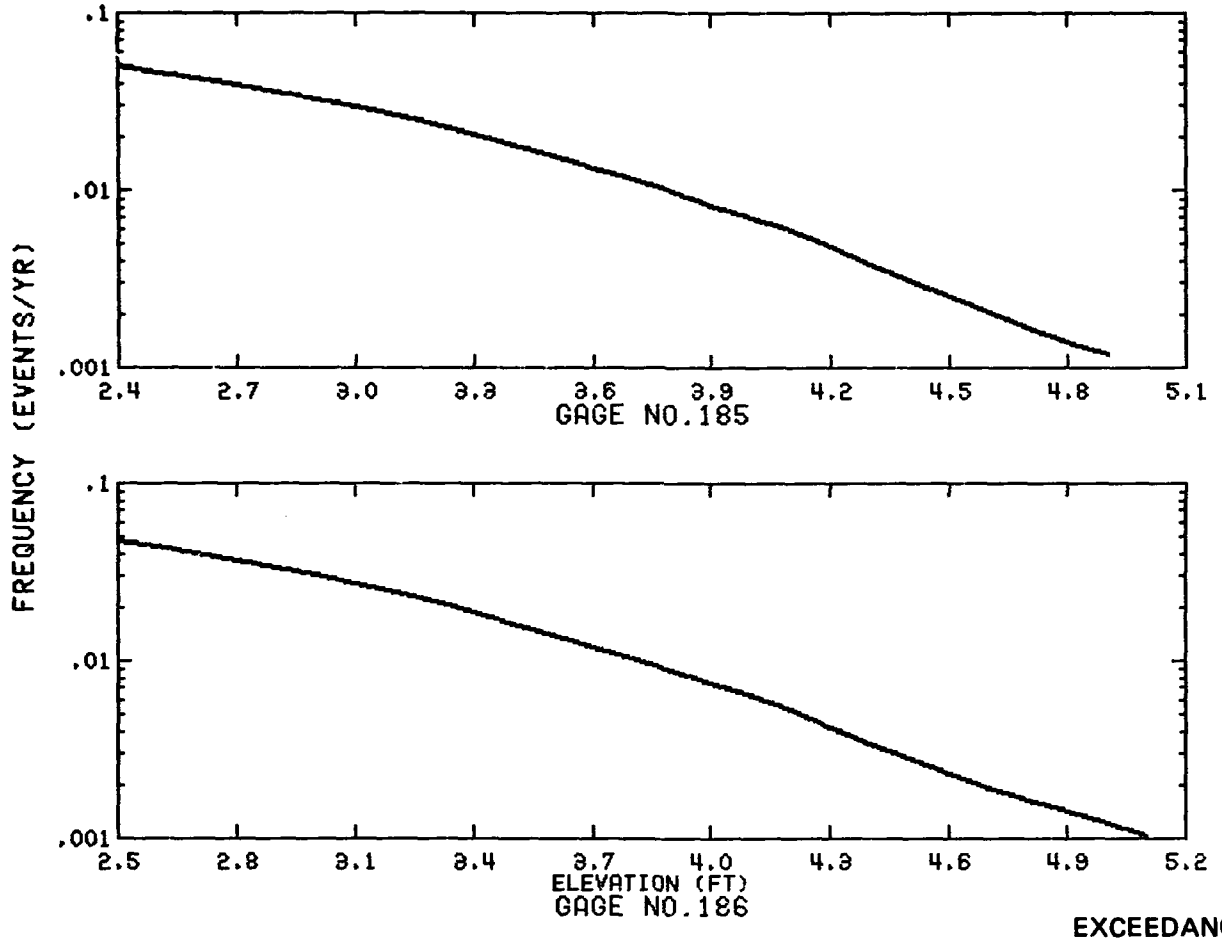

EXCEEDANCE FREQUENCY DISTRIBUTION
GAGES 185 AND 186

PLATE 93

PLATE 94

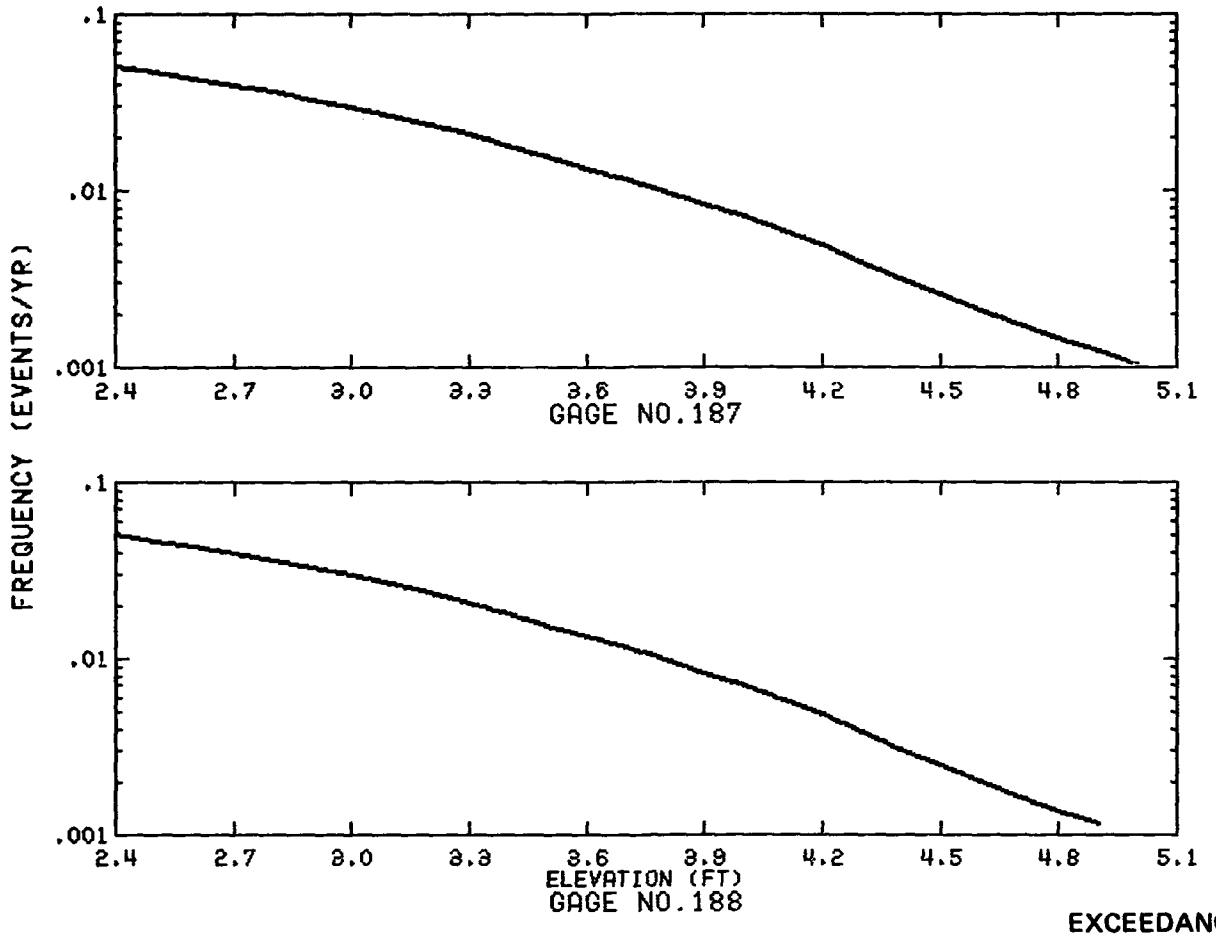

EXCEEDANCE FREQUENCY DISTRIBUTION
GAGES 187 AND 188

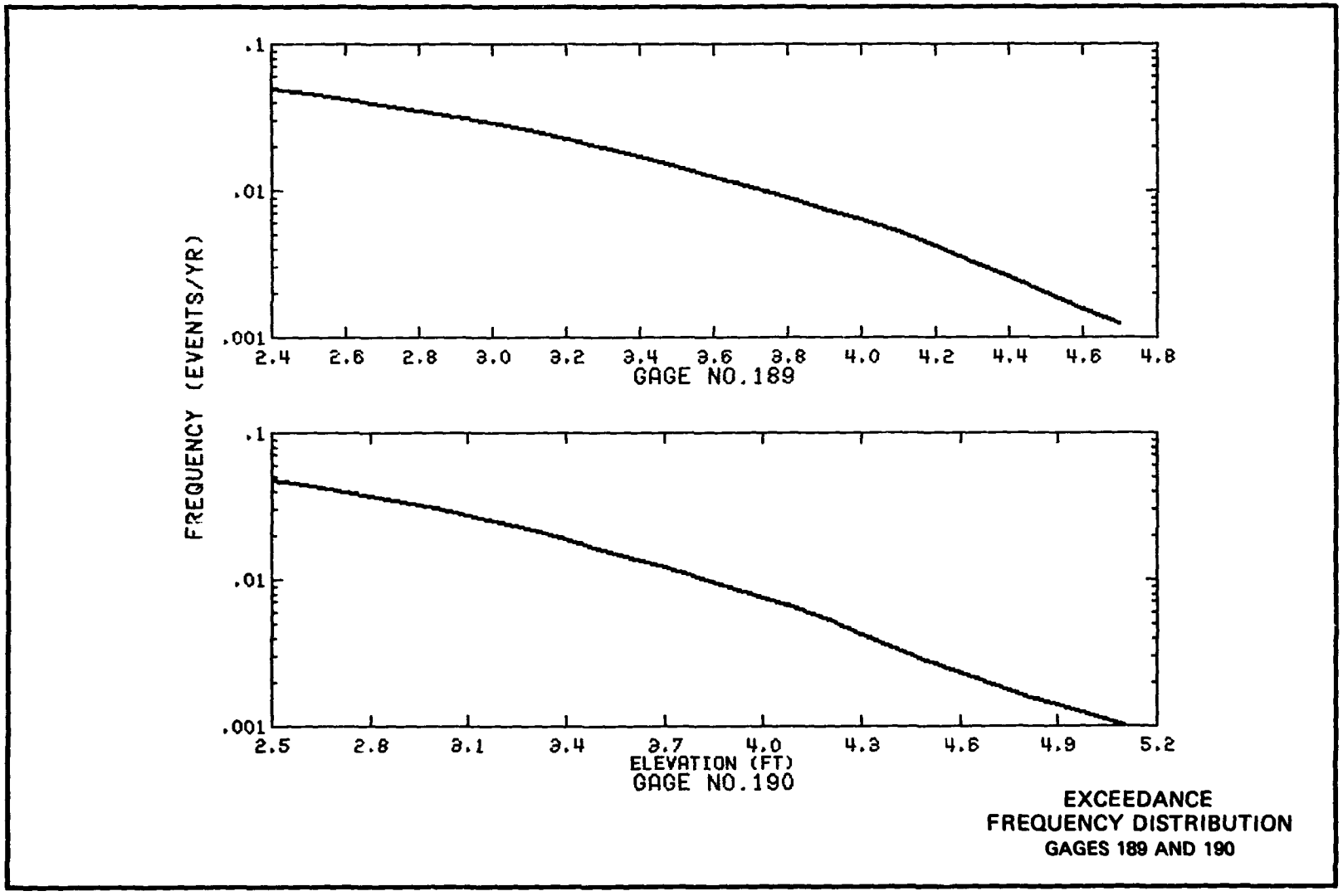

EXCEEDANCE FREQUENCY DISTRIBUTION
GAGES 189 AND 190

PLATE 95

PLATE 96

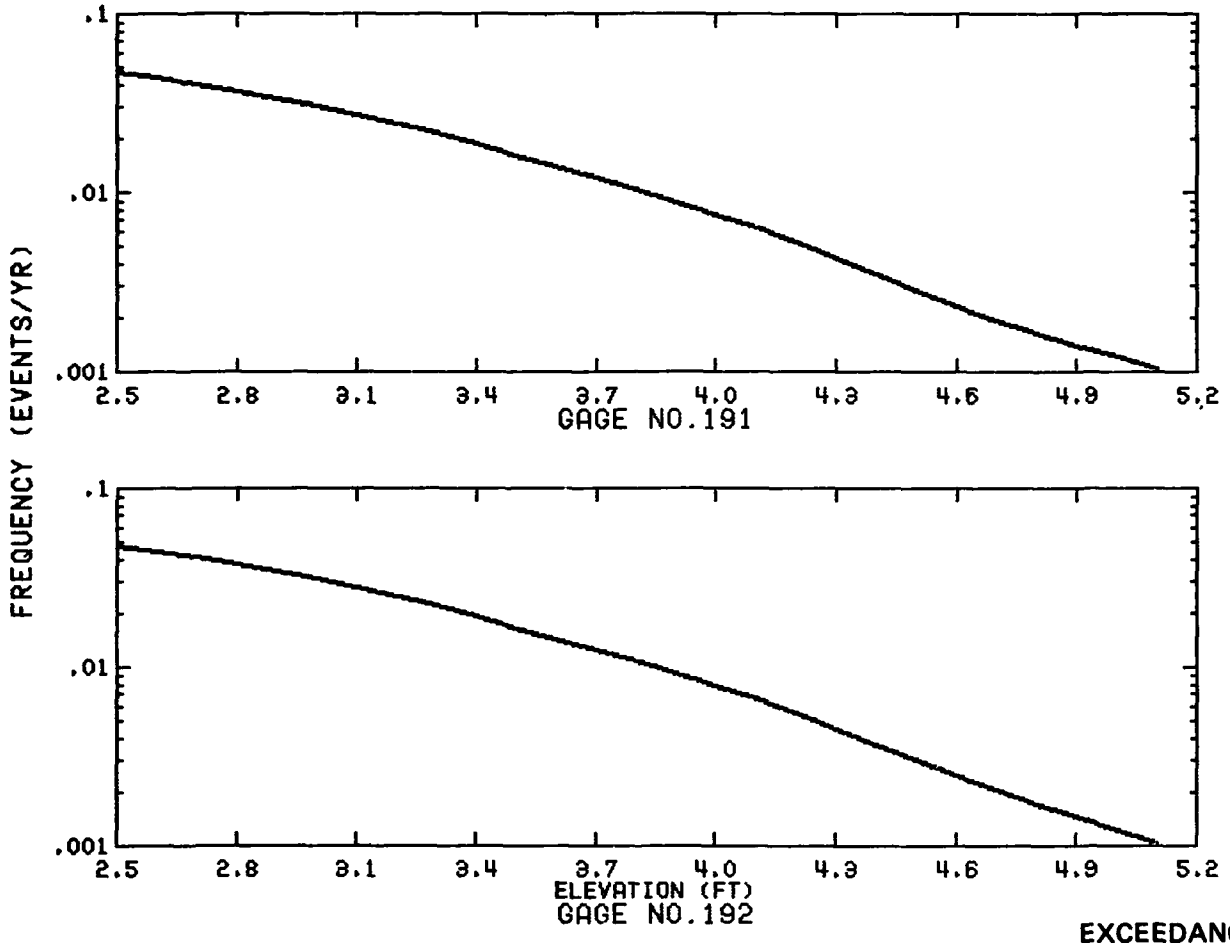

EXCEEDANCE FREQUENCY DISTRIBUTION
GAGES 191 AND 192

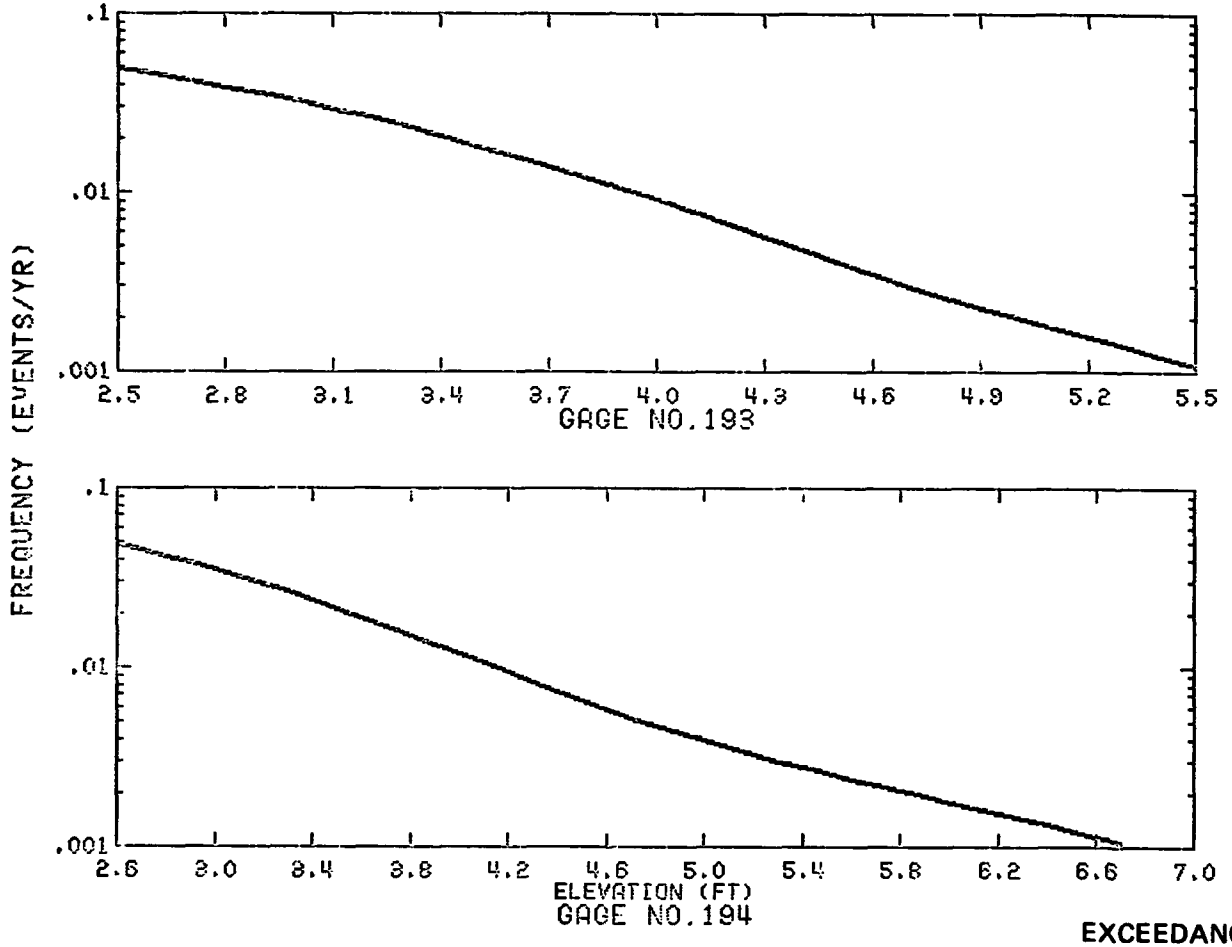

EXCEEDANCE FREQUENCY DISTRIBUTION
GAGES 193 AND 194

PLATE 97

PLATE 98

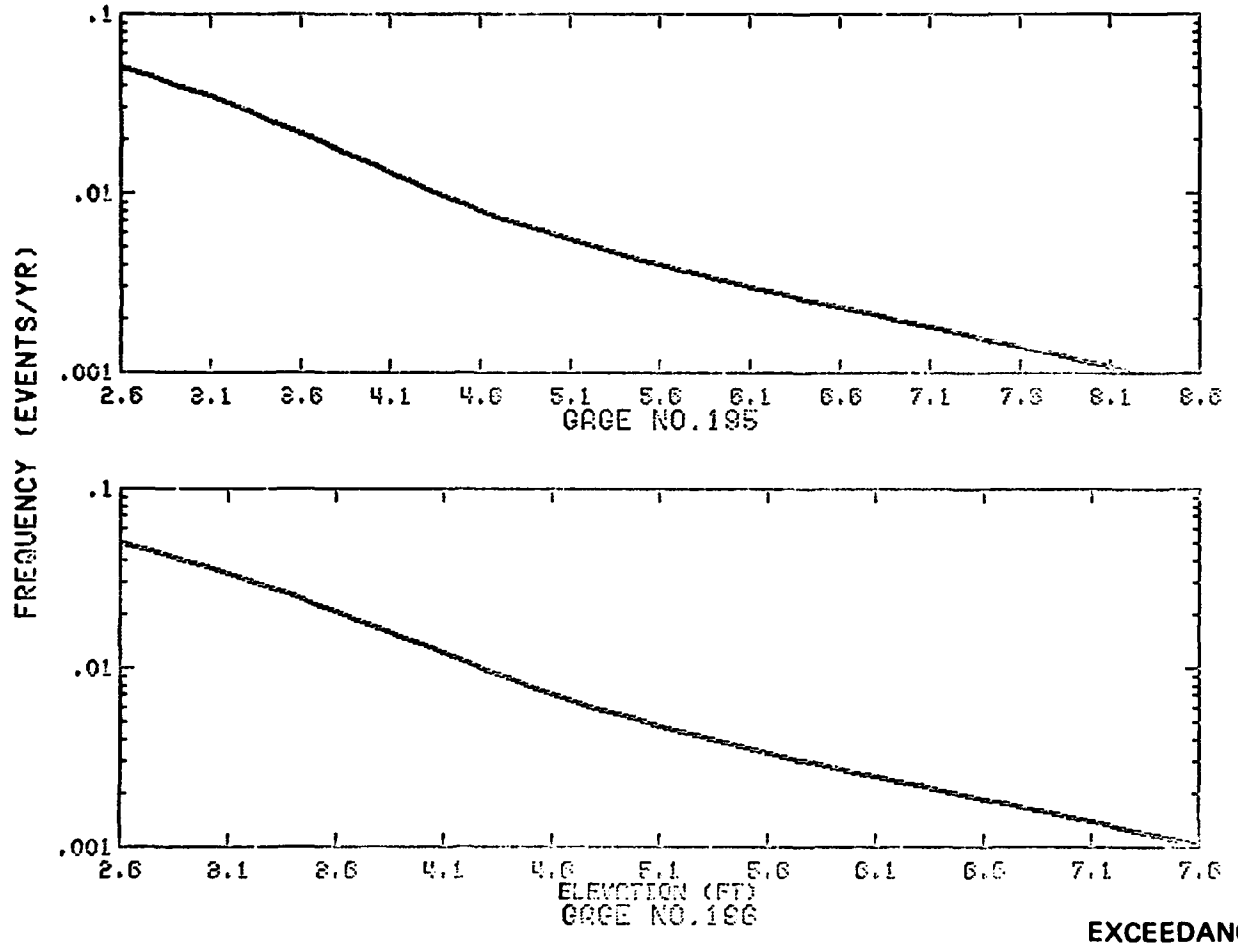

EXCEEDANCE FREQUENCY DISTRIBUTION
GAGES 195 AND 196

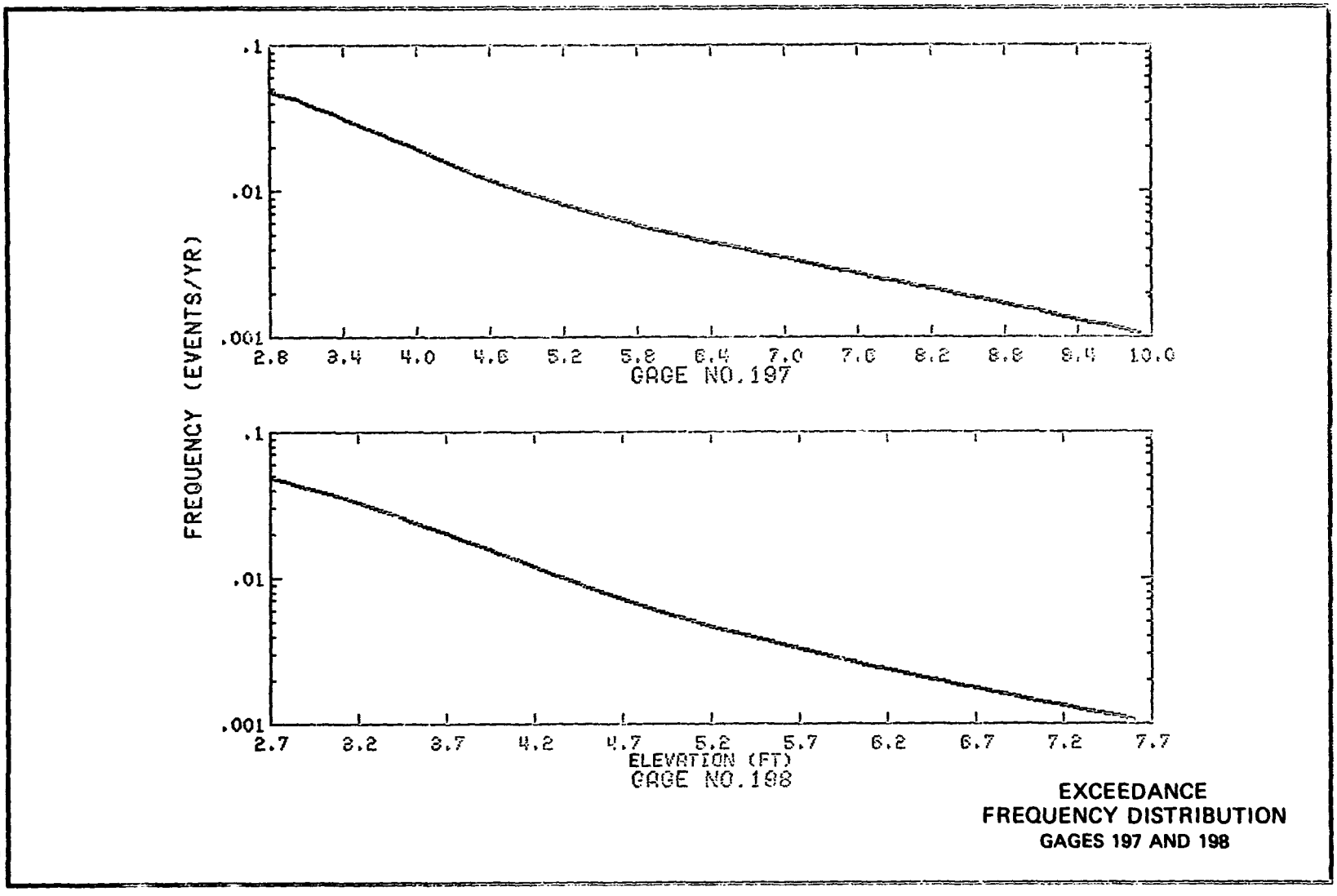

EXCEEDANCE FREQUENCY DISTRIBUTION
GAGES 197 AND 198

PLATE 99

PLATE 100

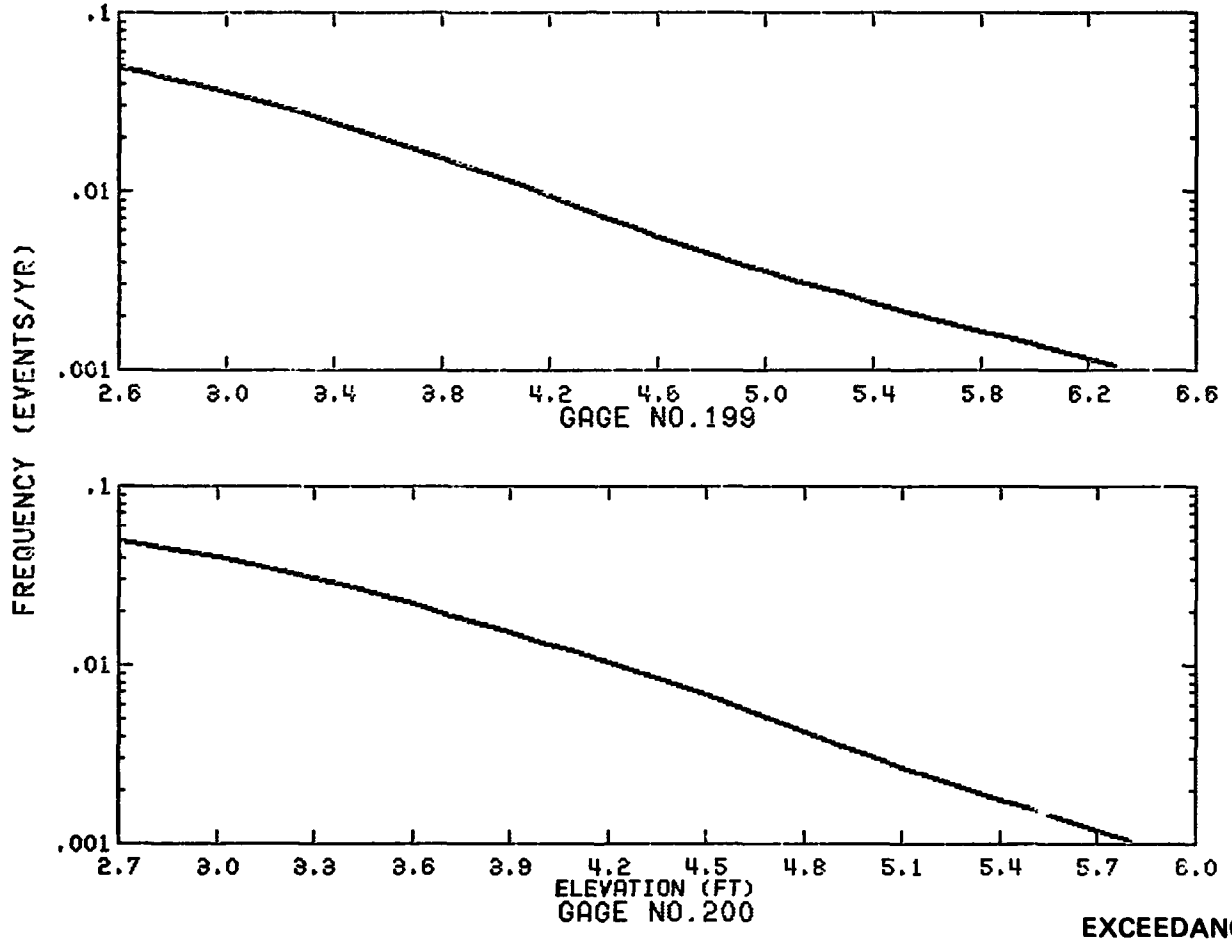

EXCEEDANCE FREQUENCY DISTRIBUTION

GAGES 199 AND 200

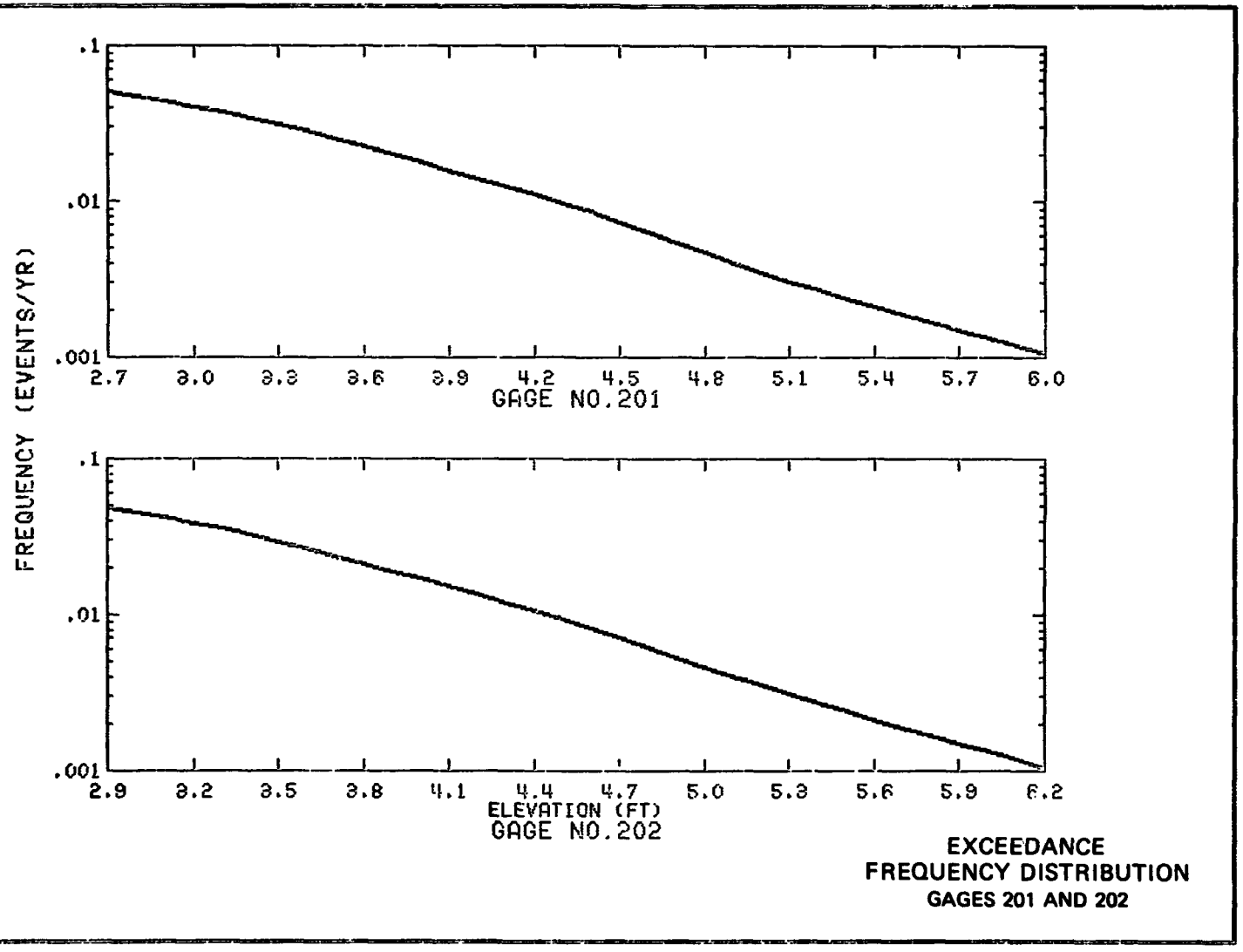

EXCEEDANCE FREQUENCY DISTRIBUTION
GAGES 201 AND 202

PLATE 101

PLATE 102

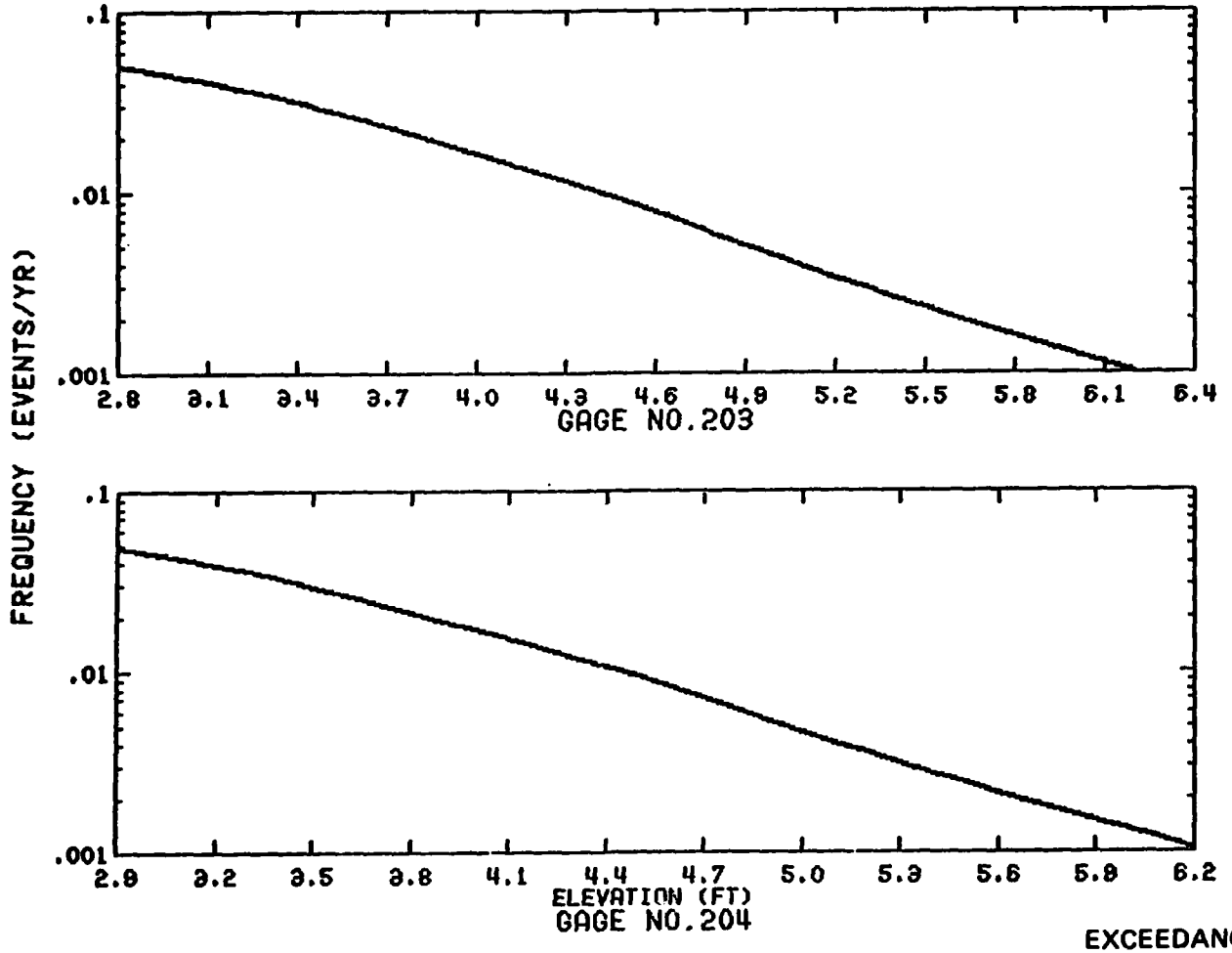

EXCEEDANCE FREQUENCY DISTRIBUTION
GAGES 203 AND 204

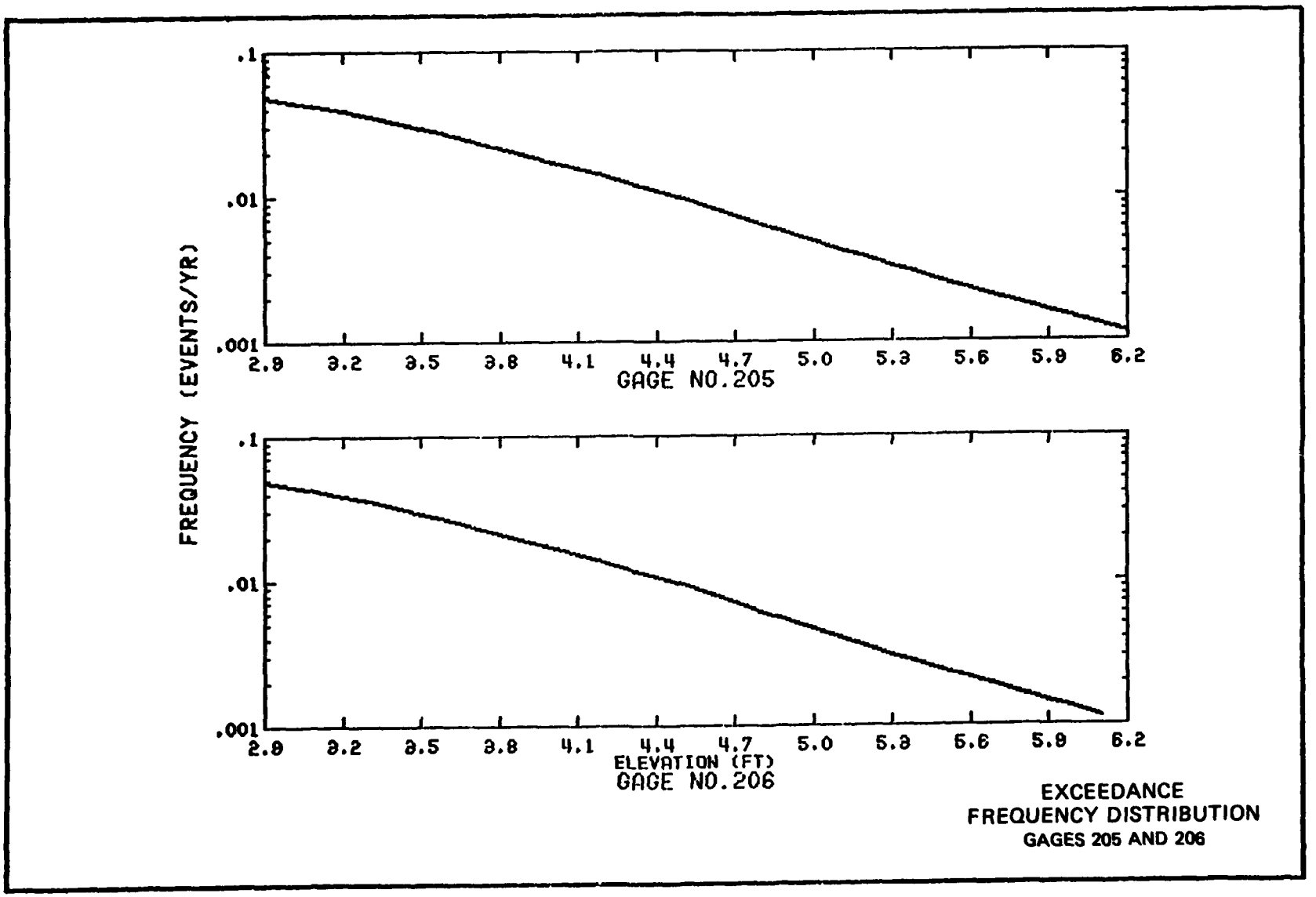

EXCEEDANCE
FREQUENCY DISTRIBUTION
GAGES 205 AND 206

PLATE 103

PLATE 104

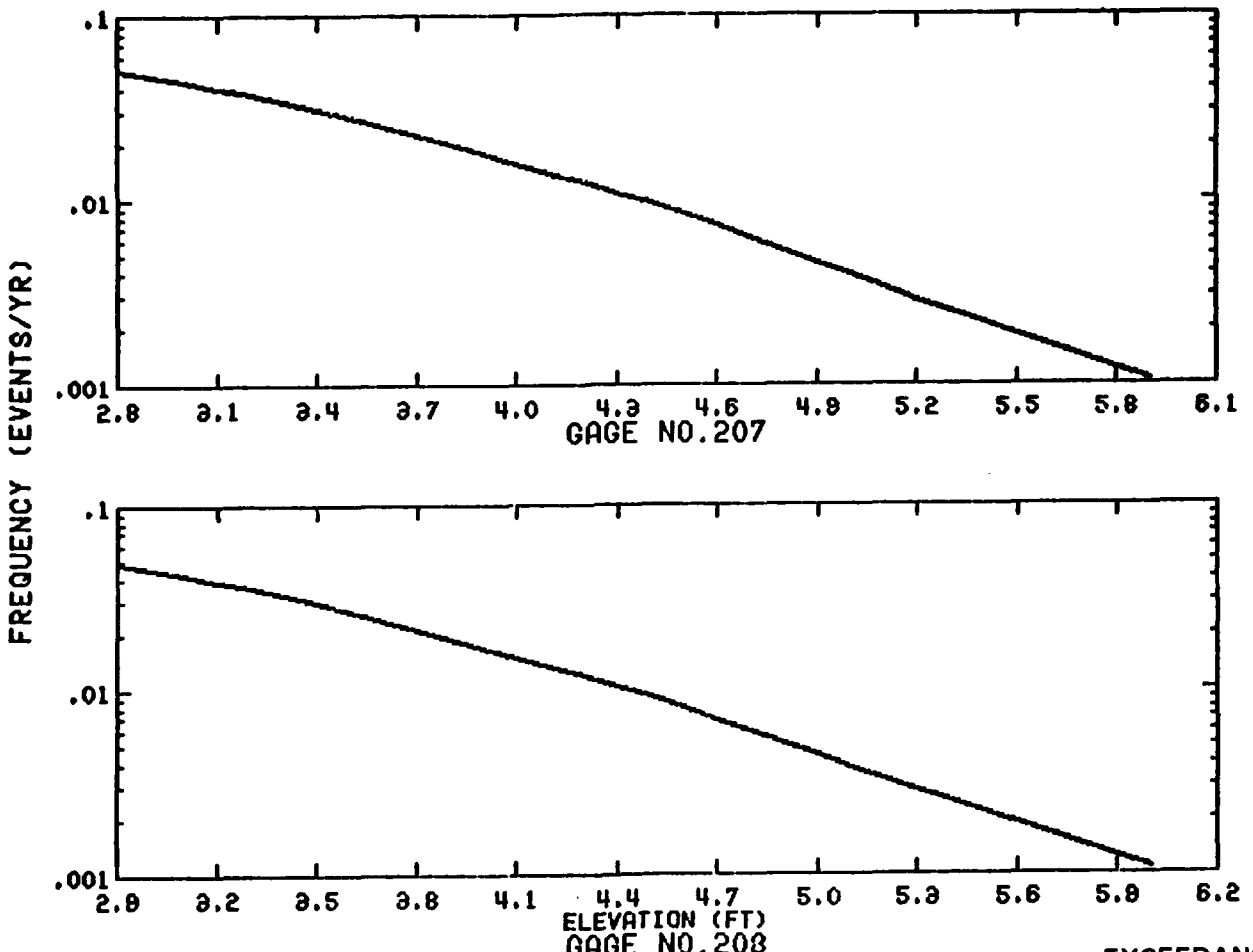

EXCEEDANCE
FREQUENCY DISTRIBUTION
GAGES 207 AND 208

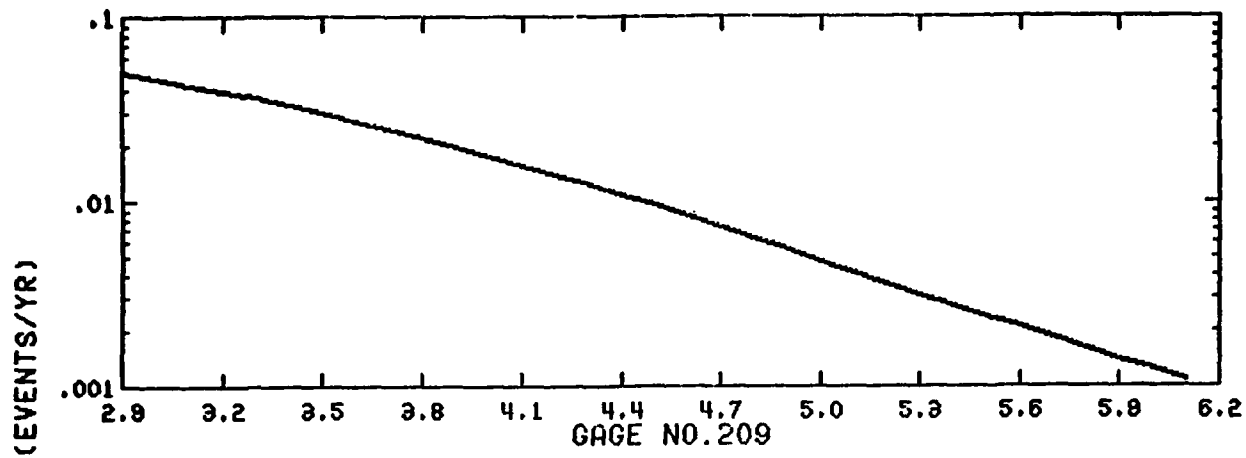

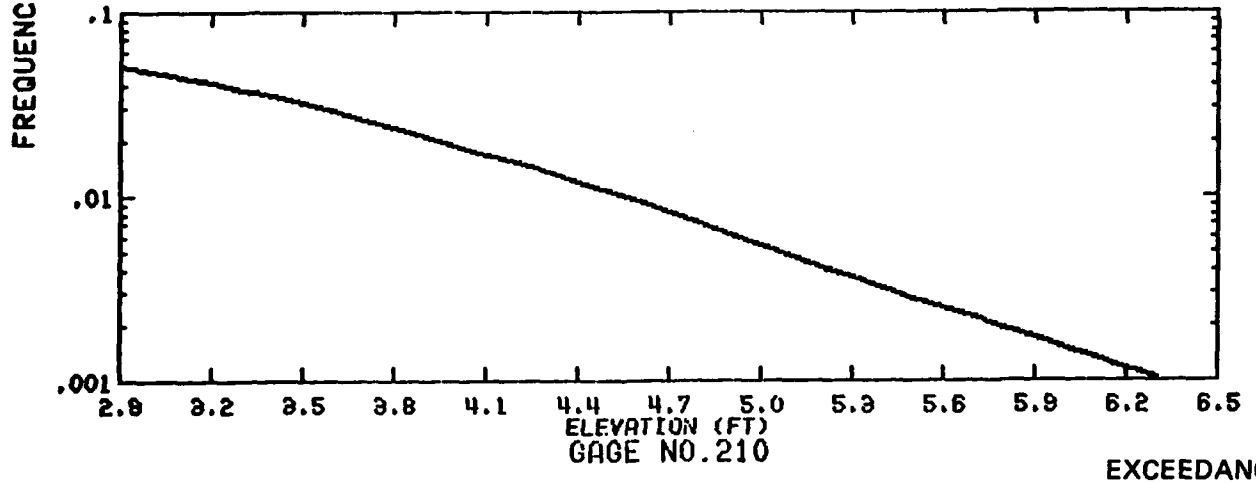

EXCEEDANCE FREQUENCY DISTRIBUTION
GAGES 209 AND 210

PLATE 105

PLATE 106

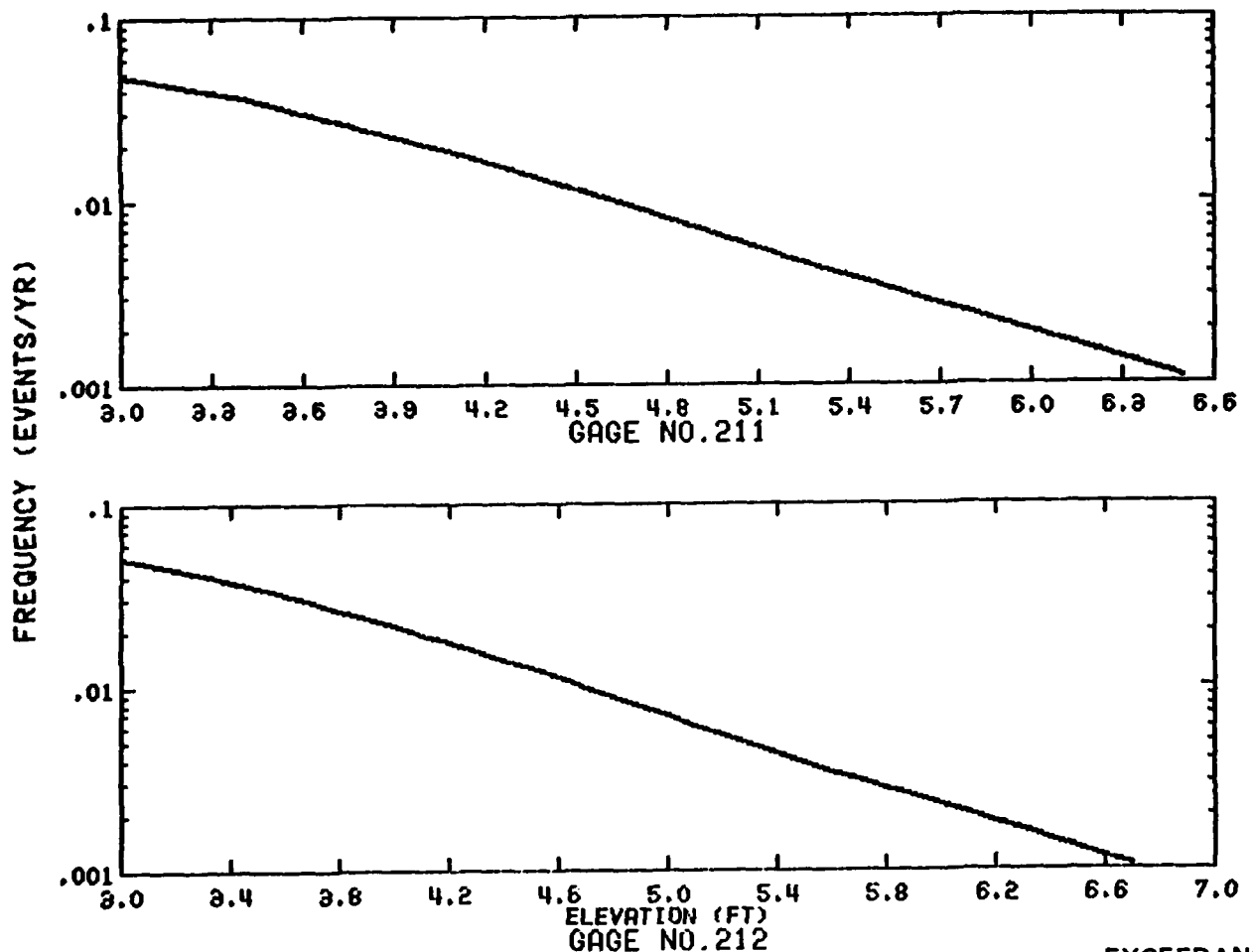

EXCEEDANCE
FREQUENCY DISTRIBUTION
GAGES 211 AND 212

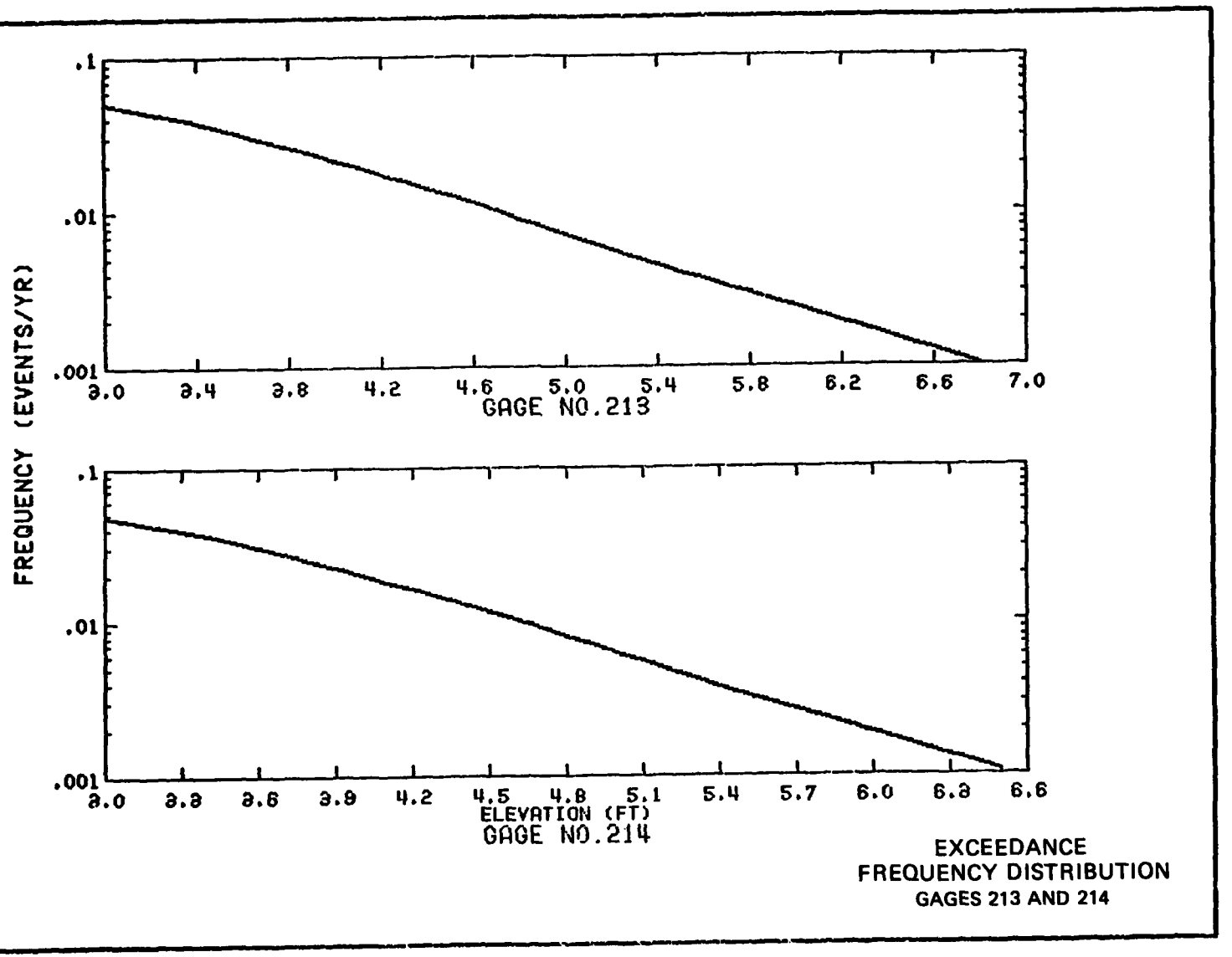

EXCEEDANCE
FREQUENCY DISTRIBUTION
GAGES 213 AND 214

PLATE 107

PLATE 108

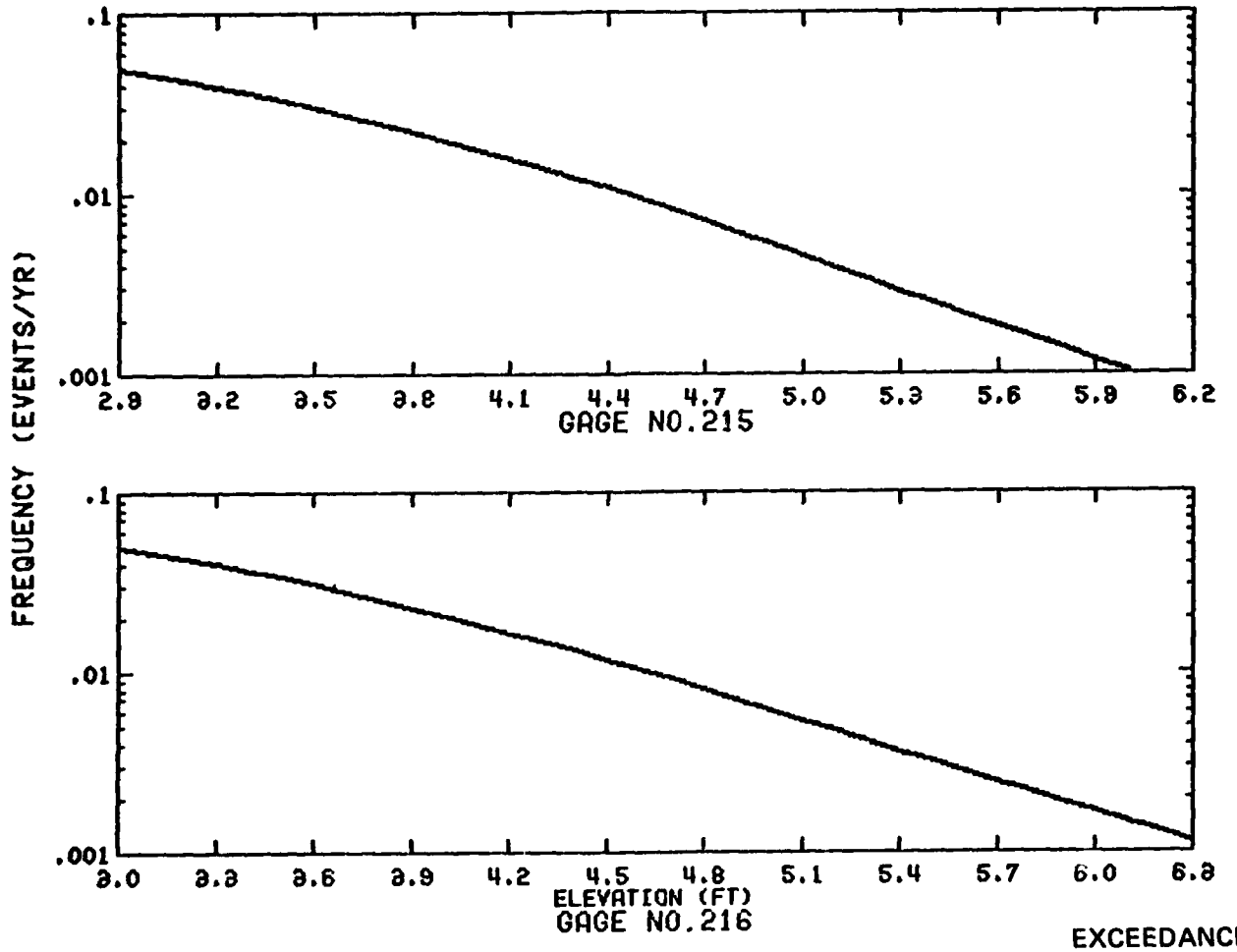

EXCEEDANCE
FREQUENCY DISTRIBUTION
GAGES 215 AND 216

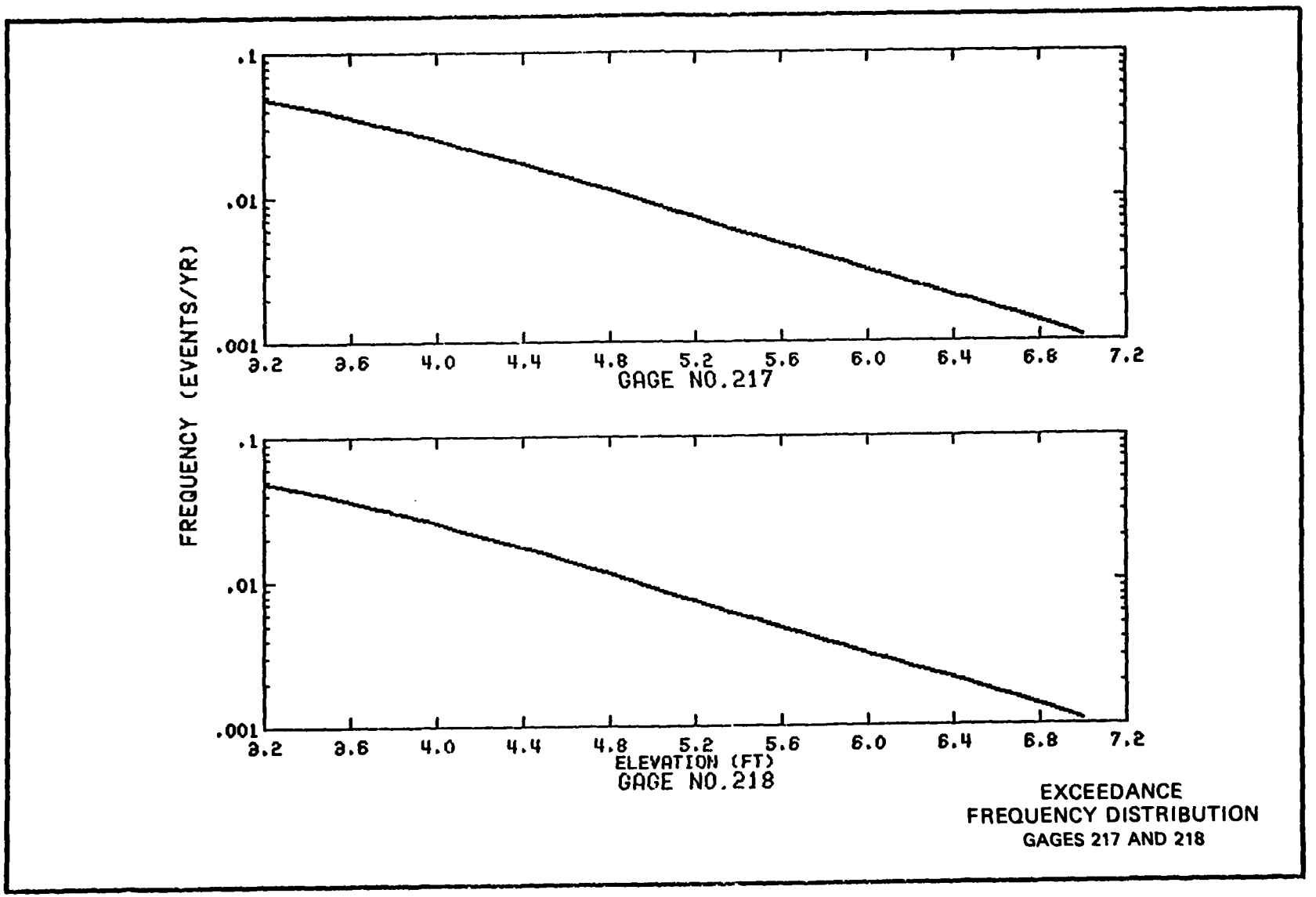

EXCEEDANCE
FREQUENCY DISTRIBUTION
GAGES 217 AND 218

PLATE 109

PLATE 110

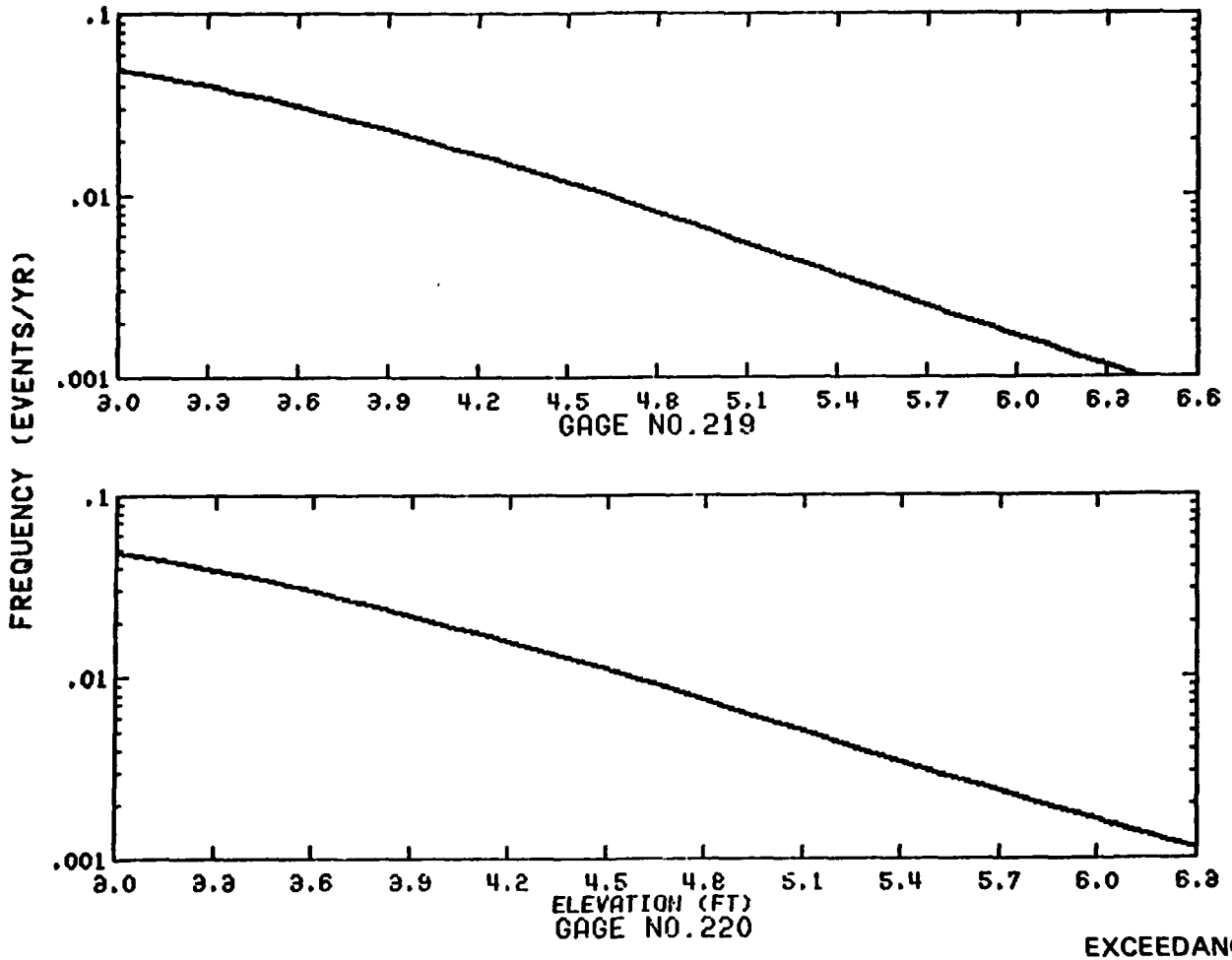

EXCEEDANCE FREQUENCY DISTRIBUTION
GAGES 219 AND 220

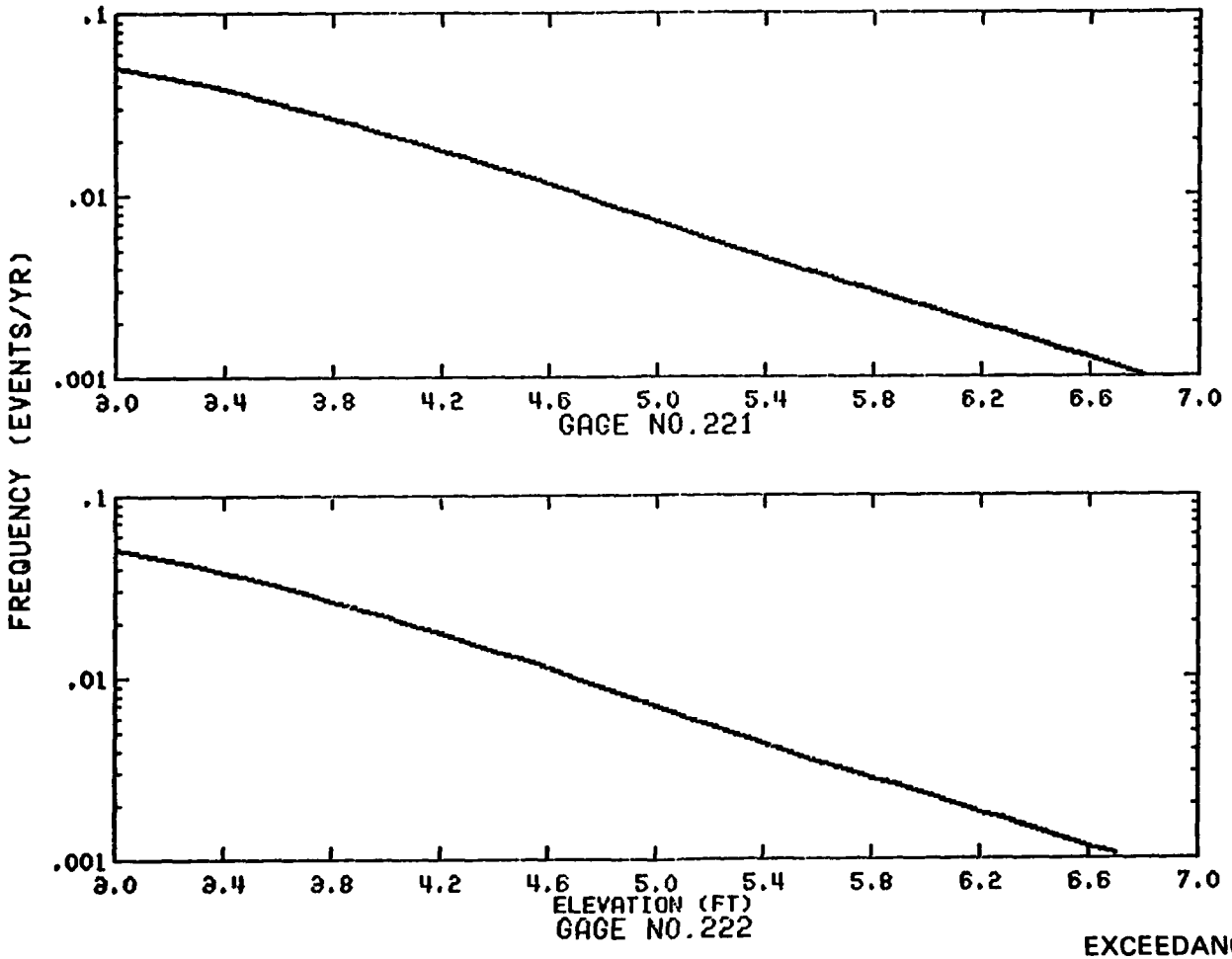

PLATE 111

EXCEEDANCE
FREQUENCY DISTRIBUTION
GAGES 221 AND 222

PLATE 112

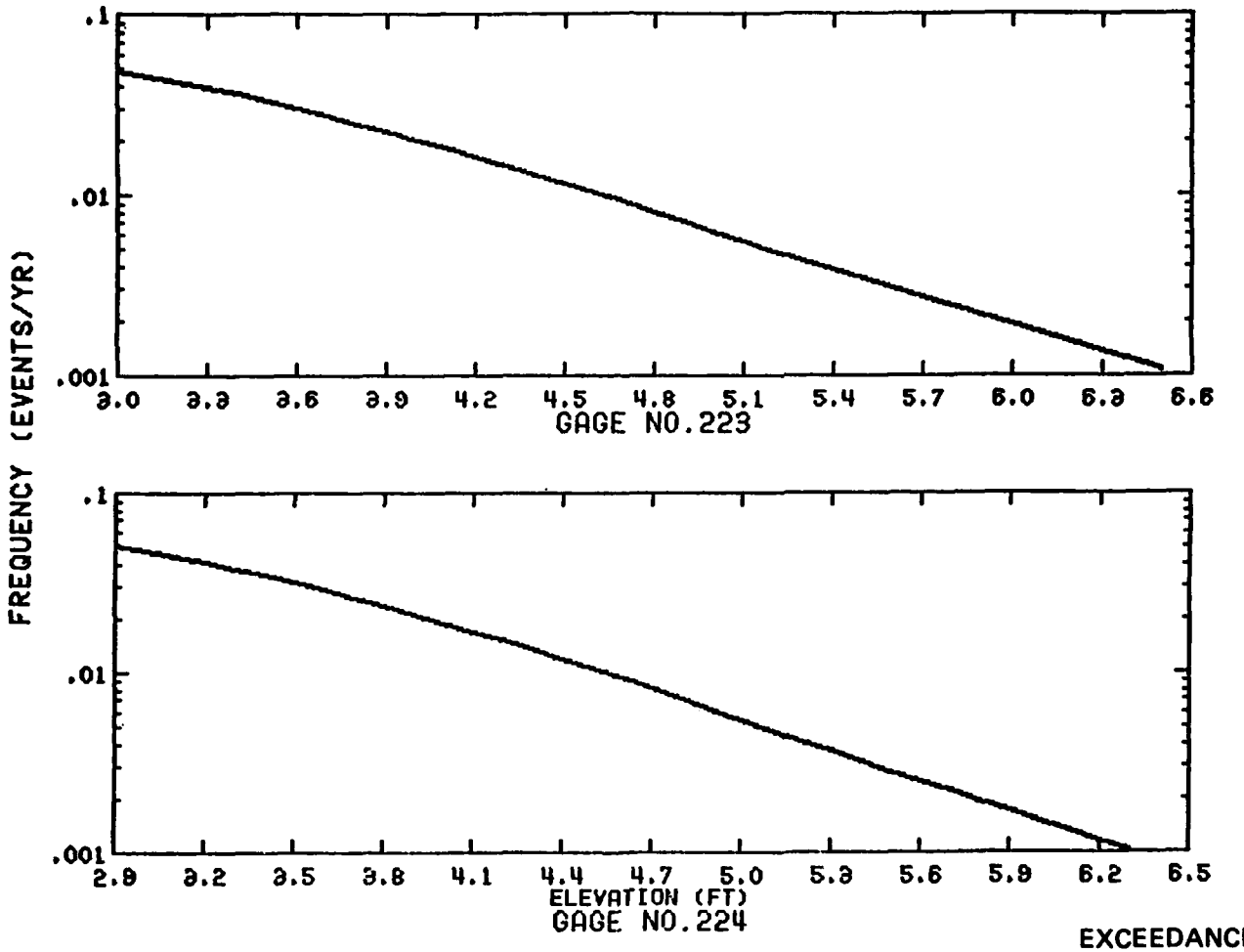

EXCEEDANCE FREQUENCY DISTRIBUTION
GAGES 223 AND 224

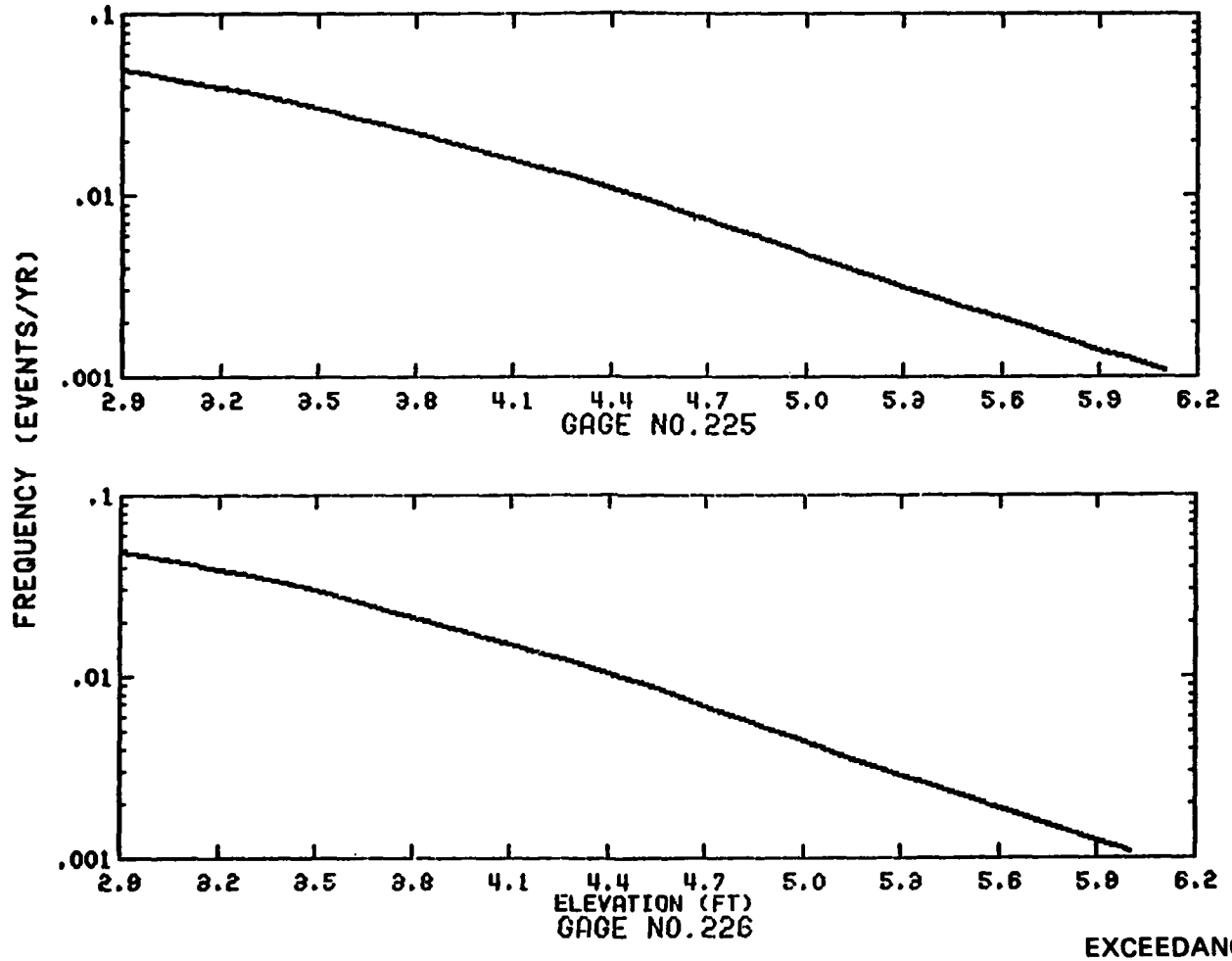

EXCEEDANCE FREQUENCY DISTRIBUTION
GAGES 225 AND 226

PLATE 113

PLATE 114

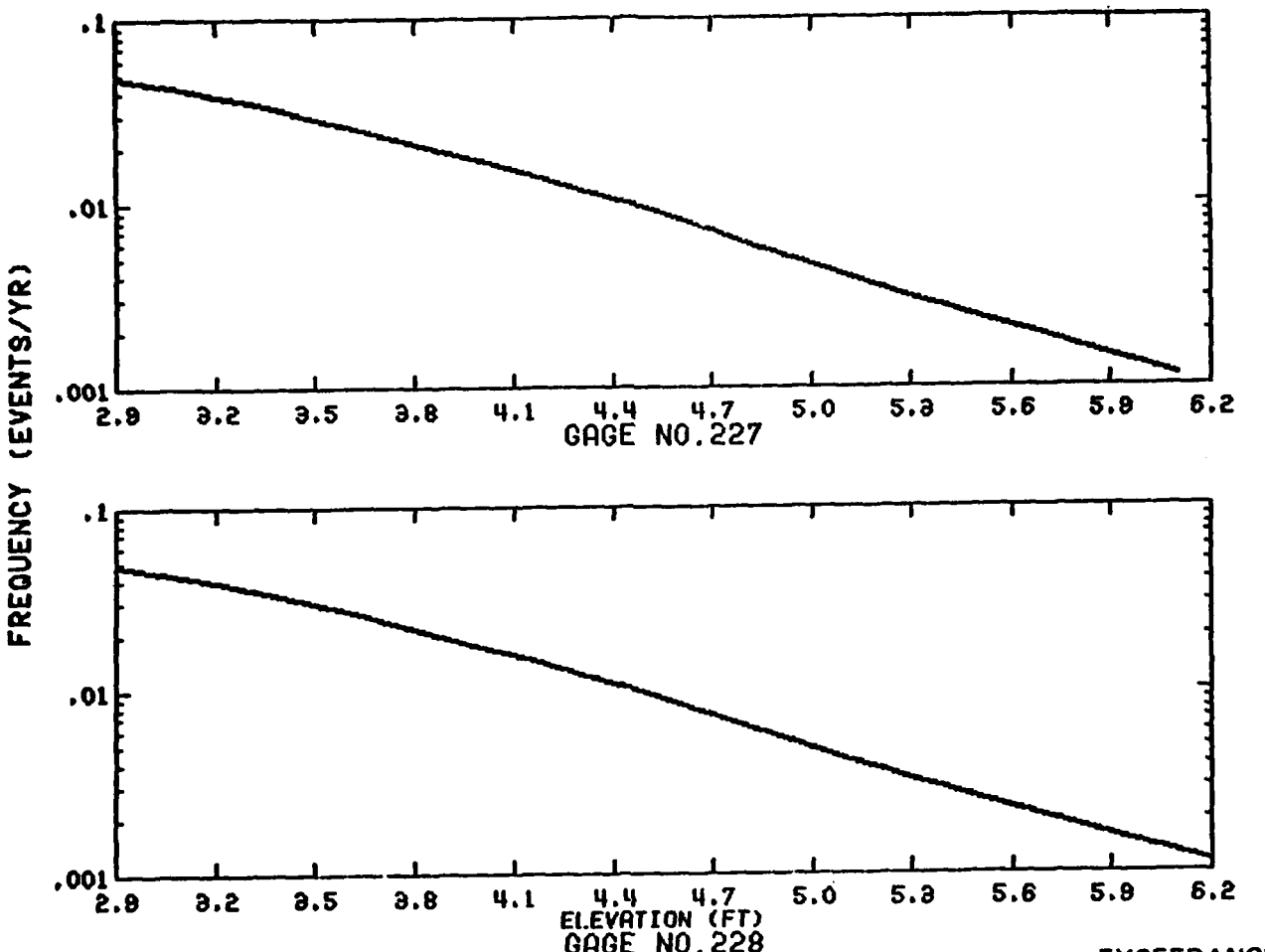

EXCEEDANCE FREQUENCY DISTRIBUTION
GAGES 227 AND 228

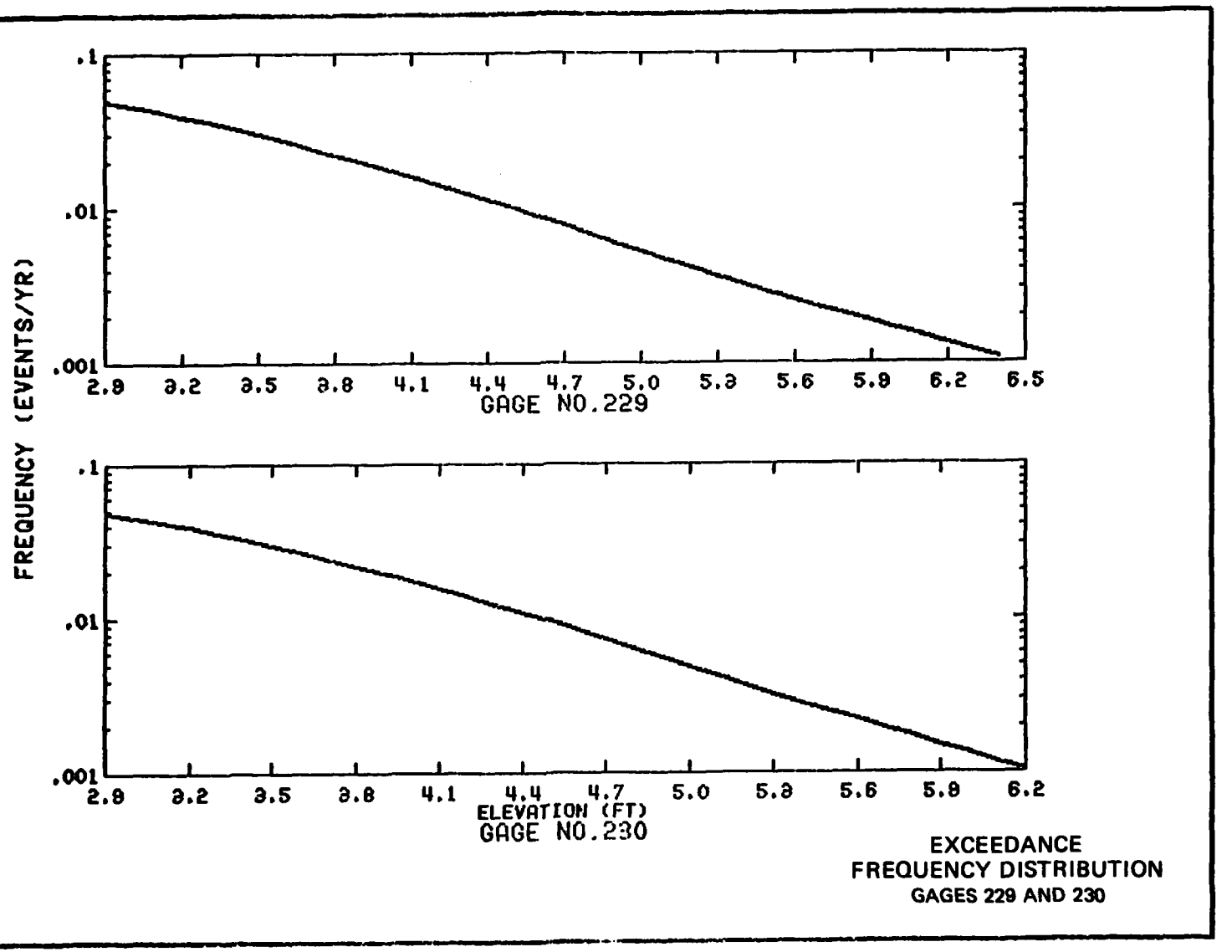

PLATE 115

EXCEEDANCE
FREQUENCY DISTRIBUTION
GAGES 229 AND 230

PLATE 116

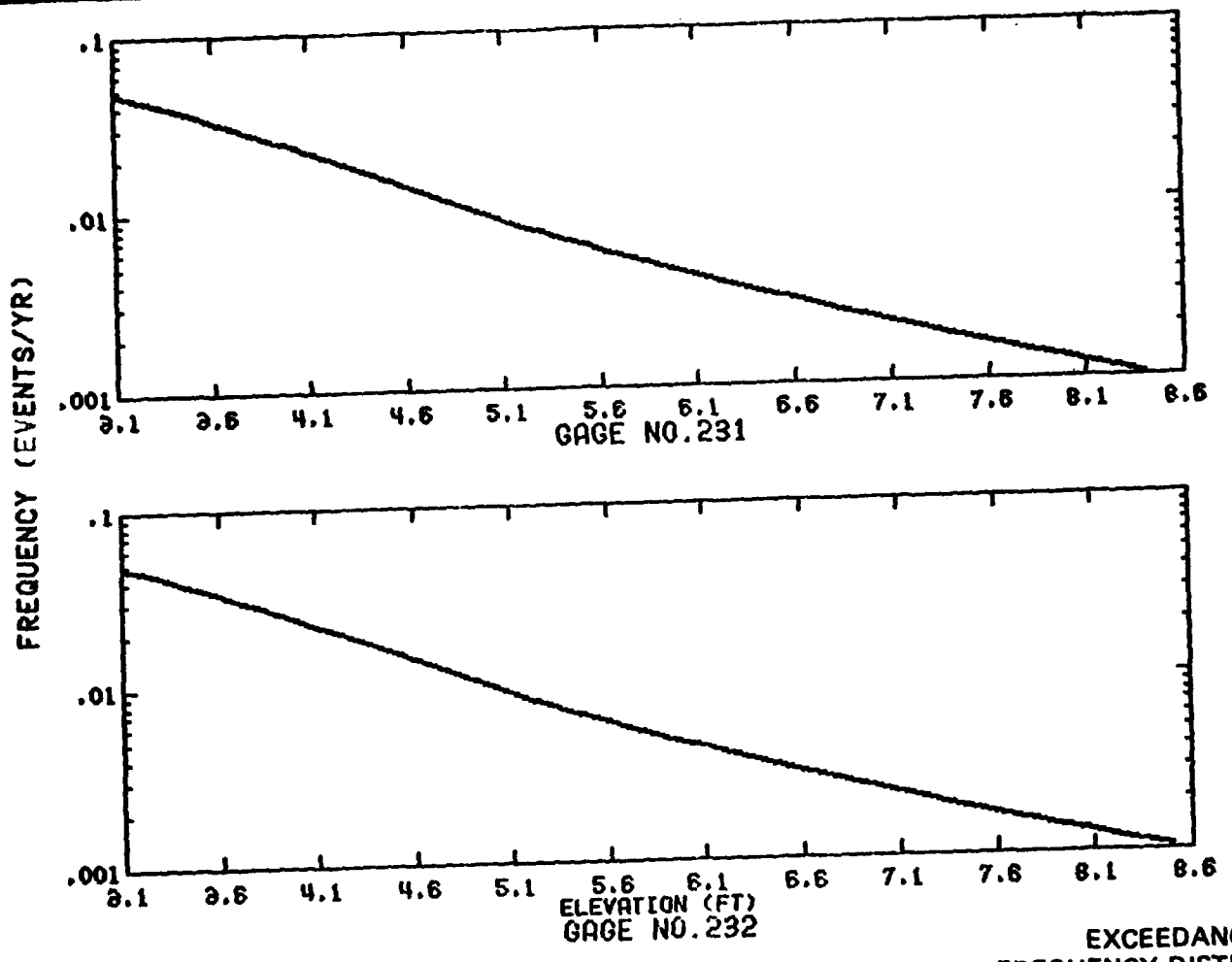

EXCEEDANCE
FREQUENCY DISTRIBUTION
GAGES 231 AND 232

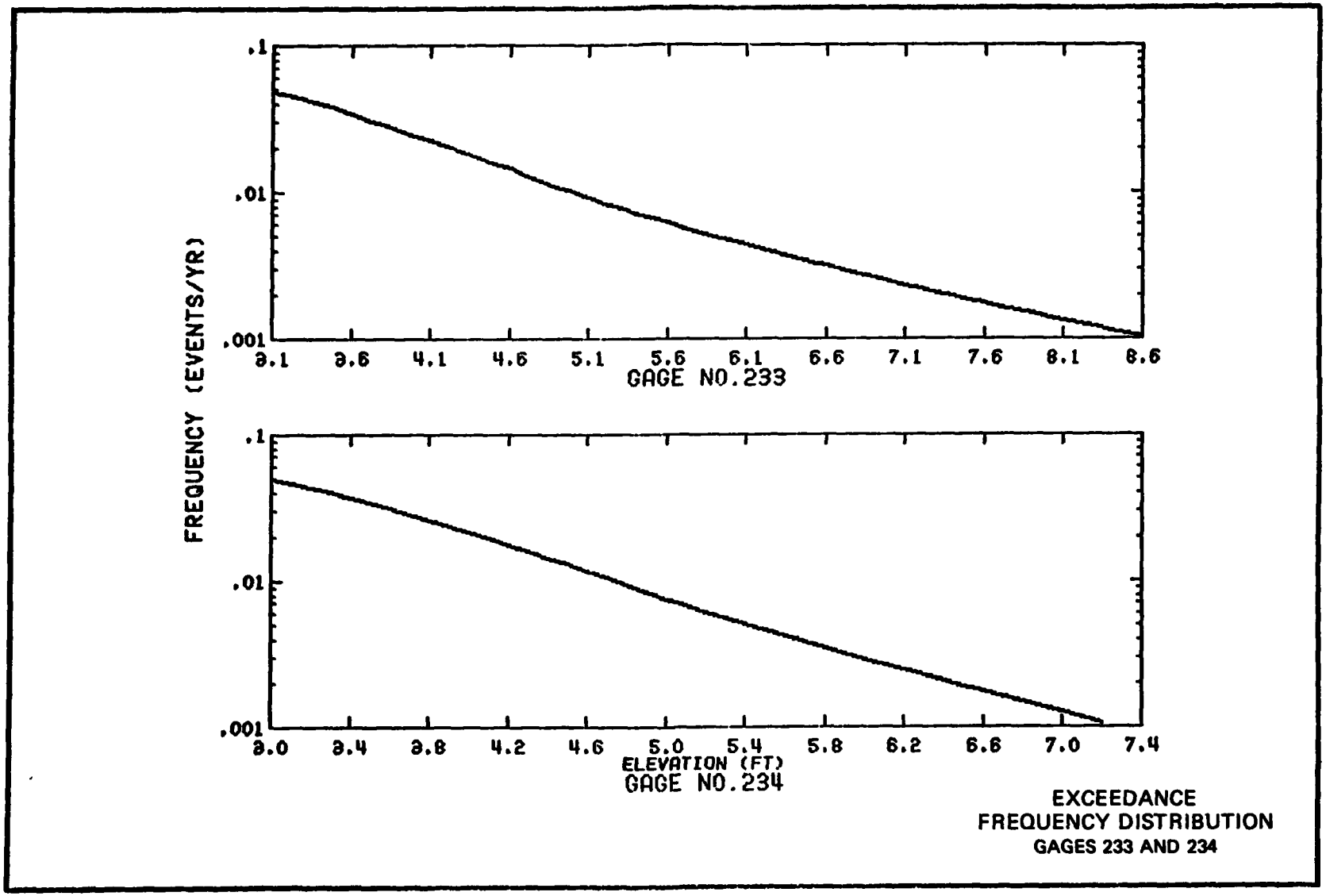

PLATE 117

EXCEEDANCE
FREQUENCY DISTRIBUTION
GAGES 233 AND 234

PLATE 118

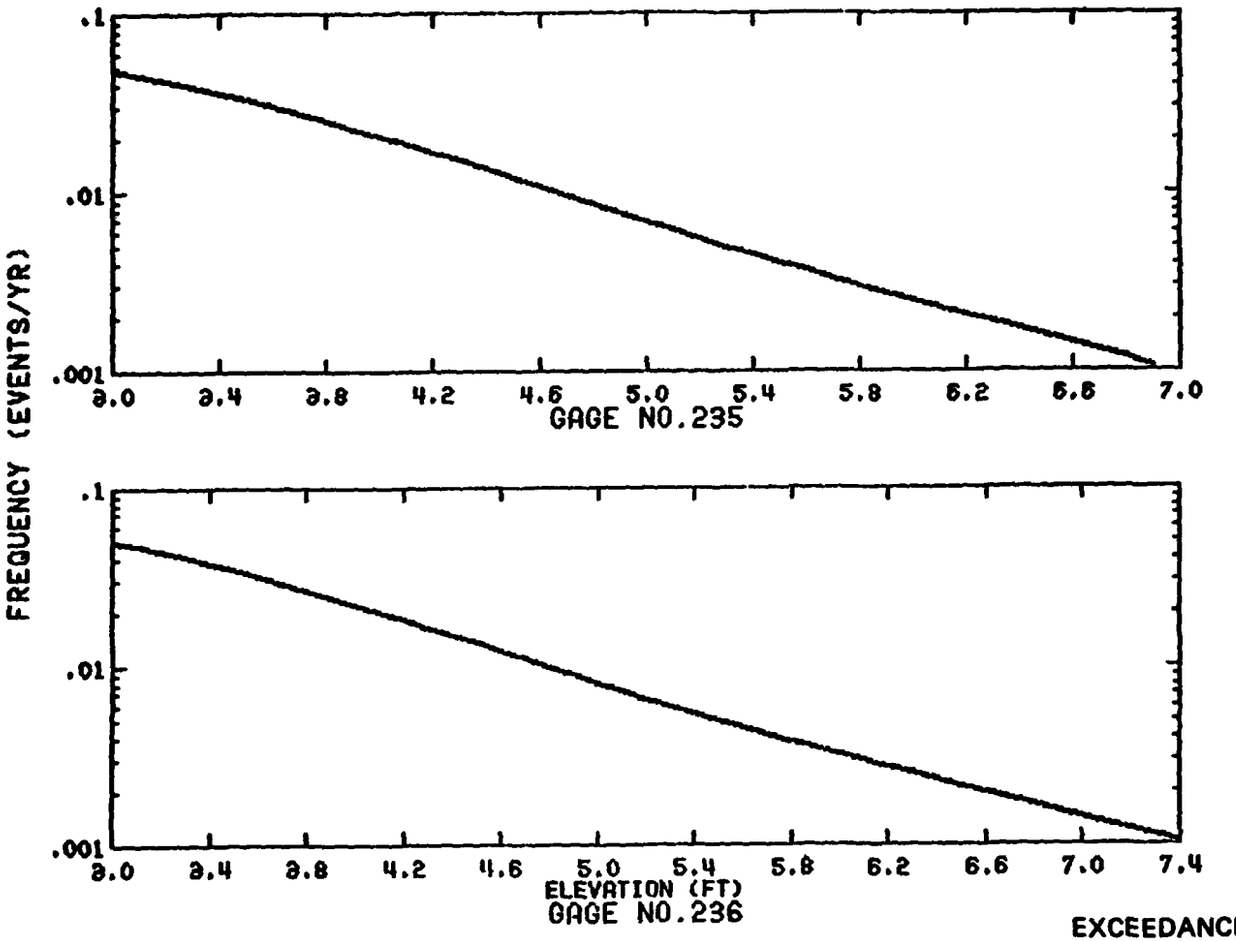

EXCEEDANCE
FREQUENCY DISTRIBUTION
GAGES 235 AND 236

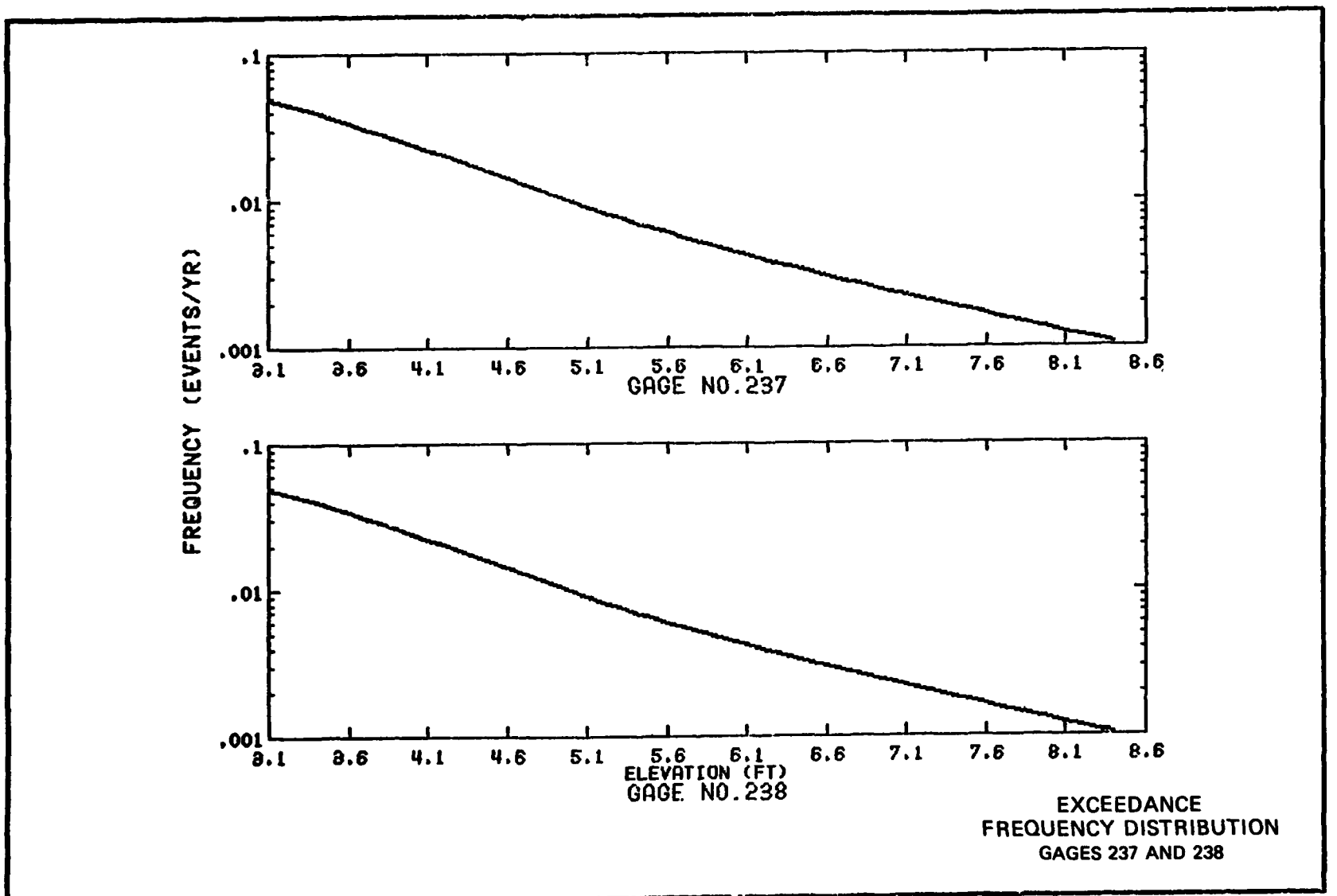

EXCEEDANCE
FREQUENCY DISTRIBUTION
GAGES 237 AND 238

PLATE 119

PLATE 120

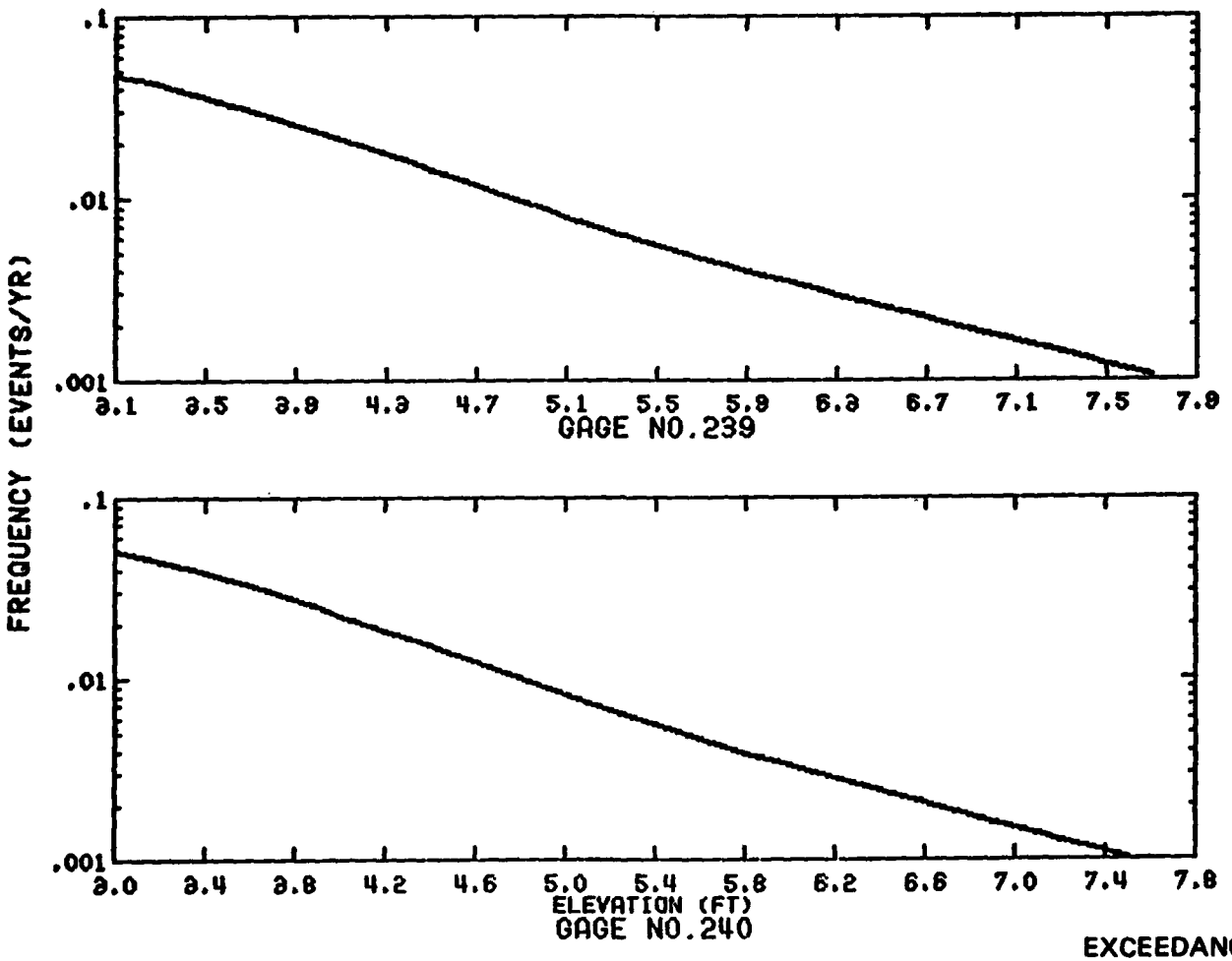

EXCEEDANCE FREQUENCY DISTRIBUTION
GAGES 239 AND 240

APPENDIX A: EFFECT OF NODE FACTOR TEMPORAL VARIATION ON JOINT PROBABILITIES

1. In constructing exceedance frequency distributions for extremal heights resulting from joint occurrences of tsunamis and the astronomical tide, a period of time for the analysis must be selected. However, the inclination of the moon's orbit to the plane of the earth's equator (called an obliquity factor) varies throughout an 18.6-yr cycle because of the revolution of the moon's node. The ratio obtained by dividing the true obliquity factor by its mean value is called a node factor since it is a function of the longitude of the moon's node. The node factor thus has an 18.6-yr cycle. If a period of time less than 18.6 yr is selected for an analysis of joint occurrences of tsunamis and the astronomical tide, the influence of the temporal variation of the node factor is neglected. In this appendix it will be shown that if a particular year (instead of 18.6 yr) is selected for the analysis, the effect of the temporal variation in the node factor on the exceedance frequency distribution is negligible. Thus only a single year instead of 18.6 yr needs to be considered in the analysis and this results in a significant reduction of required computational expense.

2. The effect of a temporal variation of the node factor on external heights resulting from joint occurrences of tsunamis and the astronomical tide can be estimated using an analytical solution described by Houston and Garcia (1974). Since tsunamis have periods much less than 18.6 yr, the variation in the node factor is assumed to be negligible during a tsunami (in fact, the node factor in standard tidal harmonic analysis is assumed to be constant over an entire year). Let

z = the water elevation at any time above local mean sea level.

$P_T(z)$ = the exceedance frequency distribution for the water level at a site being equal to or exceeding z due only to the maximum wave of the tsunami.

$P_N(z)$ = the exceedance frequency distribution of the water level at a site being equal to or exceeding z due only to the temporal variation of the node factor of the astronomical tide.

$P(z)$ = the exceedance frequency distribution of the water level at a given site being equal to or exceeding z due to both the maximum wave of the tsunami and the node factor of the astronomical tide.

3. According to Chandrasekhar (1943), $P(z)$ can be calculated from

$$P(z) = \int_{-\infty}^{\infty} f_N(\lambda) P_T(z - \lambda) d\lambda \tag{A1}$$

where

$$f_N(z) = - \frac{dP_N(z)}{dz} \tag{A2}$$

and $f_N(z)$ is the frequency density for the astronomical tide. If $P_N(z)$ is approximated by a Gaussian distribution, then

$$f_N(z) = \frac{1}{\sqrt{2\pi}\sigma} e^{-(z^2/2\sigma^2)} \tag{A3}$$

where the variance, σ^2, is given by

$$\sigma^2 = \sum_{m=1}^{\infty} C_m^2 \tag{A4}$$

and C_m equals the height variation of the node factor associated with the m^{th} tidal constituent.

4. It is well-known that the logarithm of $P_T(z)$ is linearly related to tsunami elevations (see PART III). Therefore, let

$$P_T(z) = Ae^{-\alpha z} \tag{A5}$$

Substituting Equations A3 and A5 into Equation A1 yields

$$P(z) = Ae^{-\alpha\left[z-(\alpha\sigma^2/2)\right]} \tag{A6}$$

or

$$P(z) = Ae^{-\alpha z^1} \tag{A7}$$

where

$$z^1 = z - \frac{\alpha\sigma^2}{2} \tag{A8}$$

5. Thus, the net effect of the temporal variation in the node factor is to produce a $P(z)$ identical with $P_T(z)$ except for a shift of z by an amount $\alpha\sigma^2/2$. The variance σ^2 can be determined by multiplying the nodal factor variation for each tidal constitutent (*Schureman* 1948) times the amplitude of the tidal constituents (tidal constituents available from the National Ocean Survey). This product equals C_m in Equation A4; α can be determined at a location using Plates 1-120 by approximating the curves with straight lines and determining the slope of the lines.

6. For example, gage 104 is the site of the Los Angeles tide gage. From Plate 52 α is found to be equal to approximately 0.54. σ^2 equals 0.17.

7. Thus $\alpha\sigma^2/2 \cong 0.05$ ft. Hence, the exceedance frequency distribution based upon a year for which the major tidal constituents have an average value (approximately 1.0) should be shifted relative to an 18.6-yr period by approximately 0.06 ft for all frequencies.

8. The analytic solution presented was shown to be correct by a direct numerical approach. The year 1964 was selected as the year for which the major tidal constituents have an average value. The 18.6-yr period was centered on 1964. Tsunami and tidal elevations were expressed to the nearest 0.1 ft. It was found that the exceedance frequency distributions for the 1-yr and 18.6-yr period had the same 50-yr, 200-yr, 500-yr, and 1000-yr elevations. The 100-yr elevation was different by 0.1 ft.

APPENDIX B: NOTATION

a	Length of major axis of elliptical source, miles
A	*Amplitude constant*
b	Length of minor axis of elliptical source, miles
c_m	m^{th} nodal constituent
$f(\ )$	Probability density function
F	Tsunami frequency
H_a	Wave height in direction of major axis of ellipse, ft
H_b	Wave height in direction of minor axis of ellipse, ft
H_{avg}	Average runup over a coast, m
i	Tsunami intensity
$n(\ )$	Tsunami probability function
p	Constant
$P(\ )$	Exceedance frequency distribution for combined node factor variation and tsunamis
$P_N(\ )$	Exceedance frequency distribution for node factor variation
$P_T(\ )$	Exceedance frequency distribution for tsuanmis
q	Constant
r	Constant
x	Spatial coordinate, ft
y	Spatial coordinate, ft
z	Water-surface elevation above mean sea level (msl), ft
α	Exponential constant
λ	Variable of integration
σ^2	Variance

In accordance with letter from DAEN-RDC, DAEN-ASI dated 22 July 1977, Subject: Facsimile Catalog Cards for Laboratory Technical Publications, a facsimile catalog card in Library of Congress MARC format is reproduced below.

Houston, James R
Type 19 flood insurance study: Tsunami predictions for southern California / by James R. Houston. Vicksburg, Miss. : U. S. Waterways Experiment Station; Springfield, Va. : available from National Technical Information Service, 1980.
48, [6] p., [60] leaves of plates: ill. ; 27 cm. (Technical report - U. S. Army Engineer Waterways Experiment Station ; HL-80-18)
Prepared for Federal Insurance Administration, Federal Emergency Management Agency, Washington, D. C.
References: p. 46-48.

1. Floodplain insurance. 2. Mathematical models. 3. Numerical analysis. 4. Shorelines. 5. Southern California. 6. Tsunamis. I. United States. Federal Insurance Administration. II. Series: United States. Waterways Experiment Station, Vicksburg, Miss. Technical report ; HL-80-18.
TA7.W34 no.HL-80-18